TEXAS TECH UNIVERSITY
Multidisciplinary Research in Transportation

Effects of Wet Mat Curing Time and Earlier Loading on Long-Term Durability of Bridge Decks: Compressive Strength, Maturity and Strength Durability Index (SDI)

Authors: Hector Garcia-Monzon, Sanjaya Senadheera, R. Scott Phelan

Performed in Cooperation with the Texas Department of Transportation and the Federal Highway Administration

Research Project 0-2116
Research Report 0-2116-4A
http://www.techmrt.ttu.edu/reports.php

Notice

The United States Government and the State of Texas do not endorse products or manufacturers. Trade or manufacturers' names appear herein solely because they are considered essential to the object of this report.

Technical Report Documentation Page

1. Report No.: FHWA/TX -09-2116-4A	2. Government Accession No.:	3. Recipient's Catalog No.:
4. Title and Subtitle: Effects of Wet Mat Curing Time and Earlier Loading on Long-Term Durability of Bridge Decks: Compressive Strength, Maturity and Strength Durability Index (SDI)		5. Report Date: January 2009
		6. Performing Organization Code:
7. Author(s): Hector Garcia-Monzon, Randall Scott Phelan, and Sanjaya Senadheera		8. Performing Organization Report No. 0-2116-4A
9. Performing Organization Name and Address: Texas Tech University College of Engineering Box 41023 Lubbock, Texas 79409-1023		10. Work Unit No. (TRAIS): 11. Contract or Grant No. : Project 0-2116
12. Sponsoring Agency Name and Address Texas Department of Transportation Research and Technology P. O. Box 5080 Austin, TX 78763-5080		13. Type of Report and Period Cover: Final Report 04/07/99 - 08/31/04 14. Sponsoring Agency Code:
15. Supplementary Notes: This study was conducted in cooperation with the Texas Department of Transportation and the Federal Highway Administration		

Abstract: There is increasing pressure from owners, contractors, and the public to open bridge decks sooner to full traffic loads. As a result, a set of criteria or guidelines is needed to determine when concrete bridge decks can safely be opened. Today, current practice allows many bridge decks and concrete pavements to be opened to traffic once a desired compressive strength is achieved from a representative field-cast test cylinder. Though generally untrue, many believe that this strength value serves as a measure of the durability of the placed concrete. In a collaborative research effort between Texas Department of Transportation and researchers at Texas Tech University, studies were undertaken to collect research data that could potentially lead to the development of new guidelines as to when bridge decks can be open to (a) construction traffic and (b) full traffic without sacrificing concrete durability. This report presents detailed findings of two research thrusts: compressive strength and maturity curves commonly used on bridge deck concrete mixes and comparative assessment of the effectiveness of three curing methods that led to the development of a framework for a Strength-Durability Index (SDI).

17. Key Words: concrete, bridge, deck, durability, curing, wet mat, vehicle loading, early loading		Distribution Statement No restrictions. This report available to the public through the National Technical Information Service, Springfield, Virginia 22616 www.ntis.gov	
19. Security Classif. (of this report) Unclassified	20. Security Classif. (of this page) Unclassified	21. No. of Pages	22. Price

Form DOT F 1700.7 (8-72)

EFFECTS OF WET MAT CURING TIME AND EARLIER LOADING ON LONG-TERM DURABILITY OF BRIDGE DECKS: COMPRESSIVE STRENGTH, MATURITY AND STRENGTH-DURABILITY INDEX (SDI)

by

Hector Garcia-Monzon, Randall Scott Phelan and Sanjaya Senadheera

Report 0-2116-4A

conducted for the

Texas Department of Transportation
in cooperation with the
U.S. Department of Transportation
Federal Highway Administration

by the

CENTER FOR MULTIDISCIPLINARY RESEARCH IN TRANSPORTATION

TEXAS TECH UNIVERSITY

July 2009

AUTHOR'S DISCLAIMER

The contents of this report reflect the views of the authors who are responsible for the facts and the accuracy of the data presented herein. The contents do not necessarily reflect the official view of policies of the Texas Department of Transportation or the Federal Highway Administration. This report does not constitute a standard, specification, or regulation.

PATENT DISCLAIMER

There was no invention or discovery conceived or first actually reduced to practice in the course of or under this contract, including any art, method, process, machine, manufacture, design or composition of matter, or any new useful improvement thereof, or any variety of plant which is or may be patentable under the patent laws of the United States of America or any foreign country.

ENGINEERING DISCLAIMER

Not intended for construction, bidding, or permit purposes.

TRADE NAMES AND MANUFACTURERS' NAMES

The United States Government and the State of Texas do not endorse products or manufacturers. Trade or manufacturers' names appear herein solely because they are considered essential to the object of this report.

Prepared in cooperation with the Texas Department of Transportation and the U.S. Department of Transportation, Federal Highway Administration.

Table of Contents

List of Tables

List of Figures

CHAPTER 1
INTRODUCTION

There continues to be increasing pressure from owners, contractors, and the public to open bridge decks sooner to full traffic loads. As a result, a set of criteria or guidelines is needed to determine when concrete bridge decks can safely be opened. Today, current practice allows many bridge decks and concrete pavements to be opened to traffic once a desired compressive strength is achieved from a representative field-cast test cylinder. Though generally untrue, many believe that this strength value serves as a measure of the durability of the placed concrete.

In a collaborative research effort between Texas Department of Transportation and researchers at Texas Tech University, studies were undertaken to collect research data that could potentially lead to the development of new guidelines as to when bridge decks can be open to (a) construction traffic and (b) full traffic without sacrificing concrete durability. This report presents detailed findings of the following two research thrusts:

1. Compressive strength and maturity of seven commonly used bridge deck concrete mixes subjected to varying wet-mat curing durations.
2. Comparative assessment of the effectiveness of three different curing methods using an eighth concrete mix design that led to the development of a framework for a Strength-Durability Index (SDI).

1.1 Compressive Strength and Maturity

One of the main objectives of the testing done in this project was to compare the compressive strengths of in-situ four-inch diameter cores taken from bridge decks with predicted strengths based on (a) strength-maturity curves developed from six-inch diameter field-cast cylinders, and (b) strength-maturity curves developed from six-inch diameter lab-cast cylinders. In addition, a comparison is made between in-situ strength and the conventional cylinder strength method which is currently used to determine the cast-in-place strength. Results from these tests lead to an evaluation to establish which method (i.e., maturity method or conventional method) is more appropriate to assess in-situ compressive strength. The comparisons just described are illustrated in Figure 1.1.

The comparisons made in this report as shown in Figure 1.1 support the use of the maturity method as a means to assess the compressive strength of concrete, provided that there is little to no variation between concrete mixes used to pour concrete decks and develop strength-maturity curves. With proper curing of bridge deck slabs, it has been found that 4 days of curing is adequate to attain compressive strengths equivalent to 10 days of curing, but it is still not known if 4 days of curing is adequate for concrete durability. Also, it was discovered that there exists some issues concerning quality control during concrete placement such as adding excessive water to a concrete mix, thus changing its strength gain characteristics. All of these findings will be discussed in more detail within this report.

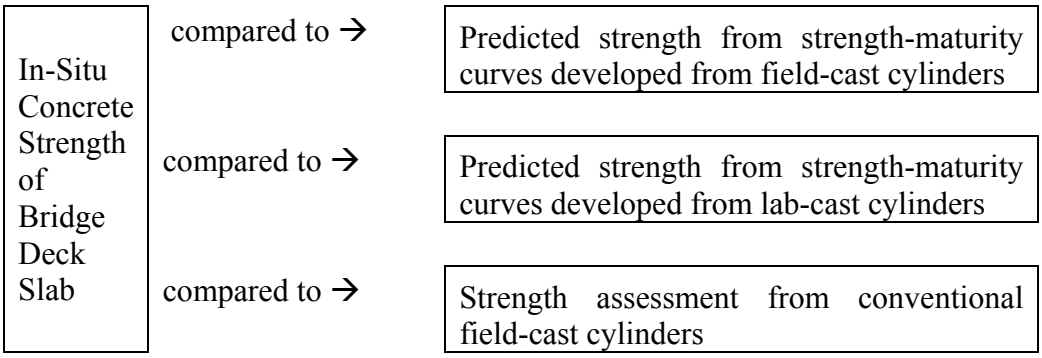

Figure 1.1 Strength Comparisons

The comparisons made in this report as shown in Figure 1.1 support the use of the maturity method as a means to assess the compressive strength of concrete, provided that there is little to no variation between concrete mixes used to pour concrete decks and develop strength-maturity curves. With proper curing of bridge deck slabs, it has been found that 4 days of curing is adequate to attain compressive strengths equivalent to 10 days of curing, but it is still not known if 4 days of curing is adequate for concrete durability. Also, it was discovered that there exists some issues concerning quality control during concrete placement such as adding excessive water to a concrete mix, thus changing its strength gain characteristics. All of these findings will be discussed in more detail within this report.

Significance of Research

Following specifications developed in 1993, the minimum requirement for wet mat curing in Texas is eight days for Type I and III cement and ten days for Type II, I/II, or mix designs with fly ash, (TxDOT, 1993). These specifications also require a minimum of 14 and 21days after termination of wet mat curing before pavements are open to ¾ ton construction traffic and full traffic load, respectively. As a result, bridge decks were open to full traffic anywhere from 29 to 31 days from the completion of the concrete pour. Special provisions to Item 420 - Concrete Structures, which were written in 1995 and adopted in 1998, allow opening the bridge deck to construction and full traffic much sooner than the 14 and 21 days required in the 1993 specifications. However, these special provisions do not reduce the wet mat curing period (TxDOT, 1998).

According to the special provisions, once the concrete is cured the minimum number of days, the pavement is allowed to dry for one day to prepare it for surface treatment. An additional day typically is needed to apply any required surface treatment. The bridge deck is then opened to full traffic only if the required compressive design strength has been gained. Thus, bridge decks can essentially be open to traffic in only 10 to 12 days from the initial pour, depending on the type of cement and if all the above criteria have been met. As a result, the current special provisions represent a significant reduction in the number of days required before bridge decks can be open to traffic.

Although, the number of days before full traffic load is allowed on bridge decks has decreased from 1993 to 1998 in Texas, there is still a desire to reduce the required curing time. The concern today is the effects shorter wet mat curing durations will have on the overall performance and durability of the concrete. By investigating different curing durations (e.g., 0, 2, 4, 8, 10, and 14 days), either (a) future updates to current specifications can be made based on results from this project or (b) the results of this research may reveal that current practice is satisfactory and no change in the specifications is necessary.

Field testing included five full-scale bridge decks that were exposed to different curing durations. The curing durations studied in this research project were for 0, 2, 4, 8, 10, and 14 days of wet mat curing (0-day curing refers to no moist curing).

Lab testing included the five mix designs used in field testing as well as two other mix designs used in the state. In the lab, strength-maturity curves were developed only for curing durations of 0, 4, and 10 days with an additional set of lab-cast cylinders that were cured for 7 days. This research focuses on compressive strength results for the 0-, 4-, and 10-day wet mat cure durations.

Since this project was very extensive and the data points are numerous, concrete mix nomenclature and cylinder testing abbreviations have been adopted to easily discuss the testing procedures. The nomenclature and abbreviations used are presented in Tables 1.1, 1.2 and 1.3. Table 1.4 displays the concrete mix constituents and quantities used for this research. All mixes used Type I or I/II cement and all used a pozzolanic material with the exception of the original Lubbock and Pharr District Mix.

Table 1.1 Concrete Mix Nomenclature

Abbreviation	Description
LBB - 1	Original Lubbock District Mix
ELP	El Paso District Mix
FTW	Fort Worth District Mix
SAT	San Antonio District Mix
HOU	Houston District Mix
PHR	Pharr District Mix
ATL	Atlanta District Mix
LBB - 2	Revised Lubbock District Mix

Table 1.2 Cylinder Type Testing and Abbreviations

Test Abbreviation	Test Description
FMAT	field-cured 6-in. diam. cylinders for strength-maturity curve development
LMAT	lab-cured 6-in. diam. cylinders for strength-maturity curve development
CONVT	field-cured 6-in. diam. cylinders for conventional in-situ strength assessment

Table 1.3 Miscellaneous Abbreviations

	Description
in-situ	cast-in-place concrete from bridge deck (usually 4" diameter cores)
N-S	Nurse-Saul – Method for calculating maturity
ARR	Arrhenius – Method for calculating maturity
LN	natural log model – Strength gain model to predict strength
FH	Freiesleben Hansen model – Strength gain model to predict strength

Table 1.4 Mix Designs

Parameter	DISTRICTS							
	LBB -1	ELP	FTW	SAT	HOU	PHR	ATL	LBB - 2
Cement Type	I/II 588 lbs	I/II 306 lbs	I/II 458 lbs	I/II 489 lbs	I/II 428 lbs	I 611 lbs	I 458 lbs	I/II 397 lbs
Mineral Admixture	none	Slag 306 lbs	Fly Ash F 131 lbs	Fly Ash C 122 lbs	Fly Ash C 157 lbs	none	Fly Ash F 128 lbs	Fly Ash F 181 lbs
Coarse Aggregate	1960 lbs	1755 lbs	1802 lbs	1823 lbs	1811 lbs	2000 lbs	1790 lbs	1854 lbs
Fine Aggregate	1133 lbs	1220 lbs	1203 lbs	1092 lbs	1088 lbs	985 lbs	1117 lbs	1174 lbs
W/C+P	0.44	0.42	0.43	0.43	0.46	0.41	0.46	0.45
Air	5%	5%	6%	6%	5%	6%	6%	6%

1.2 Comparative Assessment of Three Curing Methods

The use of concrete maturity as a non-destructive method to determine in situ strength has grown in recent years. Numerous published reports and papers reviewed by Malhotra and Carino (2004) have demonstrated this non-destructive technique to be a good indicator of compressive strength; provided, the placed concrete receives adequate curing and strict quality control is enforced at the batching plant. Although, great care may be taken to ensure adequate curing at the job site, there exists a real possibility for the degree of hydration to be less than required. It is this factor that exposes a weakness in current maturity method functions.

Current maturity functions only consider internal concrete curing temperature and concrete age to determine a maturity index, either expressed as a time-temperature factor or as an equivalent age. These maturity models do not directly consider the availability of moisture during hydration, which leads to the development of concrete properties (e.g., strength development, freeze-thaw resistance, chloride ion penetration resistance, etc.), but rather assume sufficient moisture is present during the apparent hydration of concrete.

Traditionally, concrete strength has been used as a measure to indirectly assess the durability properties of concrete. With a poor curing environment or insufficient moisture during concrete hardening/hydration, perceived maturity equivalent ages, as determined from the Arrhenius or Nurse-Saul functions, may not be indicative of the true age of the concrete and thus predict erroneous in situ strengths. This in turn could give a false sense of the developing durability properties. Therefore the maturity concept should be studied in more detail if it is to be used as a successful indicator of concrete strength and durability.

This research is a first step in determining a Strength Durability Index (SDI) that considers concrete temperature, age, and internal pore humidity. Thus, the major objective of this research was to investigate concrete pore humidity when subjected to various cure conditions. This study together with findings by other researchers in the area of concrete water diffusion help develop the framework for a better prediction tool for field-cast concrete under a variety of curing conditions.

Significance of Research

The use of the maturity method to determine in situ strength and/or strength development assumes concrete receives sufficient moisture during curing to promote hydration. This was true with the research and findings conducted by Nurse (1949) and Saul (1951) since concrete specimens were exposed to steam curing environments. Some researchers found the Nurse-Saul maturity method to be an effective tool in predicting compressive strengths while others found it not to be as reliable.

To improve on the Nurse-Saul method, researchers proposed a method which would consider the effect of curing temperature on the hydration rate of concrete. This led to the use of the Arrhenius equation to determine a maturity index expressed as an equivalent age. Experimental studies conducted with the Arrhenius maturity function proved to be better than the Nurse-Saul maturity method over a wide range of curing temperatures. Even with an improved function, the Arrhenius based maturity did not consider moisture as a parameter, but assumed it to be

satisfactory during concrete curing. Many times this assumption (having sufficient moisture) may not be the case in the field and the use of current maturity functions would not indicate proper maturity ages or compressive strengths.

Since the early maturity function has progressed to the Arrhenius function, which accounts for a temperature dependant hydration rate, the author feels further improvement to concrete maturity assessment can be made which considers moisture during concrete curing. The aim of this dissertation is to establish the framework for a relationship between internal concrete moisture, curing temperature, concrete age, and compressive strength gain. This new parameter is defined as the Strength Durability Index (SDI) of concrete. SDIs are expressed in terms of an equivalent age, similar to current maturity models. If a concrete is cured under conditions where the relative humidity is nearly 100%, then the concrete will have a SDI value similar to an equivalent age as determined by the Arrhenius function. Otherwise, if pore humidity starts to fall during concrete curing then a hydration correction age factor will be applied to the Arrhenius equivalent age to consider the slower rate of hydration. Therefore SDI values will always be equal to or less than the equivalent age as determined by the Arrhenius

Thus, SDIs would be more representative of the actual concrete maturation when considering concrete moisture and temperature histories during the curing process. Once a concrete mixture is tested under a variety of cure conditions, a reference SDI-strength curve can be developed, similar to maturity-strength curves. The author believes each concrete mixture will have a unique reference SDI-strength curve. The experimentation, process, and development are given in more detail in the dissertation.

1.3 Report Format

The format for this report is as follows:

Chapter 2 discusses the experimental set-up for the compressive strength and maturity (field-site, lab setups and testing procedures), performed by Texas Tech University researchers.

Chapter 3 provides an interpretation of the data gained from the compressive strength and maturity data.

Chapter 4 describes the experimental approach for the comparative assessment of the three curing methods. The test setup, data acquisition (e.g. concrete moisture and temperature), specimen sampling, and specimen testing are described in this chapter. This experimental setup up was conducted in a laboratory and exposed a single concrete mixture to three different cure treatments as well as varying cure durations.

Chapter 5 presents all relevant data for the comparative assessment which includes the pore humidity history for the sections under investigation. Test procedures, analysis, and findings as well as the assessment of the three moist curing methods are discussed in this chapter.

Chapter 6 discusses the framework for the establishment of the Strength-Durability Index (SDI).

Chapter 7 discusses findings, conclusions and recommendations based on the research outcomes for the compressive strength and maturity.

The appendices to this report are as follows:

Appendix A: Bridge Deck In-Situ Strength Data

Appendix B: FMAT Cylinder Strength Data

Appendix C: LMAT Cylinder Strength Data

Appendix D: CONVT Cylinder Strength Data

Appendix E: ARR Equivalent Age for Bridge Deck, FMAT, and LMAT cylinders

Appendix F: N-S Equivalent Age for Bridge Decks, FMAT, and LMAT cylinders.

CHAPTER 2
EXPERIMENTAL PLAN FOR COMPRESSIVE STRENGTH AND MATURITY

2.1 Test Approach Overview

The approach taken for this research project has been to study seven different bridge deck concrete mix designs used in seven different districts in the State of Texas. The seven mix designs tested are for the following districts: Lubbock, El Paso, Fort Worth, San Antonio, Houston, Pharr, and Atlanta.

Of these seven mix designs, five of them (LBB - 1, ELP, FTW, SAT, and HOU) were used to construct full scale bridge decks in their respective climatic region in Texas. These bridge decks were divided into six sections each. Each section received a different curing duration (e.g., 0, 2, 4, 8, 10, or 14 days). The 0-day cure section of the bridge deck slab received no moist curing, only a curing compound application. Concrete curing temperatures were monitored for each section for 28 days to determine a maturity equivalent age for each section.

Along with the bridge deck, 36 field-cured maturity (FMAT) cylinders were prepared with curing durations of 0, 4, and 10 days. The 0-day cure FMAT cylinder received no moist curing after demolding, whereas the 4- and 10-day cure FMAT cylinders were immersed in a lime bath for 3 and 9 days respectively (one day in sealed plastic molds account for one day of curing). FMAT cylinders were used to develop strength-maturity curves by monitoring concrete curing temperatures with embedded thermocouples. Maturity equivalent ages were calculated using the recorded concrete curing temperatures.

Also, 48 conventional field-cured (CONVT) cylinders were prepared at the field site. These cylinders are similar to those used in common construction practice to determine the in-situ strength of a concrete structure. CONVT cylinders were cured for durations of 0, 2, 4, 8, 10, and 14 days. These were also cured by immersing the specimens in a lime bath for the specified amount of days. CONVT cylinders were tested on days 7, 14, and 28.

As well as constructing these field sites and preparing field cast specimens, seven mix designs were tested in the lab. A total of 42 lab-cured maturity (LMAT) cylinders were prepared. Curing durations of 0, 4, 7, and 10 days were studied for the lab cast specimens. Concrete curing temperatures were monitored and maturity equivalent ages were calculated. Maturity equivalent ages and compressive data from LMAT cylinders (at 1, 3, 7, 14, and 28 days) were used to develop strength-maturity curves based on lab curing conditions.

Tables 2.1 and 2.2 illustrate the different 6-inch diameter cylinders used in this project as well as testing phases performed for each mix design. FMAT cylinders were not performed for the LBB – 1 and ELP mixes because of difficulties experienced in setting up the temperature data acquisition portion of this test. Pharr and Atlanta mixes did not have a bridge deck, thus, neither FMAT nor CONVT strength testing phases occurred for these mixes, as they were tested strictly in the lab. LMAT cylinders for LBB – 1 were not prepared or tested, because this particular mix is no longer being used. Field cured samples were prepared with the LBB – 2 mix but did not

have an accompanying bridge deck. The lab testing for LBB – 2 was performed in the Spring of 2004 but is not included in this report.

Table 2.1 Cylinder Types and Quantity

Cylinder Type	QTY.	Description
FMAT	36	field-cured cylinders used to develop strength-maturity curves
LMAT	42	lab-cured cylinders used to develop strength-maturity curves
CONVT	48	field-cured cylinders used to assess in-situ strength conventionally

Table 2.2 Testing Performed

District	Bridge Deck	FMAT	LMAT	CONVT
LBB - 1	X			X
ELP	X		X	X
FTW	X	X	X	X
SAT	X	X	X	X
HOU	X	X	X	X
PHR			X	
ATL			X	
LBB - 2		X		X

2.2. Test Setup

2.2.1 Bridge Deck Field Setup

Construction of the field test sites was designed to mimic actual TxDOT bridge design and construction procedures as closely as possible. The bridge deck field testing portion of this research involved the construction of a full scale (typically 12' x 32') bridge deck cast on site. This portion of the project proved to be challenging and the work required for completion of a site was extensive. Essentially, all bridge decks were built in a similar fashion with a few exceptions such as overall dimensions and the types of beams used. Table 2.3 details the components and dimensions of each bridge deck site constructed.

Table 2.3 Bridge Deck Descriptions

	Bridge Deck Field Site				
Component	Lubbock	El Paso	Fort Worth	San Antonio	Houston
Abutment wall height	5 ft	3 & 5 ft	4 ft	2 ft	3 ft
Beam Type	concrete	concrete	steel	steel	concrete
Bay	double	double	double	single	single
# of pre-cast panels	12	12	12	6	3
Pre-cast panel dimensions	5' x 5'	5' x 5'	5' x 5'	8' x 8'	8' x 8'
Average deck height above ground	8 ft	7 ft	7 ft	5 ft	6ft
Dimension of each bay	5’ x 12’	5’ x 12’	5’ x 12’	8’ x 10’	4’ x 10’

The few differences among the bridge decks at the field sites are discussed in this section. A double bay bridge is defined as a bridge having three beams over a span with pre-cast panels on either side of the center beam as illustrated in Figure 2.3. The single bay bridge deck has only two beams with pre-cast panels placed between them. Double bays were used on the Lubbock, El Paso, and Fort Worth District bridge decks, and single bays were used for the San Antonio and Houston District bridge decks. The construction phase, which follows, is that for a double bay bridge deck. However, the single bay bridge deck is constructed in a similar fashion.

2.2.1.1 Field Test Site (Construction Stage I) – Footings, Abutment Walls

The first phase of the field site work involved construction of the footings and of the two abutment walls. Holes for each of the two footings were typically dug 1 foot deep, 4 feet wide and 14 feet long (12 feet long for the single bays). The sides of the holes served as the formwork for the footing. Reinforcing for the footing consisted of a two layer rebar mat. To help erect the cage for the abutment walls, starter bars were installed as part of the footing. Once these tasks were performed, concrete was delivered to the site and the footings were poured, vibrated, and leveled to start the erection of the walls. The poured footings were allowed to cure and gain the necessary strength before construction commenced on the abutment walls.

The abutment wall cage was tied and secured to the starter bars to make the footing and wall act monolithically. Steel formwork was installed around the cage to provide the shape of the wall. Also to help anchor and secure the concrete beams, the top of the walls had dowel rods inserted during the pour for shear transfer and so the beams could later be accurately set into place. Bearing seat reinforcement was provided within the wall so that the beams would not shear the walls. Once all reinforcing was tied and the top of the walls was leveled to the proper height, concrete was placed in the forms in lifts to prevent the forms from failing due to the hydrostatic pressure of the concrete.

Pouring the concrete walls usually involved two lifts. After the first lift was poured, a period of about 15 minutes elapsed to allow some initial hardening of the concrete walls. After this time period the second lift was performed. After completion of the second lift, the top surface of the

wall was leveled and finished. Once the finish was applied, the top of the wall was covered to prevent moisture evaporation. Abutment walls were covered for 24 hours before coverings and forms were stripped. A completed abutment wall with the forms stripped is shown in Figure 2.1.

Figure 2.1 Abutment Wall

As listed in Table 2.3, the heights of the abutment walls varied from site to site. The bridge deck heights ranged from 5 to 8 feet. This was a result of the terrain in which the walls had to be built such as uneven ground or over creek beds. Originally, beams for the bridge deck were planned to sit on top of pre-cast blocks less than 1 foot above the ground which would yield a bridge deck height of about 4 feet. An early project change to prevent excess accumulation of humidity underneath the bridge deck resulted in the need for constructing the abutment walls and building the footings.

2.2.1.2 Field Test Site (Construction Stage II) – Bearing Strip, Panel Placement

The second construction phase involved setting the beams and pre-cast panels on top of the abutment walls. This phase required the use of a crane and typically required a second site visit for completion. As shown in Table 2.3, either concrete or steel beams were used for the bridge deck. Elastomeric bearing pads were placed on the abutment wall to help distribute the load from the beams and from the future bridge deck. As mentioned earlier, at sites with concrete beams, dowel rods were provided on the abutment walls to assure proper beam placement and to prevent slippage of the beams. For sites with steel beams, steel cross bracing was welded onto the steel beams to provide stabilization. Thus, for the steel sites, no dowels were cast into the abutment walls.

Once the beams were set in place and secured, bearing strips for the pre-cast panels were placed on the edges of the beams. Pre-cast panels were then set on the bearing strips to allow the poured concrete from the deck to flow underneath and "hug" the panel to allow composite action as shown in Figure 2.2. As the panels were being placed on the beams, three quarter inch plywood dividers were installed as shown in Figure 2.7. The five plywood dividers provided the bridge deck with 6 sections, each of which would experience a different curing period.

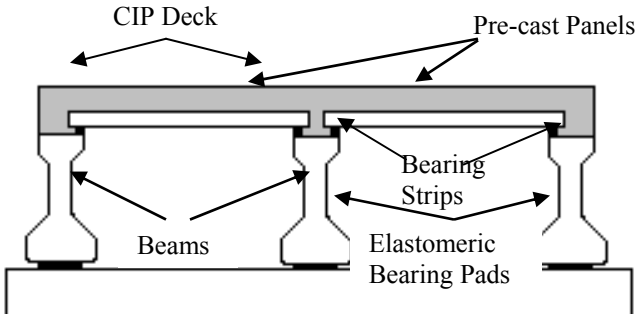

Figure 2.2 Bridge Deck Double Bay Cross-Section

Figure 2.3 Placed Concrete Beams on Abutment Walls

Figure 2.4 Placing Pre-cast Panels on Beams

Figure 2.5 Placed Pre-cast Panels on Bridge Deck (Double Bay)

2.2.1.3 Field Test Site (Construction Stage III) – CIP Deck Preparation

The third phase of site construction consisted of forming the bridge deck, tying top mat reinforcement, and setting the grade. Plywood was used as formwork around the perimeter of the deck. To provide sturdiness, half inch anchor bolts were spaced at 2-1/2 feet and used to secure the ¾ inch formwork to the side of the concrete beams when concrete beams were used. For sites with steel beams, steel angles were spaced at three feet and welded to the beams. The plywood formwork for sites with steel beams was secured to the angles with half inch bolts.

Reinforcement for the bridge was provided to mimic a real bridge deck. Reinforcement was elevated from the panels with the use of 1-inch bolster slabs (chairs). Number 4 rebar, (i.e. ½ inch diameter), spaced evenly at 9 inches center-on-center, was used for the longitudinal reinforcement. Transverse reinforcement consisted of # 5 rebar (i.e., 5/8 inch diameter) spaced at 6 inches center-on-center. Since the deck was divided into six sections, longitudinal reinforcement was not continuous throughout the entire deck; rather there were six individual rebar mats.

Once these tasks were completed, survey readings of the pre-cast panels and formwork were taken. A runoff slope of 2% was applied to the bridge deck surface by using ¾-inch chamfer strip. The chamfer strip helped the contractor finish the surface of the deck to the proper slope. Chamfer strip was placed using the survey data to ensure a 2-inch cover during the slab pour. Figures 2.9 and 2.10 show the rebar mat, formwork, dividers, and the chamfer strip.

Figure 2.6 Rebar Mat in One Section of the Bridge Deck (Double Bay)

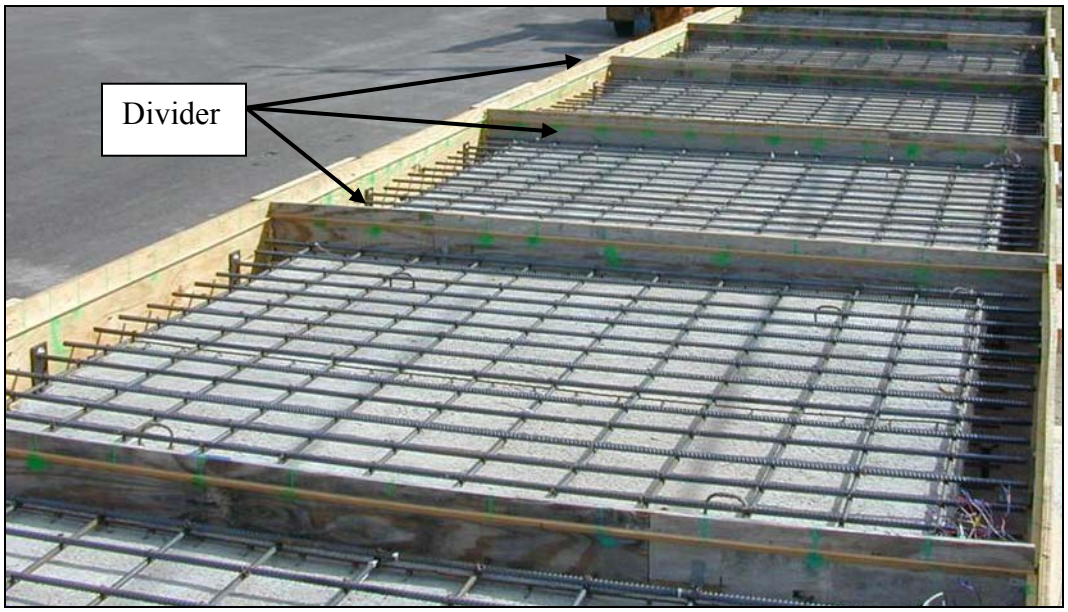

Figure 2.7 Completion of Phase 3 (Single Bay)

2.2.1.4 Field Test Site (Construction Stage IV) – Instrumentation

Phase four of site construction involved instrumentation of the bridge deck. Type "T" 22 gauge copper-constantan shielded wire was used to monitor and record the temperature of the concrete for 28 days. Shielded thermocouple wire as opposed to unshielded was necessary to minimize interference from outside noise sources. In addition, the shielding adds durability to the wires. Each of the six sections was instrumented with six thermocouples to determine an average concrete temperature in the deck slab.

Thermocouple wire was purchased in spools and thus the ends were prepared manually before temperature measurements were made. Thermocouple wire was cut to the desired length to reach data recording devices (data loggers). The shielded wire contained a tinned copper overbraid with two wires within. The ends of the two wires were stripped, twisted, and soldered together. These soldered ends were protected from corrosion by applying heat shrink tubing or brush-on electrical tape to the ends. The junction of the two different wire types, one being copper, the other copper-nickel, caused a voltage difference between the metals. This voltage difference was converted to a change in temperature by an internal program of the data logger.

Locations for temperature data were taken at the four corners of each bay, which accounted for four thermocouples, and two in the middle of the section for a total of six thermocouples per bay. Thermocouples were placed at mid-depth of the deck slab (approximately 2 to 2-1/2 inches from the top surface of the deck). Thermocouple ends were placed in the middle of the rebar grid; taking care not to let the ends touch the rebar as shown in Figure 2.8. Lead wires were secured to the outside perimeter of the reinforcement mat by plastic ties and routed to one side of the bridge deck. After the lead wires were secured and labeled, they were fed through a hole in the formwork. The path of the lead wires ran from the formwork along the underside of the bridge

deck for protection against accidental damage or vandalism. From the bridge deck, all the lead wires were buried underground until they reached an on-site shed which housed the data loggers.

The on-site instrument shed served as the data gathering station for the bridge deck as well as for the FMAT specimens. Along with concrete temperature monitoring capabilities, the instrument shed contained weather instruments to record ambient conditions such as temperature, humidity, rainfall, and wind speed for possible future analysis.

Figure 2.8 Shielded Type "T" Thermocouples

2.2.1.5 Field Test Site (Deck Pour)

Completion of phase four of the test site marked the end of the pre-testing construction activities (i.e., required activities prior to the pouring and monitoring of the bridge deck and all field test specimens). Phase five of the test site involved pouring and finishing the concrete deck. A TxDOT Class "S" concrete mix design was used for each concrete deck mix, whereas TxDOT Class "C" was used on relevant pre-testing construction activities (e.g., footings, abutment walls).

Whenever possible, a contractor from the area was hired to complete the bridge deck to help simulate actual field conditions. On several occasions, it was observed that extra water was added to the concrete mix by the contractor to increase workability. Obviously, this increased the water cement ratio and thus reduced the compressive strength of the field concrete.

Concrete was carefully placed in each section to avoid damage to the thermocouples. The concrete was vibrated, floated, and finished using practices common to the local area. In general, bridge decks had broom and/or tine finishes.

Figure 2.9 Placement of Concrete

2.2.1.6 Field Test Site (Curing)

After the bridge deck was poured, curing compound was sprayed on the surface of each section to prevent moisture loss. This process was usually done within the first half hour after the pour. Once the concrete achieved initial set, cotton mats were laid on the 2-, 4-, 8-, 10-, and 14-day cure sections of the concrete surface and wetted to provide the necessary moisture for hydration continuation. An automated system consisting of a water tank, a pump with a timer, and a series of soaker hoses was employed to maintain moisture in the cotton mats. Since periodic supervision was not possible at the field site, evaporation of moisture from the cotton mats was minimized by placing plastic sheeting on top of the cotton mats. This allowed any evaporation to condense on the plastic and fall back onto the mats and is an example of sealed curing.

Since the primary objective of this research project involves evaluation of the effects of different curing durations on the durability of concrete, cotton mats and plastic sheeting were removed according to predetermined durations. As mentioned before, the curing periods studied are 0-, 2-, 4-, 8-, 10-, and 14-day wet mat cures. Curing periods were measured and terminated based on actual calendar days irrespective of any extreme temperature fluctuations that might have occurred and not as the maturity or equivalent age of the concrete. The 0-day cure section of the bridge deck did not receive any moist curing, though curing compound was applied to its surface. After each section attained its specified curing duration, cotton mats were removed for

that section. For example after 2 days of curing, cotton mats and plastic sheeting were removed from the 2-day cure section. Similarly, after 4 days the same was done for the 4-day cure section and so forth. This process was repeated up until 14 days when curing of the bridge deck site was complete, and all curing media from the 14-day cure section was removed.

Monitoring of ambient conditions and concrete temperatures continued for 28 days. Sampling of the bridge deck for compressive strength consisted of 72 4-inch diameter cores within the first 28 days of the pour.

Figure 2.10 Freshly Poured Deck with Finish and Curing Compound

Figure 2.11 Finished Bridge Deck with Curing Media

2.2.2 Field Specimen Setup (FMAT & CONVT Cylinders)

FMAT cylinders were cast to develop strength-maturity curves. They were cured near the bridge deck to experience similar atmospheric conditions. Standard 6-inch diameter plastic molds were used to make these cylinder specimens according to ASTM C-31. For each of the five field-cured cylinder portions, a total of 90 cylinders were cast. Of these cylinders, 36 were FMAT cylinders for development of strength-maturity curves and 48 were CONVT cylinders (as indicated in Table 2.2) to determine a representative strength assessment of the bridge deck using conventional cylinder breaks. Thus, strengths from the deck and the 48 CONVT cylinders were compared based on calendar days, as opposed to considering the maturity of the deck or cylinders. Also, extra cylinders (usually 6) were prepared in the event of accidental damage to the specimens from the demolding process or improper preparation of the sample.

Field-cured cylinders were prepared according to ASTM C31 standards. Molds were filled in three layers. After each layer, concrete was rodded 25 times with a tamping rod and tapped on the sides to reduce honeycombing. Once the mold was filled, excess concrete was "struck off" from the top surface, leveled, and finished. The cylinders were then capped with lids and set aside for 24 hours until demolding was performed.

Figure 2.12 Preparing Field Cast Cylinders

For strength-maturity curve development, six of the 36 FMAT cylinders were instrumented with thermocouple wire to monitor concrete temperature. Thermocouples were inserted to mid-depth of the FMAT cylinders as recommended by ASTM C1074. Although, six different curing durations were studied for the bridge deck, strength-maturity curves were developed only for three curing durations (i.e., for 0, 4, and 10 days of curing). Each of the three curing durations had two cylinders with embedded thermocouples. Concrete curing temperature was monitored for the FMAT cylinders and the average curing temperature for each set was used to determine maturity equivalent ages. These curing periods are chosen because it is believed that they provide adequate data of the strength gain behavior of concrete.

The 0-day cure cylinders were the control group. These cylinders were evaluated to determine the effects of no curing on strength development. The 4-day cure duration was chosen since concrete pavements have been opened in as few as 4 days when using the maturity method (i.e., when the special provisions allowed by TxDOT have been followed) as was the case during the reconstruction of the North Central Expressway in Dallas (Texas Quality Initiative 1999). The North Central Expressway project required only 4 days of curing as additional specifications were closely followed. For example, among other things, tight restrictions on the source and quality of the concrete ingredients were followed.

After a 24-hour period from initial cylinder preparation, caps were removed from the field cast cylinders and demolded. Great care was taken when demolding FMAT cylinders as not to damage the thermocouple wire. The cylinders were properly labeled for tracking. The labeling on the cylinders identified when curing terminated and when testing was to be performed.

Figure 2.13 Demolded Field Cast Cylinders

Once all cylinders were properly labeled, they were put into a lime bath for curing in the field with the exception of the 0-day cure cylinders. The 0-day cure cylinders were left outside the bath after demolding with no additional covering or protection. Other cylinders were removed from the bath according to predetermined durations (2, 4, 8, 10, and 14 days). Cylinders which received 2 days of curing were removed from the bath after 2 days from the pour. The same procedure was carried out for the remaining cylinders with different curing durations.

Cylinders were then tested based on a developed schedule by the researchers of this project. CONVT cylinder breaks were performed on Day 7, 14, and 28 from the time of the initial pour. As will be discussed in the following section, FMAT cylinder testing days for strength-maturity development are 1, 3, 7, 14, and 28 days as recommended by ASTM C1074.

Since a number of factors influence the strength gain of concrete, (i.e., curing temperature, curing method, etc.), an attempt was made to expose the cylinders to the same atmospheric conditions as experienced by the bridge deck. Thus, the curing lime baths were not kept at a constant curing temperature, (i.e., 68 °F, 20 °C), but instead, were left to experience ambient temperature fluctuations.

Figure 2.14 Lime Bath and Cylinders with Embedded Thermocouples

2.2.3 Lab Cast Cylinder Setup (LMAT Cylinders)

As discussed field cast maturity (FMAT) cylinders were allowed to cure in ambient conditions. Lab cast maturity (LMAT) cylinders were also cast to serve as a control for curing conditions. By curing cylinders in the lab, temperature fluctuations were minimized due to the absence of hot or cold days experienced in the field. Also, climatic variables experienced in the field were eliminated in the lab. As a result, strength-maturity curves developed from the LMAT cylinders did not experience field curing conditions. The developed strength-maturity curves from both FMAT and LMAT cylinders are compared to determine the effect of field variables on maturity calculation. Similar to the testing approach of the FMAT cylinders, concrete temperature monitoring was performed for the 0-, 4-, and 10-day cure durations. However, an additional 7-day curing duration was added to the lab testing portion.

Of the seven mix designs presented, six have been tested in the lab. Forty-two cylinders were prepared and tested in the lab. All of the dry ingredients from each mix were brought to the lab from the local area where the mix is used. Thus, the coarse and fine aggregates used in the lab samples were from the same quarry sources as used for the bridge deck and field-cured cylinder pours. Even the same water (usually local drinking water) from the area was used for the concrete mix. All these ingredients are stored in bins and tanks at a Texas Tech research facility until they are ready to be tested.

Concrete mixed in the lab was made with a 6 cubic foot concrete mixer located in Texas Tech lab facilities. Before mixing, the individual constituents of the mix were weighed according to the size of the batch. The procedure used to mix the concrete was to (a) first moisten the basin drum of the mixer with a small amount of regular water, (b) switch on the mixer, and (c) then empty the water from the basin.

First, the coarse aggregate was added into the basin drum. Then, half of the mix water along with any chemical admixtures was added to the drum. The specified amount of fine aggregate was

then added to the mixture. With the addition of mix water as the second step in the mixing process, the surface of the coarse aggregate becomes moist and thus the fine aggregate sticks to the surface of the coarse aggregate. Cement and any mineral admixture (e.g., fly ash, slag) were then added. The rest of the mix water was then added and the constituents were allowed to mix for about 5 minutes. Once the ingredients were thoroughly mixed, a slump test was performed to confirm the design slump.

Cylinder molds for the LMAT cast specimens were identical to those used in the field. The preparation procedures were also similar, which followed ASTM C192. Cylinders were prepared by first pouring a single layer one third of the height of the cylinder. This layer was rodded 25 times with a tamping rod and the sides of the cylinder tapped to assure proper consolidation. This process was repeated two more times until the cylinder was finished. Once the entire process was complete, the cylinders were finished, capped with lids, and stored for 24 hours. After the initial 24-hour period, cylinders were demolded, labeled and put into a lime bath. Lime baths were kept at room temperature.

Figure 2.15 Slump Test

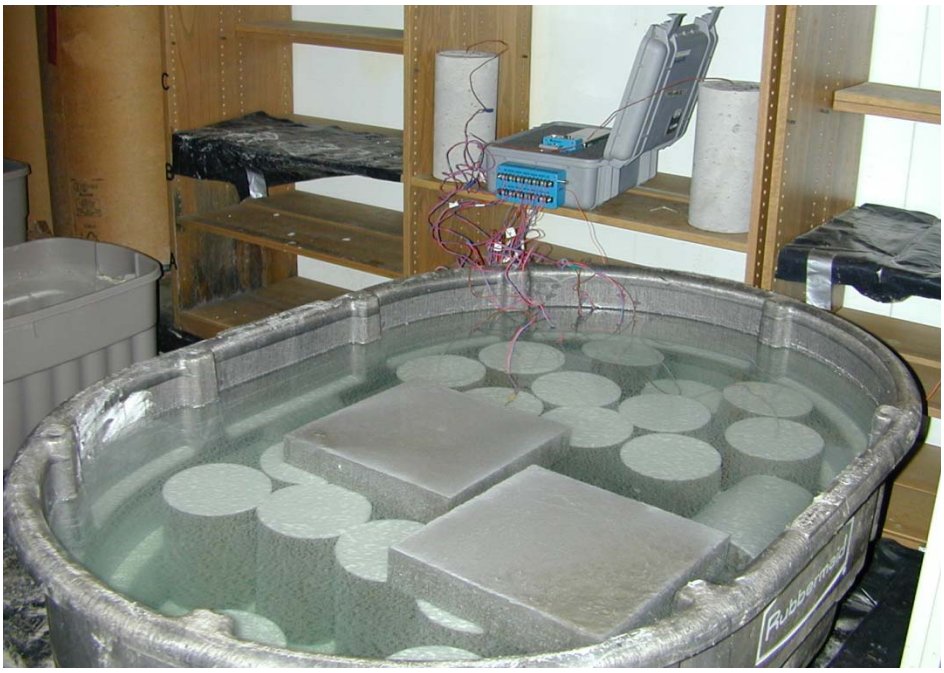

Figure 2.16 Lab Cylinders with Embedded Thermocouples in Lime Bath

A total of 45 lab-cured cylinders were prepared for each mix. For the lab portion, durations of 0, 4, 7, and 10 day cures were considered. All of the curing durations were the same as those for the field with the exception of the 7-day cure. Although the 7-day cure duration was not investigated on the bridge deck, the 7-day cure strength gain comparison with the 4- and 10-day cure cylinders was of interest and therefore added to the lab testing portion.

As discussed previously, 42 LMAT cylinders were used to develop strength-maturity curves. Thermocouples were inserted at mid-depth in eight of the cylinders. The ends of the lead wires were then connected to a data logger to record temperature data. For each curing duration, two cylinders were instrumented with thermocouples to record an average curing temperature and thus determine a maturity value.

The remaining three cylinders were used to monitor heat development with the use of calorimeter drums. These cylinders were prepared in the similar fashion as the compressive cylinders. After completion of the cylinders, they were capped, and a temperature sensor was inserted into the cylinder. Each cylinder was then lowered into a calorimeter drum with the use of a cylinder holder. The placed concrete specimen was then sealed within the calorimeter drum. Heat development and loss was monitored and used to develop a heat signature profile for that particular mix design. Data collected from the heat development of the different concrete mixes was collected for future analysis.

Figure 2.17 Calorimeter Drums and Data Logger

2.3 Sampling and Testing

2.3.1 Bridge Deck

Determining the in-situ strength of the bridge deck required taking a compressive strength sample, typically from a 4-inch diameter core sample. Cores were taken with a portable coring machine using a four inch inside diameter coring bit as shown in Figure 2.18. These coring bits were water cooled and diamond tipped to help expedite the cutting. To minimize contact with the reinforcing mat, the bridge deck surface was marked where rebar was known to be.

The coring depth for each core was approximately 4-1/2 to 5 inches (usually just below the pre-cast panel). Once the coring bit reached this depth, the bit was retracted. To remove the core, the bond between the cast-in-place concrete and the pre-cast panel was broken by gently prying the core at an angle with the use of a wedge. Once the bond was broken, the core was retracted and inspected for damage. If there appeared to be no apparent damage to the core, the sample was labeled and kept for testing.

Figure 2.18 Coring Machine

Figure 2.19 Four-Inch Concrete Core Being Retracted

Before cores could be tested, the ends of the core must be level and absent from any jagged edges. Therefore, the ends were cut with a concrete saw at the field site. Samples were then wrapped in moist paper towels and sealed in plastic bags. They were carefully packed in special foam protected carrying cases, and transported back to the Texas Tech lab via ground or air transportation.

Sampling and testing of the bridge deck occurred on Days 4, 7, 10, 14, and 28. These testing dates were set as part of the proposal for the current ongoing research. A total of 72 4-inch

diameter compressive core samples were taken over the sampling and testing period of 28 days. For each section, three cores were taken on any given sampling date to determine an average compressive strength for the curing duration being tested. Table 2.4 lists the sampling number and testing days for the 4-inch diameter cores of the bridge deck.

Table 2.4 Schedule for Bridge Deck Sampling and Testing

		Curing Duration					
		0-day	2-day	4-day	8-day	10-day	14-day
Sampling and Testing Day	4	3	3	3	-	-	-
	7	3	3	3	3	-	-
	10	3	3	3	3	3	-
	14	3	3	3	3	3	3
	28	3	3	3	3	3	3

As observed from the previous table, no cores were taken from the 8, 10, or 14 day cure section on the fourth day of sampling and testing. Cores were not taken from the above mentioned curing sections because curing mats and plastic sheeting still covered these sections. Data gathered from the 4-day cure sample would be used as a representative compressive strength for the 8, 10, and 14-day cure sections for that particular day. The same scenario applied for testing Day 7 for the 10 and 14-day cure section and testing Day 10 for the 14-day cure sections of the bridge deck.

Once the bridge deck core samples were received in the lab, they were unpacked and prepared for testing. The height for each core was measured and recorded. Differences in core height were due to sample preparation by different researchers and core heights ranged anywhere from 4 – 4 ½ inches. Height measurements were necessary to apply a height to diameter correction factor on the compressive strength value obtained from the test for each core to make the strength comparable to a 6-inch diameter cylinder according, to Section 25 of Tex-424-A (TxDOT 1999). A condensed form of the correction factors is listed in Table 2.5.

Table 2.5 Concrete Core Correction Factors

H/D	Factor	H/D	Factor	H/D	Factor
1.00	0.870	1.35	0.942	1.70	0.976
1.05	0.882	1.40	0.948	1.75	0.980
1.10	0.894	1.45	0.954	1.80	0.984
1.15	0.906	1.50	0.960	1.85	0.988
1.20	0.918	1.55	0.964	1.90	0.992
1.25	0.930	1.60	0.968	1.95	1.000
1.30	0.936	1.65	0.972	2.00	1.000

After the heights were recorded, the cores were prepared for testing by applying steel caps with neoprene inserts. Cores were tested at a pressure loading rate between 20 to 50 psi per second as suggested by ASTM C42. The target pressure loading rate was the median value which is 35 psi per second. The pressure loading increase was continued until failure occurred in the specimen. The compressive strength recorded for a particular set was taken to be the average of the three core specimens in the set. These compressive strengths were then compared to predicted strengths from developed FMAT and LMAT strength-maturity curves, as well as the strength from a CONVT cylinder break.

The testing apparatus for compression testing is a hydraulic powered machine, having a load bearing capacity of 500 kips. The compression machine consists of two units, one being the actual compression unit with the testing hydraulic piston and the other being a stand alone LCD display unit. The LCD unit controls the loading rate, displays strength readouts, and houses the hydraulic pump. Calibration for the compression machine is performed once a year.

2.3.2 Field Cylinder (FMAT & CONVT Cylinders)

Field cylinder testing consisted of two types of cylinders, FMAT cylinders and CONVT strength cylinders. FMAT cylinders were samples used to develop strength-maturity curves whose temperatures were monitored over a 28-day period. CONVT strength cylinders were samples that were cured along with the field cast concrete. Strength assessment of the cast-in place concrete was based on the CONVT cylinders, irrespective of time, and on the curing temperature history of the concrete.

Testing of FMAT maturity cylinders was done by a local testing lab. This approach was taken as it was soon realized that numerous trips to the field site, either using ground or air transportation, were needed to transport samples back to the lab. Air transportation was not a viable option due to the numerous (and heavy) concrete cylinders (i.e., 18 6-inch diameter cylinders at one time), and the weight restrictions imposed by the airlines. Driving would also require many consecutive trips to the site within the first seven days. Therefore it was decided it would be most beneficial if the testing was performed by a local testing lab.

The local testing labs were certified and had previously provided testing services on TxDOT projects. Technicians from the local lab picked up cylinders from the field on specified days. These technicians knew when and how many cylinders to pick up as they were provided a testing schedule similar to that shown in Table 2.6. They were also provided with a list of the labeled cylinders which were to be picked up on the given testing days. Cylinders were transported to the local lab and tested. Data from the compressive strength results were mailed to Texas Tech, where results were recorded to a database and linked to their respective maturity values using either the Arrhenius or Nurse-Saul Equivalent Age functions.

As discussed, only the 0-, 4-, and 10-day curing durations were chosen to develop strength-maturity curves. Compression tests were performed on days 1, 3, 7, 14, and 28 days as suggested by ASTM C1074. Strength-maturity curves were then developed based on compression data for each curing period and linked with respective maturity values. On Day 1 of testing, only three cylinders were tested, all of which were from the 0-day cure cylinders. Since all the cylinders were sealed and kept in their molds for the first 24 hours, the 4- and 10-

day cure cylinders experienced the same amount of curing as the 0-day curing cylinders. Therefore, the average compressive strength for the 0-day cure cylinder on Day 1 represents the first compressive strength data point for all curing durations for development of the strength-maturity curves.

Table 2.6 FMAT Cylinder Testing Schedule

		Curing Duration		
		0-day	4-day	10-day
Testing Day	1	3	-	-
	3	3	3	-
	7	3	3	3
	14	3	3	3
	28	3*	3*	3*

* 2 of 3 cylinders with embedded thermocouples

CONVT strength cylinders were transported back to the Texas Tech lab as opposed to having them tested by a local testing lab. It was decided that transportation of these cylinders back to Lubbock was reasonable due to mandatory visits to the field site on days 7, 14, and 28, which also correspond to testing days of the conventional cylinders as listed in Table 2.7. The mandatory visits were due to coring of the bridge deck on the days listed in Table 2.4.

When transporting CONVT strength cylinders back to Lubbock, they were covered with wet cotton mats. Once in the lab, cylinders were inspected for any damage and prepared for testing. These cylinders were capped with steel plates with neoprene inserts and loaded into a compression machine for testing. CONVT cylinders were tested according to ASTM C39 with the exception of continually keeping cylinders moist after removal from the lime bath. CONVT cylinders were not kept moist because the effects of different curing durations on strength gain were being investigated. Testing was performed with a pressure loading rate range of 20 to 50 psi per second. Again, the target pressure loading rate was 35 psi per second. CONVT cylinders were tested until failure and the strength was recorded to a database.

Table 2.7 CONVT Strength Cylinder Testing Schedule

		Curing Duration					
		0-day	2-day	4-day	8-day	10-day	14-day
Testing Day	7	3	3	3	3	-	-
	14	3	3	3	3	3	3
	28	3	3	3	3	3	3

2.3.3 Lab Cast Cylinder (LMAT Cylinders)

LMAT cylinder testing was done in a similar manner as for the FMAT cylinders. LMAT cylinders were batched and prepared according to ASTM C192, and cured in laboratory facilities. Lab cylinders were cured for Days 0, 4, 7, and 10. Testing of the 42 LMAT cylinders were tested on days as specified in Table 2.8.

LMAT cylinders were tested in accordance with ASTM C39. Maturity values for the LMAT cylinders were determined from the Arrhenius and Nurse-Saul Equations. Compressive strengths for each curing duration and testing day were linked with its corresponding maturity values. Strength-maturity curves were developed based on the FH and natural log strength gain models.

Table 2.8 Testing of LMAT Cylinders

		Curing Duration			
		0-day	4-day	7-day	10-day
Testing Day	1	3	-	-	-
	3	3	3	-	-
	7	3	3	3	-
	14	3	3	3	3
	28	3*	3*	3*	3*

* 2 of 3 cylinders with embedded thermocouples

Monitoring adiabatic heat generation of concrete mixes was another portion of the lab testing. Cylinders were placed in calorimeter drums and heat generation profiles (i.e., heat signature curves), were developed with the use of the Quadrel® software (DSS 2000). Data gained from the heat signature curves for each concrete mix will be used for future analysis.

2.4 Expected Results for Test Setup

Results gained from the testing procedures discussed in this chapter are presented in Chapter 3. Results include development of strength-maturity curves for FMAT and LMAT cylinders using both Nurse-Saul and Arrhenius Equivalent Age functions. The following strength-maturity curves can be generated for any given mix:

- FMAT strength-maturity curves developed with Arrhenius function
- FMAT strength-maturity curves developed with Nurse-Saul function
- LMAT strength-maturity curves developed with Arrhenius function
- LMAT strength-maturity curves developed with Nurse-Saul function

The predicted strengths from the above mentioned strength-maturity curves and CONVT cylinder strength breaks are compared to in-situ strengths. Results presented in Chapter 3 are further discussed in Chapter 7.

CHAPTER 3
RESULTS AND ANALYSIS OF COMPRESSIVE STRENGTH AND MATURITY DATA

As an attempt to determine the reliability of the maturity method, strength-maturity curves were developed from both FMAT and LMAT cylinders using both the Arrhenius and Nurse-Saul functions. In order to accomplish this task, several steps were taken. These included (a) monitoring concrete temperatures for bridge decks and FMAT and LMAT cylinders, (b) computing maturity equivalent ages using the Arrhenius and Nurse-Saul functions for bridge decks, FMAT, and LMAT cylinders, (c) developing strength-maturity curves from FMAT and LMAT cylinders, (d) comparing predicted strength values from developed strength-maturity curves to the in-situ strength, and (e) comparing maturity equivalent ages and strengths from field-cured conditions to lab-cured conditions. Also, to help verify the reliability of the maturity method, strengths for the bridge deck were compared to CONVT cylinders (i.e. strengths based on calendar days, which is the common practice for determining in-situ concrete strengths).

3.1 Temperature Histories

3.1.1 Bridge Deck

The curing temperature of the concrete deck was monitored and recorded by data loggers for 28 days. This was done to compare the temperature curing histories between different curing durations and determine the maturity based on an equivalent age. Equivalent ages are computed using the temperature history of the deck along with the maturity equations mentioned in the literature review of the previously submitted report.

Concrete curing bridge deck temperature histories for the LBB – 1, ELP, FTW, SAT, and HOU districts are shown in Figures 3.1 through 3.5 Although, the curing temperature was monitored for 28 days, only the first 450 hours (almost 19 days) are displayed in the figures. For each graph, bridge deck curing temperatures are shown for the 0-, 2-, 4-, 8-, 10-, and 14-Day cure durations along with the ambient temperature history with the exception of the Houston Bridge Deck. Bridge deck curing temperatures for the 0-, 2-, 4-, and 8-day curing sections of the Houston bridge deck were unavailable due to problems with the data logger used to monitor these sections, as well as the ambient temperature history.

From Figures 3.1 through 3.5, temperature rise ranging from 10 to 20 °F (due to heat of hydration) was experienced by the slabs the first 24 hours when compared to the ambient temperature. After the first 24 hours, it is observed that while the curing media remained on the surface of the slabs, the concrete curing temperature fluctuations were usually minimized. Once sections had the curing media removed, the concrete temperature closely followed the ambient temperature. If one studies the temperature history plots carefully, one can determine when the curing media was removed for a given curing duration. This is apparent in Figures 3.1 and 3.2. The bridge deck curing histories for FTW, SAT, and HOU do not clearly display the different in curing temperature but are better illustrated in the curing histories of the FMAT cylinders.

The bridge deck slab curing temperatures for each site are given in the following table.

Table 3.1 Bridge Deck Maximum and Minimum Curing Temperatures

District	Max. Temp. (first 24 hrs)	Max. Temp. (first 19 days)	Min. Temp. (first 19 days)
LBB – 1	107 °F	120 °F	54 °F
ELP	118 °F	118 °F	74 °F
FTW	115 °F	115 °F	42 °F
SAT	124 °F	124 °F	75 °F
HOU	101 °F	105 °F	65 °F

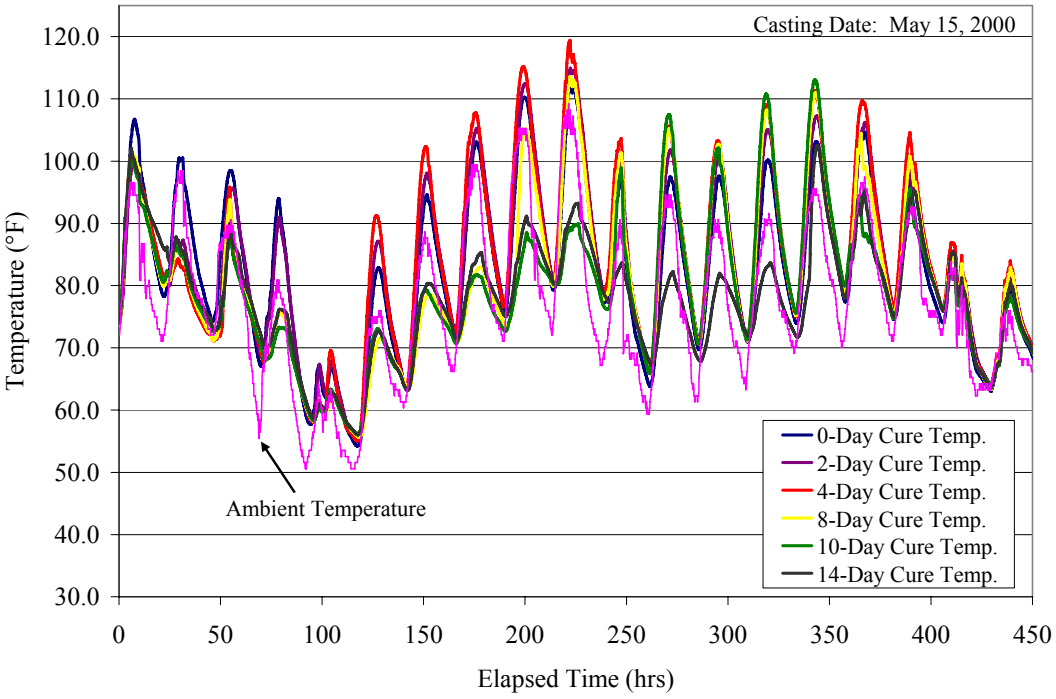

Figure 3.1 LBB -1 Bridge Deck Temperature History

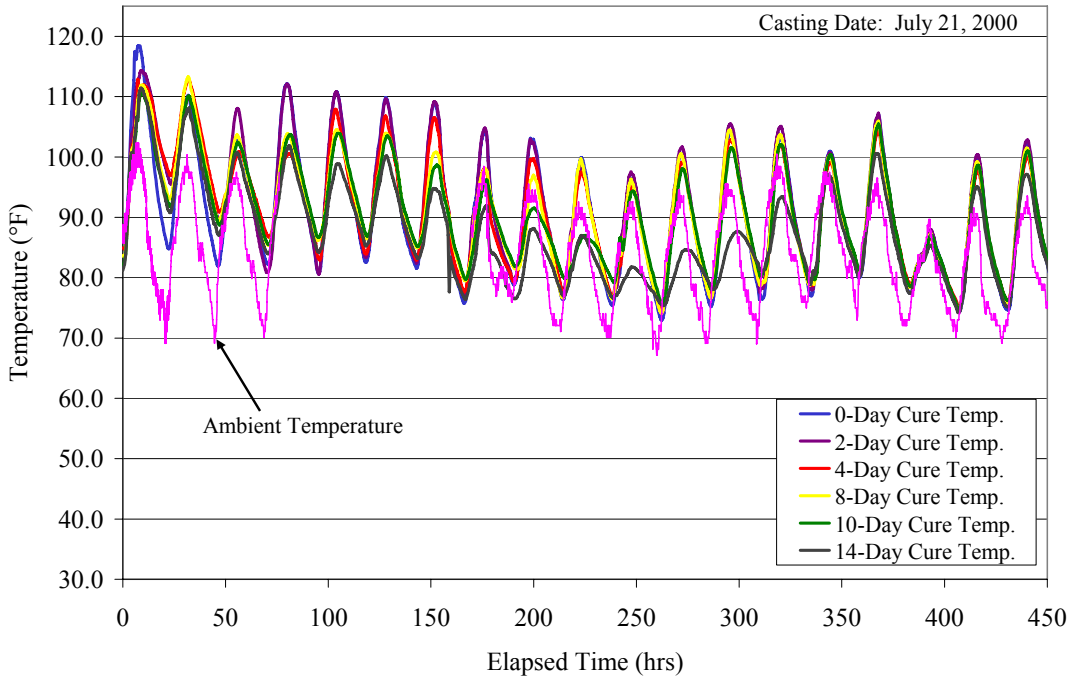

Figure 3.2 ELP Bridge Deck Temperature History

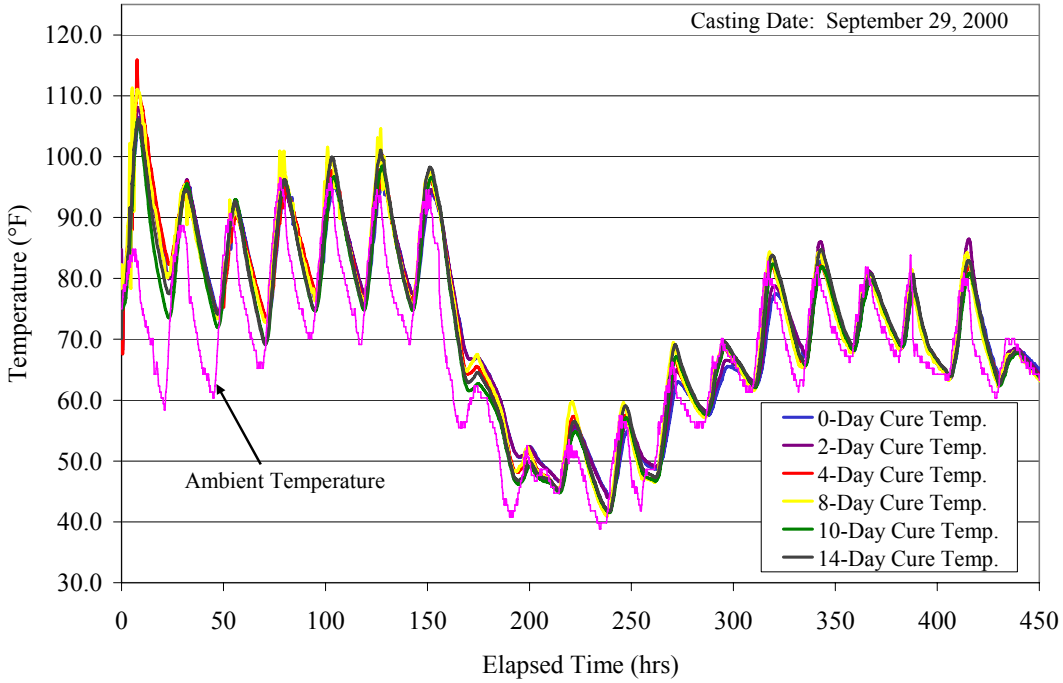

Figure 3.3 FTW Bridge Deck Temperature History

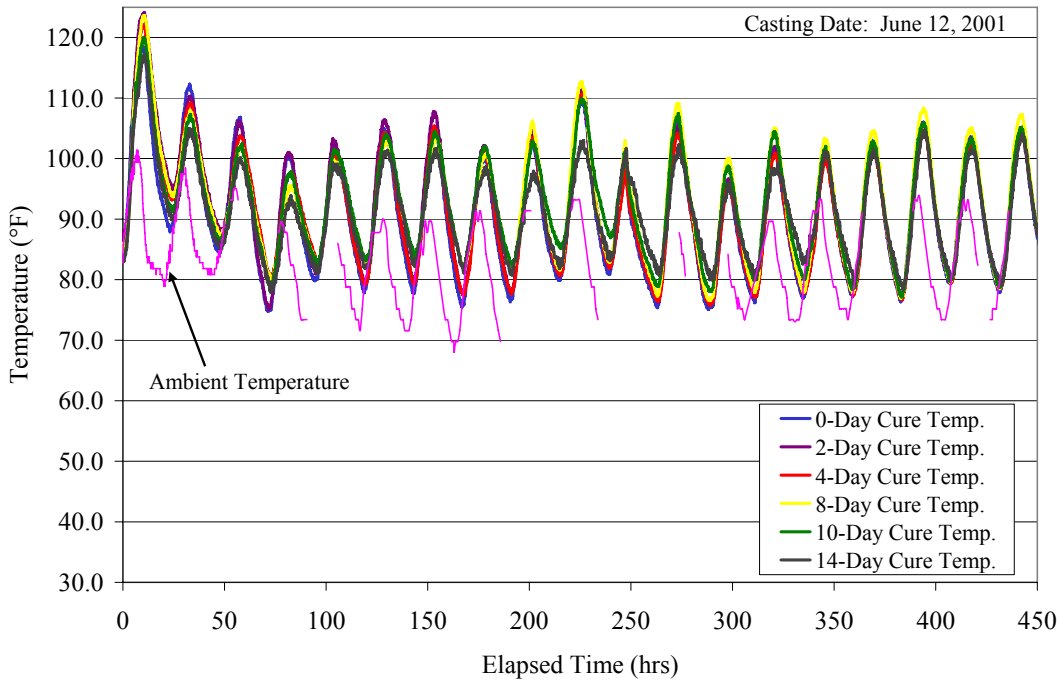

Figure 3.4 SAT Bridge Deck Temperature History

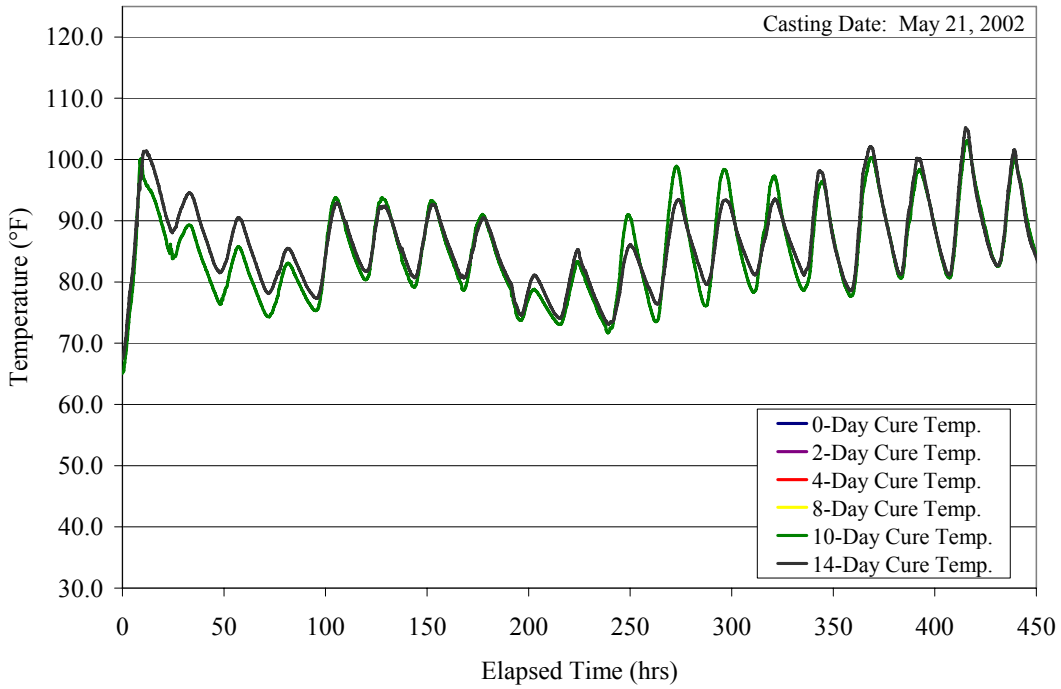

Figure 3.5 HOU Bridge Deck Temperature History

3.1.2 FMAT Cylinders

Concrete curing temperatures for the FMAT cylinders were monitored by embedding thermocouples in two cylinders for each of the curing durations (i.e., 0, 4, 10 days). The average curing temperature for the two cylinder set is used to develop the curing temperature history and used to compute the maturity values for the FMAT cylinders. FMAT cylinder curing temperature histories for FTW, SAT, HOU, and LBB-2 are shown in Figures 25 through 28. Comparing the peak temperatures for the first 24 hours for the bridge deck and FMAT cylinders show that the same temperature rise is experienced. However, after the first 24 hours most FMAT cylinder temperatures do not follow the same trend as the bridge deck temperatures. Only the 0-day cure cylinders follow approximately the same curing temperature as the bridge deck. These trends are accounted for since the 0-day cure FMAT cylinders were exposed to ambient conditions soon after demolding (24 hours), and the 4 and 10-day cure FMAT cylinders were immersed in a lime bath.

The 4- and 10-day cure cylinders maintain a less fluctuating temperature. This is attributed to the lime bath in which the cylinders are placed. Even though the lime baths are not temperature controlled, the water in the baths require sufficient heat energy and time to adjust to ambient temperatures, thus a more constant curing temperature results. It is only when FMAT cylinders are removed from the lime bath that curing temperature fluctuates with the extremes of the ambient temperature. The 4-day cure cylinders experience lime bath temperatures until approximately 100 hours after the pour. At this time the 4-day cure FMAT cylinders are removed from the bath and exposed to ambient conditions. The same is also true for the 10-day cure FMAT cylinders at approximately the 250 hour mark. After this time, all FMAT cylinders experienced ambient curing temperatures.

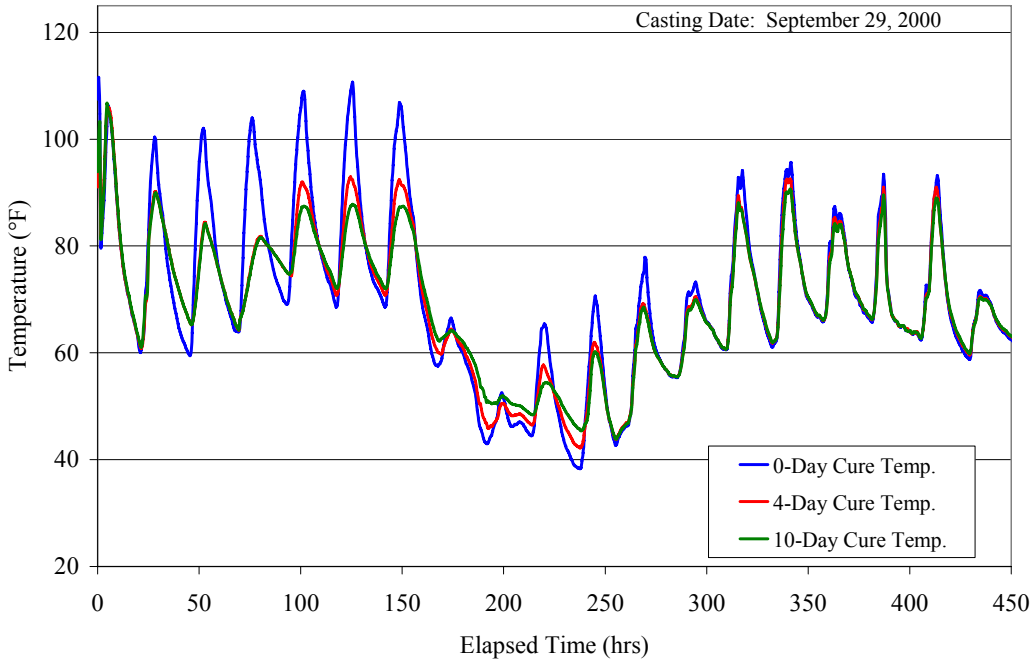

Figure 3.6 FTW FMAT Temperature History

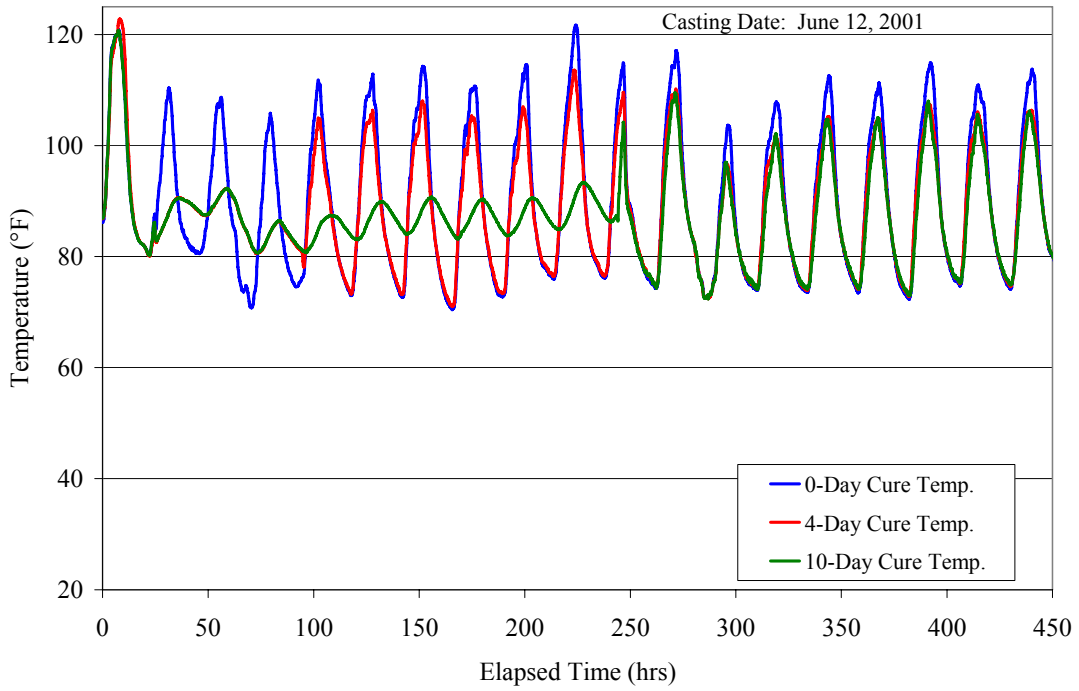

Figure 3.7 SAT FMAT Temperature History

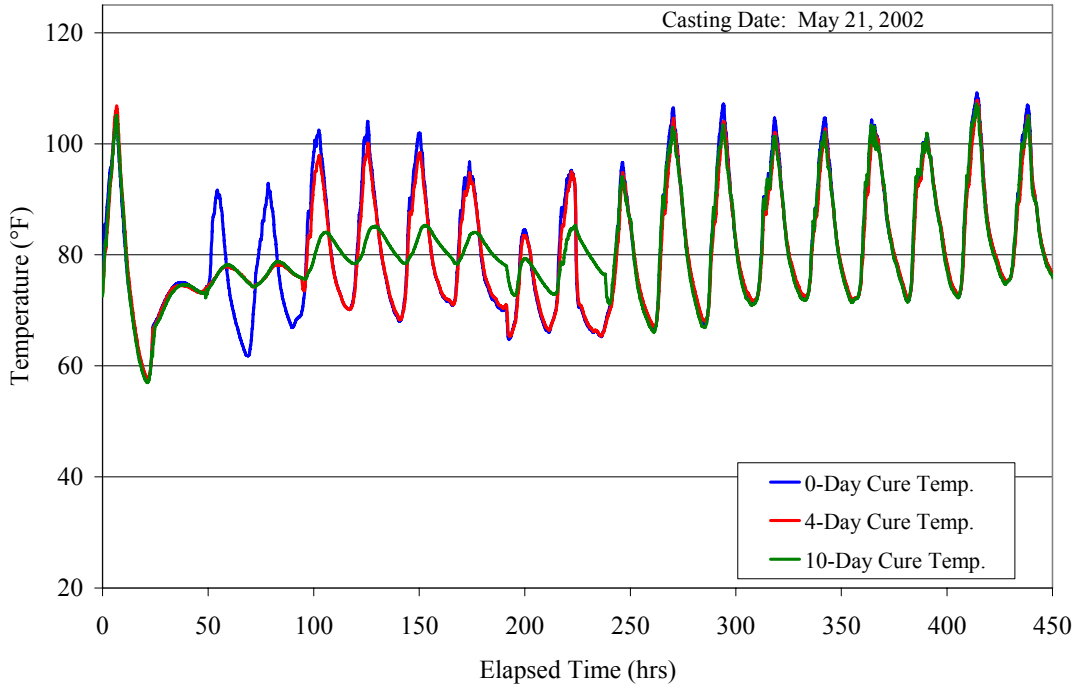

Figure 3.8 HOU FMAT Temperature History

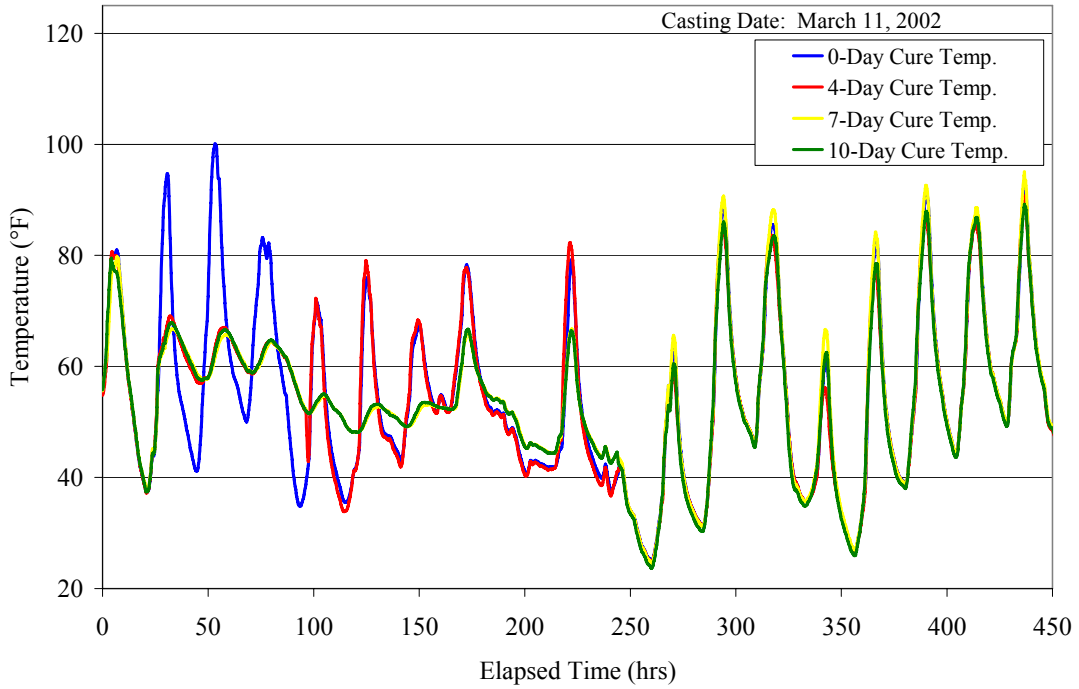

Figure 3.9 LBB – 2 FMAT Temperature History

3.1.3 LMAT Cylinders

Another portion of testing involved the generation of strength-maturity curves from LMAT cylinders. These developed curves were then used to see how well strengths could be predicted for the bridge deck. Three of the concrete mixes used in the field site have been tested. These include concrete mixes for the Fort Worth, San Antonio, and El Paso districts.

The process for developing lab maturity curves was performed in the same manner as for the FMAT cylinders. Curing concrete temperatures for the cylinders were monitored by thermocouples and recorded by data-loggers. Temperature histories for the LMAT cylinders were then utilized to determine maturity equivalent ages using both the Arrhenius and Nurse-Saul Equivalent Age functions for days when cylinder testing was performed. Cylinder breaks were performed on Days 1, 3, 7, 14, and 28 as recommended by ASTM C1074-93. The scheduled testing and number of cylinder breaks are shown in Table 3.8.

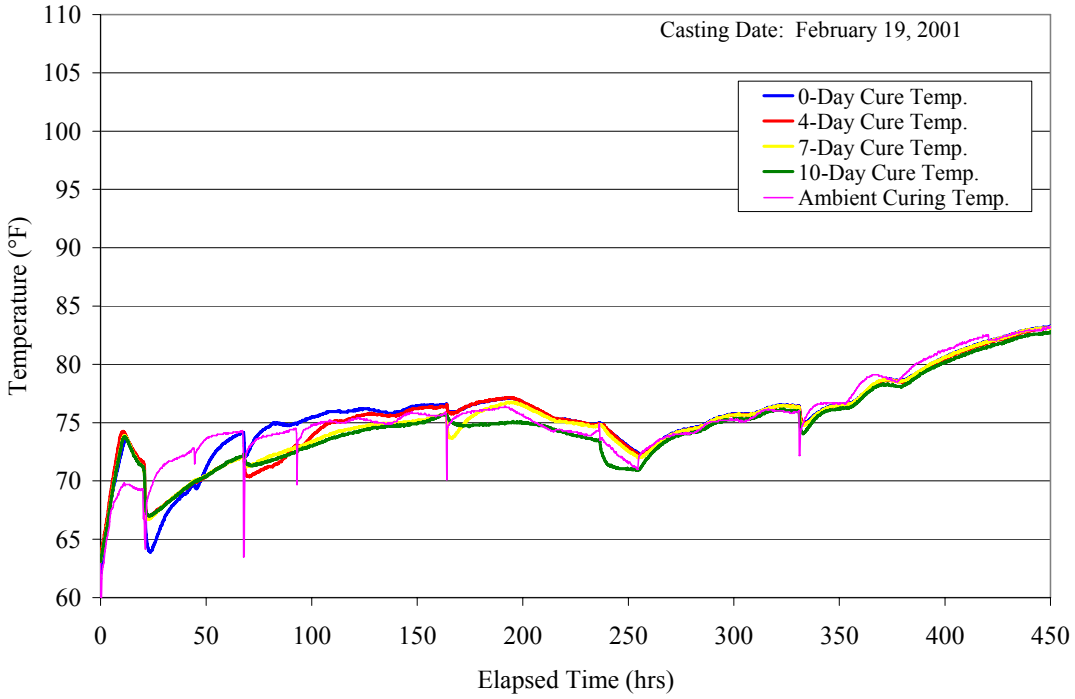

Figure 3.10 ELP LMAT Temperature History

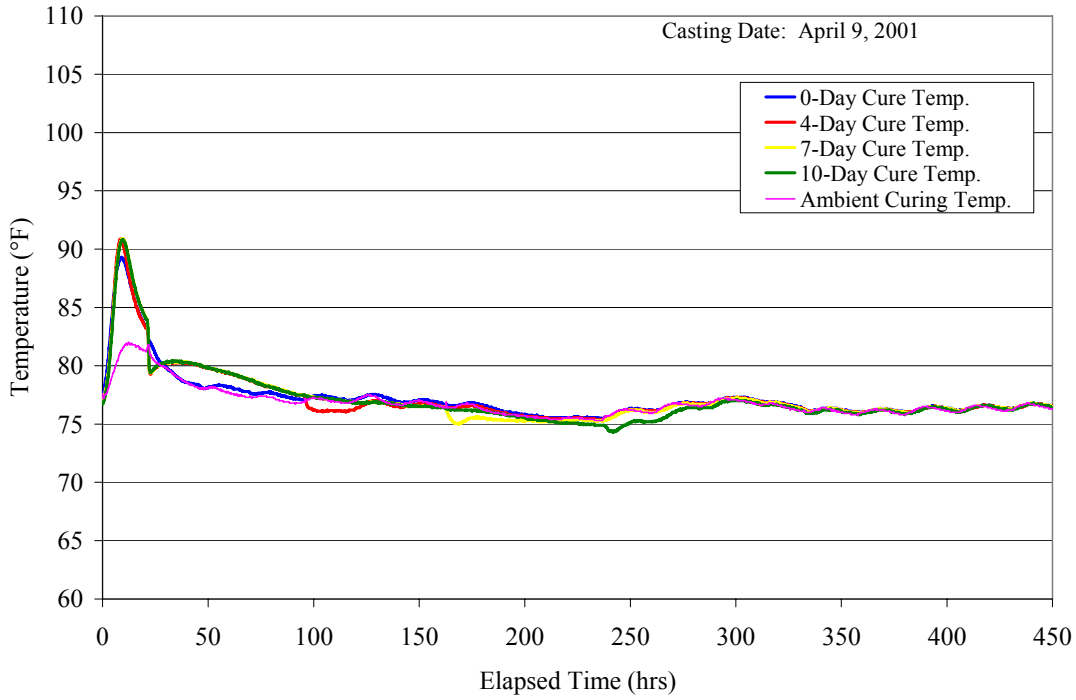

Figure 3.11 FTW LMAT Temperature History

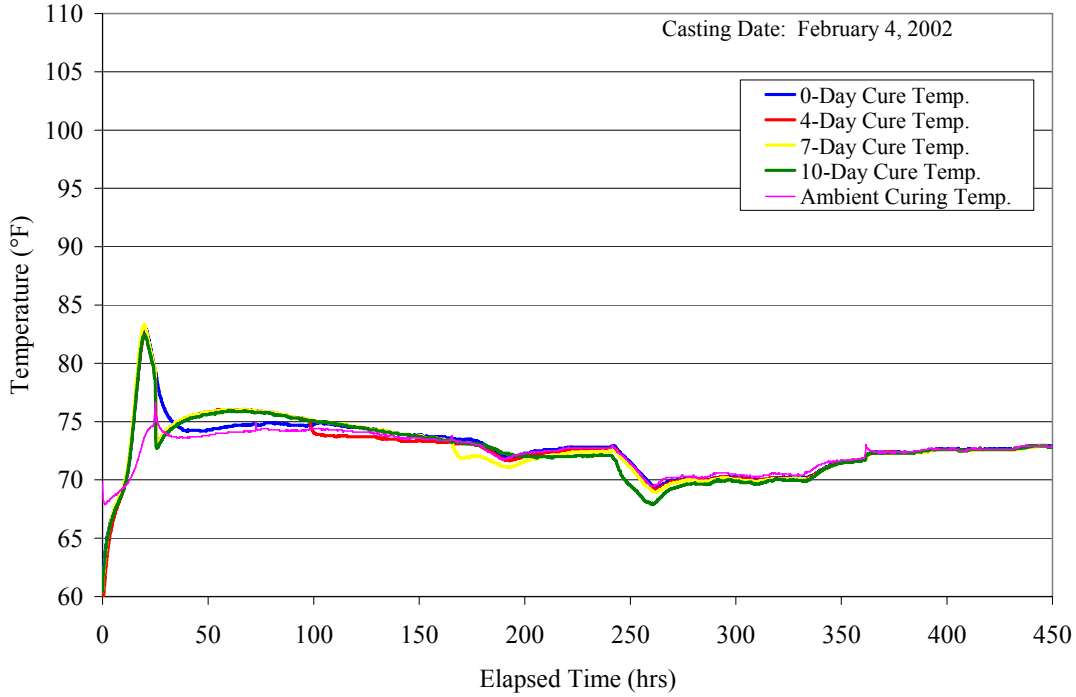

Figure 3.12 SAT LMAT Temperature History

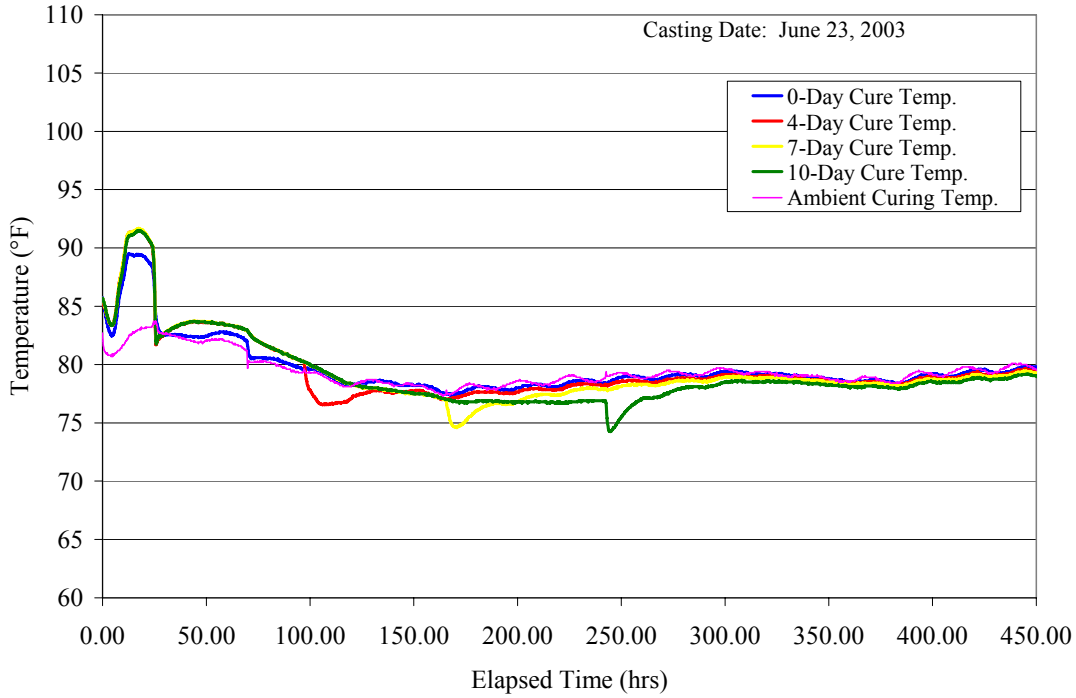

Figure 3.13 HOU LMAT Temperature History

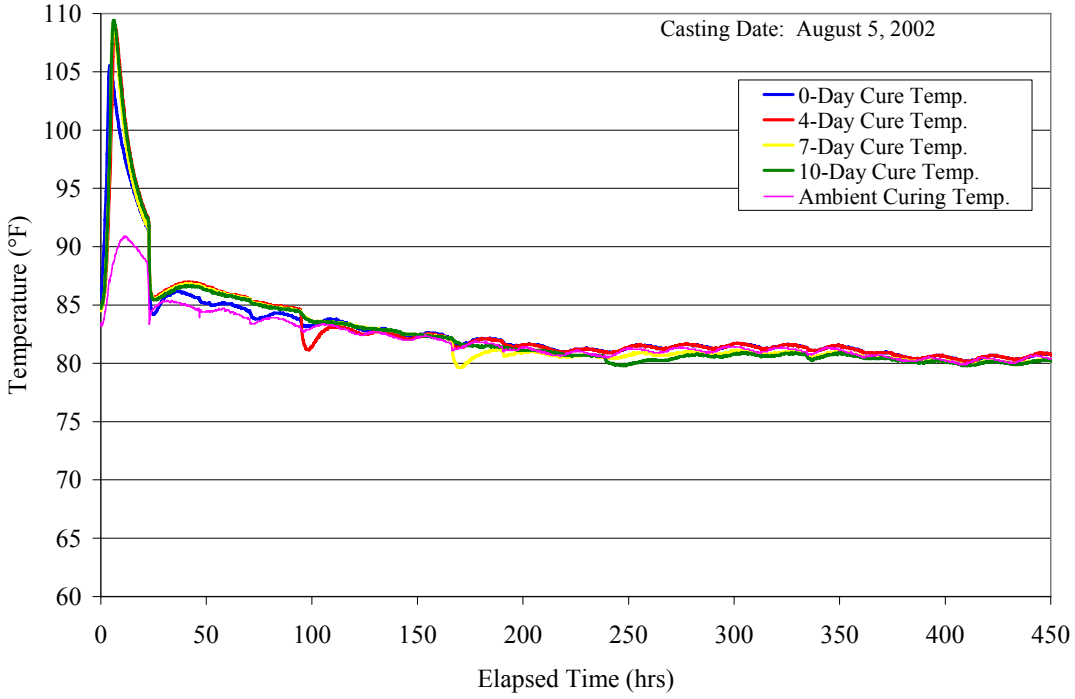

Figure 3.14 PHR LMAT Temperature History

3.2 Compressive Strength Developed and Strength-Maturity Curves

3.2.1 Bridge Deck Strength Gain Curves

As seen in Table 2.4, sampling and testing of bridge deck cores occurred on Days 4, 7, 10, 14, and 28. For each set of four-inch diameter core breaks, two maturity values were calculated, one from the Arrhenius function, the other from the Nurse-Saul Function. These maturity values are used later in this report to compare the strengths from the strength-maturity curves developed from the FMAT and LMAT cylinders.

In-situ strengths for the bridge decks with their different curing durations are plotted in Figures 3.15 through 3.19. These figures are plotted based on the average compressive strength for a set of cores for any given testing day. A natural log best fit curve is displayed for each set of data to observe strength gain characteristics.

Curing durations of four days or more yielded very similar strength gain characteristics. It is clearly seen that no days of moist curing greatly affects the strength gain characteristics and ultimate strength of the slab when compared to slabs which received some duration of curing. The exception to this observation is for the Houston 0-Day cure slab. The strength gain for this section was far greater than the sections receiving moist curing. This strength gain is attributed

to the difference in the amount of mix water used for this section (i.e. less mix water was used for the 0-Day section and more was used for the other sections).

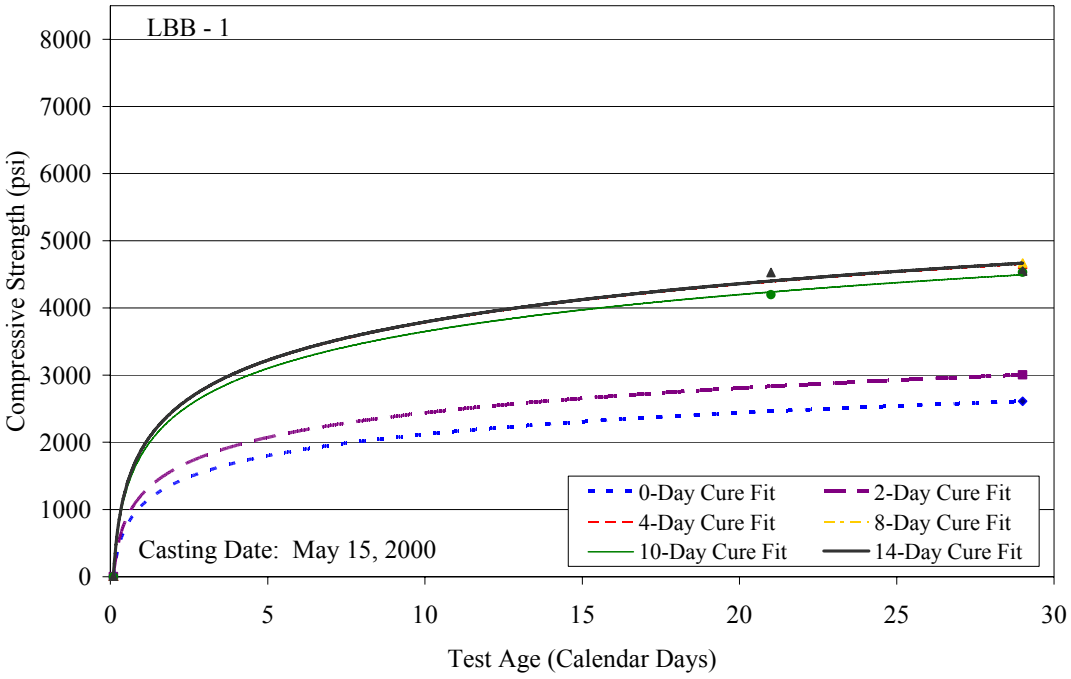

Figure 3.15 LBB – 1 Bridge Deck Compressive Strength Development

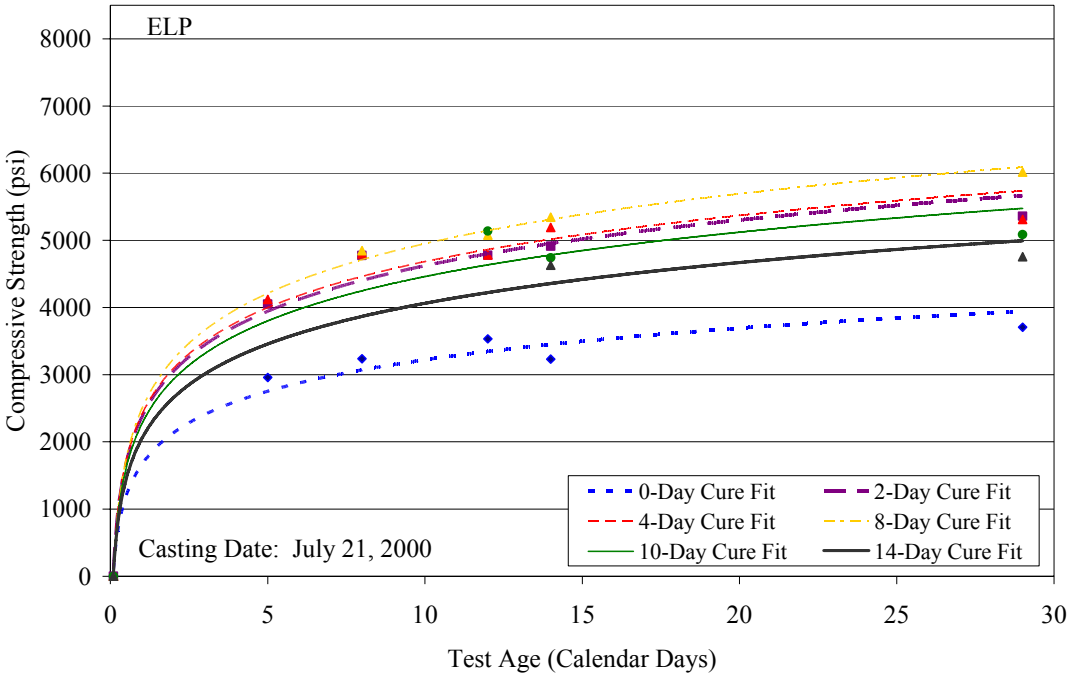

Figure 3.16 ELP Bridge Deck Compressive Strength Development

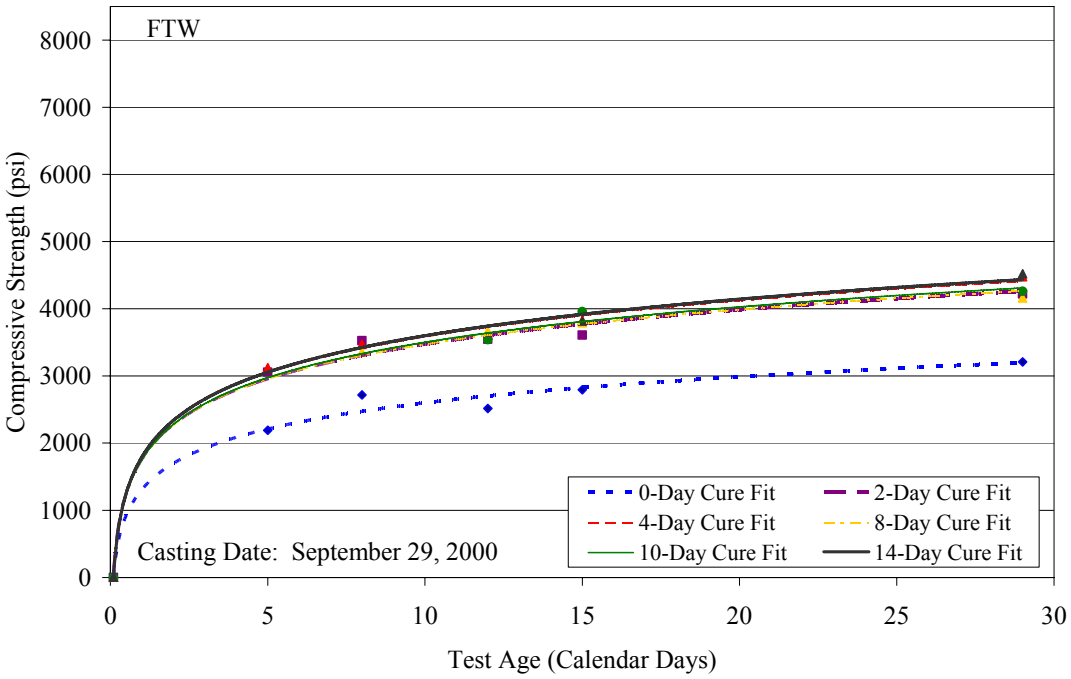

Figure 3.17 FTW Bridge Deck Compressive Strength Development

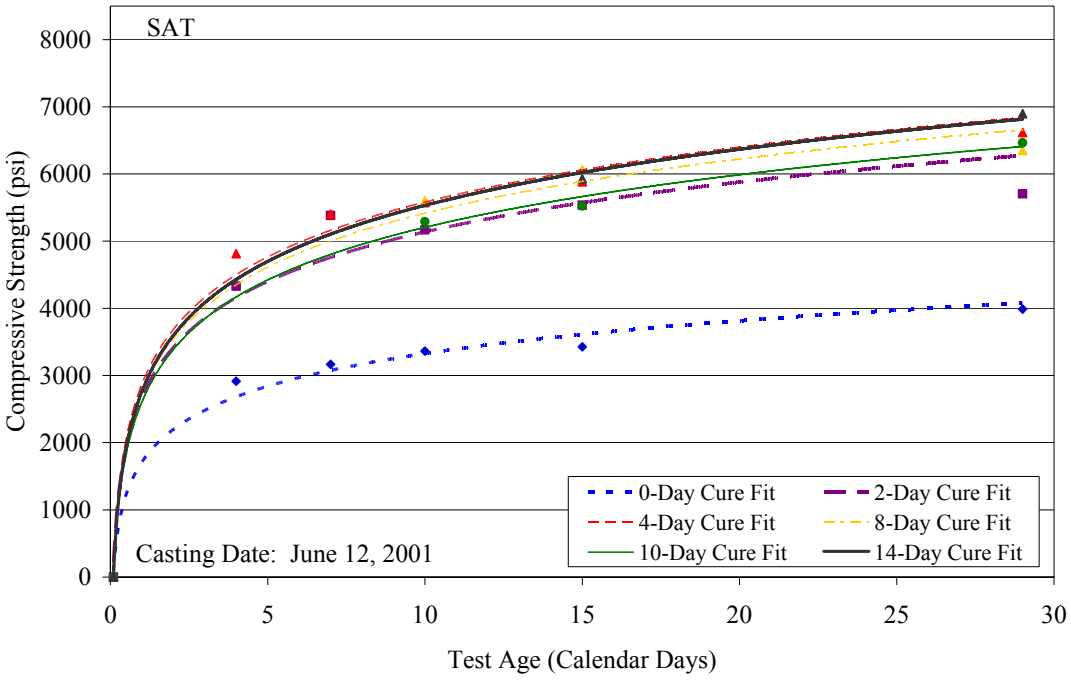

Figure 3.18 SAT Bridge Deck Compressive Strength Development

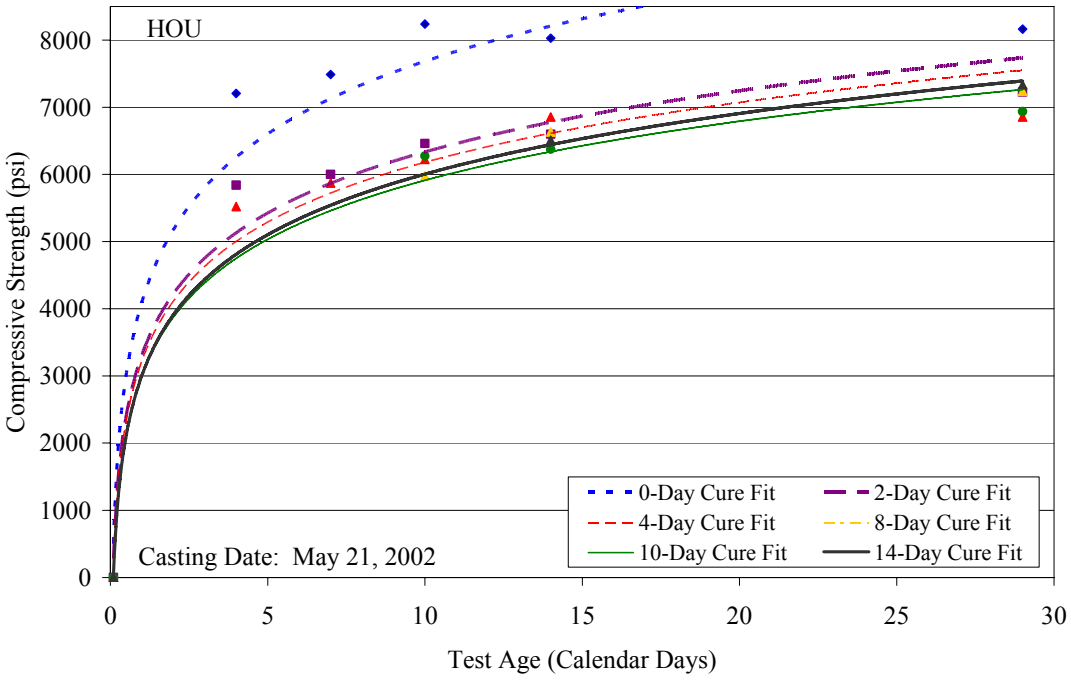

Figure 3.19 HOU Bridge Deck Compressive Strength Development

3.2.2 FMAT Cylinder Strength-Maturity Curves

Development of strength-maturity curves involves the temperature histories of the FMAT cylinders discussed in the previous section along with their corresponding compressive strengths performed on Days 1, 3, 7, 14, and 28. Strength-maturity relationships were developed using both the Arrhenius and Nurse-Saul equivalent age functions. The following sections (a) discuss the development of these curves using the respective strength gain model for each maturity function as well as (b) provide the constants required for the curve of best fit.

3.2.2.1 FMAT Arrhenius Maturity Curves

Temperature data collected by the data loggers was uploaded to a server maintained by Digital Site Systems, Inc. (DSS) of Pittsburgh, Pennsylvania. The software developed by (DSS) is called Quadrel®. Quadrel® uses temperature data to compute an equivalent age based on the Arrhenius function. Compressive strengths and equivalent ages for Days 1, 3, 7, 14, and 28, as suggested by ASTM C1074, are entered in the server to develop strength-maturity curves. A best-fit curve is generated by Quadrel® based on the Freiesleben Hansen (FH) strength gain model (i.e., Equation 3.1). For each curing duration, coefficients for the best-fit curves are listed in Table 3.2, and Figures 3.20 through 3.23 illustrate the developed strength-maturity curves.

$$S(t_{ea}) = S_{\inf} e^{-\left(\frac{\tau}{t_{ea}}\right)^{\alpha}} \qquad \text{[Equation 3.1]}$$

where
$S(t_{ea})$ = compressive strength as a function of equivalent time (t_{ea})
S_{inf} = final value of strength S
τ = strength time constant
t_{ea} = Arrhenius equivalent age at the reference temperature.

S_{inf} is the asymptotic value of concrete strength associated with an infinite equivalent age.

The strength time constant, τ, is the maximum equivalent age value of the differential of compressive strength (S) with respect to the log of t_{ea} as shown in Equation 3.2.

$$\tau = \max\left[\frac{dS}{d\log(t_{ea})}\right] \qquad \text{[Equation 3.2]}$$

The strength curvature factor, α, is the rate of strength development. The strength time constant, τ, is the maximum equivalent age value of the differential of compressive strength (S) with respect to the log of t_{ea} as shown in Equation 3.2.

Since one of the objectives of this research project is to determine appropriate curing durations, one can conclude from the developed strength-maturity curves that 4 days of curing usually provides approximately equal strength as 10 days of curing. This can be seen as the curve for the 4-day cure closely follows the trend of the 10-day curve in Figures 3.20 through 3.23.

One might initially conclude that 4 days of curing is adequate to achieve desired compressive strengths. However, a lack of confidence still exists due to inadequate testing to be able to state with confidence that the durability of the concrete is the same for the 4- and 10-day cures. Also, though it is evident that the 0-day cure cylinder strengths are not much lower than the strengths for the 4- and 10-day cure cylinders, this is not the case for the 0-day cure section of the bridge deck. Since cylinders for the 0-day cure are sealed from moisture loss for the first 24 hours, these cylinders are actually going through a critical period of hydration unlike the bridge deck, which is not covered and is susceptible to drying due to evaporation.

Table 3.2 Coefficients for FH Model (FMAT Cylinders)

District	Curing Duration	S_{inf}	α	τ
FTW	0	5034.76	0.4293	49.666
	4	5324.03	0.5602	57.285
	10	5653.04	0.5734	68.199
SAT	0	7466.84	0.4612	28.956
	4	9076.28	0.4676	55.808
	10	9840.67	0.3786	66.185
HOU	0	6625.87	0.4827	37.746
	4	7668.13	0.5812	41.492
	10	7374.41	0.5432	39.693
LBB - 2	0	8586.94	0.4468	68.880
	4	8074.14	0.6141	44.648
	10	8804.05	0.5951	52.893

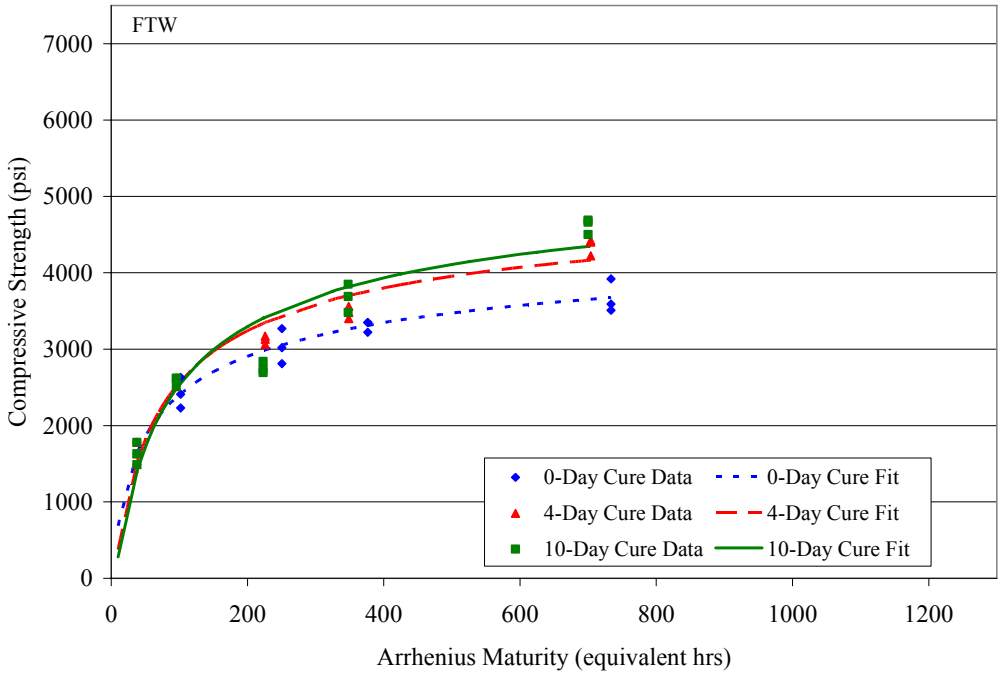

Figure 3.20 FTW Arrhenius FMAT Curves

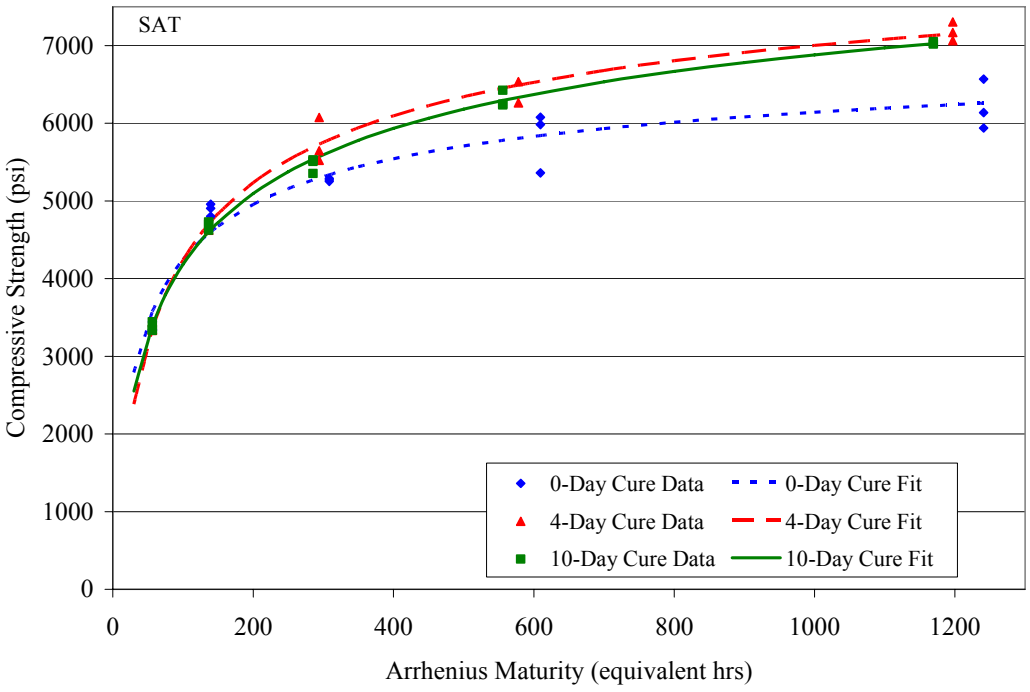

Figure 3.21 SAT Arrhenius FMAT Curves

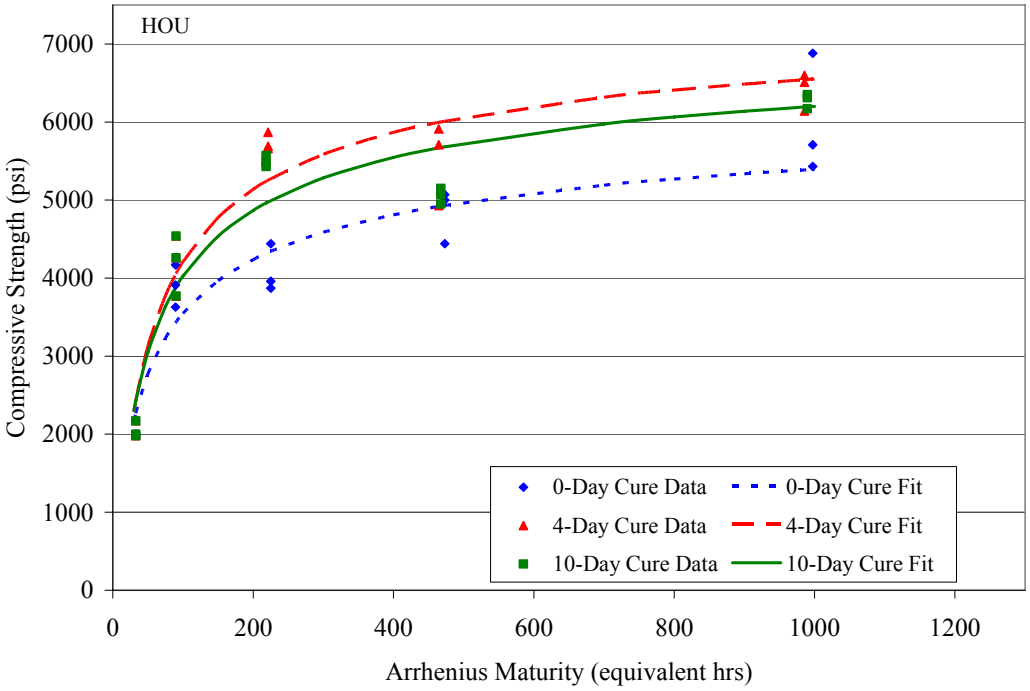

Figure 3.22 HOU Arrhenius FMAT Curves

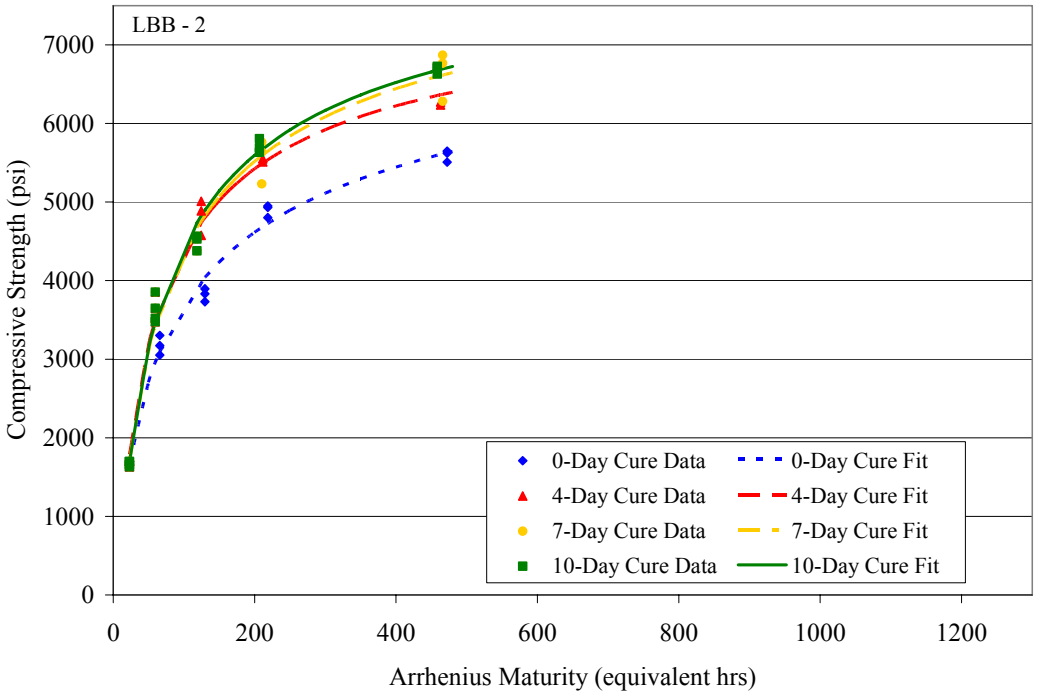

Figure 3.23 LBB – 2 Arrhenius FMAT Curves

3.2.2.2 FMAT Nurse-Saul Maturity Curves

In an attempt to verify which maturity function best serves to predict concrete compressive strengths, strength-maturity curves were also developed for the Nurse-Saul Equivalent Age function. The same temperature history data was used to determine a maturity value based on Equation 3.2 with a datum temperature of 14 °F (-10 °C) and a reference temperature of 68 °F (20 °C).

$$S(t_{ens}) = a_1 \ln(t_{ens}) + a_2 \qquad \text{[Equation 3.3]}$$

where

$S(t_{ens})$ = compressive strength as a function of equivalent age (t_{ens})

a_1 = natural log best-fit curve constant

a_2 = natural log best-fit curve constant

and

$$t_{ens} = \frac{\sum_{0}^{t}(T - T_o)\Delta t}{T_r - T_o}$$ [Equation 3.4]

where

t_{ens} = Nurse-Saul equivalent age at the reference temperature

T_r = reference temperature, usually taken as 68 °F (20 °C).

t = time after pour

Δt = elapsed time between temperature readings

M_s = concrete maturity at age t expressed as a "temperature-time factor"

T = average temperature between Δt

T_o = datum temperature, usually taken as 14 °F (-10 °C).

Coefficients for the Natural Log Strength Gain Model (LN model) are listed in Table 3.3. Figures 3.24 through 3.27 show the developed strength-maturity curves based on the Nurse-Saul Equivalent Age function with a natural log best-fit curve.

Maturity values using the Nurse-Saul Equivalent Age function are lower than those for the Arrhenius Equivalent Age function for curing temperatures above 68 °F (-10 °C). Since curing temperatures were usually above 68°F, it should be expected that equivalent ages due to the Arrhenius function will be higher than those for the Nurse-Saul function.

Table 3.3 Coefficients for LN Model (FMAT Cylinders)

District	Curing Duration	a_1	a_2
FTW	0	663.1	-597.7
	4	839.3	-1261.3
	10	918.6	-1645.4
SAT	0	864.7	464.8
	4	1191.3	-928.9
	10	1166.0	-873.4
HOU	0	1056.8	-1282.4
	4	1233.7	-1589.7
	10	1139.0	-1272.3
LBB - 2	0	1308.0	-2478.0
	4	1567.2	-3127.4
	10	1659.8	-3520.7

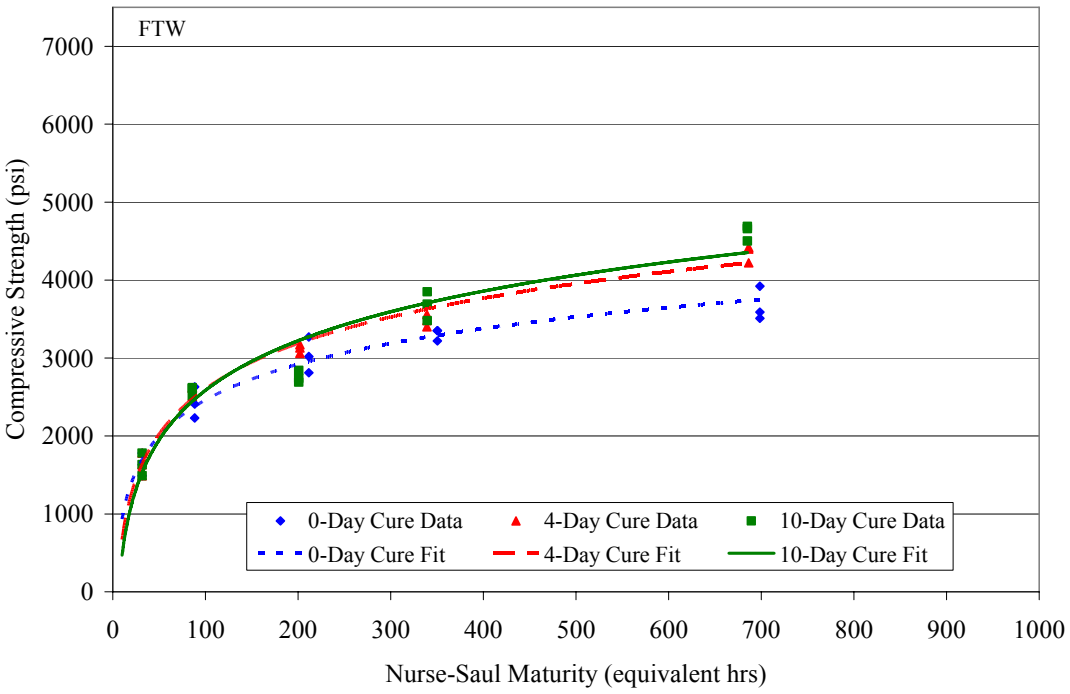

Figure 3.24 FTW Nurse-Saul FMAT Curves

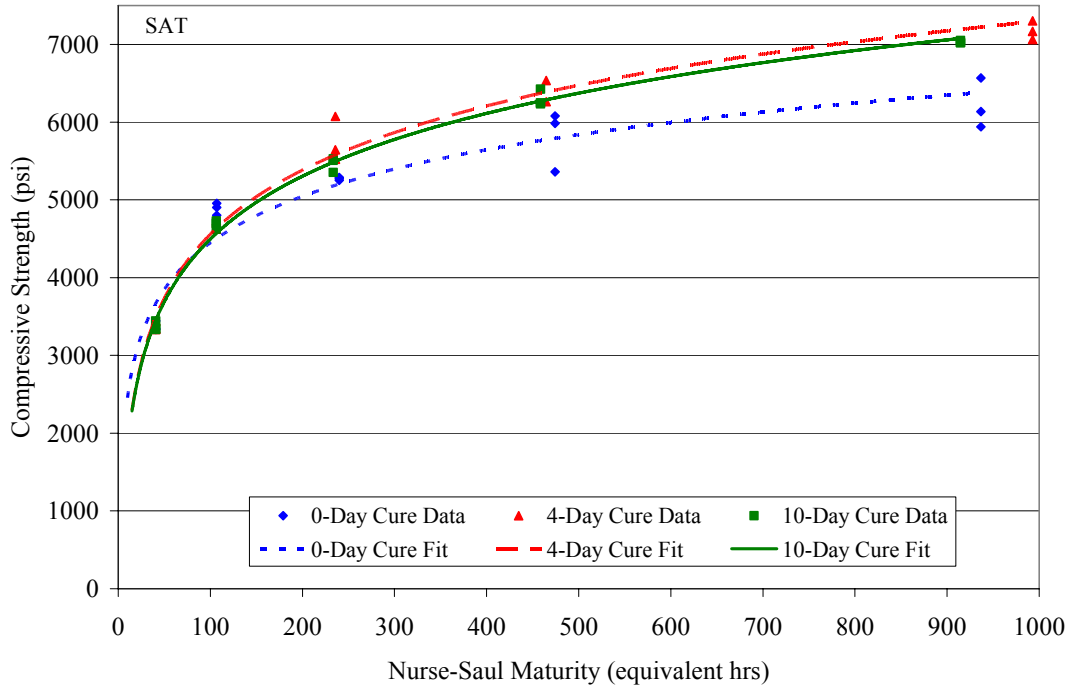

Figure 3.25 SAT Nurse-Saul FMAT Curves

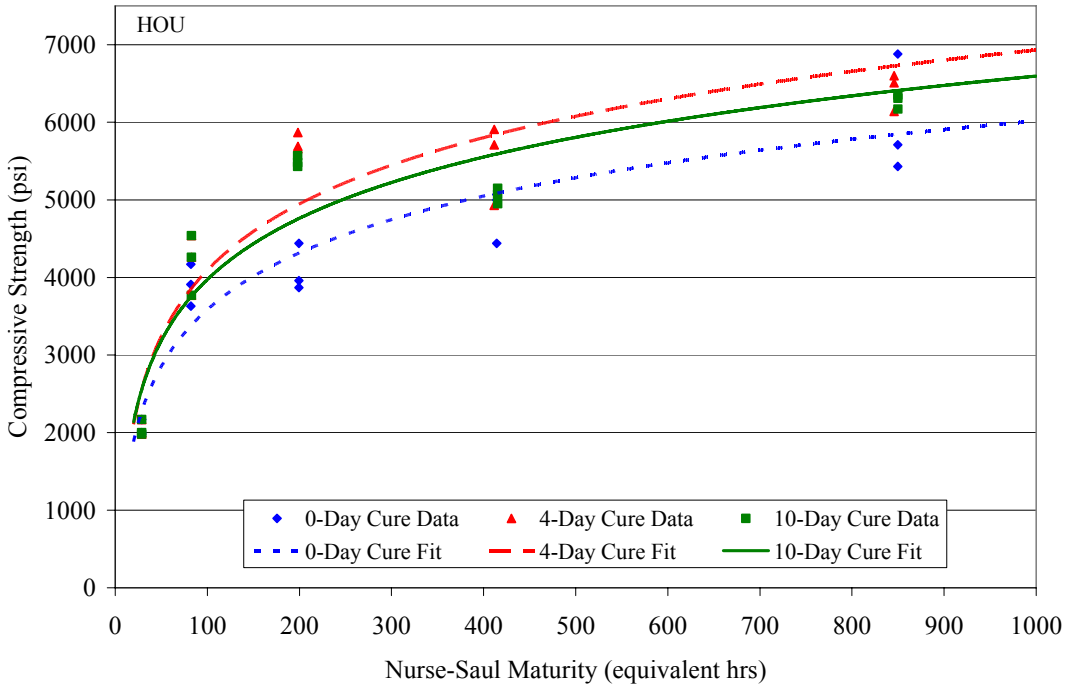

Figure 3.26 HOU Nurse-Saul FMAT Curves

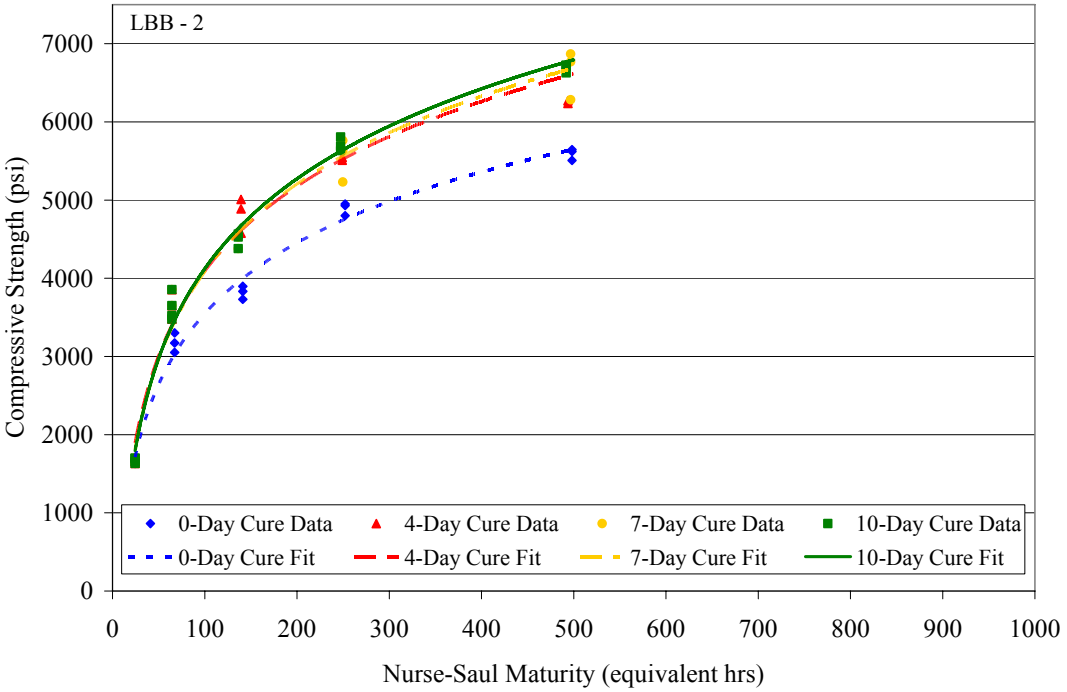

Figure 3.27 LBB – 2 Nurse-Saul FMAT Curves

3.2.3 CONVT Cylinder Strength

As a means to validate which method (i.e. conventional cylinder or maturity), indicates more closely in-situ concrete strength, conventional field-cured cylinder and concrete core strengths were compared based on actual calendar days. Evaluations between the in-situ concrete strength and conventional field-cured cylinders were made for Days 7, 14, and 28 due to the common testing dates between the concrete deck cores and conventional field cylinders.

3.2.3.1 CONVT Strength Gain Curves

It can be seen that conventional field-cured cylinders deviate from in-situ concrete deck strengths. Other than for a few exceptions, such as the 4- and 10-day curing durations for the Fort Worth mix, overall comparison errors were highly variable. Moderate deviations, as will be defined herein as an error range of 10 to 30%, were common for the 4- and 10-day curing periods.

Deviations for the 0-day cure period were anywhere from 20 to 80% with the exception of the El Paso concrete mix. The high variability of strengths between the field cylinder and bridge deck for the 0-day curing duration could be accounted for by the different conditions each experiences in the first 24 hours as discussed in the following.

As mentioned earlier, the 0-day cure portion of the bridge deck does not receive any moist curing (i.e. wet mats), after initial placement, but a curing compound is applied to the surface, which may or may not completely prevent the evaporation of mix water in the concrete mix. Furthermore, this portion of the bridge deck is not covered and therefore is exposed directly to the atmosphere, which allows generated heat of hydration to dissipate more easily. On the other hand for the first 24 hours, the 0-day cure cylinders are within plastic molds and capped with lids, which prevents evaporation of mix water and provides sufficient insulation to prevent large amounts of heat loss due to the hydration process.

Overall, the strength assessment of the in-situ concrete deck strength based on conventional field-cured cylinders strengths is less indicative of in-place strength. Utilizing the maturity method to determine the strength of in-situ concrete appears to be more accurate than conventional cylinders, provided that mix proportions used to develop strength-maturity curves are the same for the bridge deck.

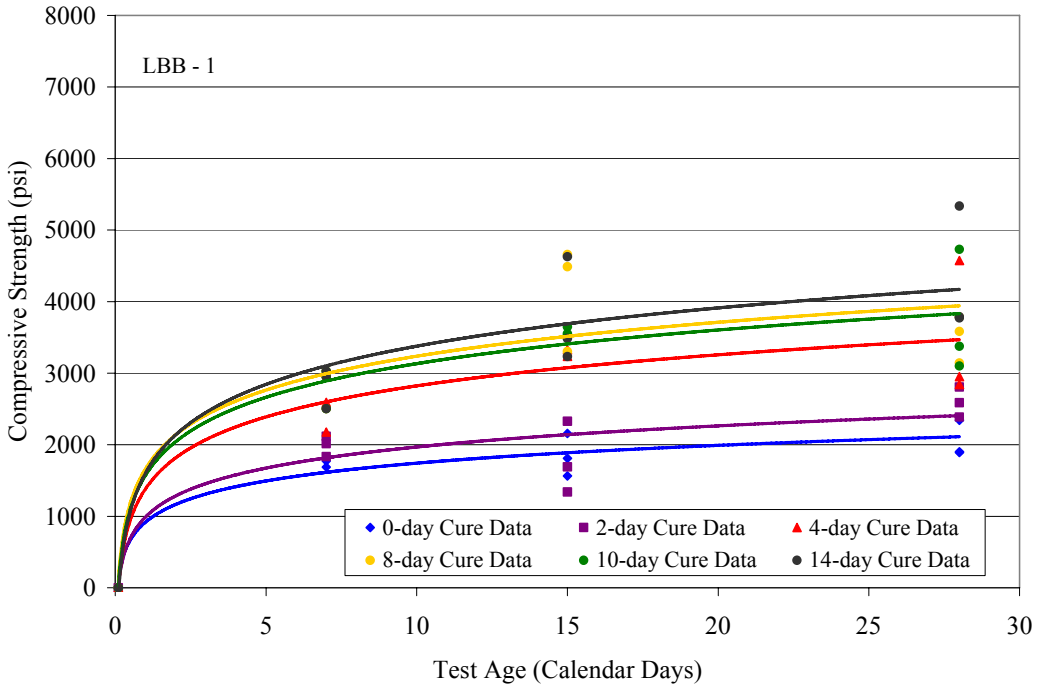

Figure 3.28 LBB – 1 CONVT Strength Gain

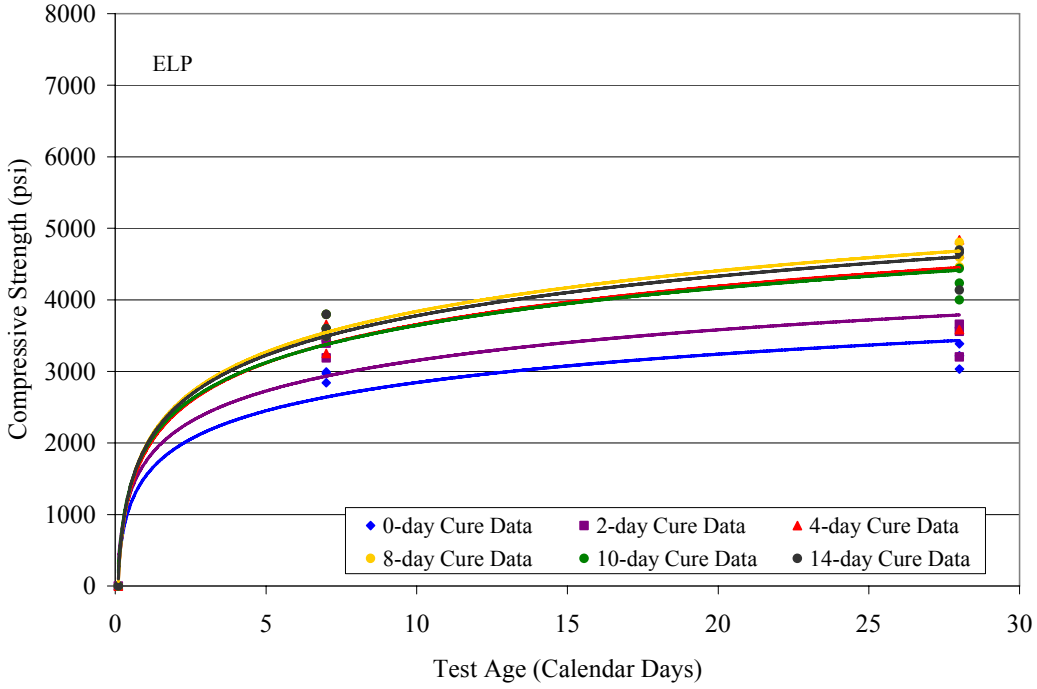

Figure 3.29 ELP CONVT Strength Gain

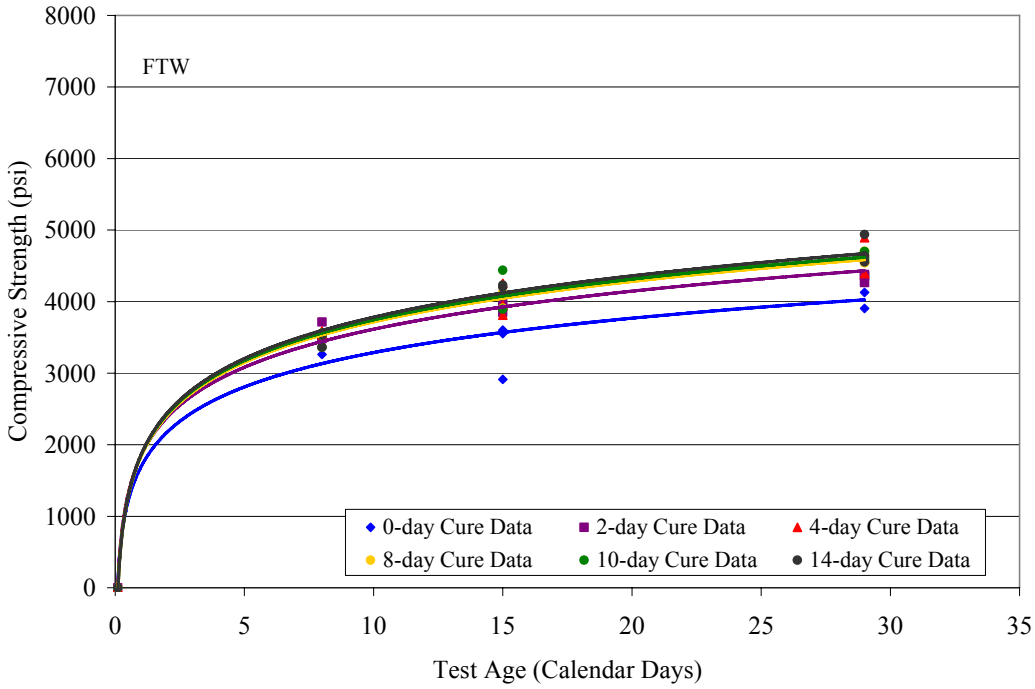

Figure 3.30 FTW CONVT Strength Gain

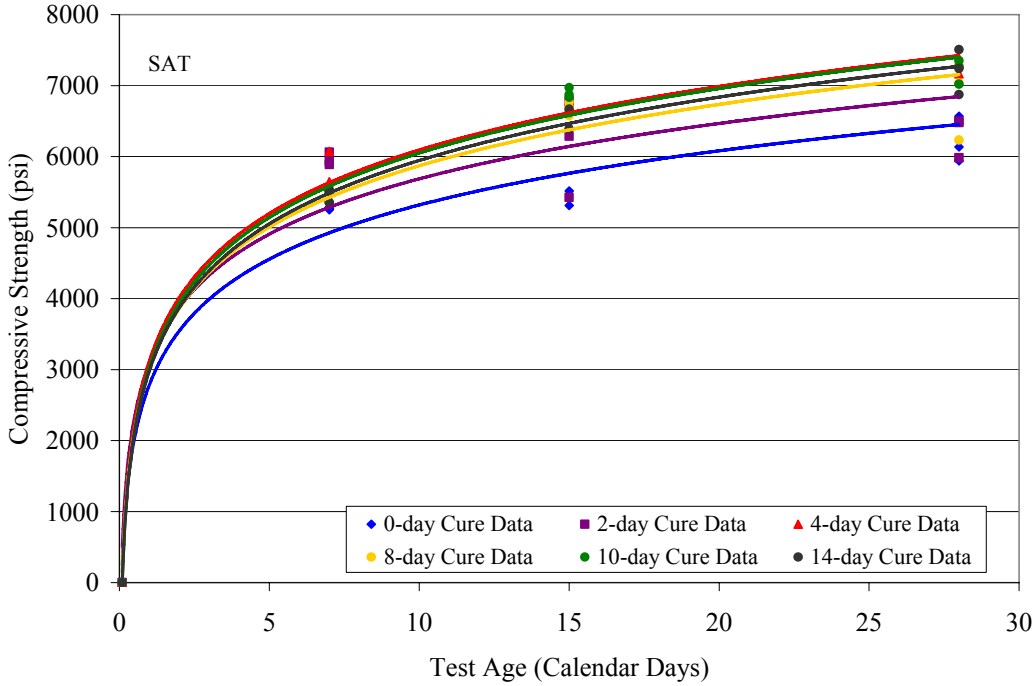

Figure 3.31 SAT CONVT Strength Gain

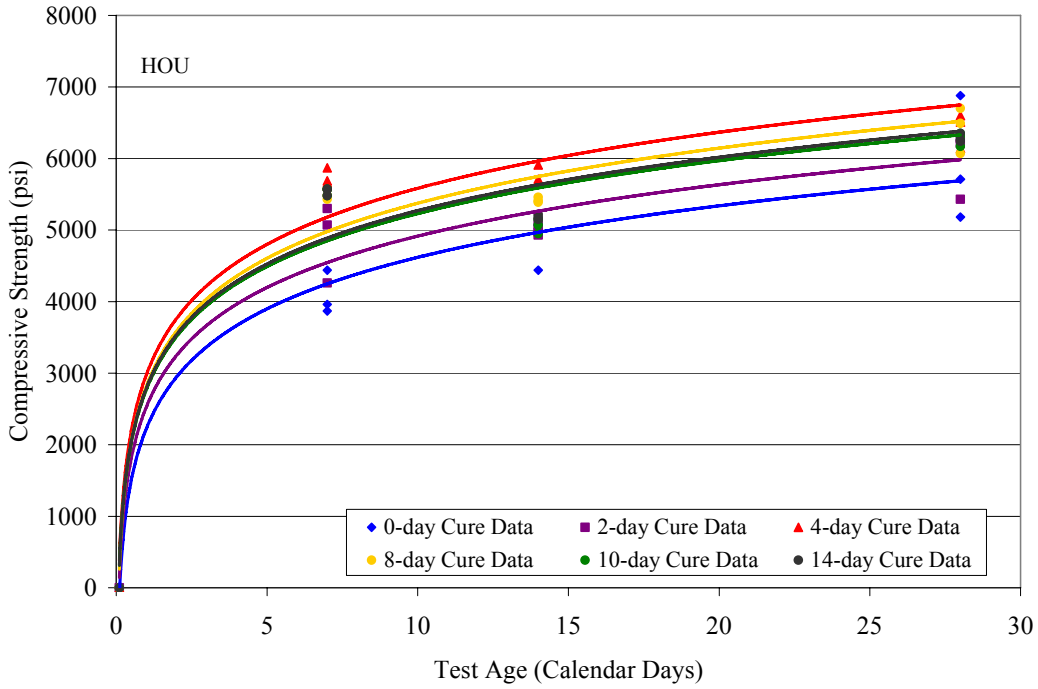

Figure 3.32 HOU CONVT Strength Gain

3.2.3.2 In-Situ Strength Compared to CONVT Strength

As a means to validate which method (i.e. conventional cylinder or maturity), indicates more closely in-situ concrete strength, conventional field-cured cylinder and concrete core strengths were compared based on actual calendar days. Evaluations between the in-situ concrete strength and conventional field-cured cylinders were made for Days 7, 14, and 28 due to the common testing dates between the concrete deck cores and conventional field cylinders. Since the focus has been on curing durations of 0, 4, and 10 days for this thesis, concrete strength comparisons are presented only for these curing durations in Table 3.4.

Referring to the data presented in Table 3.4, it can be seen that conventional field-cured cylinders deviate from in-situ concrete deck strengths. Other than for a few exceptions, such as the 4- and 10-day curing durations for the Fort Worth mix, overall comparison errors were highly variable. Moderate deviations, as will be defined herein as an error range of 10 to 30%, were common for the 4- and 10-day curing periods.

Deviations for the 0-day cure period were anywhere from 20 to 80% with the exception of the El Paso concrete mix. The high variability of strengths between the field cylinder and bridge deck for the 0-day curing duration could be accounted for by the different conditions each experiences in the first 24 hours as discussed in the following.

As mentioned earlier, the 0-day cure portion of the bridge deck does not receive any moist curing (i.e. wet mats), after initial placement, but a curing compound is applied to the surface, which

may or may not completely prevent the evaporation of mix water in the concrete mix. Furthermore, this portion of the bridge deck is not covered and therefore is exposed directly to the atmosphere, which allows generated heat of hydration to dissipate more easily. On the other hand for the first 24 hours, the 0-day cure cylinders are within plastic molds and capped with lids, which prevents evaporation of mix water and provides sufficient insulation to prevent large amounts of heat loss due to the hydration process.

Overall, the strength assessment of the in-situ concrete deck strength based on conventional field-cured cylinders strengths is less indicative of in-place strength. Utilizing the maturity method to determine the strength of in-situ concrete appears to be more accurate than conventional cylinders, provided that mix proportions used to develop strength-maturity curves are the same for the bridge deck.

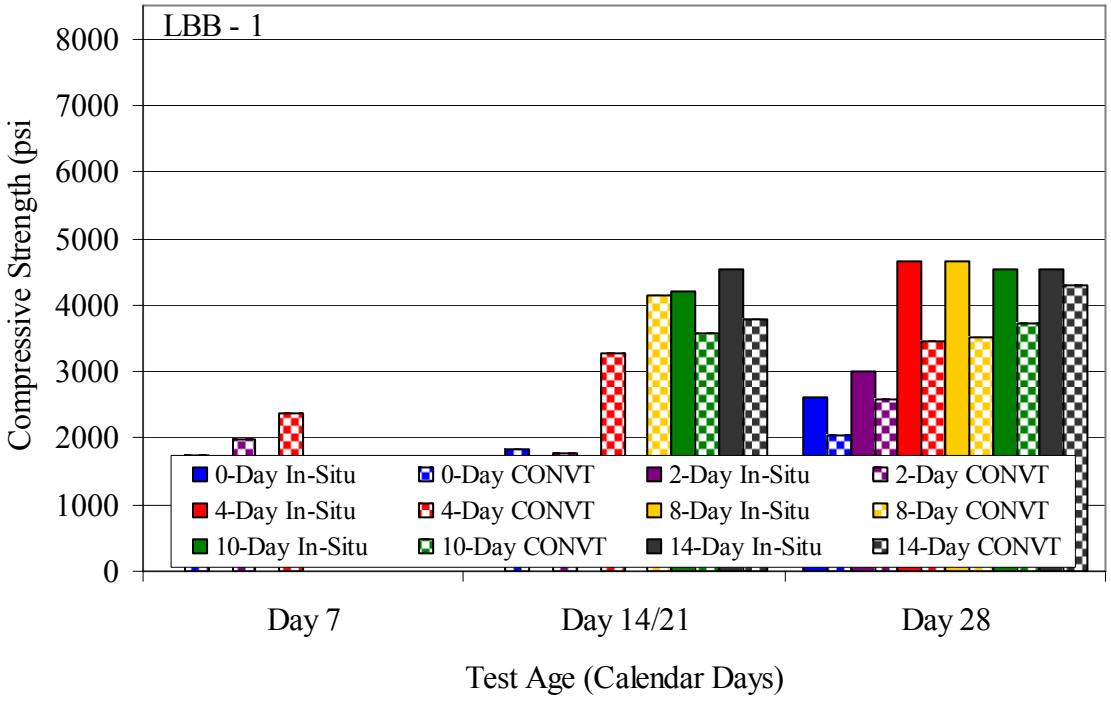

Figure 3.33 LBB – 1 In-Situ Strength Compared to CONVT Strength

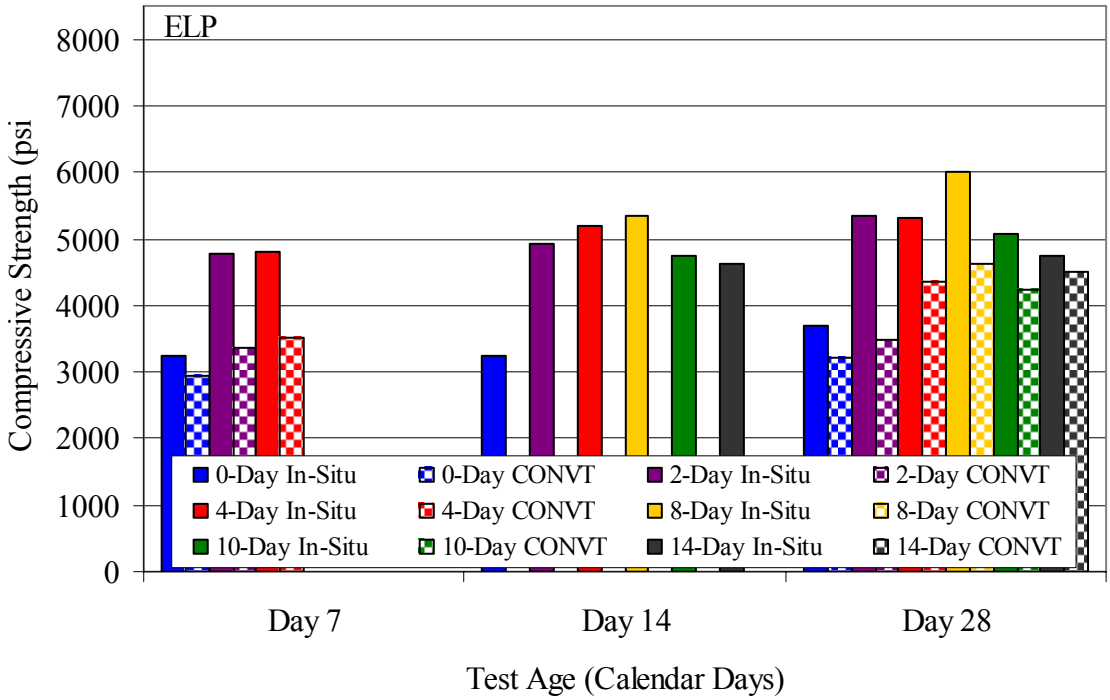

Figure 3.34 ELP In-Situ Strength Compared to CONVT Strength

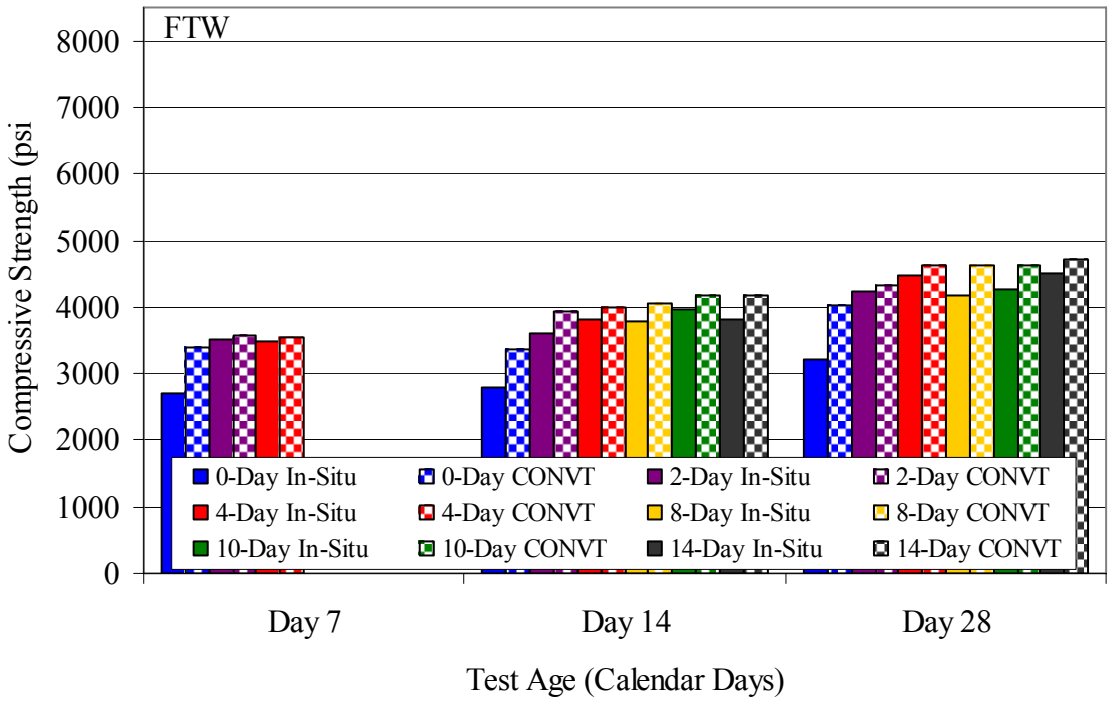

Figure 3.35 FTW In-Situ Strength Compared to CONVT Strength

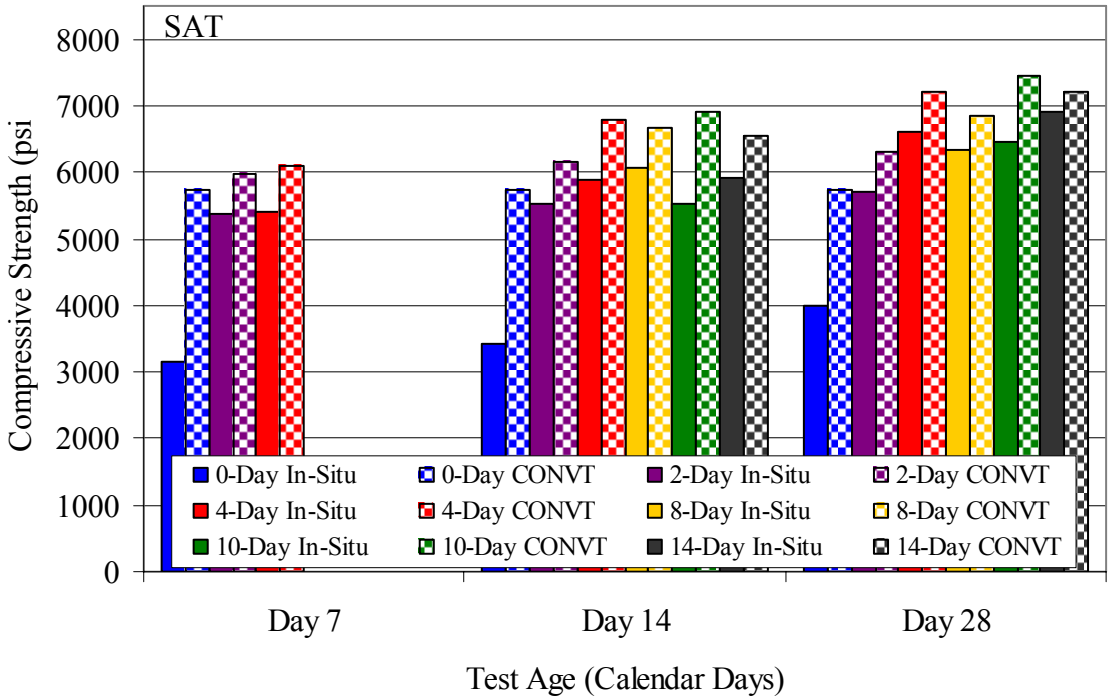

Figure 3.36 SAT In-Situ Strength Compared to CONVT Strength

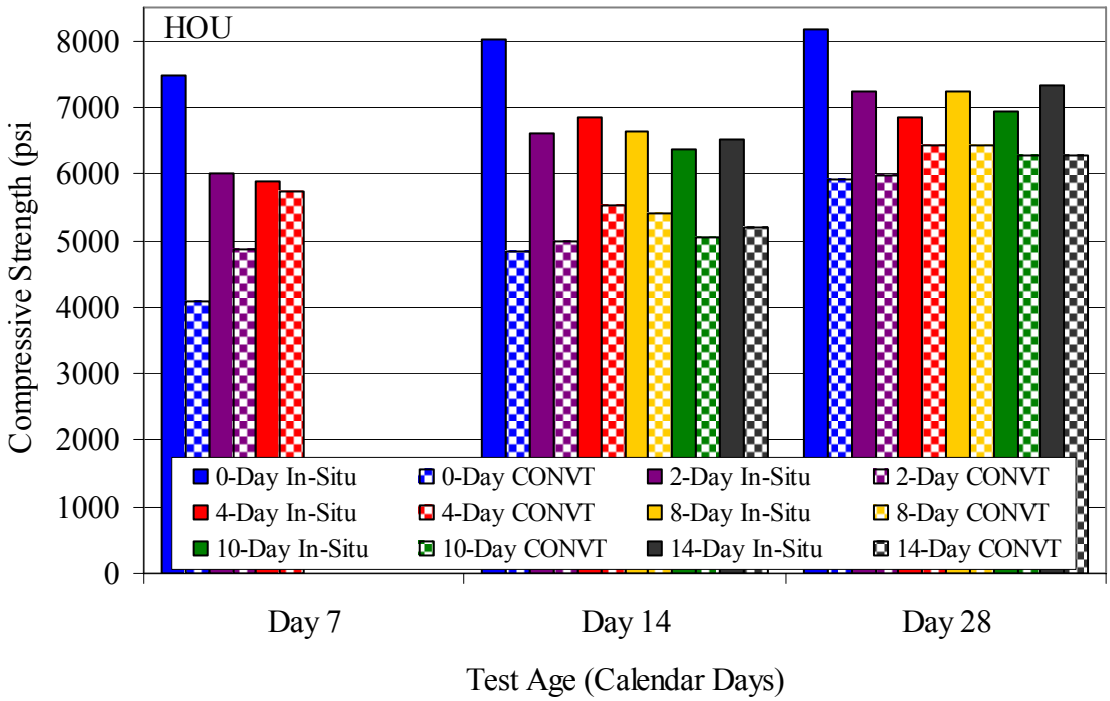

Figure 3.37 HOU In-Situ Strength Compared to CONVT Strength

Table 3.4 In-Situ Strength Compared to CONVT Cylinder

			Testing Age (days)		
			7	14	28
FTW	0-day cure	In-Situ Strength (psi)	2717	2796	3210
		CONVT Cylinder (psi)	3385	3355	4016
		% Error	25	20	25
	4-day cure	In-Situ Strength (psi)	3470	3824	4477
		CONVT Cylinder (psi)	3559	4004	4626
		% Error	3	5	3
	10-day cure	In-Situ Strength (psi)	–	3959	4262
		CONVT Cylinder (psi)	–	4166	4632
		% Error	–	5	9
SAT	0-day cure	In-Situ Strength (psi)	3167	3429	3989
		CONVT Cylinder (psi)	5731	5740	5743
		% Error	81	67	44
	4-day cure	In-Situ Strength (psi)	5404	5882	6616
		CONVT Cylinder (psi)	6098	6795	7211
		% Error	13	16	9
	10-day cure	In-Situ Strength (psi)	–	5525	6464
		CONVT Cylinder (psi)	–	6894	7448
		% Error	–	25	15
HOU	0-day cure	In-Situ Strength (psi)	7489	8027	8165
		CONVT Cylinder (psi)	4090	4837	5923
		% Error	45	40	28
	4-day cure	In-Situ Strength (psi)	5872	6854	6855
		CONVT Cylinder (psi)	5740	5517	6417
		% Error	2	20	6
	10-day cure	In-Situ Strength (psi)	–	6375	6937
		CONVT Cylinder (psi)	–	5057	6277
		% Error	–	21	10
ELP	0-day cure	In-Situ Strength (psi)	3239	3233	3707
		CONVT Cylinder (psi)	2933	N/A	3212
		% Error	9	–	13
	4-day cure	In-Situ Strength (psi)	4800	5193	5311
		CONVT Cylinder (psi)	3506	N/A	4355
		% Error	27	–	18
	10-day cure	In-Situ Strength (psi)	–	4742	5086
		CONVT Cylinder (psi)	–	N/A	4224
		% Error	–	–	17

N/A = Data is Not Available

3.2.4 LMAT Cylinder Strength-Maturity Curves

Once all compressive data had been collected and linked with its corresponding equivalent age, strength-maturity curves were generated. Maturity curves for the LMAT cylinders were developed with the FH strength gain model using Quadrel® software and the LN strength gain model using a spreadsheet with their respective equivalent ages. Coefficients for both of the strength gain models are tabulated in Tables 3.5 and 3.6. Since the temperature data for the ATL specimens were insufficient, the compressive strength was plotted against the actual testing age.

Table 3.5 Coefficients for FH Model (LMAT Cylinders)

District	Curing Duration	S_{inf}	α	τ
ELP	0	4129.25	0.528	68.765
	4	8300.76	0.710	96.795
	10	7732.54	0.724	83.875
FTW	0	6814.33	0.439	55.477
	4	10212.62	0.410	115.786
	10	7702.38	0.605	66.93
SAT	0	5719.42	0.594	55.362
	4	7950.58	0.705	67.451
	10	9882.33	0.742	82.5
HOU	0	6841.06	0.467	47.422
	4	7378.46	0.536	61.329
	10	7514.22	0.582	66.874
PHR	0	5905.24	0.511	22.882
	4	6669.49	0.521	33.479
	10	6486.86	0.4387	28.646

Table 3.6 Coefficients for LN Strength Gain Model (LMAT Cylinders)

District	Curing Duration	a_1	a_2
ELP	0	713.67	-1496.3
	4	1790.7	-5051.9
	10	1695.8	-4606.5
FTW	0	934.69	-1093
	4	1408.3	-2767.4
	10	1326.8	-2527.4
SAT	0	1038	-2011.6
	4	1663	-4006.3
	10	2195.9	-5968.0
HOU	0	969.97	-1186.4
	4	1202.3	-2208.0
	10	1303.1	-2663.6
PHR	0	704.6	517.0
	4	857.6	-35.1
	10	722.94	433.2

Figures 3.38 through 3.43 are strength-maturity curves developed using the Arrhenius function and Figures 3.44 through 3.49 are those for the Nurse-Saul function. Even though coefficients for the 7-day cure LMAT cylinders are not listed in Tables 3.5 and 3.6, the 7-day cure strength-maturity relationships are plotted along with the 0-, 4-, and 10-day cure curves as shown in the figures just mentioned.

Again, as observed from the generated strength-maturity curves for the LMAT cylinders, four days of curing attains approximately the same strengths as cylinders with 10 days of curing. This was also true for strength-maturity curves developed from FMAT cylinders. With the addition of the 7-day cure strength-maturity curve, a comparison could be made between the 4-, 7-, and 10-day cure lab cylinders. Strength gain trends for curing durations of 4 days or more seem to be similar, which suggests that 4 days of curing may be adequate to achieve a desired compressive strength but it is still not known if 4 days is adequate for concrete durability. Also, it is recognized that the 0-day cure cylinders achieve significantly lower strengths than those cylinders with any amount of moist curing.

The exception to the above-mentioned observation (4-day cure is adequate for strength gain) is that for the lab poured San Antonio concrete mix. Since LMAT cylinders for the 0-, 4-, 7-, and 10-day cure durations were made from different batches, it is possible that the batch used for the 4-day cure cylinders varied slightly from the other batches (i.e., 0-, 7-, and 10-day cure) for this particular mix.

When comparing the developed strength-maturity curves for the LMAT cylinders to those developed for the FMAT cylinders, concrete strength development was higher for LMAT cylinders as opposed to FMAT cylinders. The differences in strength gain could be attributed to several factors such as not having the same concrete mix in the field or in the lab. In the field, the differences could be a result of differences in concrete mix delivered by a ready-mix manufacturer. In the lab, such differences could occur from variations in lab mixing due to having different batches in the lab with a 6-foot cubic capacity concrete mixer. Another quality control factor could be the frequent addition of varying amounts of water by the contractor to increase the workability. Since, strength gain models for the lab generated curves yielded consistently higher strengths than those for the FMAT generated curves, it should be noted that strength predictions for the concrete bridge deck based on LMAT generated curves should deviate from in-situ strengths.

3.2.4.1 LMAT Arrhenius Maturity Curves

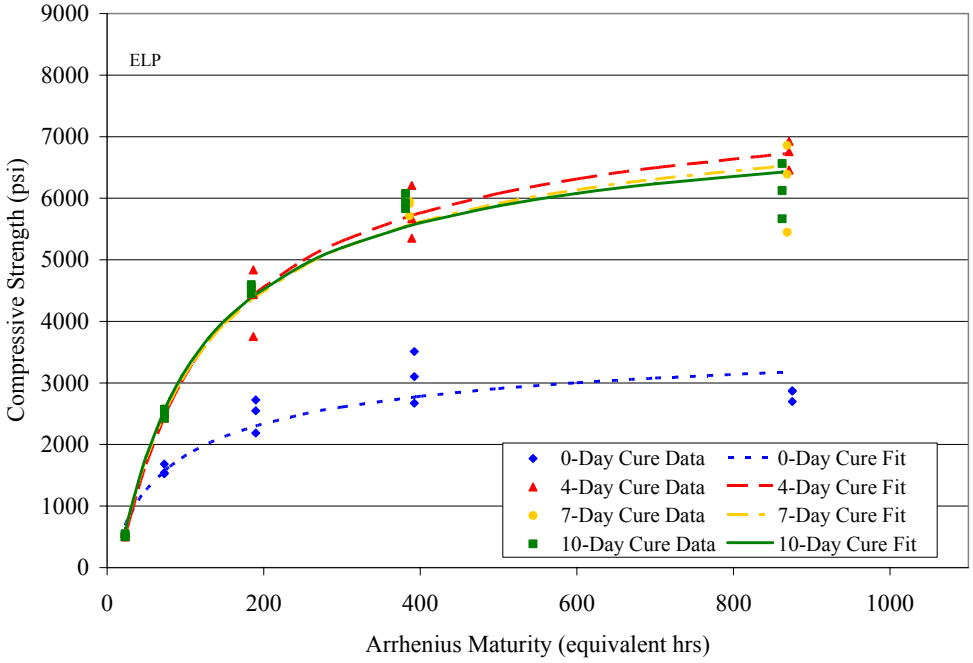

Figure 3.38 ELP Arrhenius LMAT Curves

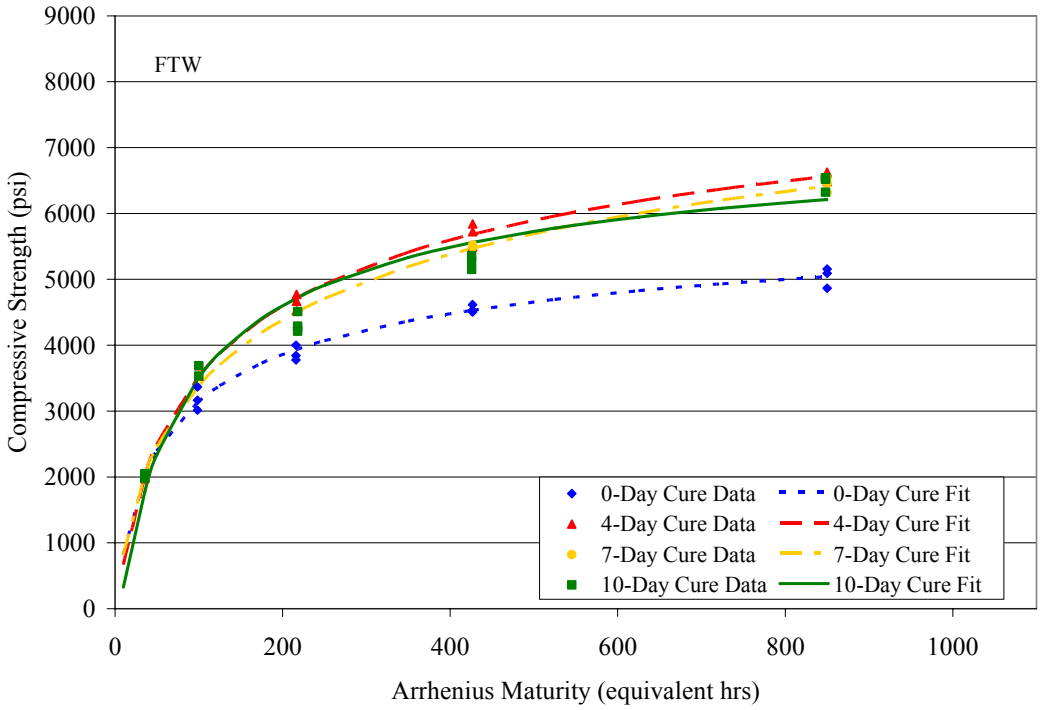

Figure 3.39 FTW Arrhenius LMAT Curves

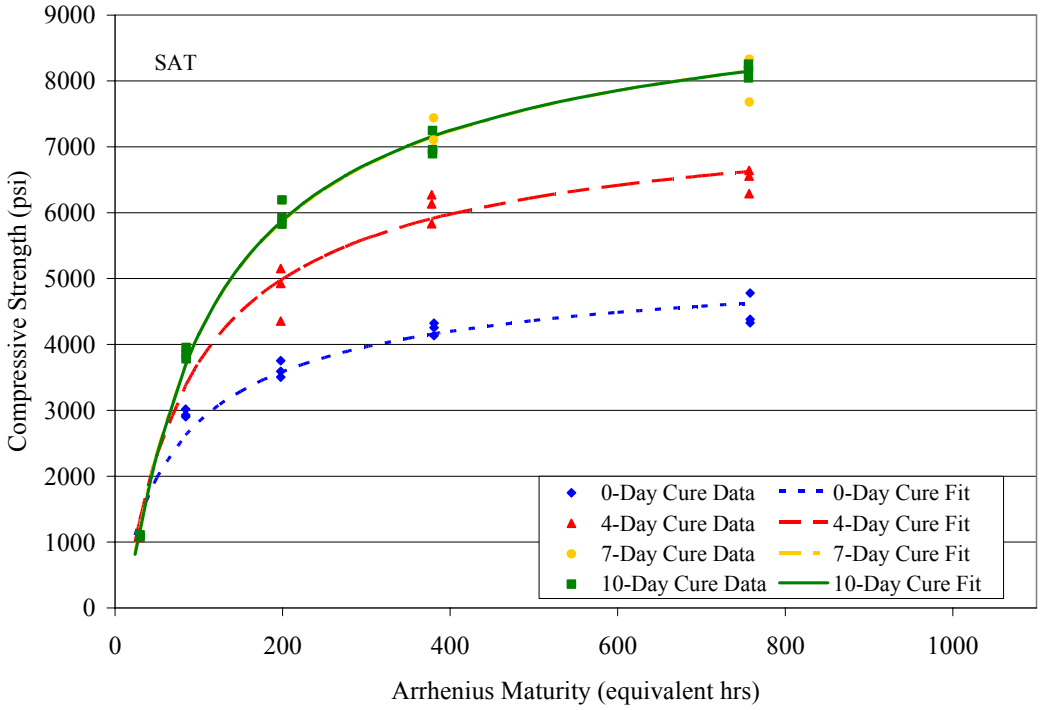

Figure 3.40 SAT Arrhenius LMAT Curves

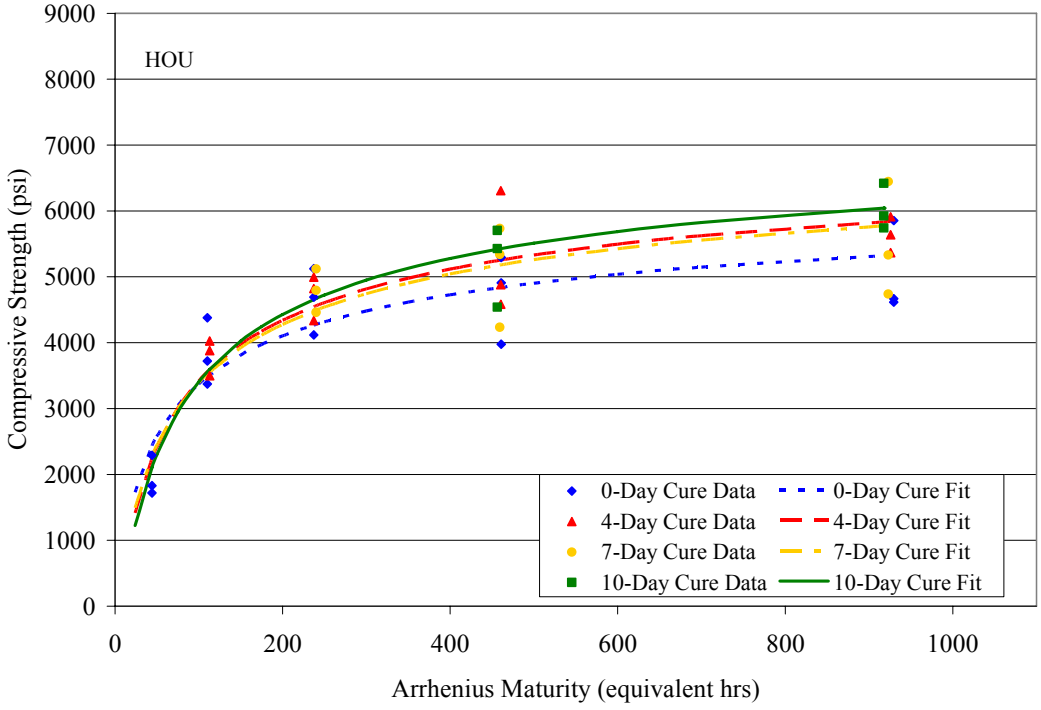

Figure 3.41 HOU Arrhenius LMAT Curves

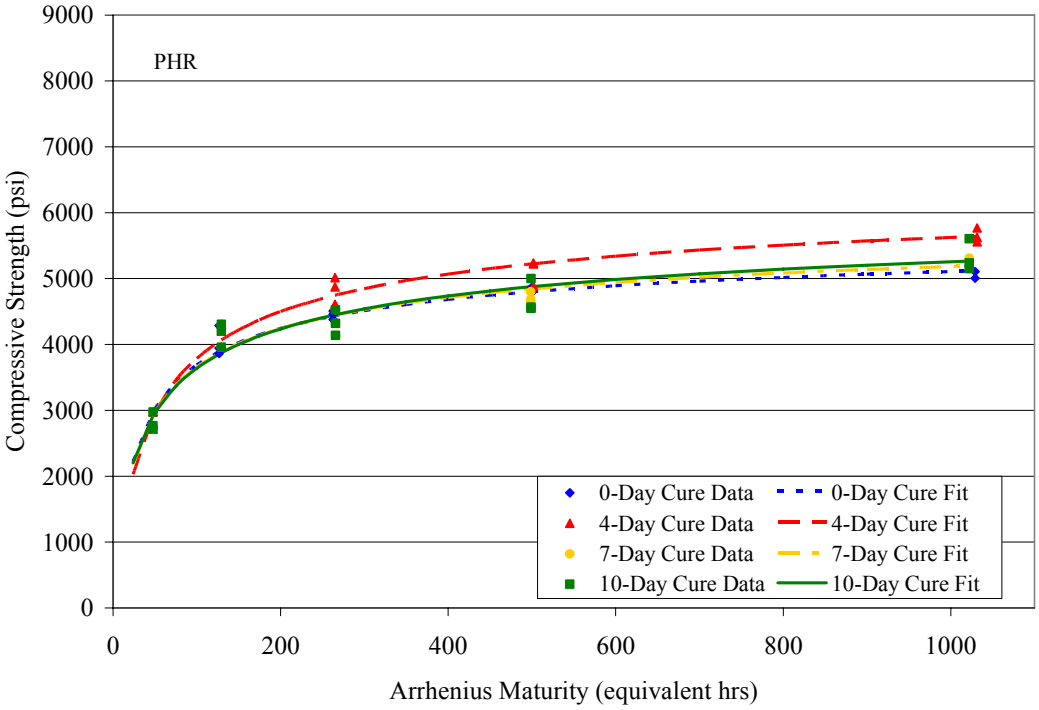

Figure 3.42 PHR Arrhenius LMAT Curves

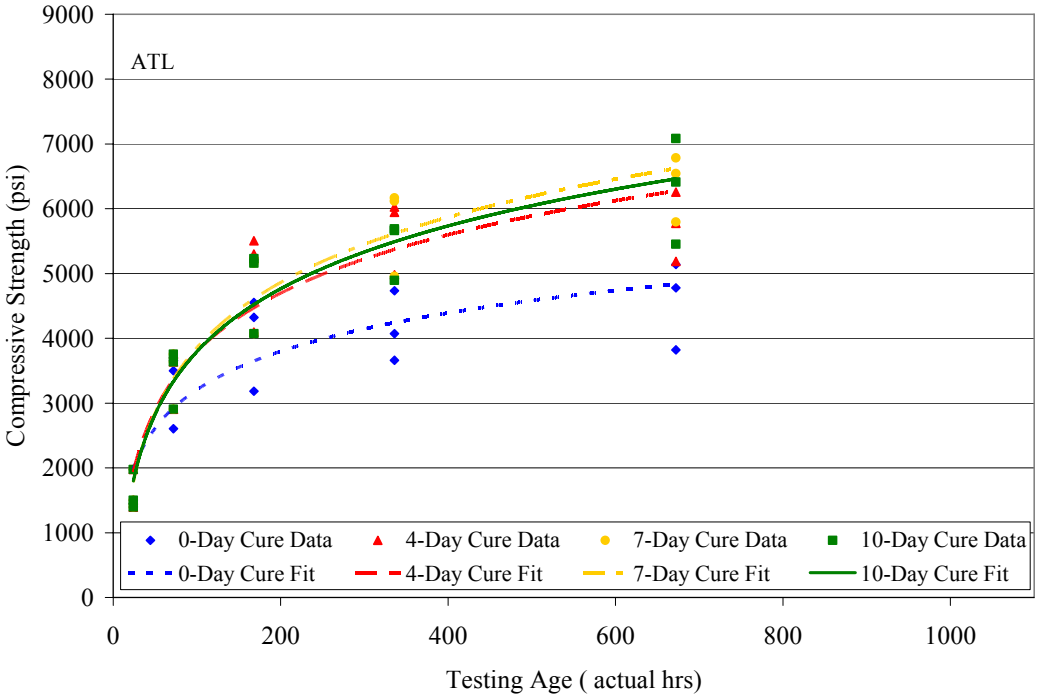

Figure 3.43 ATL Lab Strength Development Curves

3.2.4.2 LMAT Nurse-Saul Maturity Curves

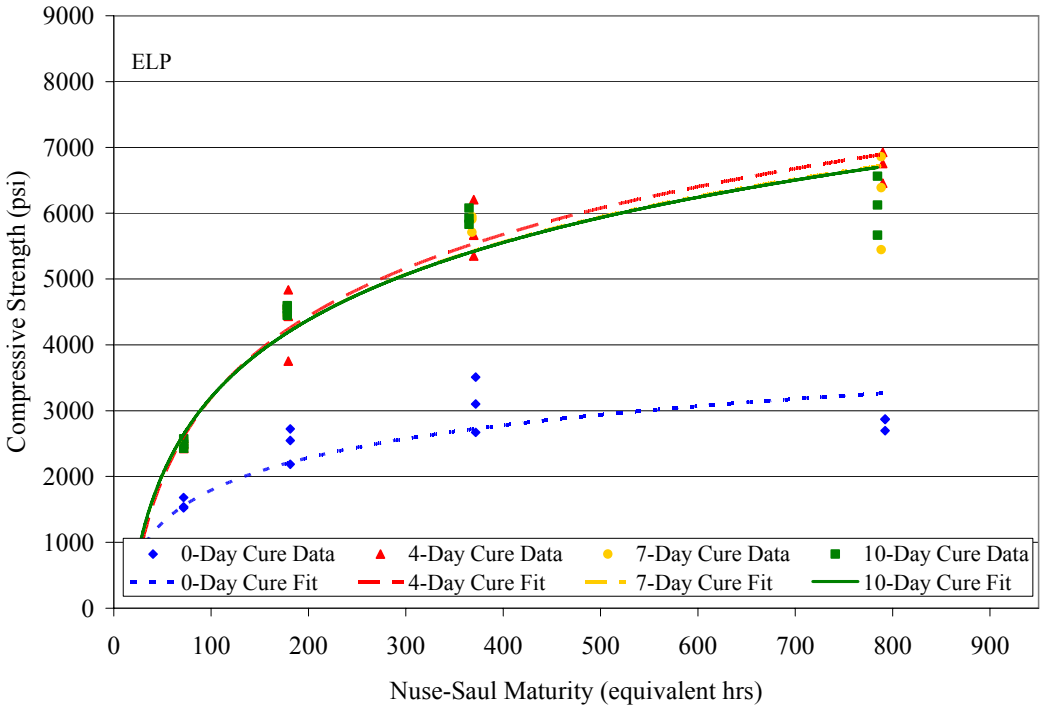

Figure 3.44 ELP Nurse-Saul LMAT Curves

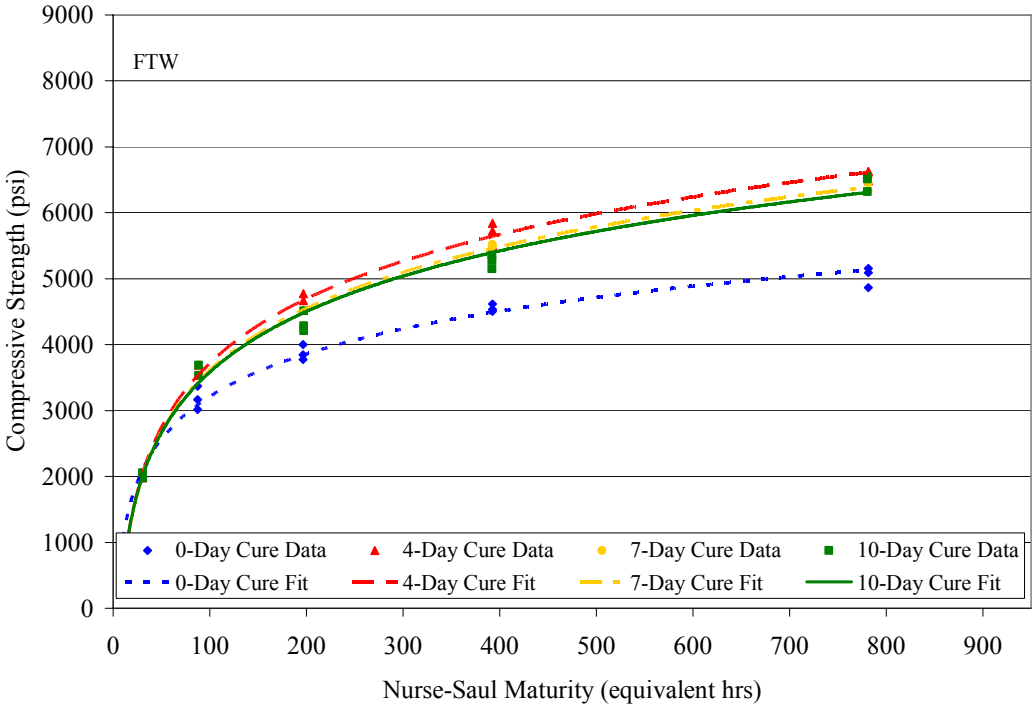

Figure 3.45 FTW Nurse-Saul LMAT Curves

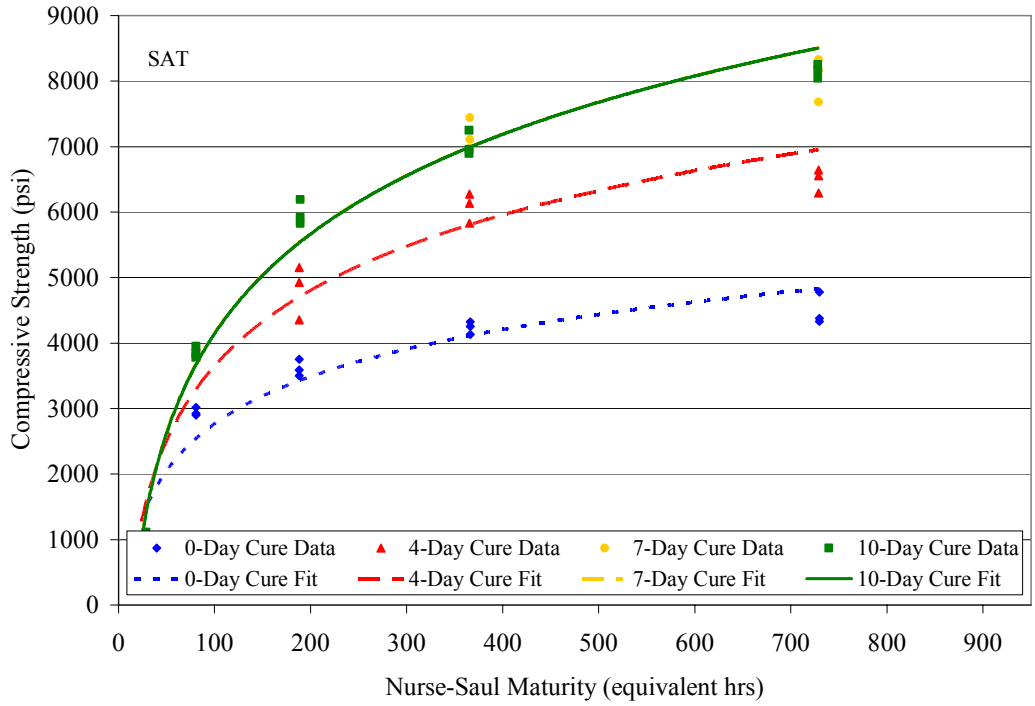

Figure 3.46 SAT Nurse-Saul LMAT Curves

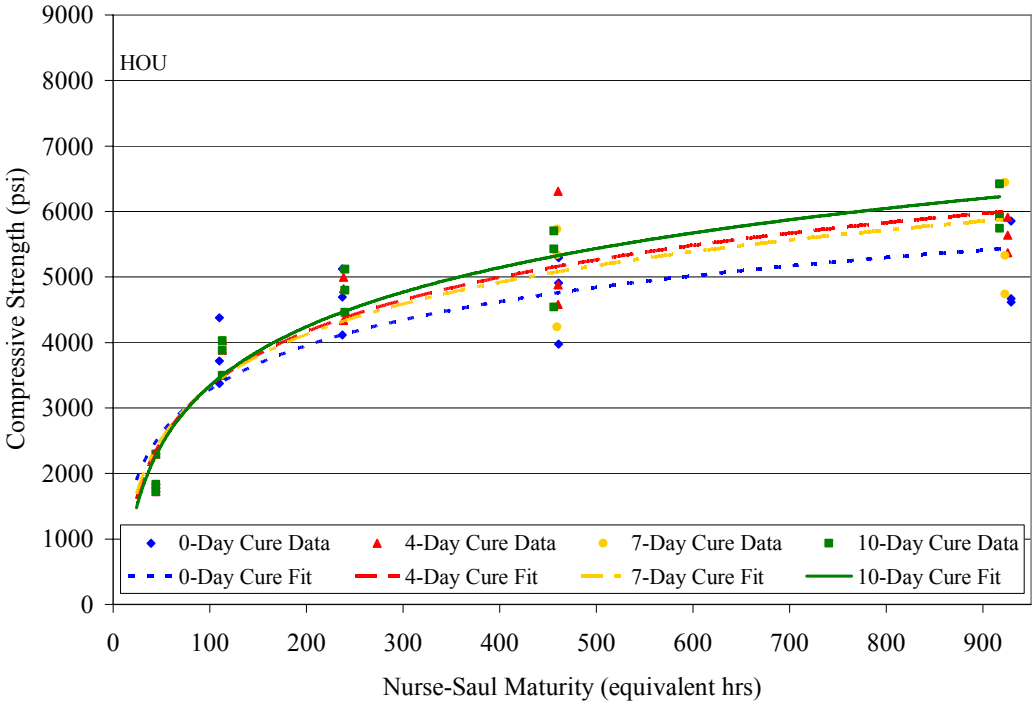

Figure 3.47 HOU Nurse-Saul LMAT Curves

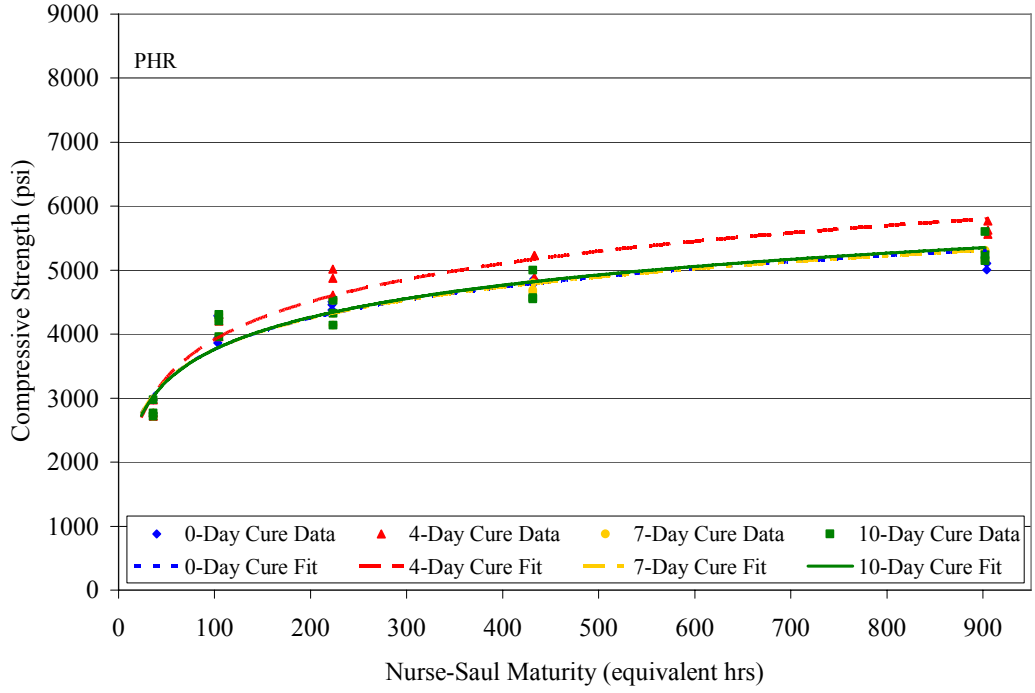

Figure 3.48 PHR Nurse-Saul LMAT Curves

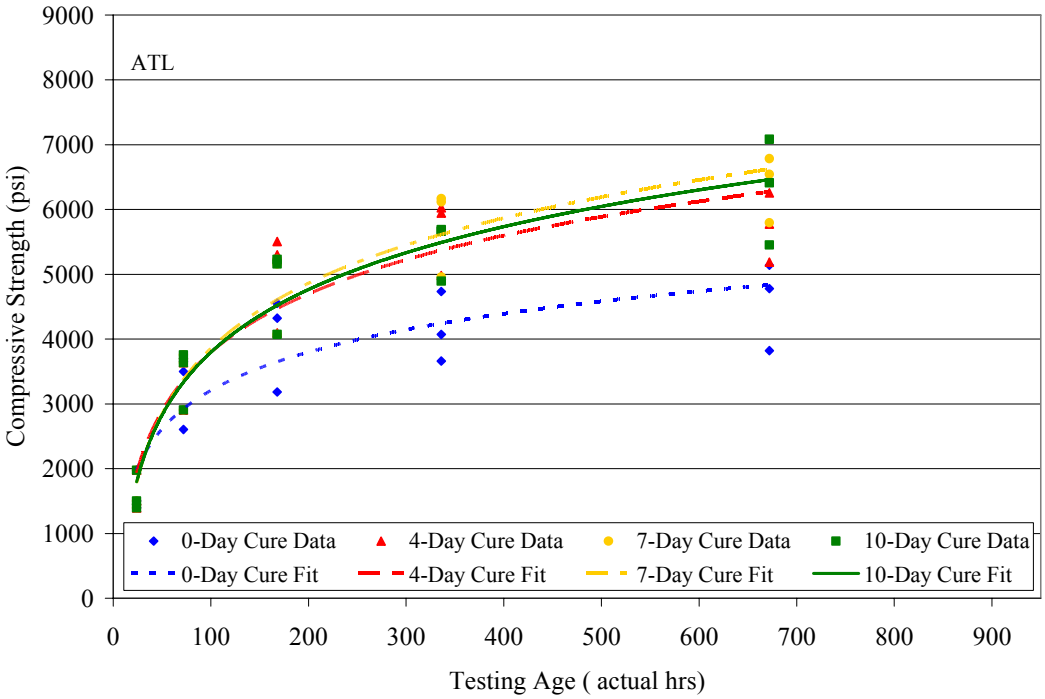

Figure 3.49 ATL Lab Strength Development Curves

3.3 Bridge Deck In-Situ Strength Compared to Predicted Strength

With the development of strength-maturity curves, in-situ concrete strength can be compared to predicted strengths from both the Arrhenius and Nurse-Saul generated curves. First, the in-situ equivalent age of the bridge deck is determined. By utilizing the temperature history of each concrete deck section, two equivalent ages for each section were determined using both the Arrhenius and Nurse-Saul functions. Thus, two maturity equivalent ages were computed for each section of the bridge deck. When determining equivalent ages, it is assumed that an entire bridge deck section (i.e., 0, 2, 4, 8, 10, or 14-day cure section) experienced approximately the same curing temperature and thus has the same maturity value throughout that specific concrete slab section.

Three concrete cores from each curing section of the bridge deck were sampled and tested on Days 4, 7, 10, 14, and 28 with the exception of the 10-day cure section. Concrete cores were sampled and tested only on Days 10, 14, and 28 for the 10-day cure section because curing cotton mats and plastic sheeting covered this section during earlier testing days. Since no samples were taken for Days 4 and 7 for the 10-day cure slab, no compressive data was available for these days. Therefore, maturity values for the bridge deck on specified sampling and testing days were determined to predict concrete strength of the deck based on the developed FMAT strength-maturity curves.

3.3.1 FMAT Predicted Strength

Once maturity values were determined for the bridge decks, strength predictions were made based on developed strength-maturity curves from the FMAT cylinders. The Freiesleben Hansen and natural log strength gain models with their respective coefficients were used to determine predicted concrete bridge deck strengths. Strength gain models, coefficients, and in-situ equivalent ages were entered in a spreadsheet to compare the accuracy of both the Arrhenius and Nurse-Saul Equivalent Age functions. Comparison of in-situ to predicted strengths for the FTW, SAT, and HOU bridge decks based on strength-maturity curves from FMAT cylinders are shown in Tables 3.7 through 3.9 and shown in Figures 3.50 through 3.52.

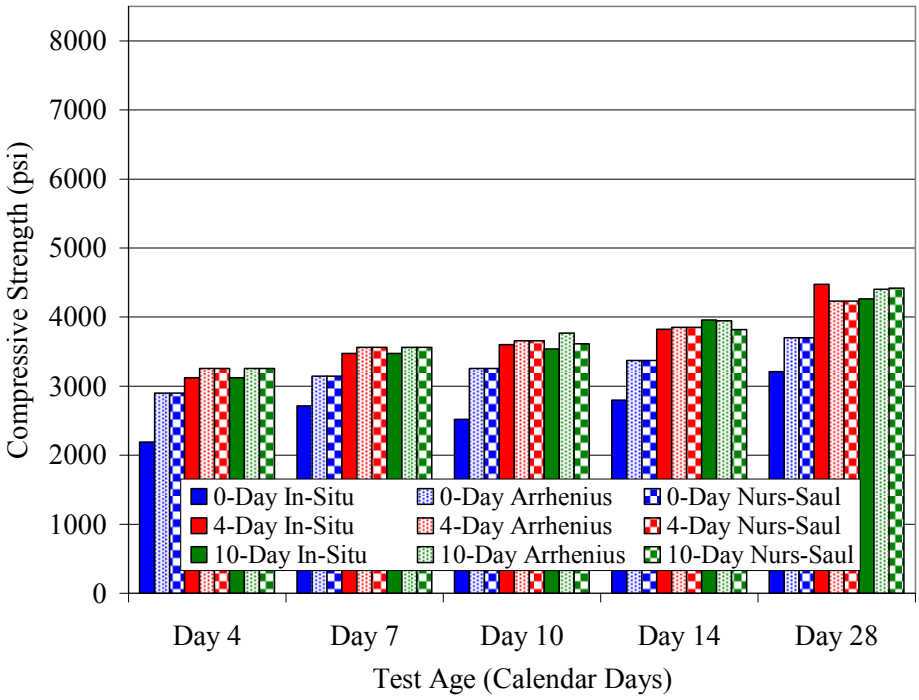

Figure 3.50 FTW In-Situ Strength Compared to FMAT Predicted Strength

Table 3.7 FTW In-Situ Strength Compared to FMAT Predicted Strength

		Test Age (Calendar Days)				
		4	7	10	14	28
0-day cure	In-Situ Strength (psi)	2191	2717	2517	2796	3210
	ARR Predicted Strength (psi)	2899	3144	3253	3373	3700
	% Error	32	16	29	21	15
	N-S Predicted Strength (psi)	2791	3054	3218	3359	3788
	% Error	27	12	28	20	18
4-day cure	In-Situ Strength (psi)	3122	3470	3603	3824	4477
	ARR Predicted Strength (psi)	3256	3563	3659	3851	4229
	% Error	4	3	2	1	6
	N-S Predicted Strength (psi)	3037	3360	3566	3747	4290
	% Error	3	3	1	2	4
10-day cure	In-Situ Strength (psi)	–	–	3540	3959	4262
	ARR Predicted Strength (psi)	–	–	3767	3949	4401
	% Error	–	–	6	1	3
	N-S Predicted Strength (psi)	–	–	3614	3817	4419
	% Error	–	–	2	4	4

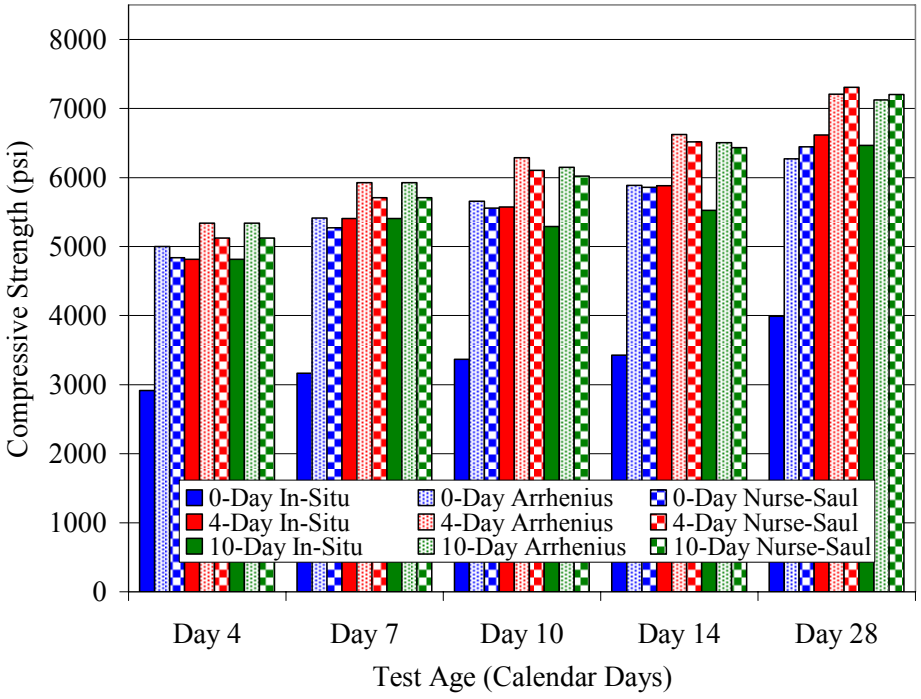

Figure 3.51 SAT In-Situ Strength Compared to FMAT Predicted Strength

Table 3.8 SAT In-Situ Strength Compared to FMAT Predicted Strength

		Test Age (Calendar Days)				
		4	7	10	14	28
0-day cure	In-Situ Strength (psi)	2917	3167	3365	3429	3989
	ARR Predicted Strength (psi)	5001	5411	5658	5886	6272
	% Error	71	71	68	72	57
	N-S Predicted Strength (psi)	4839	5271	5557	5860	6442
	% Error	66	66	65	71	62
4-day cure	In-Situ Strength (psi)	4815	5404	5572	5882	6616
	ARR Predicted Strength (psi)	5340	5927	6290	6624	7205
	% Error	11	10	13	13	9
	N-S Predicted Strength (psi)	5122	5710	6102	6514	7310
	% Error	6	6	10	11	11
10-day cure	In-Situ Strength (psi)	–	–	5290	5525	6464
	ARR Predicted Strength (psi)	–	–	6148	6504	7122
	% Error	–	–	16	18	10
	N-S Predicted Strength (psi)	–	–	6022	6432	7202
	% Error	–	–	14	16	11

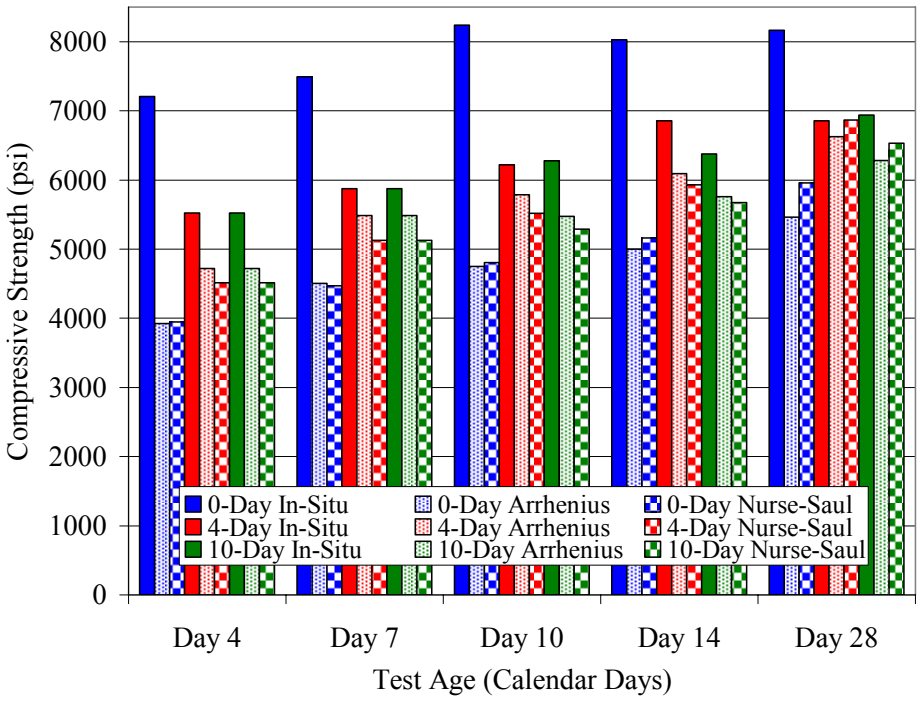

Figure 3.52 HOU In-Situ Strength Compared to FMAT Predicted Strength

Table 3.9 HOU In-Situ Strength Compared to FMAT Predicted Strength

		Test Age (Calendar Days)				
		4	7	10	14	28
0-day cure	In-Situ Strength (psi)	7206	7489	8237	8027	8165
	ARR Predicted Strength (psi)	3924	4506	4749	4998	5463
	% Error	46	40	42	38	33
	N-S Predicted Strength (psi)	3949	4471	4807	5161	5961
	% Error	45	40	42	36	27
4-day cure	In-Situ Strength (psi)	5521	5872	6223	6854	6855
	ARR Predicted Strength (psi)	4720	5483	5788	6092	6629
	% Error	15	7	7	11	3
	N-S Predicted Strength (psi)	4517	5127	5519	5932	6866
	% Error	18	13	11	14	1
10-day cure	In-Situ Strength (psi)	–	–	6275	6375	6937
	ARR Predicted Strength (psi)	–	–	5472	5759	6279
	% Error	–	–	13	10	10
	N-S Predicted Strength (psi)	–	–	5291	5672	6534
	% Error	–	–	16	11	6

As shown in Figures 3.50 through 3.52, predicted strengths from developed strength-maturity curves for the 0-day cure sections deviate drastically from the in-situ strengths of the bridge deck. This is a result of not providing any type of moist curing to the surface of the deck after the initial pour and only applying a curing compound. Apparently, the curing compound did not provide adequate protection against moisture loss for the 0-day cure portion of the deck slab during the first 24 hours of hydration, which is a critical period during hardening and strength gain for concrete. On the other hand, the 0-day cure cylinders were capped after preparation for the initial 24 hours after the pour. By preventing moisture loss for the 0-day cure cylinders during the first 24 hours, adequate concrete hydration occurred from the concrete mix water and resulted in higher strength gains for these cylinders, thus higher strength data was used to develop strength-maturity curves. As a result of higher strength data for the 0-day cure FMAT cylinders, strength-maturity curves developed using either the FH or LN strength gain models predicted higher strengths for the bridge deck.

From Figures 3.50 and 3.51 and referring to Tables 3.7 and 3.8, predicted strengths for the 0-day cure section, whether using the Arrhenius (FH model) or Nurse-Saul (LN model) functions, were higher than actual in-situ strengths for the section. Predicted strengths for the Fort Worth and San Antonio bridge decks deviated anywhere from 12 to 72% of in-situ 4-inch diameter core strengths.

In contrast, predicted strengths for the 0-day cure Houston bridge deck were actually lower than those of the actual in-situ bridge deck strength with no curing. The deviation for the 0-day cure Houston bridge deck ranged anywhere from 27 to 46% of actual in-situ strength. Also, it is seen in Figure 3.49 that 0-day cure sections of the bridge deck had higher compressive strengths than the 4- and 10-day cure sections. This observation was not expected as it is normally believed

that concrete with some curing would have higher compressive strengths than concrete with no curing. Reasons for this discrepancy could be due to any, or a combination, of the following: (a) high relative humidity at the Houston site resulting in ongoing curing for the 0-day cure section and (b) lack of quality control of the delivered concrete. Most of the Houston bridge deck (i.e., 4-, 10-, and 14-day cure sections), FMAT and CONVT cylinders were poured with a concrete mix having a slump of 6 inches, which deviated from the 3 ½-inch design slump. The remaining sections (0- and 2-day cure sections) were poured from a concrete mix having a slump of 4 inches – though the second mix delivered from the plant should have been identical to the first.

When comparing the strength predictions for the 4- and 10-day cure sections, it was observed that deviations from the in-situ strength were much less when compared to the 0-day cure section. For the 4- and 10-day cure sections, the predicted strength errors ranged anywhere from 0.3 to 17.7% and 1.0 to 16.4% with the use of the Arrhenius and Nurse-Saul functions, respectively. Even with lower percentage errors for the 4- and 10-day cure sections, it was evident that error percentages were still somewhat large when compared to errors for the Fort Worth and San Antonio concrete mixes. Usually a percentage error of 10% or less would seem to be more desirable, even though currently there is no known rule of thumb or guideline to determine an acceptable percentage error.

For instance, the strength predictions for the 4- and 10-day cure section of the Fort Worth bridge deck were very similar to the in-situ concrete strength. The 4- and 10-day cure strength predictions only varied 1 to 6% from in-situ strength using either the Arrhenius or Nurse-Saul functions as shown in Table 3.7. With percentage errors at or below 6% for the 4- and 10-day cure sections of the Fort Worth bridge deck, one is inclined to have confidence in using the maturity method as a means to predict in-place strength. Note that this agreement is much closer than was found using traditional cylinder breaks.

Predicted strength percentage errors for the San Antonio and Houston bridge decks were slightly larger than those for the Fort Worth bridge deck. The percentage differences between the predicted strengths and the 4- and 10-day cure San Antonio in-situ strengths ranged from 6 to 18% using either the Arrhenius or Nurse-Saul functions with their respective strength gain models. For Houston, the differences ranged from 1 to 18%.

Although, there are some percentage errors above 10% for the San Antonio and Houston bridge deck, most of the percentages fall below the 15%. Of the predicted strengths, only 5 of the 32 strengths had percentage errors greater that 15%. In fact, 27 of the 32 predictions had an error of 15% or less. Again, since there is no guideline to determine an acceptable error, engineering judgment should be used to determine if these errors would be acceptable.

As observed, percentage errors varied for each of the test sites and could be a result of scatter of the 4-inch diameter in-situ core or FMAT cylinder strength data. The compressive strength data for in-situ cores and FMAT cylinders is shown in Appendix A and B respectively. Referring to Tables 3.7 through 3.9, one should notice that some of the in-situ strengths for earlier test dates have higher compressive strengths than for later test dates. For instance on the 0-day cure section for the Fort Worth Deck (Table 3.7), compressive strengths of 2717 and 2517 psi were attained on Day 7 and 10, respectively. Of course, it is highly unlikely that concrete compressive strength actually went down. In this case, it is theorized that the variability of concrete strengths

is a result of poor concrete placement practices such as lack of consolidation when vibrating concrete, variability of current testing practices, and/or the non-homogeneous nature of concrete.

Also, concrete mixes used for the bridge deck did not necessarily reflect the actual mix design as stated in the specifications. For example, the Houston concrete mix specified a 3 ½-inch design slump, but the trucks delivered a concrete mix with slumps of 6 and 4 inches. On numerous occasions, extra water was added to the concrete mix, as is common practice when placing concrete in the field. Adding extra water to the mix was usually the decision of the contractor in order to increase the workability of the concrete.

Although it is obvious that there was a lack of quality control during concrete placement, it was not the intent of this project to monitor quality control. The objective of the overall project is to determine appropriate wet mat curing durations to ensure durability of concrete with current concrete placement practices. This meant having contractors pour concrete in the same manner as would be done on any other construction project. As a result of the variability of field practices, Texas Tech researchers believed it would be beneficial to perform lab tests on these same mixes.

3.3.2 LMAT Predicted Strength

With two different sets of prediction models (i.e. FMAT and LMAT generated strength-maturity curves), a comparison could be made to determine which prediction model best predicted the in-situ strength of the bridge deck. Comparison of the predicted strengths from the FMAT and LMAT generated strength-maturity curves based on the Arrhenius and Nurse-Saul functions to the in-situ concrete strength are presented in Figures 3.53 through 3.58 and Tables 3.10 through 3.15.

Figure 3.55 and 3.58, along with Tables 3.12 and 3.15; also show a comparison of the predicted strengths for only the LMAT generated strength-maturity curves to in-situ concrete strengths for the El Paso bridge deck. As mentioned earlier, the El Paso site was one of the sites without FMAT cylinders and thus only an evaluation is made between LMAT cylinders and the bridge deck.

As discussed earlier, predicted strengths from the LMAT generated strength-maturity curves should be higher than in-situ concrete strengths. Again, this difference could be associated with the specific concrete placement practices employed. Usually additional water was added to the concrete mix at the site. The resulting increase in water to cement ratio gave lower strengths when compared to strengths associated with lab mixed concrete.

Analyzing the prediction values for developed LMAT strength-maturity curves, one can observe that all strength predictions were higher than actual field samples for all cases with the exception of the 4-day cure lab cylinders for the San Antonio mix. Referring back to the LMAT generated strength-maturity curves, one can see that the 4-day cure strength trend varied from the 7- and 10-day cure cylinders, as opposed to the general trend observed for all other developed strength-maturity curves whether generated from FMAT or LMAT cylinders. One may conclude that the batch for preparation of the 7- and 10-day cure cylinders could have had a lower water-cement ratio than batches for the 0- and 4-day cure LMAT cylinders, thus resulting in higher strengths

for the 7- and 10-day cure LMAT cylinders. When comparing strengths from the 4-day cure LMAT strength-maturity curve and in-situ strength for the San Antonio mix in Tables 3.11 and 3.14, observed percentage errors ranged from 6% to 11% and 3% to 13% for the Arrhenius and Nurse-Saul functions, respectively.

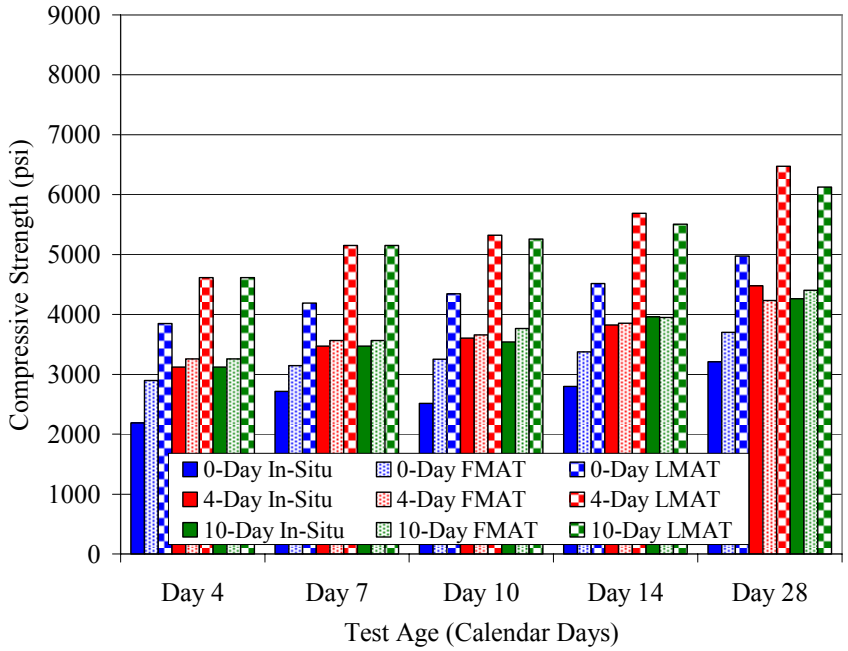

Figure 3.53 FTW In-Situ Compared to FMAT and LMAT Predicted Strength (FH Model)

Table 3.10 FTW In-Situ Compared to LMAT Predicted Strength – FH Model

		Test Age (Calendar Days)				
		4	7	10	14	28
0-day cure	In-Situ Strength (psi)	2191	2717	2517	2796	3210
	In-Situ Equivalent Age (hrs)	198.2	287.1	341.8	418.1	771.0
	LMAT Predicted Strength (psi)	3848	4193	4346	4515	4975
	% Error	75.6	54.3	72.7	61.5	55.0
4-day cure	In-Situ Strength (psi)	3122	3470	3603	3824	4477
	In-Situ Equivalent Age (hrs)	203.5	291.8	329.9	428.8	788.0
	LMAT Predicted Strength (psi)	4618	5150	5326	5691	6475
	% Error	47.9	48.4	47.8	48.8	44.6
10-day cure	In-Situ Strength (psi)	**	**	3540	3959	4262
	In-Situ Equivalent Age (hrs)	**	**	328.7	407.8	763.6
	LMAT Predicted Strength (psi)	**	**	5257	5509	6124
	% Error	**	**	48.5	39.1	43.7

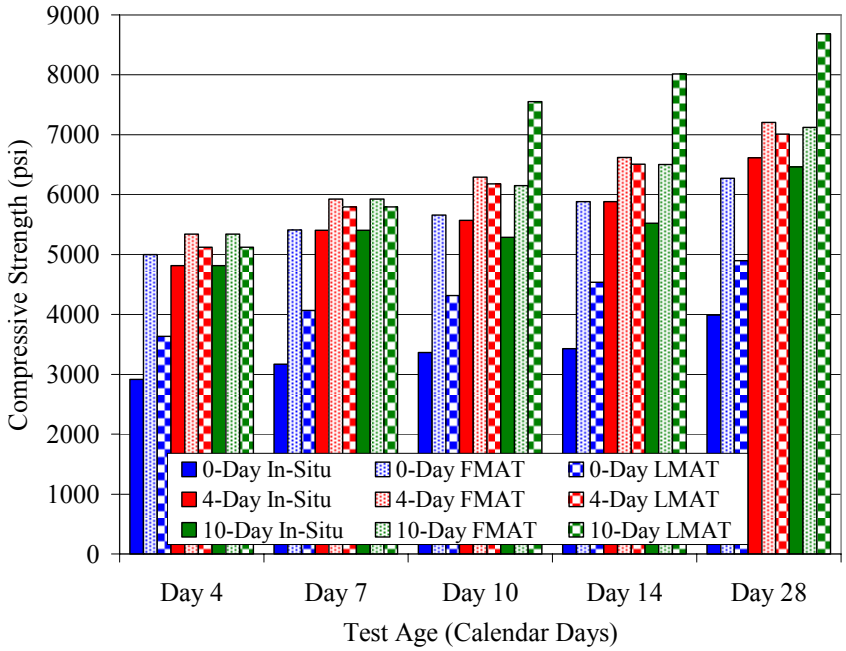

Figure 3.54 SAT In-Situ Compared to FMAT and LMAT Predicted Strength (FH Model)

Table 3.11 SAT In-Situ Compared to LMAT Predicted Strength – FH Model

		Test Age (Calendar Days)				
		4	7	10	14	28
0-day cure	In-Situ Strength (psi)	2917	3167	3365	3429	3989
	In-Situ Equivalent Age (hrs)	210.3	337.9	467.0	651.0	1276.8
	LMAT Predicted Strength (psi)	3637	4064	4314	4537	4897
	% Error	24.7	28.3	28.2	32.3	22.8
4-day cure	In-Situ Strength (psi)	4815	5404	5573	5882	6616
	In-Situ Equivalent Age (hrs)	216.5	345.9	477.1	660.4	1283.2
	LMAT Predicted Strength (psi)	5122	5796	6180	6507	7013
	% Error	6.4	7.3	10.9	10.6	6.0
10-day cure	In-Situ Strength (psi)	–	–	5290	5525	6464
	In-Situ Equivalent Age (hrs)	–	–	485.3	679.5	1305.6
	LMAT Predicted Strength (psi)	–	–	7555	8017	8688
	% Error	–	–	42.8	45.1	34.4

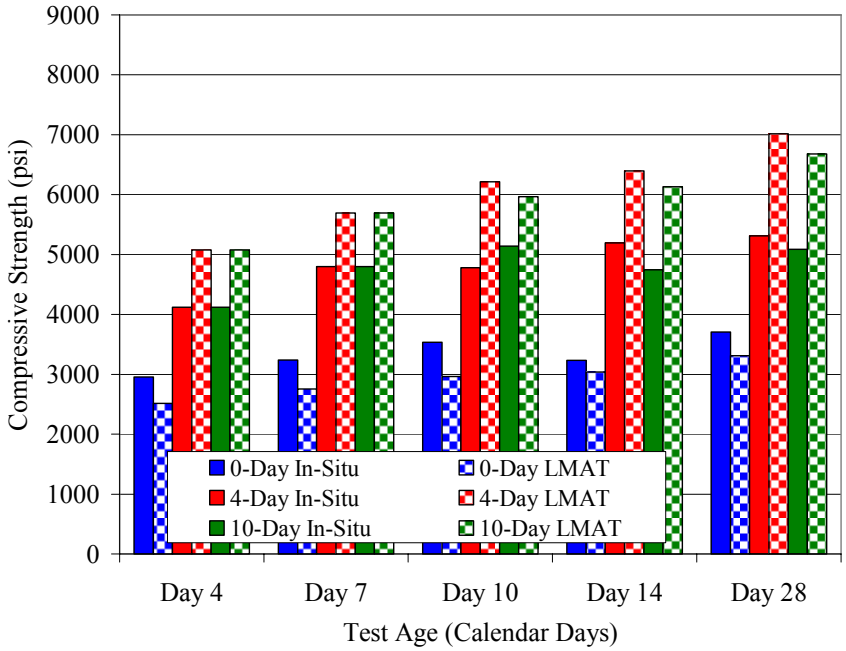

Figure 3.55 ELP In-Situ Compared to LMAT Predicted Strength (FH Model)

Table 3.12 ELP In-Situ Compared to LMAT Predicted Strength – FH Model

		Test Age (Calendar Days)				
		4	7	10	14	28
0-day cure	In-Situ Strength (psi)	2958	3239	3535	3233	3707
	In-Situ Equivalent Age (hrs)	258.7	383.2	555.7	645.6	1200.0
	LMAT Predicted Strength (psi)	2513	2758	2963	3039	3311
	% Error	15.1	14.9	16.2	6.0	10.7
4-day cure	In-Situ Strength (psi)	4120	4800	4783	5193	5311
	In-Situ Equivalent Age (hrs)	262.9	383.4	554.3	643.4	1198.5
	LMAT Predicted Strength (psi)	5075	5697	6213	6397	7020
	% Error	23.2	18.7	29.9	23.2	32.2
10-day cure	In-Situ Strength (psi)	**	**	5139	4742	5086
	In-Situ Equivalent Age (hrs)	**	**	540.6	630.2	1193.2
	LMAT Predicted Strength (psi)	**	**	5964	6129	6679
	% Error	**	**	16.1	29.2	31.3

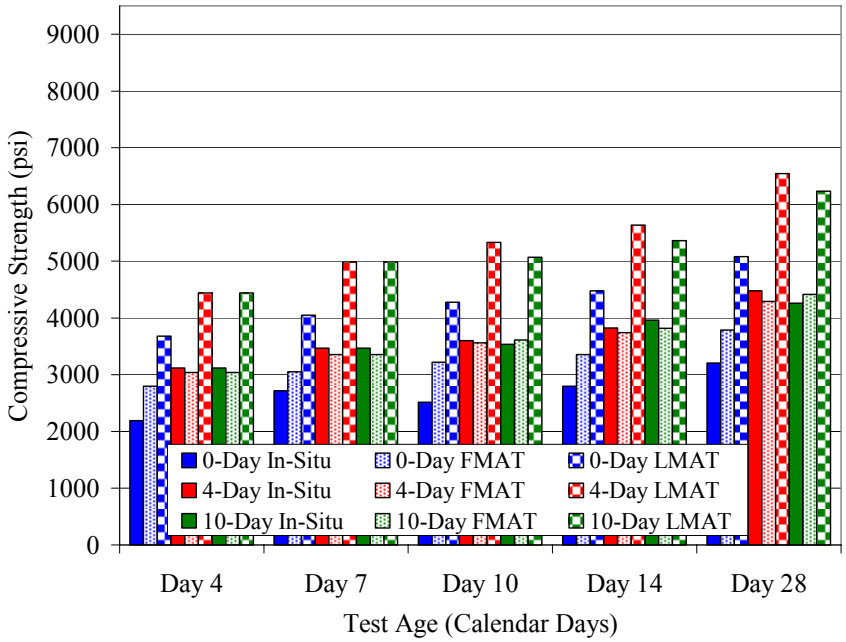

Figure 3.56 FTW In-Situ Compared to FMAT and LMAT Predicted Strength (LN Model)

Table 3.13 FTW In-Situ Compared to LMAT Predicted Strength – LN Model

		Test Age (Calendar Days)				
		4	7	10	14	28
0-day cure	In-Situ Strength (psi)	2191	2717	2517	2796	3210
	In-Situ Equivalent Age (hrs)	165.8	245.3	314.1	388.6	742.3
	LMAT Predicted Strength (psi)	3684	4050	4281	4480	5084
	% Error	68.1	49.0	70.1	60.2	58.4
4-day cure	In-Situ Strength (psi)	3122	3470	3603	3824	4477
	In-Situ Equivalent Age (hrs)	167.5	246.2	314.6	390.2	745.4
	LMAT Predicted Strength (psi)	4444	4987	5332	5635	6547
	% Error	42.4	43.7	48.0	47.4	46.2
10-day cure	In-Situ Strength (psi)	**	**	3540	3959	4262
	In-Situ Equivalent Age (hrs)	**	**	306.7	382.6	736.8
	LMAT Predicted Strength (psi)	**	**	5070	5363	6233
	% Error	**	**	43.2	35.5	46.2

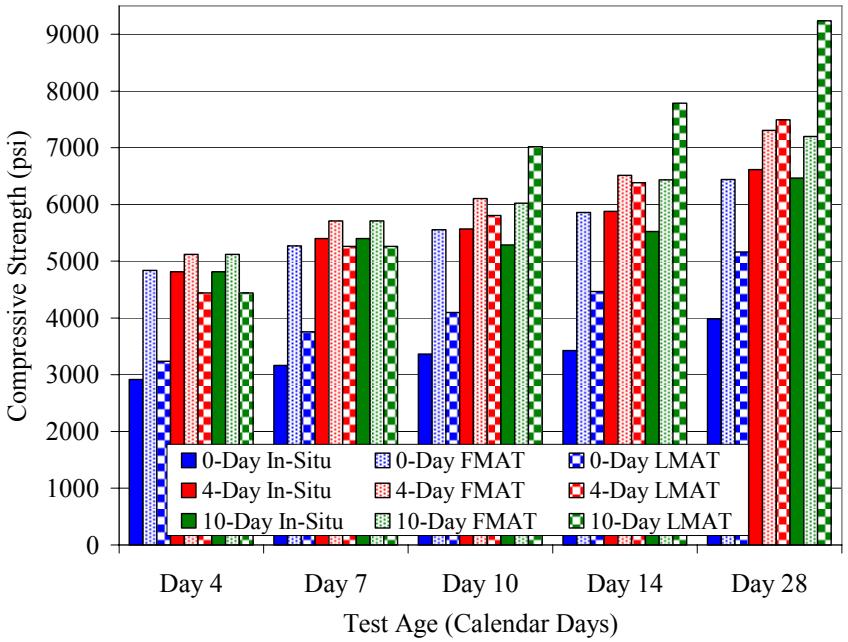

Figure 3.57 SAT In-Situ Compared to FMAT and LMAT Predicted Strength (LN Model)

Table 3.14 SAT In-Situ Compared to LMAT Predicted Strength – LN Model

		Test Age (Calendar Days)				
		4	7	10	14	28
0-day cure	In-Situ Strength (psi)	2917	3167	3365	3429	3989
	In-Situ Equivalent Age (hrs)	157.4	259.4	361.1	512.2	1004.4
	LMAT Predicted Strength (psi)	3239	3758	4101	4464	5163
	% Error	11.1	18.7	21.9	30.2	29.4
4-day cure	In-Situ Strength (psi)	4815	5404	5572	5882	6616
	In-Situ Equivalent Age (hrs)	160.6	263.1	365.8	516.8	1007.9
	LMAT Predicted Strength (psi)	4440	5261	5809	6384	7494
	% Error	7.8	2.6	4.2	8.5	13.3
10-day cure	In-Situ Strength (psi)	**	**	5290	5525	6464
	In-Situ Equivalent Age (hrs)	**	**	370.1	525.9	1018.5
	LMAT Predicted Strength (psi)	**	**	7018	7790	9241
	% Error	**	**	32.7	41.0	43.0

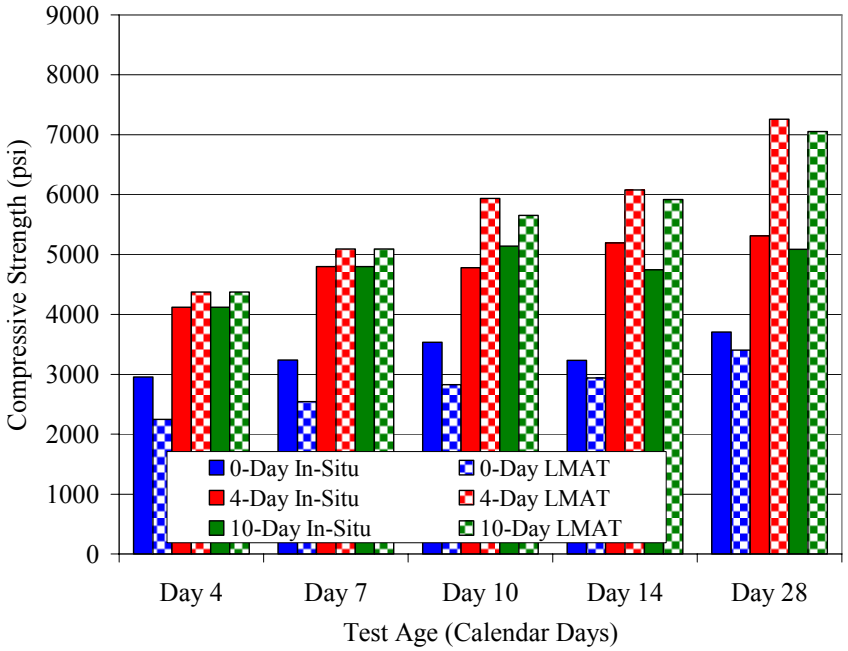

Figure 3.58 ELP In-Situ Compared to LMAT Predicted Strength (LN Model)

Table 3.15 ELP In-Situ Compared to LMAT Predicted Strength – LN Model

		Test Age (Calendar Days)				
		4	7	10	14	28
0-day cure	In-Situ Strength (psi)	2958	3239	3535	3233	3707
	In-Situ Equivalent Age (hrs)	190.8	287.4	428.4	499.7	966.0
	LMAT Predicted Strength (psi)	2250	2543	2828	2937	3408
	% Error	23.9	21.5	20.0	9.1	8.1
4-day cure	In-Situ Strength (psi)	4120	4800	4783	5193	5311
	In-Situ Equivalent Age (hrs)	193.2	288.4	462.8	500.2	967.8
	LMAT Predicted Strength (psi)	4374	5091	5938	6077	7259
	% Error	6.2	6.1	24.2	17.0	36.7
10-day cure	In-Situ Strength (psi)	**	**	5139	4742	5086
	In-Situ Equivalent Age (hrs)	**	**	424.3	495.6	966.4
	LMAT Predicted Strength (psi)	**	**	5654	5917	7050
	% Error	**	**	10.0	24.8	38.6

3.4 Strength Comparison between 4 and 14 - Day Cure Concrete

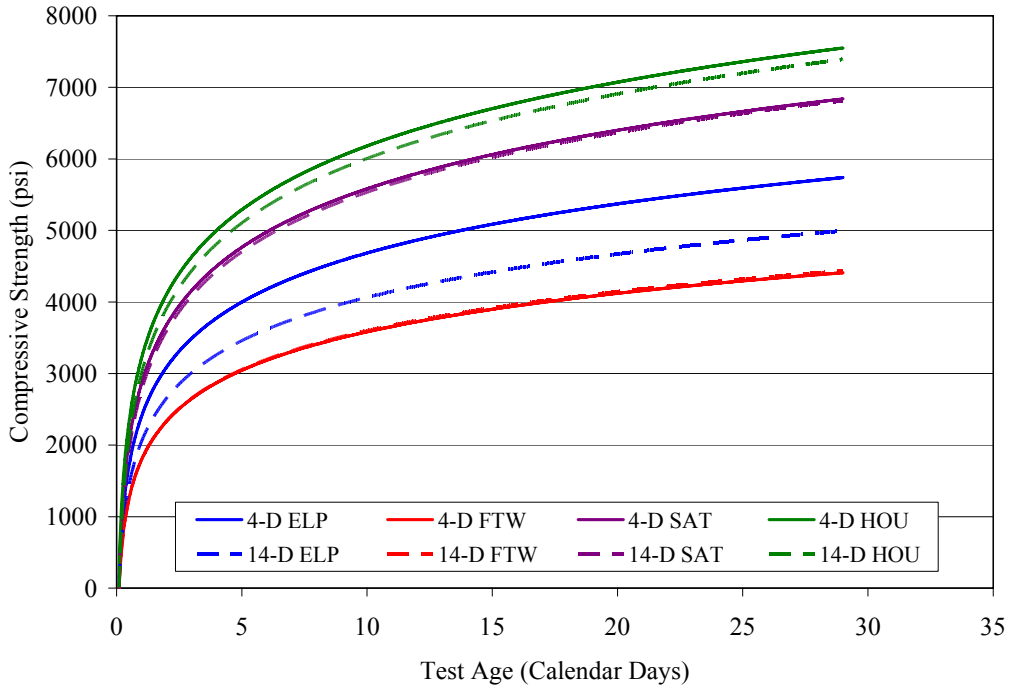

Figure **3.59** 4-Day and 14-Day Cure In-Situ Strength Comparison

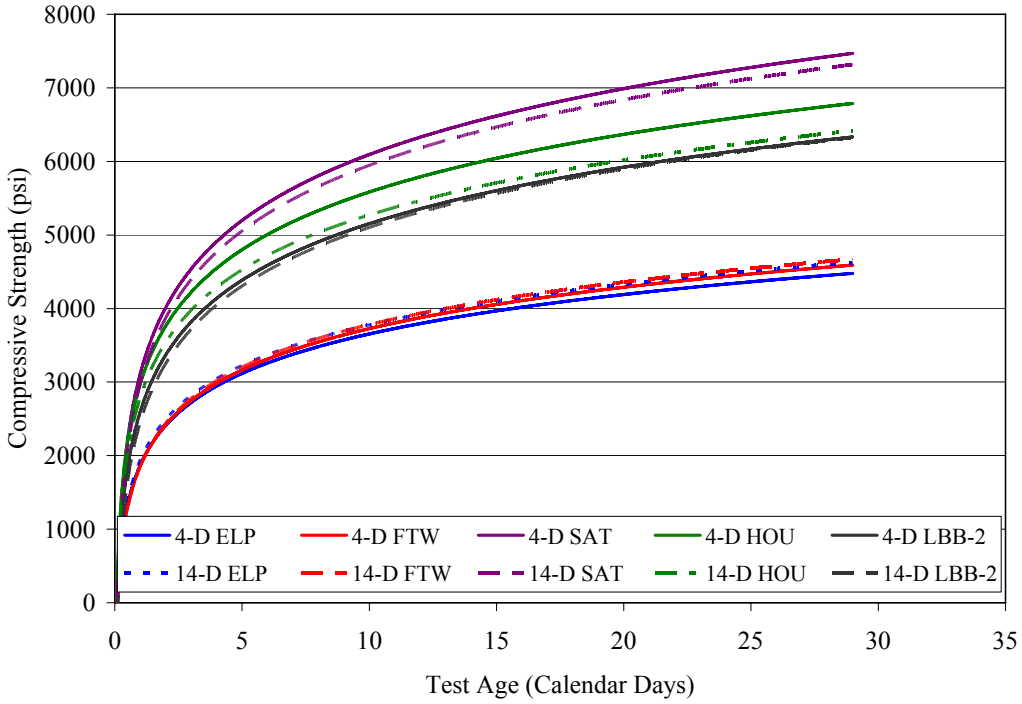

Figure 3.60 4-Day and 14-Day Cure Field Cylinder Strength Comparison

CHAPTER 4
EXPERIMENTAL PLAN FOR COMPARATIVE ASSESSMENT OF THREE CURING METHODS

As discussed in the previous chapter, concrete strength assessment based on the maturity method can lead to a misrepresentation of in situ strength. Thus, an erroneous evaluation of durability can be made if strength is used as the primary indicator of such assessment. Therefore, the objective of this portion of the study is to make changes to the maturity method by considering moisture presence during hydration for a better indicator of concrete strength and durability.

Results from the previous portion of this study demonstrated a comparable correlation between strength and permeability resistance. Increased strength typically indicated a less permeable concrete. Low permeability concrete was usually produced by subjecting the specimen to some period of moist curing, (e.g. 4 days or more of moist curing). Therefore, the presence of moisture during hydration proves to be critical for adequate permeability resistance and in turn, strength development. As part of this portion of the study, concrete moisture is monitored during the curing process to help determine a relationship between maturity, strength, and permeability.

The following sections describe the procedures used to accomplish the objectives of this study. The experimental setup included testing a single concrete mixture typically used in the Amarillo (AMA) District. The components of the six-sack concrete mixture used for this portion of the study are listed in Table 4.1. This mixture was subjected to varying curing durations and different moist cure treatments. Details of the cure durations and moist cure treatments are discussed in later sections.

As part of data collection, internal concrete temperature and moisture were monitored during curing with numerous sensors. Physical properties of the concrete mixtures such as strength and permeability were determined from core samples and prepared test specimens. Temperature and moisture data will aid in establishing relationships between strength, permeability, and maturity properties. This data and the correlations from this portion of the investigation are discussed in the subsequent chapter.

Table 4.1 Amarillo Concrete Mixture

Mix Description	AMA	
Cement	*Type*	I/II
	Quantity	367 lbs
Mineral Admixture	*Type*	Fly Ash C
	Quantity	158 lbs
Cement Replacement[1]	35%	
Coarse Aggregate	*Type*	Siliceous Gravel
	Quantity	1976 lbs
Fine Aggregate	*Quantity*	1231 lbs
W/(C+P)	0.40	
Air	5%	

[1] Cement replacement by volume

4.1 Laboratory Setup

The experimental setup for this investigation was performed in February 2004 in the structures laboratory at Texas Tech University. Although the placed concrete was shielded from environmental elements, (i.e., snow, wind, rain, and sunlight), the experiment was not in a totally controlled environment. Atmospheric ambient conditions coupled with existing ongoing experimental work in the structures laboratory, (e.g. leaving overhead door open to move items in and out of the laboratory), caused internal laboratory temperature and relative humidity to fluctuate at times.

4.1.1 Slab Descriptions

Three concrete slabs were placed and cured in the laboratory conditions just described. Each concrete slab was 18-feet long, 4-feet wide and 4 ½-inches thick. The slabs were elevated approximately six inches from the laboratory floor by resting plywood formwork on steel C-channels. This slab elevation was the only option at the time of testing. The slab was sloped longitudinally approximately 1.5% by adjusting the height of the steel C-channels with wood blocks and shims. By elevating and sloping the slabs, the accumulation of humidity underneath the slab was minimized and proper surface water drainage was provided.

Each slab was divided into six sections, similar to the previously tested bridge deck sites. Each section had an area of 3 feet by 4 feet and 4 ½-inches thick. Reinforcement mats were placed in each section. Number 4 rebar was spaced 9 inches center-to-center in the overall longitudinal direction of the slab while number 5 rebar was spaced 6 inches on center in the transverse direction. Slab bolsters were used to maintain the rebar mat 1 ½-inches from the bottom of the formwork. To help establish the proper slab thickness, a ¾-inch chamfer strip was used to outline the top surface perimeter of each section. The formwork and rebar layout for the slabs are shown in Figures 4.1 and 4.2, respectively.

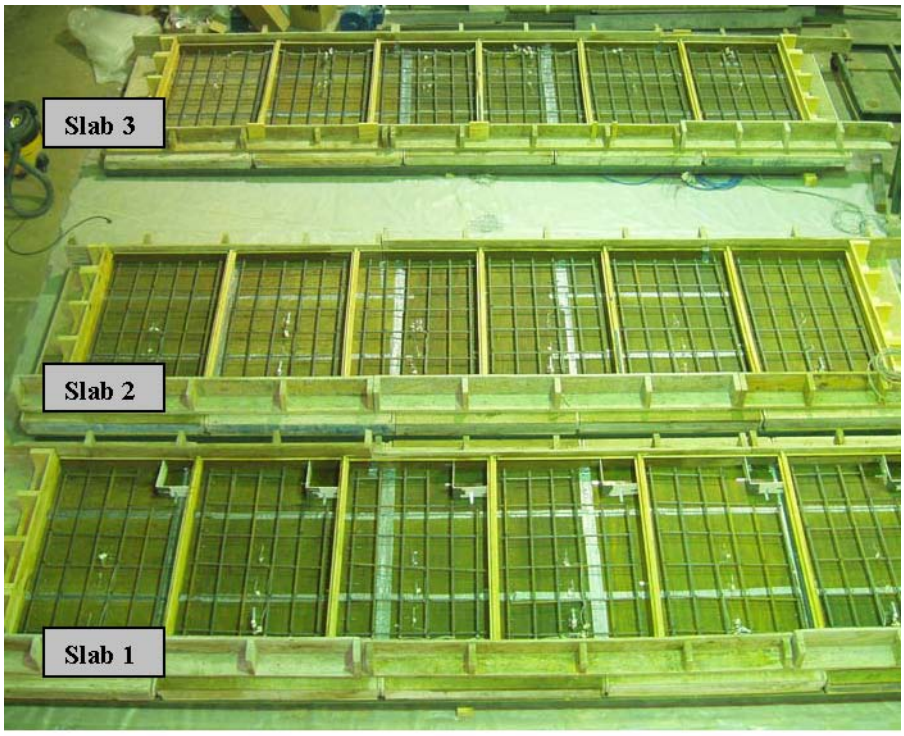

Figure 4.1 Slab Arrangement in Structures Laboratory.

Figure 4.2 Rebar Layout of Slab Arrangement in Structures Laboratory

4.1.2 Temperature and Moisture Sensors

Since temperature and moisture are of interest during curing, each slab was instrumented with thermocouples and a number of digital temperature/moisture sensors. Thermocouples were made from type "T" shielded copper-constantan wire. The ends of thermocouple wires were protected from corrosion with heat-shrink tubing. Relative humidity within the slabs was

measured with SHT75 temperature and humidity sensors from Sensirion. These sensors record relative humidity (RH) within ± 2% between the range of 10% to 90% RH and recorded temperature within ± 3 °F between the range of 40°F to 200°F. The two types of sensors used for instrumentation are shown in Figure 4.3.

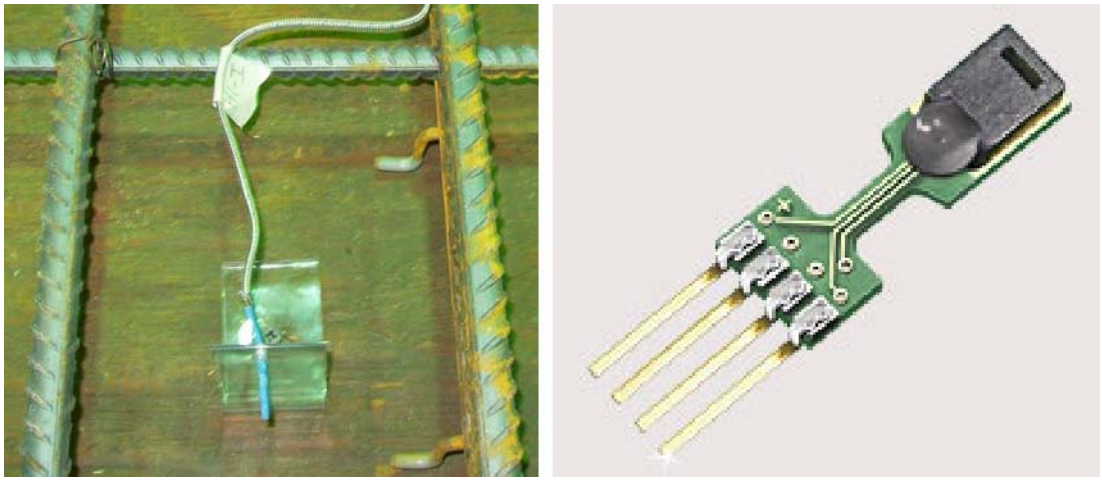

(a) Type "T" thermocouple (b) Sensirion digital moisture sensor

Figure 4.3 Data Acquisition Sensors

To protect the digital chip sensor during concrete placement and from direct exposure to plastic concrete, each sensor was housed in PVC tubing. The tubing was ½inch in diameter and 4-inches long with a nylon screen attached to one end with duct tape. The nylon screen was used to prevent direct contact between the concrete and sensor, yet allowed the internal concrete humidity and temperature to be measured. Sensors were inserted through the open end of the tubing to approximately ½-inch from the nylon screened end. The open end of the PVC tubing was sealed with plumber's putty to secure the sensor wire in place and to prevent concrete from reaching the housed digital chip sensor. Digital sensor depths were maintained by securing the PVC housing with Plexiglas brackets as shown in Figure 4.4.

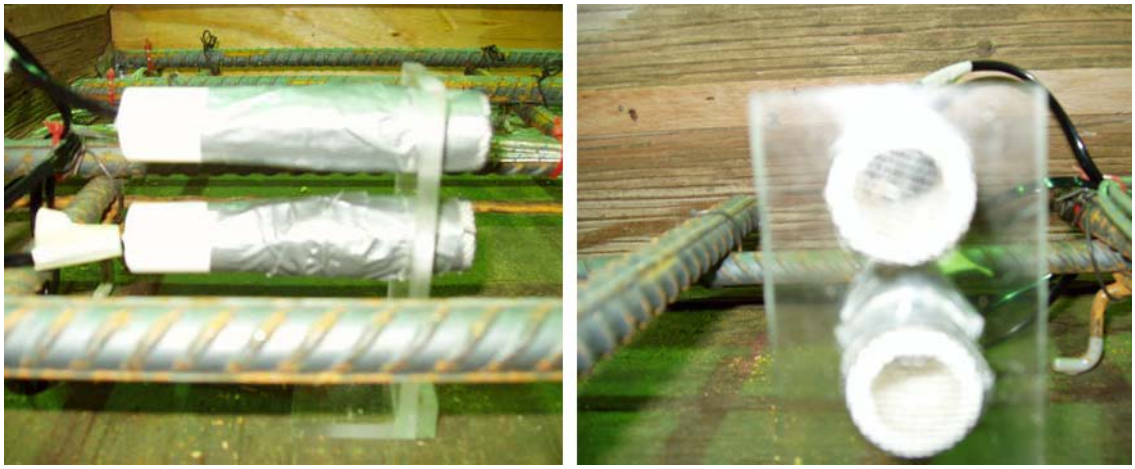

(a) Side view (b) Front view

Figure 4.4 Digital Chip Sensor Enclosures

Data was recorded continuously to either a data logger or a computer hard drive for both type "T" thermocouple and SHT75 sensors. All lead wires from the sensors were secured to the steel reinforcement with zip ties and routed towards the exterior of the slab. Lead wires were bundled and connected to their respective channel inputs at the data acquisition hub as shown in Figure 4.5.

Figure 4.5 Data Acquisition Hub

Type "T" thermocouples were placed at mid-depth and in the center of the rebar grid in locations of the slab as shown in Figure 4.6 (rebar location is shown with a dashed line). The depth of thermocouples was maintained by inserting thermocouple ends through a secured plastic bracket as depicted in Figure 4.3a.

Due to the high cost of Sensirion digital sensors, only 20 sensors were purchased. These sensors were placed in select sections of the slab, for 0-, 4-, and 10-day cures. Sensirion sensors were placed near the longitudinal edge of the slabs. Sensors along the edge were at two different depths, mid-depth (approximately 2 ¼-inches below the surface) and 1-inch below the surface. The digital Sensirion sensors were also placed at mid-depth in the center of the 10-day cure section for slabs 2 and 3 (i.e. "throw-on" and mist cure slabs, respectively, as described in the next section). A typical layout identifying sensor locations is shown in Figure 4.6.

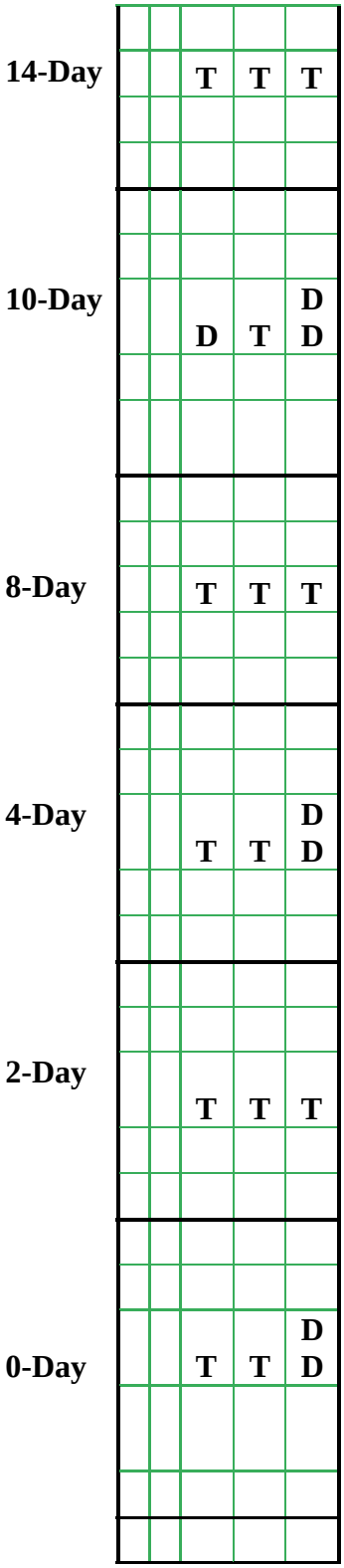

Figure 4.6 Typical Layout Identifying Sensor Locations

All sensors are placed at mid-depth and center of rebar grid. Where D appears twice within a cell, sensors are placed at mid-depth and 1-in below concrete surface.

LEGEND	
T =	Type "T" thermocouple
D =	Digital temperature/moisture sensor

DIMENSIONS
Total slab is 18' x 4'
Each slab is divided into 6 sections
Each section is 3' x 4'

4. 2 Cure Treatments

Work presented in this chapter investigates varying moist-cure durations as well as three different types of curing treatments. Each cure treatment is applied to its respective slab for durations of 0, 2, 4, 8, 10, and 14 days. Different cure treatments are studied to evaluate any 0-2116-4A

differences in concrete property development. The three cure treatments applied to the slabs are referred to as either conventional, "throw-on," or "mist." These are described in more detail in subsequent sections. Two areas of interest are a) the availability or presence of moisture and b) the retention of heat during hydration each of the cure treatments and durations provide.

4.2.1 Conventional Cure

The conventional moist cure treatment is the same treatment used in previous detailed work. After placement of concrete, the surface was finished with a broom texture. Type I-D pink-pigmented curing compound was applied to the concrete surface approximately 45 minutes to 1 hour after placement. Once final set of the concrete is achieved, approximately 3 hours after placement, saturated cotton mats were placed on the concrete surface and covered with 4 mil thick polyethylene sheeting. Curing media was kept in place for durations of 2, 4, 8, 10, and 14 days. After a section of a slab received its predetermined duration cure, curing media were removed and the concrete was exposed to laboratory conditions. The 0-day cure section of the conventional cure slab received a curing compound treatment but no additional moist curing. The conventional cure slab prior to covering with wet mats and polyethylene is shown in Figure 4.7.

Figure 4.7 Conventional Slab with Curing Compound Prior to Wet Mat Placement

4.2.2 Throw-On Cure

The second treatment used is referred to as a "throw-on" cure. Once the concrete in each section was placed and floated, saturated cotton mats were placed on the smooth finished surface and covered with polyethylene. Curing compound was not applied to any surfaces of the "throw-on" slab. Moisture in the cotton mats was retained with polyethylene and periodic cotton mat soaking. Curing media was in place for the durations of 2, 4, 8, 10, and 14 days on certain

sections of the slab. The 0-day cure section of this slab had a smooth finish with no curing compound or moist cure treatment applied. This section was exposed to laboratory conditions at all times and evaporation of mix water was not deterred. The "throw-on" cure slab prior to polyethylene sheet placement is shown in Figure 4.8.

Figure 4.8 "Throw-on" Cure Slab with Saturated Cotton Mats

4.2.3 Mist Cure

The third treatment was a "mist" cure. After placement of concrete, each section was leveled, floated, and a broom finish applied. None of the sections of the slab received a curing compound application. Immediately after final finish of the surface, an elevated polyethylene sheeting canopy was set in place over individual sections. The misting canopy assembly was comprised of a wooden frame, plastic sheeting, and water misters. A hose and a number of water misters were secured to the interior of the wooden frame. The wooden frame was fitted with polyethylene sheeting to help prevent moisture loss. After placement of the misting canopy assemblies over concrete sections, care was taken to prevent any exposure to the atmosphere by securing overlapping polyethylene sheeting to formwork. Hoses from each of the canopies were connected to a water manifold. Water misters were turned on periodically within the first 24 hours when needed based on a visual inspection. A slight sheen of water on the concrete surface indicated saturated conditions.

Misting canopies were removed after the initial 24 hours and counted for 1 day of curing. After removal of misting canopies, saturated cotton mats and polyethylene sheets were placed over the curing concrete surfaces. This curing media was left in place for the remainder of the predetermined curing duration for each section. For example, the 4-day cure section received 1 day of mist canopy curing followed by 3 days of saturated cotton mat curing, (i.e. a total of 4 days of curing). The 0-day section of the "mist" cure slab was similar to the "throw-on" cure

slab as neither section received a curing compound application and was exposed to laboratory conditions throughout the investigation. The two differed since the 0-day section of the "mist" slab received a broom finish as opposed to the smooth finish of the "throw-on" slab. A misting canopy assembly and the "mist" cure slab after concrete placement are shown in Figure 4.9.

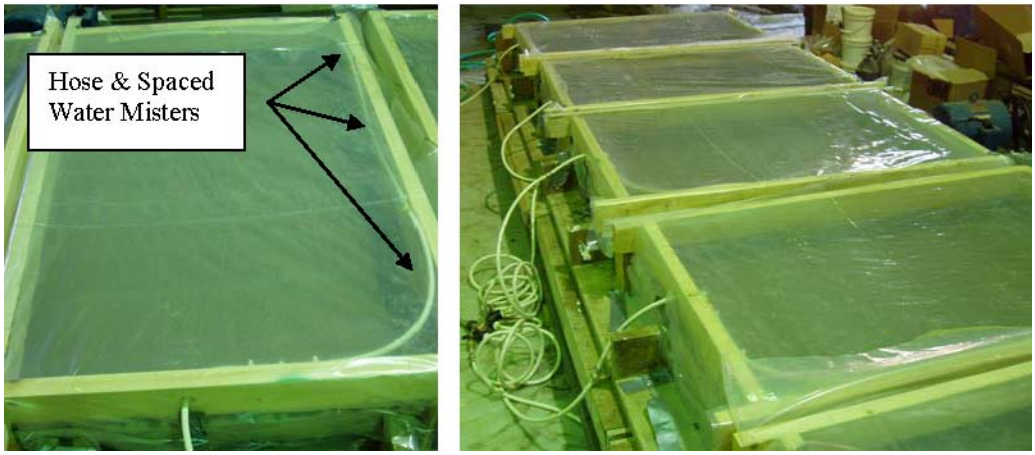

(a) Misting canopy assembly (b) Placed canopy assemblies

Figure 4.9 "Mist" Cure Slab

4.3 Concrete Test Specimens

In addition to the concrete slabs, numerous concrete test specimens were prepared and cured within the structures laboratory environment. Six-inch diameter cylinders and rectangular prismatic specimens were used to determine the strength and permeability properties of the AMA concrete mixture. These specimens, however, were not exposed to different cure treatments, but were exposed to different durations of curing in lime saturated water baths.

Over sixty six-inch diameter cylinders were cast from the AMA concrete mixture. ASTM C 192 procedures were followed in the preparation of test cylinders. Several cylinders were instrumented with thermocouples to monitor concrete curing temperatures. Once prepared, cylinders were capped with plastic lids to maintain moisture during the first 24 hours, which accounted for one day of curing. After this initial period, concrete cylinders receiving additional curing were removed from their plastic molds and submerged in a non-temperature controlled saturated lime water bath. Similar to sections of the slabs, sets of cylinders were cured for durations of 2, 4, 8, 10, and 14 days. The 0-day cylinders were subjected to laboratory ambient conditions once removed from their molds after the 24 hour period.

Ponding specimens were 12"x12"x4" prismatic slabs. Concrete was placed in two layers and consolidated sufficiently between layering. Surfaces received a smooth finish and were covered with polyethylene sheets for the first 24 hours to minimize mix water evaporation. After this period, samples were removed from their molds and submerged in a non-controlled temperature

lime bath for the remainder of their specified curing duration. Ponding samples were subjected to 2, 4, 8, 10, and 14 days of curing while the 0-day cure samples were exposed to the ambient conditions once removed from their molds. Test specimens for strength (6-inch diameter cylinder) and permeability (ponding slab) are shown in the following figures.

(a) Being prepared (b) Completed

Figure 4.10 Six-inch Test Cylinders

(a) Being prepared (b) Completed Figure

Figure 4.11 Ponding Slabs

4.3.1 Compressive Strength Sampling and Testing

In situ strength for the different cure methods was determined from 4-inch diameter cores. Samples were drilled with a portable coring machine fitted with a water-cooled diamond core bit (Figure 4.12a). During drilling, reinforcement bars were avoided by marking the reinforcement grid on the surface of the slabs (Figure 4.12b). Strength for a section on a given age was taken as

the average of 3 core samples. Compressive strengths for the slabs were determined for 4, 7, and 14 days of age.

(a) Portable coring machine (b) Cored slab section

Figure 4.12 Sampling Laboratory Bridge Deck Slabs

Although testing dates were set for 4, 7, and 14 days after casting, not all sections were accessible for sampling since curing media were still in place for sections incurring longer curing durations. Table 4.2 details the number of cores taken from a section on a specified test day. Compressive strength cores were typically tested 1 day after they had been removed from the slab. ASTM C 42 testing procedures were followed and the average strength for a section was determined from the average of three cores.

Table 4.2 Four-Inch Core Strength Sampling Schedule

Age	Curing Duration					
(days)	0-day	2-day	4-day	8-day	10-day	14-day
4	3	3	3	-	-	-
7	3	3	3	-	-	-
14	3	3	3	3	3	3

In addition to in situ slab strengths, concrete strengths were determined from standard 6-inch diameter cylinders. A schedule detailing the number of cylinders tested for a particular age is shown in the following table. Cylinders were tested for compressive strength at ages of 1, 3, 7, 14, and 28 days. Cylinders were subjected to varying moist cure durations as the slabs, (i.e. 2, 4, 8, 10, & 14 days). Cylinder strengths were determined from the average of three test specimens. Since cure duration is one of the variables of the investigation, test specimens were not moisture preconditioned, as suggested by ASTM C 39, but were rather tested in their moisture state at time of testing, (i.e. no moisture preconditioning prior to the test).

Table 4.3 Concrete Cylinder Testing Schedule.

Age (days)	Curing Duration					
	0-day	2-day	4-day	8-day	10-day	14-day
1	3	-	-	-	-	-
3	3	3	3	-	-	-
7	3	3	3	3	-	-
14	3	3	3	3	3	3
28	3	3	3	3	3	3

4.3.2 Permeability Sampling and Testing

Permeability for the AMA concrete mixture was determined by both the RCPT and chloride ion ponding test methods. Four-inch diameter cores were used to determine the electrical resistivity of the in situ concrete. Drilled cores were taken during the ages of 56 and 57 days for this purpose. Due to problems with coring equipment and procedures, core sampling was performed over two days and limited to the sections shown in the Table 4.4. Table 4.4 lists the number of cores taken for a particular section of a slab.

Table 4.4 Day 56/57 4-inch Core RCPT Sampling Schedule

Cure Treatment	Curing Duration					
	0-day	2-day	4-day	8-day	10-day	14-day
conventional	3	3	3	3	3	3
"throw-on"	3	-	3	-	-	3
"mist"	3	-	3	-	-	3

After removal from the slab, cores were wrapped with moist paper towels and sealed in plastic bags. Samples were kept in this state until testing. Testing of RCPT core sets (4 cores in a set) started at a 100 day age. A total of 9 core sets were tested and each set required a 24-hour period for preparation and testing. Thus, a total of 9 days was required to complete testing of all cores.

Before testing, samples were prepared by first removing the top ¼-inch of each core and sawing off a bottom portion leaving a 2-inch thick disk specimen. Disk specimens were further conditioned and tested following ASTM C 1202 procedures. A RLC Instrument Company 164A 4-cell model was used to determine the electrical resistivity of the disk samples.

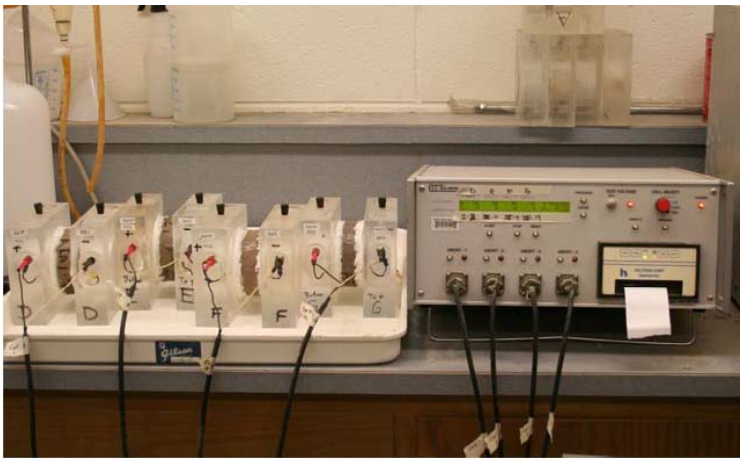

Figure 4.13 RCPT Four Cell Apparatus Setup

Chloride ion permeability potential was determined by ponding a salt solution on the specimen slabs. A setup of the ponded specimen is seen in Figure 4.14. AASHTO T 259 was used as a guideline but a few variations from the procedure were used. Since cure duration was a variable for this study, specimens were not cured for the specified 28 days but rather moist cured for durations of 2, 4, 8, 10, and 14 days. During the interval between moist curing and salt ponding, specimens were stored under standard laboratory conditions, (i.e. at room temperature with approximately 50% R.H.). Ponding of AMA specimens started at 29 days of age and the solution was maintained on the surface for a period of 120 days instead of the recommended 90 days.

Once specimens underwent the 120-day period of ponding, the salt solution was removed and the surface was brushed to remove salt crystal buildup. The surface was further abraded to simulate traffic wear. Four different powder samples from each specimen slab were taken with a rotary hammer at 4 different depth ranges. The depth ranges were as follows: 0" – ¼", ¼" – ¾", ¾" – 1 ¼", 1 ¼" – 1 ¾". Once powder samples were collected, the water soluble chloride content was determined by preparing the samples according to AASHTO T 260. After this step, a calibrated chloride ion selective electrode (ISE) was used to determine the water soluble chloride content of the concrete. The modified approach used to determine chloride content is detailed in Ghanem's work (2004).

(a) Close-up view (b) A group of specimens

Figure 4.14 Ponding Specimen Slabs

CHAPTER 5
COMPARATIVE ASSESSMENT OF THREE CURING METHODS

5.1 Conditions for Curing

Data from the experimental setup for different cure treatments (detailed in Chapter 4) is presented in this chapter. Due to the large amount of data and to maintain consistency with previously presented data, comparisons and discussion are limited to the three different cure durations of 0, 4, and 10 days. At times other cure durations may be presented to distinguish trends in data.

First, ambient atmospheric conditions are presented to relate any influence diurnal patterns may have had on concrete curing within the laboratory. Concrete curing temperatures for the first 15 days are presented for certain concrete sections of the AMA slabs. Additionally, concrete internal moisture, (i.e. measured as a R.H.) is presented. This includes the pore humidity of the slabs during the first 15 days and drying potentials after curing media had been removed.

Concrete strength and electrical resistivity are examined for the three different cure treatments and specified cure durations. Compressive strength development from 6-inch diameter cylinders is presented to determine the behavior of the AMA mix under controlled conditions. For a more accurate depiction of concrete permeability resistance, ponding results from 12-inch by 12-inch slab specimens are presented.

5.1.1 Ambient Conditions during Curing

Temperature and relative humidity conditions were not available for the interior of the structures laboratory for the first 14 days due to data logging equipment errors. Therefore outside atmospheric conditions were acquired from a local weather station to determine any influences ambient patterns may have had on curing temperature or moisture state. Figure 5.1 displays data for the first 14 days from date of pour. Concrete slabs were cast on February 6, 2004. The average outside temperature for the first 5 days was approximately 40 °F and dropped to about 25 °F between day 5 and 8. Thereafter, outside temperatures gradually increased to an average temperature of about 40 °F to 55 °F between days 8 and 14.

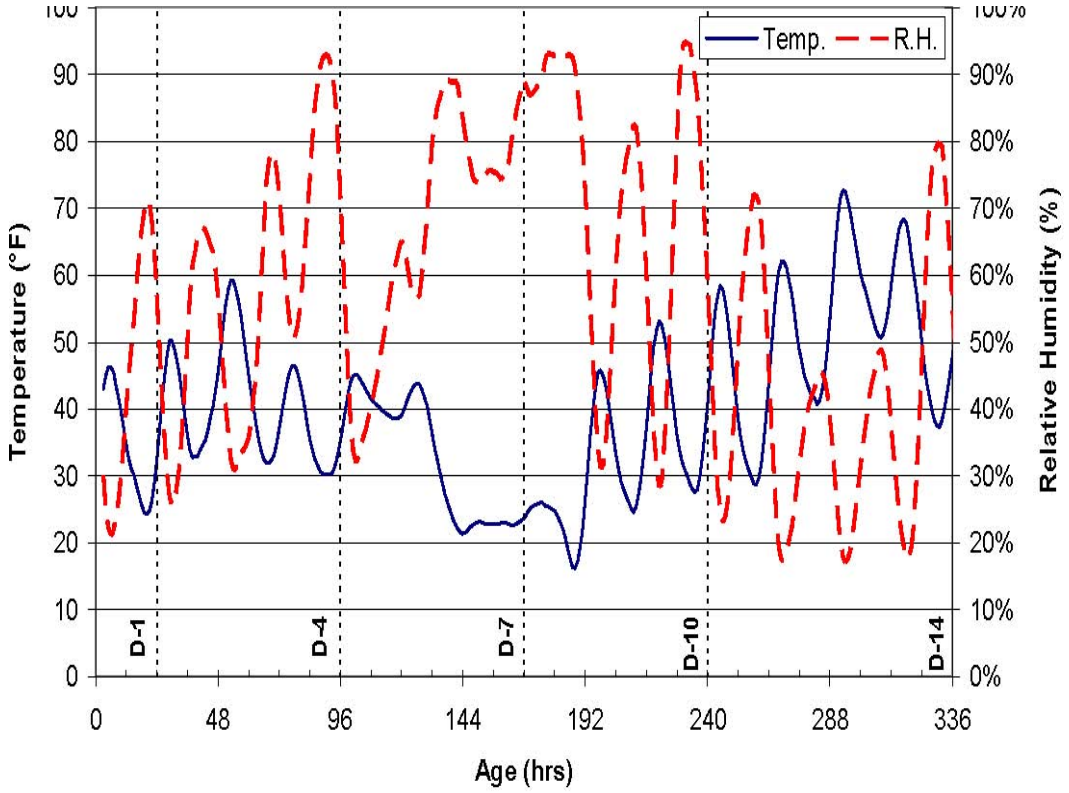

Figure 5.1 Ambient Temperature and Relative Humidity Conditions in Lubbock, TX

Although laboratory temperature data was not available the first 14 days, errors with the data logging equipment inside the laboratory were fixed and recordings revealed laboratory temperature to range between 60 and 70 °F (Figure 5.2). The laboratory temperature history shown in Figure 5.2 is for the period between day 14 and 24 (i.e. February 20, 2004 to March 1, 2004). During this period, outside temperatures approximately fluctuated between 70 °F and 28 °F. Even with low outside temperatures between days 18 and 20, laboratory temperatures remained above 60 °F. Therefore, for discussion purposes, the average laboratory temperature during the curing period will be considered as approximately 65 °F.

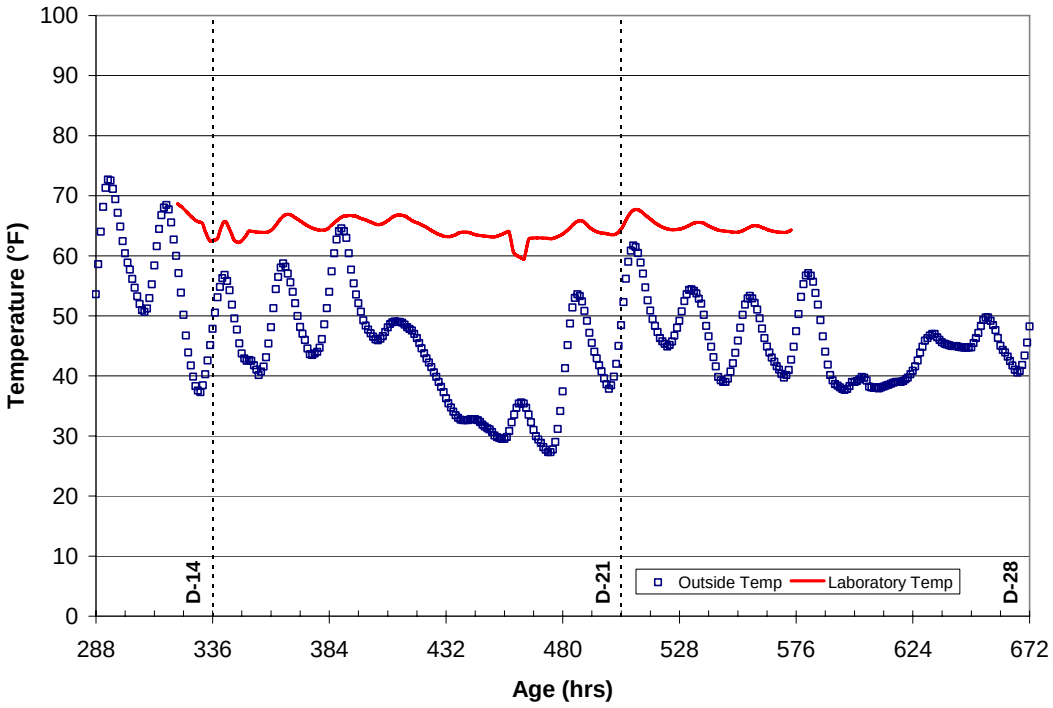

Figure 5.2 Outside and Laboratory Temperature History

5.1.2 Concrete Slab Temperature History

Figures 5.3 through 5.5 depict the concrete temperature history of the slabs during the first 15 days after casting. Dotted vertical lines have been provided to distinguish the concrete age at Days 1, 4, 7, 10, and 14. Additionally, a solid vertical line indicates the removal of curing media from a section (Figures 5.4 and 5.5). The evaluation made in each figure is between sections with similar cure durations but different cure treatments.

Concrete temperature during placement ranged between 46 and 47 °F for all sections of the slabs. These figures also depict when coring of the slab occurred by a sudden drop in temperature. This resulted from the cooling effect of the water used while taking core specimens. This temperature drop is apparent on Days 4 and 7 for the 0-, and 4-day cure sections (Figures 5.3 and 5.4). This is also true on Day 14 for the three curing durations. A sudden drop in temperature does not occur for the 10-day concrete until Day 14 since it does not undergo any wet drilling until this time.

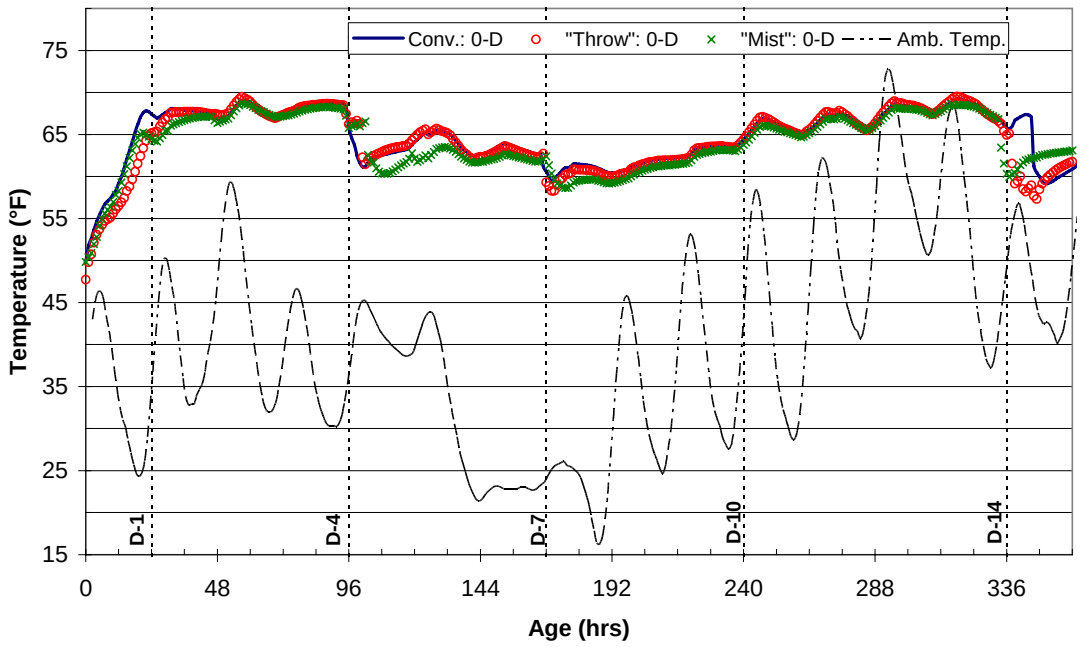

Figure 5.3 Slab Temperature History for 0-Day Cure Section

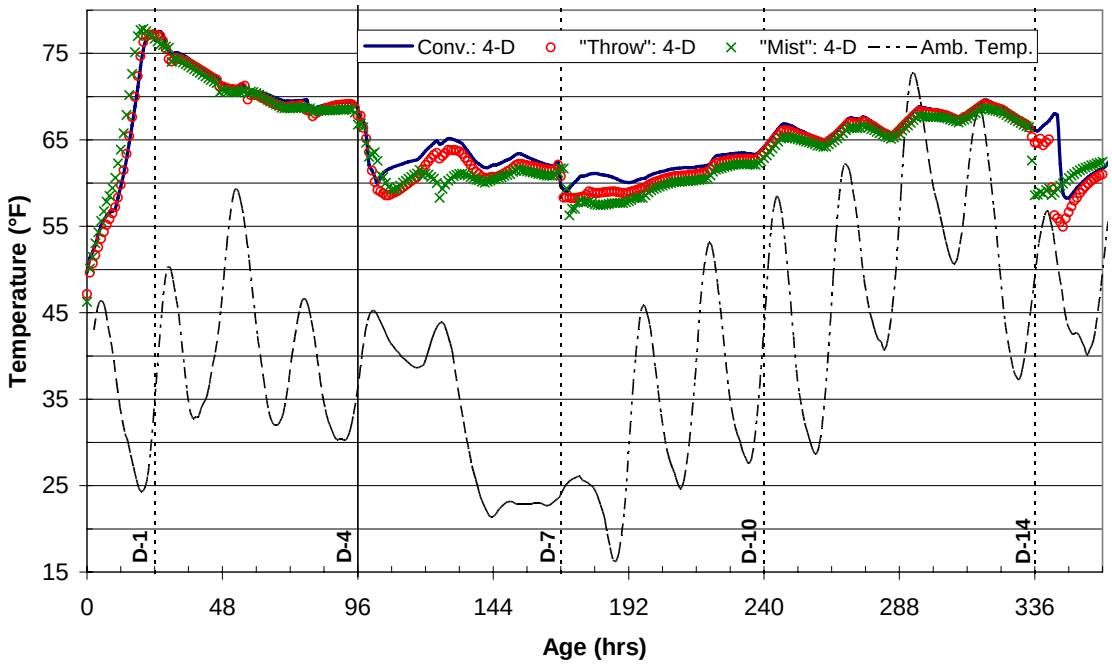

Figure 5.4 Slab Temperature History for 4-Day Cure Sections

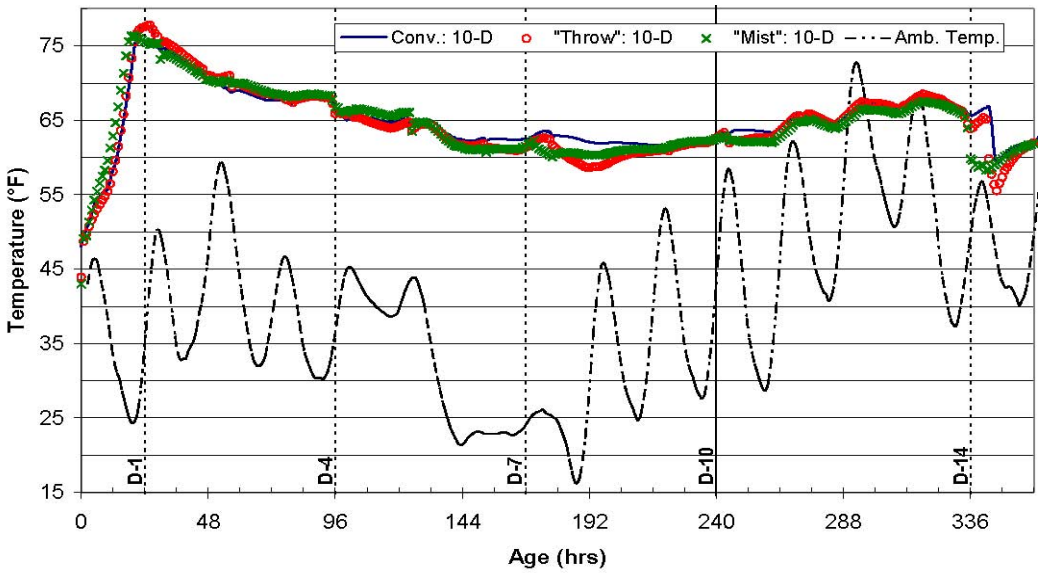

Figure 5.5 Slab Temperature History for 10-Day Cure Sections.

The 0-day cure temperature history (Figure 5.3) shows a slight divergence in peak temperature between the conventional cure and the other two cure treatments at about 24 hours from casting. The slight increase of temperature for the conventional cure is attributed to the application of a curing compound to this section while the other two sections received no protection at all. Under conditions of this experimental work, the curing compound helped increase the initial peak temperature of the 0-day cure duration by approximately 2 to 3 °F. Concrete curing temperatures for the 0-day sections ranged between 60 and 70 °F between the ages of 1 and 15 days. For the most part, temperatures between the different 0-day cure treatments were similar and usually within 1°F of each other (the exception being for a period between Day 4 and 6 for the "mist" cure treatment which showed a lower temperature).

5.1.3 Slab Temperature for AMA 4-day Sections

An increase in peak temperature is observed within the initial 24-hour period when a cure treatment is applied to the slab surfaces (Figures 5.4 and 5.5). The 4-day cure sections peaked at a temperature of 77 °F around the 20^{th} hour. After this time, concrete temperature gradually decreased until Day 4 and then a sudden drop occurred. At such time curing media was removed from this section and coring was also performed. Once coring activities were complete and each section rebounded from the cooling effects of the water, the concrete slab temperatures appear to be within the range of 60 and 70 °F, similar to laboratory temperatures. The three cure treatments used for the 4day cure duration show no drastic differences in curing temperature between each other, except that the conventional cured concrete tends to retain slightly more heat.

5.1.4 Slab Temperature for AMA 10-day Sections

Sections receiving 10 days of curing reflect the same temperature profile as the 4day cure sections for the first 4 days. Initial peak temperatures were similar between the 4- and 10-day sections. The protection provided by the prolonged duration of the 10-day cure is noticeable when comparing Figure 5.4 and 5.5. The 10-day cure sections have less erratic temperature fluctuations between ages 4 and 10 days. After the removal of curing media from the 10-day section, there was no immediate drop in concrete temperature since coring was not scheduled on this day. However, a sudden drop is noticed on Day 14 which is the first coring opportunity for these sections. Generally 10day cure sections did not experience extreme temperature differences between cure treatments and temperatures were typically between 60 and 70 °F after the 2-day age.

5.1.5 Slab Temperature for Different Cure Treatments

Figure 5.6 depicts the temperature profiles of the conventional cure slab for 0-, 4-, and 10-day cure durations. As mentioned before, the 0-day cured concrete has a lower peak temperature during the first 24 hours when compared to sections with some duration of moist curing. Once curing media is removed from the 4-day section, the slab temperature of this section is similar to the 0-day section. The 10-day section also tends to follow the 0- and 4-day temperature pattern once the curing media is removed from its surface. A similar temperature pattern, as described for the conventional treatment, is observed for the "throw-on" and "mist" cured slabs and are not included in this section but appear in Appendix C.

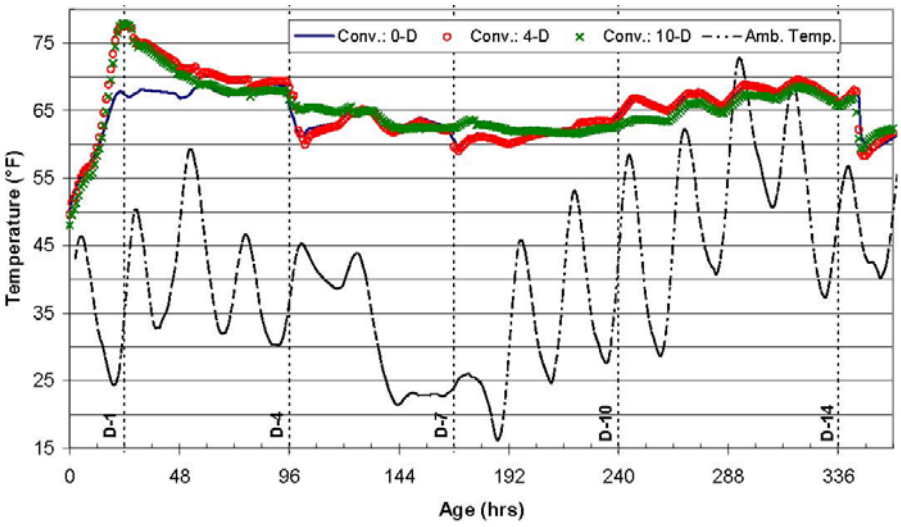

Figure 5.6 Temperature History for Conventional Cure Treatment
Arrhenius Equivalent Ages Determined from AMA Slab Temperature Data

From Figures 5.3 to 5.5, it is observed that the type of curing treatment did not greatly influence curing temperatures but curing duration did have an effect. Therefore, it can be deduced that sections with the same cure duration could have similar maturity ages based on the parameters (i.e. temperature and concrete age) current models use. Table 5.1 lists the Arrhenius maturity

age of each concrete section at age of testing based on its respective temperature history. The tabulated maturity equivalent ages show the 4- and 10-day sections generally had slightly higher values when compared to the 0-day sections at any particular testing age. However, differences in equivalent age are small (usually within 12 equivalent hours for a given test age) that they can be considered to be approximately the same age. Although all the 0-, 4-, and 10-day sections may have similar equivalent ages at 360 hours of age, it is inherent that all 0-day section (lower moisture availability) would have less desirable concrete properties compared to the 4- and 10-day sections. Therefore pore humidity during curing should be considered when determining equivalent age. Slab relative humidity is explored in more detail in upcoming sections.

Table 5.1 Maturity Equivalent Ages for Different AMA Slab Sections

Concrete Age (hr)	Arrhenius Equivalent Age (hrs)								
	Conventional			Throw-On			Mist		
	0-D	4-D	10-D	0-D	4-D	10-D	0-D	4-D	10-D
120 192	117.9	125.3	--	116.0	124.2	--	114.7	125.2	--
360	177.0	182.9	338.1	173.7	179.9	330.2	170.5	178.5	331.4
	334.0	338.8		327.5	332.2		324.5	330.0	

5.2 Slab Moisture

5.2.1 Slab Moisture History

Figures 5.7, 5.8 and 5.9 display pore humidity histories within respective slab sections measured as a relative humidity (RH). The values shown in part "a" of the figures are the averaged RH values between the top, (i.e. 1-inch below the surface), and mid-depth sensor, (i.e. 2 ¼-inches below the surface) while part "b" represents a liner humidity range between the top and mid-depth sensors within the slab sections. Each figure is for a given cure duration and compares cure treatments. Average internal RH is shown for the first 15 days while the humidity range is for 30 days. Solid vertical lines are provided to indicate the time when curing media is removed. During the initial 24 hours, pore humidity readings increased for all sections indicating possible migration and condensation of mix water into the sensor enclosure.

Sections receiving no moist curing, (i.e. 0-day) exhibited continuous drying after the apparent 24-hour period for sensor equilibrium (Figure 5.7a). At times moisture increased as a result of water from core drilling, (i.e. Days 4, 7, and 14). The 0-day section treated with a curing compound, conventional cure, retained more moisture when compared to the other two 0-day untreated sections. The 0-day conventional section lost moisture at a much lower rate and had less potential to absorbing water during coring activities. Both the "throw-on" and "mist" cure sections had similar moisture profiles. This was expected since both sections received no curing compound or moist coverings. More moisture was present in the conventional 0-day cure section at Day 14 when compared to the other two 0-day sections. Additionally at 30 days of age, the 0-day conventional sections had a mid-depth RH of approximately 94% while the other two treatments resulted in a RH of approximately 88% (Figure 5.7b).

Figure 5.8a, which compares 4-day curing using different cure methods, reveals a period of sustained moisture while the curing treatments are in place. Thereafter, the concrete gradually dries but regains moisture with core drilling activity on Day 7. Once curing media is removed, the drying rate for the "mist" cure is higher and appears to be more sensitive to water presence when compared to the other two treated sections. This is apparent following coring on Day 7. The "mist" section showed a greater increase in moisture during coring activity and a higher drying rate after coring (Figure 5.8a). The ease of moisture increase or decrease for the "mist" section suggests the concrete may be more permeable when compared to conventional and "throw-on" sections. Figure 5.8b reveals the pore humidity at 30 days of age to be approximately 80% for the 4-day conventional and "throw-on" sections while the "mist" section is at 74% at the same age. For this cure duration, the conventional and "throw-on" treated section attain similar pore humidity profiles.

High RH's were maintained throughout the moist cure period for 10-day cured sections (Figure 5.9a). The 10-day conventionally cured concrete recorded a lower RH than the two other treatments during the cure treatment period. A difference between the 4- and 10-day "throw-on" cure is noticed between Figures 5.8a and 5.9a. Between the ages of 24 and 96 hours, the 4-day "throw-on" cure had a lower RH when compared to the 10-day "throw-on" cure. This of course was not anticipated since both sections were nearly identical and experienced the same type of treatment and care during this period. An explanation to this disparity could be possible condensation of mix water inside the enclosure used to protect the digital sensor.

The following section will present the average drop in pore humidity per day for each of the cured sections. This parameter will be referred to as the drying rate. The drying rate will help distinguish the effectiveness of the cure treatment by disregarding initial pore humidity and focusing on pore humidity loss potential. Presenting data in this manner minimizes the error introduced by condensation presence or hardware calibration/functionality.

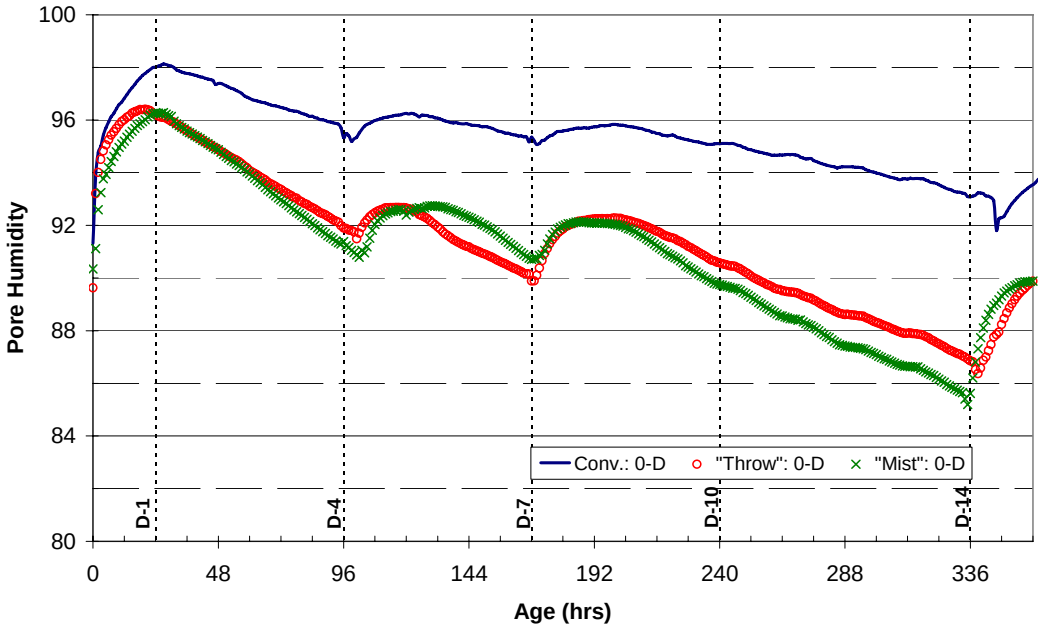

(a) Average Humidity Profile for First 14 Days

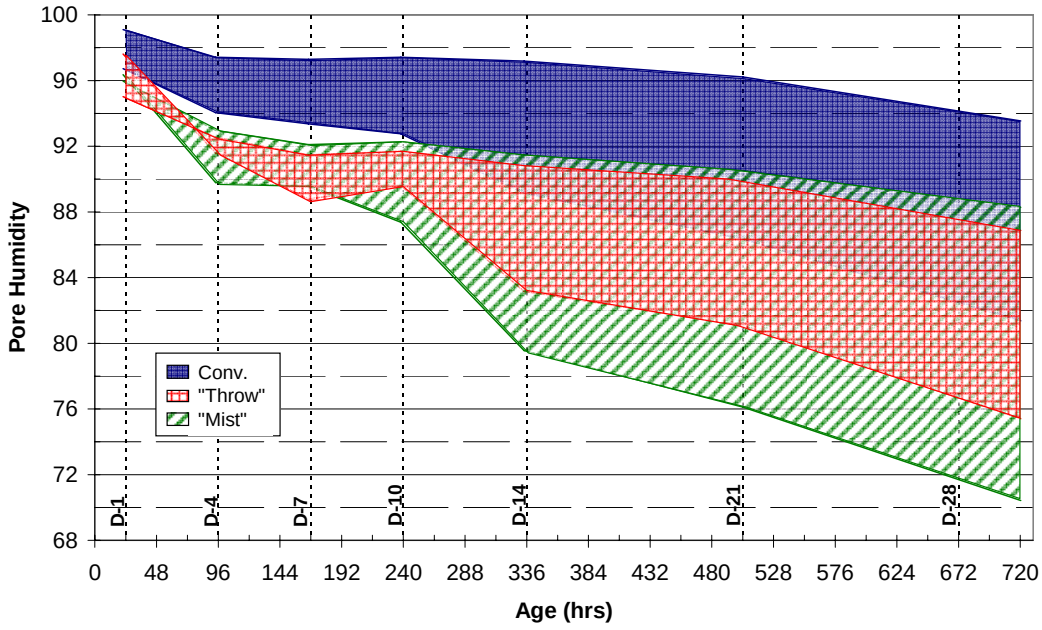

(b) Humidity range between top and middle of slab for first 30 days

Figure 5.7 Pore Humidity for 0-Day Cure Sections.

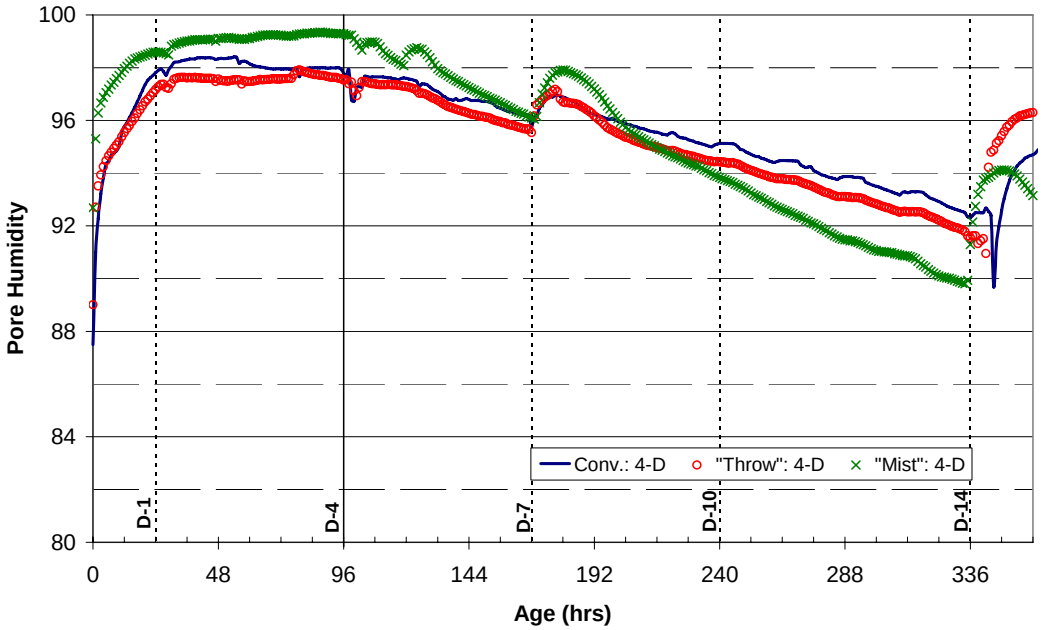

(a) Average Humidity Profile for First 14 Days

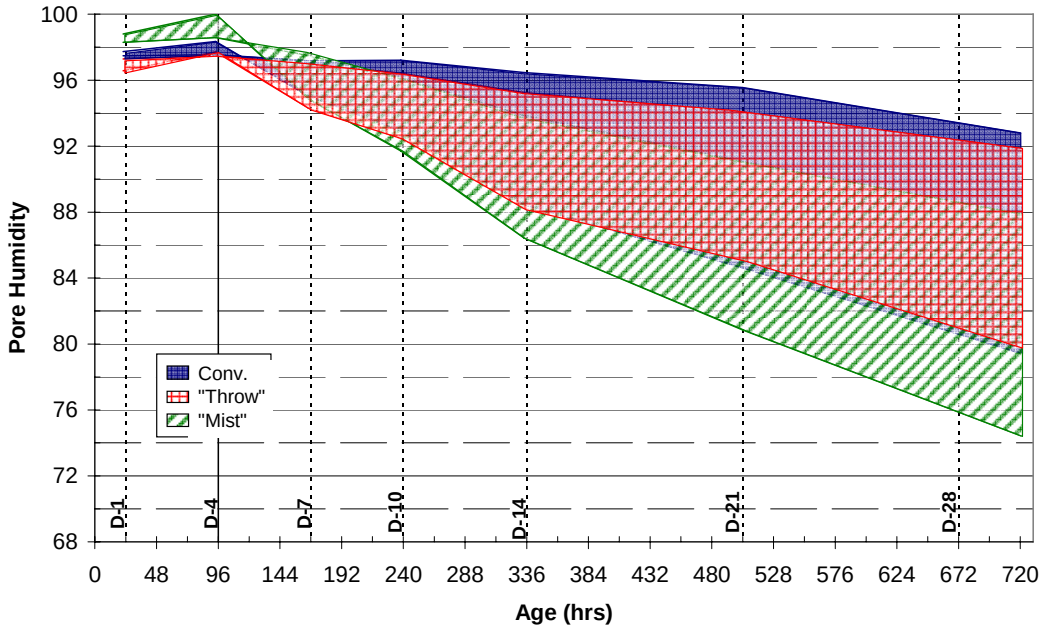

(b) Humidity range between top and middle of slab for first 30 days

Figure 5.8 Pore Humidity for 4-Day Cure Sections.

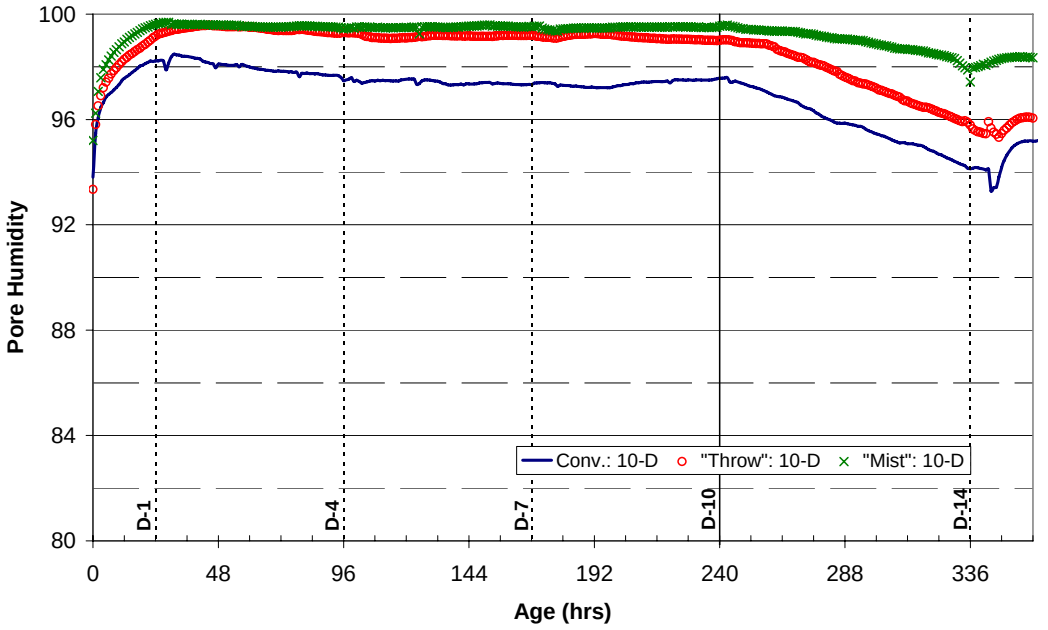

(a) Average Humidity Profile for First 14 Days

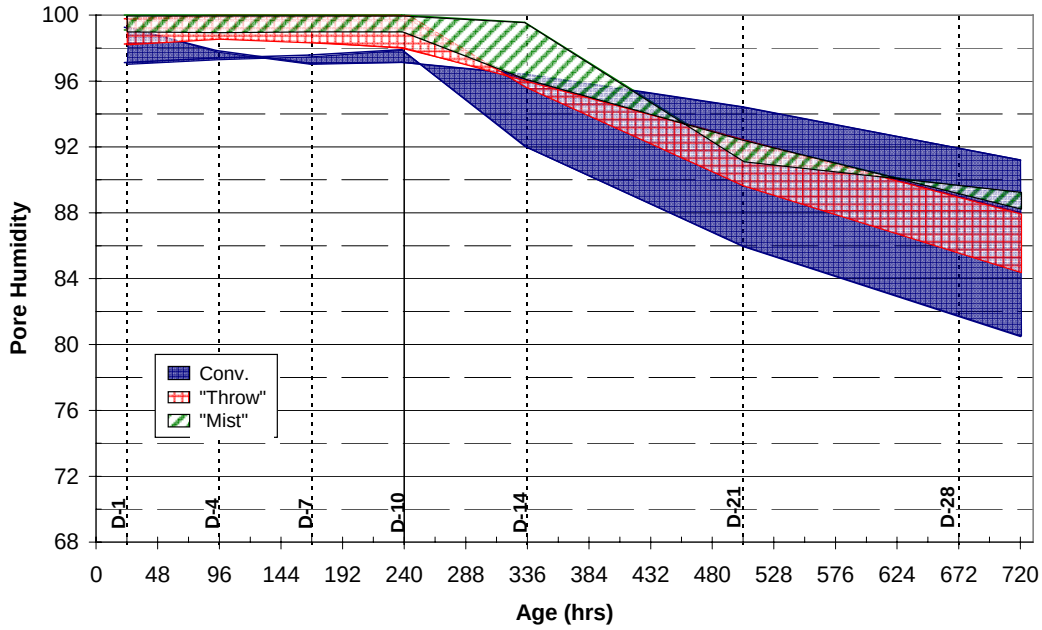

(b) Humidity Range Between Top and Middle of Slab for First 30 Days

Figure 5.9 Pore Humidity for 10-Day Cure Sections

5.2.2 Slab Moisture Retention/Drying for Different Cure Methods

Drying rates for the slab sections are presented in Figures 5.10 and 5.11. Drying rate for the slabs is expressed as the average change in RH per day based on the average RH between top and mid-depth sensors, (i.e. part "a" of Figures 5.7 to 5.9). Figure 5.10 shows the average drying rate of the slabs for the period between 11 and 14 days of age. The conventional cure sections

show an increasing drying rate with increasing cure duration, but this should not be misinterpreted as a negative effect as a result of a longer curing period. The increase in drying rate is due to the amount of moisture present in the conventional sections at the beginning of Day 11. The more moisture present in a slab results in a higher potential of drying. Since the 0-day conventional cure section had been drying for some time, less moisture is present at Day 11 and a lower drying rate results during the period depicted in Figure 5.10.

The "throw-on" cure shows no clear trend regarding drying rate with change in cure duration. The lack of drying trend can be explained by the immediate placement of saturated cotton mats on the surface after the pour. Water from the saturated mat could have increased the water-cement ratio resulting in a marred surface. From visual inspections made 15 minutes after placement of saturated mats, the surface makeup appeared to be non-uniform. Some areas had a glossy appearance, indicating moisture concentration, while other areas appeared to be dry. This surface inconsistency could be the reason for the lack of trend in drying rate with an increase in cure duration for the "throw-on" treatment. It should also be noted that the 0-day "throw-on" section had a higher drying rate than the 0-day conventional section since the conventional section had a curing compound applied to it and helped retain more moisture.

"Mist" cure sections demonstrate decreasing drying rate with prolonged cure duration. The combination of mist canopies for 24 hours along with wet mat curing after canopy removal appears to have helped retain more moisture. Since "mist" curing did not involve direct contact with the surface for the first 24 hours, the water-cement ratio was not changed. Concrete was allowed to harden during this time while retaining and receiving moisture from the mist canopy enclosures. The longer cotton mats were left in place, the less moisture was lost. As seen in Figure 5.10, the 10-day cure "mist" section had a lower drying rate when compared to the 4-day section.

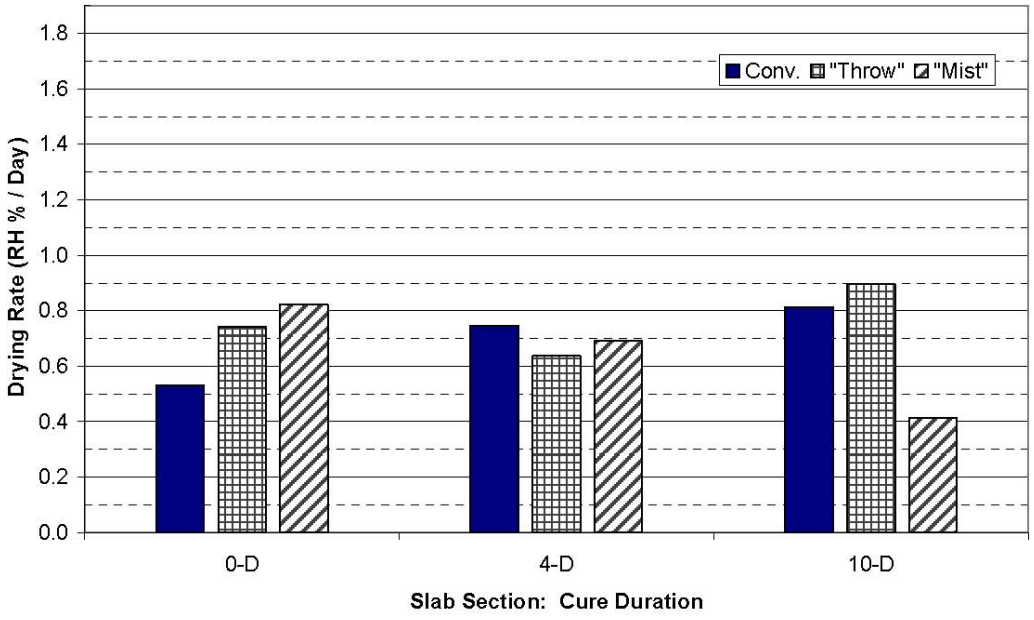

Figure 5.10 Drying Rate for Period between Age of 11 and 14 Days

Figure 5.11 presents the drying rate potential 48 hours after the removal of curing treatments. The drying rate shown for the 0-day sections is 48 hours after moisture stabilization, (i.e. 72 hour concrete age). Conventional cured sections revealed little to no difference in drying rate with increase in cure duration. Both the "throw" and "mist" cure sections had the greatest drying rate when considering the 0-day sections. This again demonstrates the ability of the curing compound to retain some of the moisture.

As mentioned before, the "throw" treatment fails to produce any clear trend with respect to drying. This again can be due to the change in water-cement ratio from the immediate placement of saturated mats.

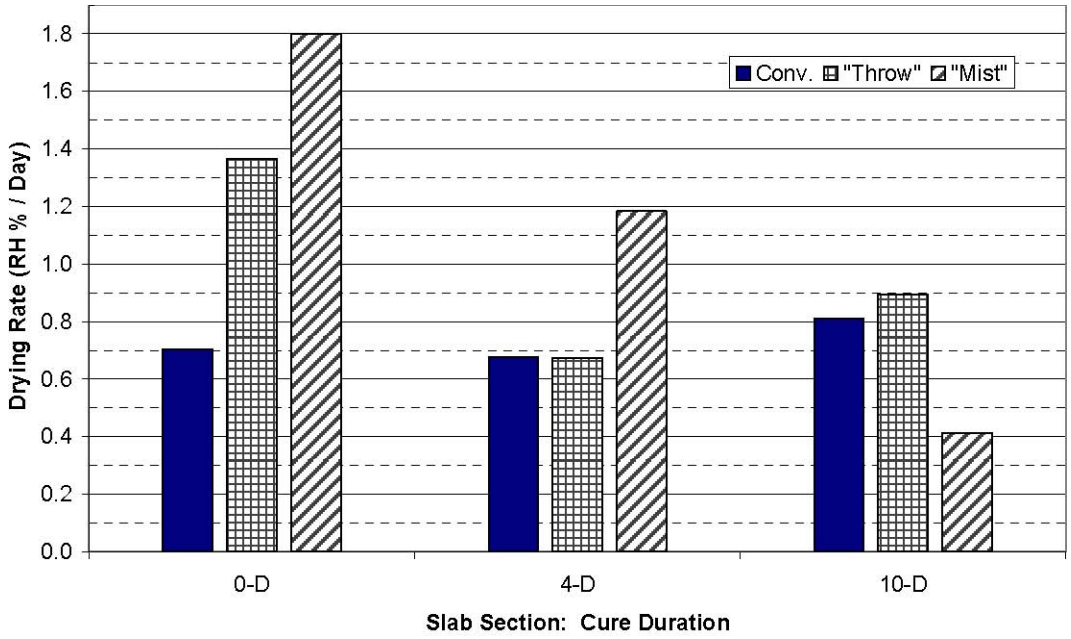

Figure 5.11 Drying Rate 48 Hours after Removal of Curing Media

Figure 5.11 shows the high drying potential of the unprotected 0-day "mist" cure section. With some protection, as seen with the 4- and 10-day "mist" cure sections, the drying rate can be reduced gradually. Leaving the curing media in place for 10 days shows drying rates to be lower when compared to the 4- and 0-day rate. The curing protection from the 10-day "mist" treatment reduces the amount of moisture loss and thus would imply a less permeable concrete.

5.2.3 Effectiveness of Cure Treatment on Concrete Moisture

The previous sections dealt with the drying potential of the slabs under different cure treatments and durations. This section focuses on the amount of moisture present in a concrete slab section for a given time. Table 5.2 lists the average RH values between the top and mid-depth of the slab sections at 306 hours of age (approximately 30 hours before Day 14) and 672 hours (Day 28). Pore humidity values for these two ages are presented since the 306 hour age represents a

time when all curing media has been removed but prior to coring on Day 14 and the 672 hour age is chosen due to the common practice of evaluating compressive strengths at 28 days of age.

The values in Table 5.2 give the impression that the 0-day conventional cure section may be a better treatment when compared to the 4-day cure duration. The application of the curing compound seems to retain moisture and minimize moisture fluctuations and gives reason as to why the 0-day conventional cure appears to perform better than the 4-day "throw-on" and "mist" treatments.

To better quantify the effectiveness of each treatment, the values in Table 5.2 are normalized with their respective 0-day cure treatment RH value for each measurement age. Therefore normalized values are relative to the value in the first row for each cure treatment and age shown in Table 5.2. The normalized data are displayed in Figures 5.12 and 5.13 and illustrate how a prolonged curing duration can retain more pore humidity for each respective cure treatment. By establishing the 0-day cure of each treatment as the bench-mark, it is seen that extended cure durations help increase the moisture content at ages 306 and 672 hours with the exception of the conventional cure.

Table 5.2 In Situ Relative Humidity of Slab Sections

Cure	306 hour age			672 hour age		
Duration	Conv.	"Throw"	"Mist"	Conv.	"Throw"	"Mist"
0-D	93.82	88.08	86.81	88.50	82.29	80.58
4-D	93.28	92.62	90.97	87.20	86.87	82.59
10-D	95.23	96.95	98.74	86.89	87.29	89.73

From the following figures, little increase or decrease in moisture is noticed when comparing the different durations of the conventional treatment at 306 or 672 hours of age. The moisture percent difference among the conventional cure sections is ±2% from respective 0-day cure RH values. Although there may be little difference in the amount of moisture present among same-age conventional cure sections, it does not necessarily mean they are the same quality concrete. In fact, compressive strengths and permeability resistance results will show each of the three sections to be unique. Therefore, the observation made from this treatment demonstrates the amount of moisture present at a particular time is not as important as the cumulative moisture history up to a certain time (Figures 5.7 – 5.9).

Sections receiving the "throw-on" and "mist" treatments do show some type of improvement with increase in cure duration. Of course any increase in moisture is expected since the 0-day cure section of both these treatments had no protection at all (i.e. no curing compound). With "throw-on" and "mist" treatments in place for 4 days, moisture was increased by more than 4% at 306 hours when compared to their 0-day counterparts at the same age. An increase in moisture was also noticed for the 4-day cure "throw-on" and "mist" treatments at 672 hours when compared to their respective 0-day cure sections. These increases were about 5% and 2% for "throw-on" and "mist" treatments, respectively.

The 10-day cure duration yielded the highest RH for the "mist" cured slab section. The 10-day

cure "mist" section had a 12% higher RH when compared to its 0-day counterpart at 306 hours. "Throw-on" treatments for the 10-day cure had an increase of 10% compared to the 0-day section at the same age. Similar trends are noticed for both treatments at 672 hours of age. At this age, the "throw-on" and "mist" sections had 6 and 11% more moisture, respectively, than their companion 0-day slab sections.

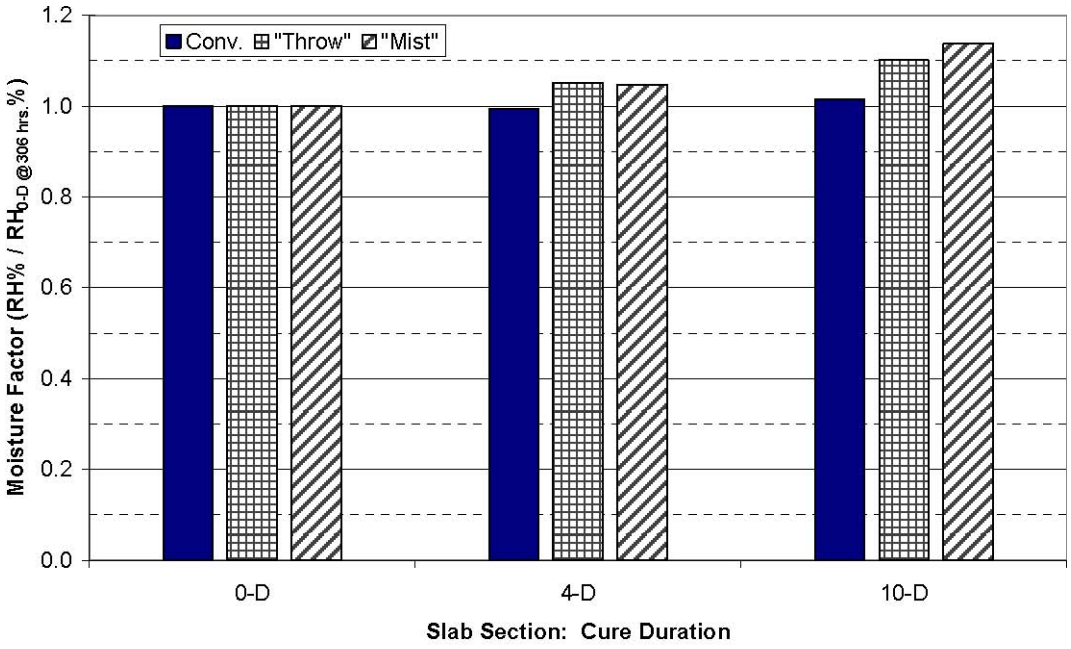

Figure 5.12 Moisture with Respect to 0-Day Cure Sections at 306-hr Age.

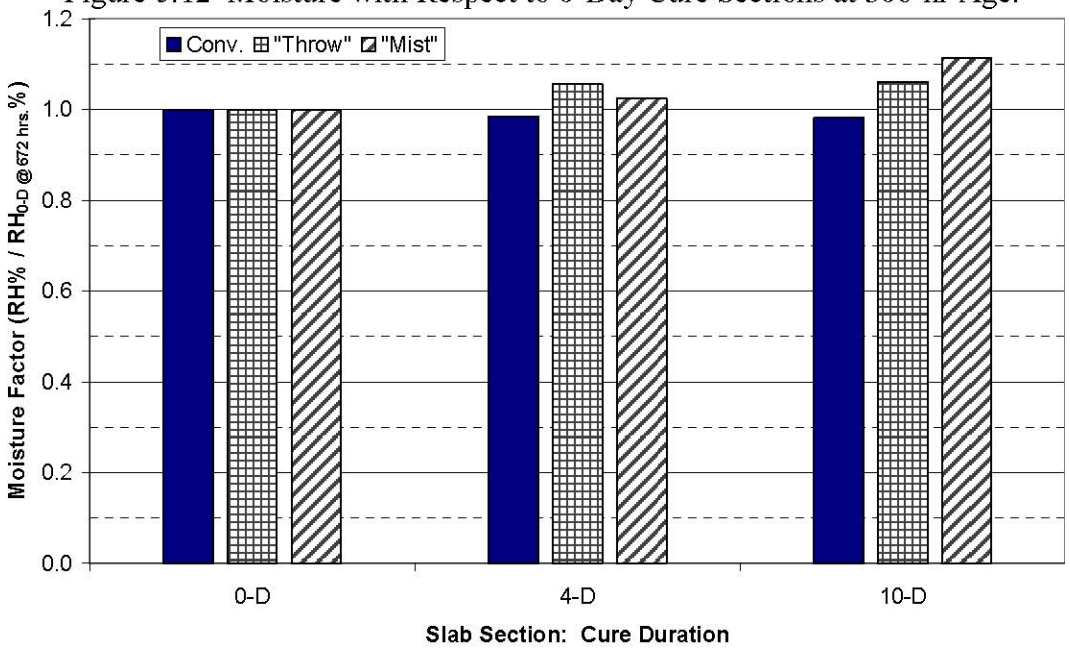

Figure 5.13 Moisture with Respect to 0-Day Cure Sections at 672-hr Age.

5.3 AMA Slab Strength

5.3.1 AMA Slab Strength Comparison

Slab strengths for each section were determined from the average strength of three drilled cores. Table 5.3 lists the average strengths for the different cure treated slab sections at test ages of 5, 8, and 15 days. Values are not available for 10-day cure sections at 5 and 8 days of age since the curing media was still on the slab surface.

Table 5.3 Average Compressive Strengths for Slab Sections

Test Age (day) (hrs)		0-Day			4-Day			10-Day		
		Conv.	"Throw"	"Mist"	Conv.	"Throw"	"Mist"	Conv.	"Throw"	"Mist"
5	120	2688	3132	2920	3661	3639	4042	-	-	-
8	192	3133	3592	3639	4224	4601	4253	-	-	-
15	360	2883	3962	3630	4589	4966	4832	4527	5598	5103

-Values are in pounds per square inch

Average compressive strength values have a wide range when considering different cure treatments and duration at Day 15. The lowest strength value corresponds to the 0-day conventional cure (2883 psi) and the highest is for the 10-day "throw-on" cure (5598 psi). This is an approximate difference of 2700 psi between these two sets of samples.

For a better comparison, compressive strength data in Table 5.3 is presented in relative terms in Table 5.4. Current TxDOT Standards (2004) specify a minimum of 10 curing days for concrete mixtures containing Type I/II cement; therefore all displayed compressive strength data in Table 5.4 is relative to the 10-day conventional cure strength. The conventional cure treatment is chosen as the cure treatment bench-mark since it is the most common method in practice. With the absence of 28-day slab compressive strengths, the 15-day age compressive strength is used as a datum. Thus all values in Table 5.4 are relative to the 10-day conventional cure at 15 days of age.

Table 5.4 Strength Ratios Relative to 10-Day Conventional Cure at 15-Day Age

(day) (hrs) Test Age		0-Day			4-Day			10-Day		
		Conv.	"Throw"	"Mist"	Conv.	"Throw"	"Mist"	Conv.	"Throw"	"Mist"
5	120	0.59	0.69	0.65	0.81	0.80	0.89	-	-	-
8	192	0.69	0.79	0.80	0.93	1.02	0.94	-	-	-
15	360	0.64	0.88	0.80	1.01	1.10	1.07	1.00	1.24	1.13

The information displayed in Table 5.4 reveals several things about strength gain characteristics of the different cure scenarios. First, all 0-day cure compressive strengths, irrespective of cure

treatment or test age, were generally lower when compared to the 4day cure treatments at 5 days of age (the only exception is the 0-day "throw-on" cure at age 15). Given the curing histories between the 0-day conventional, "throw-on," and "mist" treatments, one would intuitively reason the conventional cure treatment would yield higher strengths since a curing compound was applied to this section, which would provide protection from drying. In fact, the amount of humidity present in the conventional section was higher when compared to the other two treated sections. Table 5.2 lists the pore humidity at 306 hours of age for 0-day cure conventional, "throw-on," and "mist" treatments as 93.82%, 88.08%, and 86.81%, respectively. Previous studies have shown specimens with drier moisture states at time of testing to have higher strengths (Bloem 1968, Malhotra 1977, Bartlett and MacGregor 1994). In this case, both the 0-day "throw-on" and "mist" specimens are drier and have higher strengths compared to the 0-day conventional specimen and thus agree with findings from other researchers.

Additionally the difference associated with the 0-day specimens may be due to the degree of hydration. Conventional cured specimens indicate a higher moisture presence which would suggest the possibility of a higher degree of hydration which would result in a stronger more brittle concrete. Malhotra (1977) found that "stronger concrete offers more resistance to drilling and, in the process, may introduce micro-cracks or other damages to the cores." Given the combination of a more brittle concrete and higher moisture presence, the result is a lower compressive strength for the 0-day conventional slab section when compared to the other 0-day sections.

Findings by Bloem (1968) found concrete exposed to favorable cure conditions, (i.e. adequate moisture during curing), had a slower decrease in internal pore humidity. This would imply the 0-day conventional section would have a better degree of hydration when compared to the other two 0-day cure regimens (Figures 5.10 and 5.11).

All slab sections receiving 4 days of curing had similar or slightly better strengths at 15 days of age when compared to the standard specimen (10-day conventional cure section at Day 15). Of course this does not necessarily suggest the sections cured for 4 days are better than the "standard" 10-day cure period. The reason for the higher strengths associated with the 4-day cured sections can be attributed to the moisture state of the specimens. Referring to Table 5.2, the 4-day cure sections generally had lower pore humidity compared to 10-day cure sections. Recalling that drier samples tend to produce higher strength values, the 4-day cure specimens appear to have enhanced compressive strengths.

Compressive strength results for the 4-day cure sections at 15 days of age (Table 5.4) reveal the "throw-on" and "mist" cure schemes to yield higher values than the conventional cure. Exploring the moisture content and drying rate of each section can help explain the degree of compressive gain. Among the 4-daycure sections, the conventionally treated concrete had the highest moisture content (93.28%) and the highest drying rate (0.75 RH/day) which resulted in the lowest compressive strength within the group. A high moisture state at time of testing has been shown to reduce compressive strength while a relatively high drying rate is indicative of poor curing.

The 4-day cure "throw-on" section had the lowest drying rate (0.64 RH/day) and a median pore humidity content (92.62 %) compared to the other two cure treatments at 306 hours of age

(Figure 5.10 and Table 5.2). This combination of drying rate and moisture content resulted in the highest compressive strength among the 4-day cure group at Day 15. The 4-day "mist" cured specimens had the lowest moisture content (90.97 %) among the 4-day cure group and a lower drying rate than the 4-day cure conventional section (0.69 RH/day). The moisture and drying conditions of the "mist" treated concrete yielded a compressive strength slightly lower than the "throw-on" specimens.

Strengths for 10-day cure specimens deviate from the moisture and drying condition patterns associated with the 0- and 4-day cure specimens. Specimens undergoing a "throw-on" treatment yielded the highest compressive strength at Day 15 followed by "mist" and conventional treatments, respectively (Table 5.4). However, "throw-on" specimens had the highest drying rate among the 10-day cure group at 306 hours of age (Figure 5.10) which suggests a less desirable cure since, according to Bloem (1968), better cured concrete dries out slower. This is not the trend among the 10-day cure group.

Specimens subjected to 10 days of "mist" curing appear to have the best curing based on its low drying rate of 0.41 RH/day at 306 hours of age among the 10-day cure sections (Figure 5.10). The 10-day conventional cured slab, which is characterized as the "standard" section, had the least moisture at a 306 hour age (Table 5.2) among the 10-day group and a drying rate that is double of that of the 10-day "mist" cured specimens. The low moisture content and high drying rate of the 10-day conventionally cured sections attribute to the lower compressive strengths when compared to the other two treatments.

It appears prolonged cure durations, such as 10 days, help increase strength for "throw-on" and "mist" treatments at later test ages. Strength assessment for the 10-day specimens is less dependent on drying rate and moisture presence at time of testing. Noting this last point, a curing duration threshold may exist when concrete strengths are no longer dependent on the drying rate or presence of pore humidity.

5.3.2 Slab Strength Development and Equivalent Age

This section graphically displays the compressive strength gain for the first 15 days of concrete sections subjected to different cure treatments and durations (Figures 5.14 – 5.16.) These figures illustrate the data range of three cores for a particular cure duration, treatment, and age. A vertical line is provided to indicate one standard deviation from each side of the average from the set of three cores. In addition, straight trend lines are provided to connect the average value from each set of cores to the next test age. The solid, dotted, and broken trend lines correspond to the conventional, "throw-on", and "mist" cures, respectively.

Each figure compares the strength development of the three different treatments with the same cure durations. Along with strength development, equivalent ages are provided in a table within each figure for each set of cores. Equivalent ages were determined with the Arrhenius function and the recorded slab temperature histories (Figures 5.3 – 5.7). It should be noted that compressive strength values are not available for 10-day cured section during the first two test

dates since curing media was still in place. Therefore, Figure 5.16 only includes data points at Day 15.

Evaluating the equivalent ages for the 0-day sections reveal that they are relatively close to each other for any given test age. At 360 hours of age, the conventionally cured slab sections had the higher equivalent age among the 0-day sections, yet had the lowest strength among this set (Figure 5.14). Reasons for the lower strength values can be due to moisture content, brittleness of the concrete, and the application of a curing compound as previously mentioned. Both the 0-day "throw-on" and "mist" treated sections show similar strength gain trends and depart from the conventional treated sections and is expected since the 0-day "throw-on" and "mist" sections are nearly identical.

Concrete subjected to cure durations of 4 days do not show the disparity as shown by the 0-day cured sections. Compressive strengths for this cure group (4 days) at each test age for the three cure treatments generally were close to each other (Figure 5.15). Equivalent ages for this cure duration also exhibited similar trends as the 0-day cure sections. The equivalent ages were similar for the three treatments at any given test age.

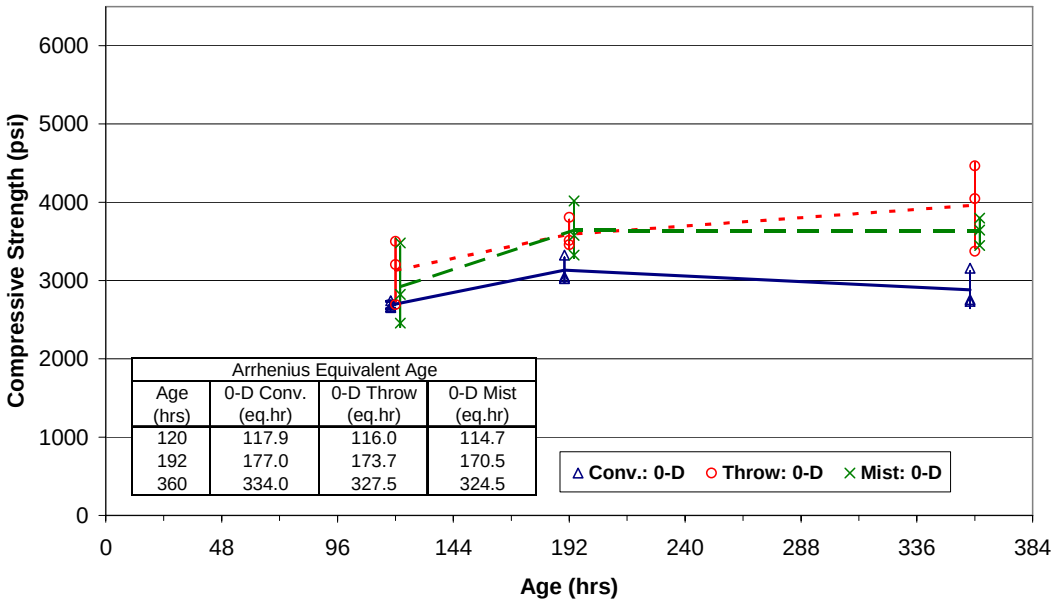

Age (hrs)

Figure 5.14 Slab Strength Development of 0-Day Cure Sections

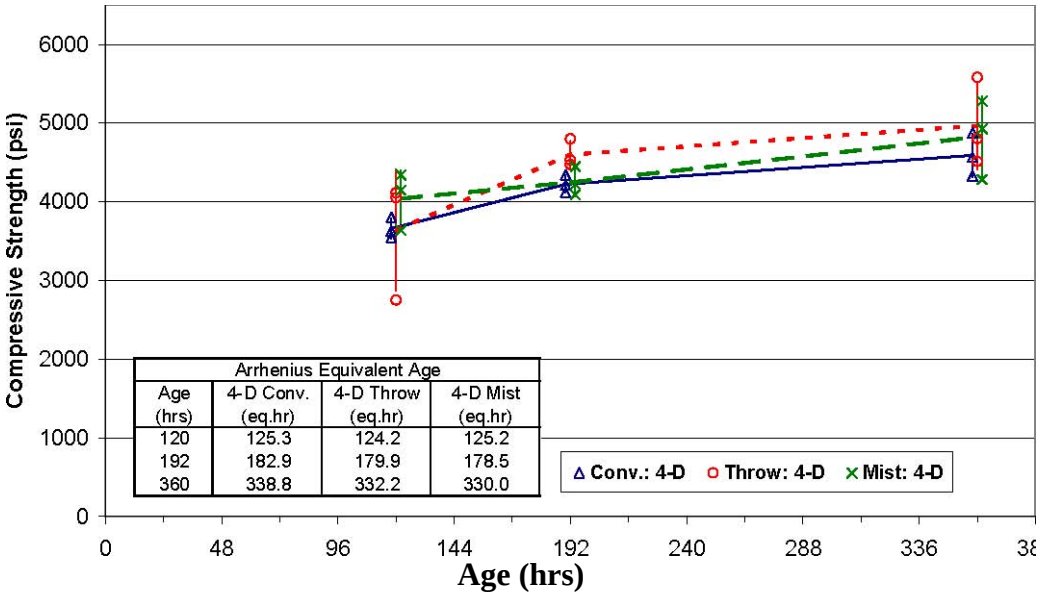

Figure 5.15 Slab Strength Development of 4-Day Cure Sections

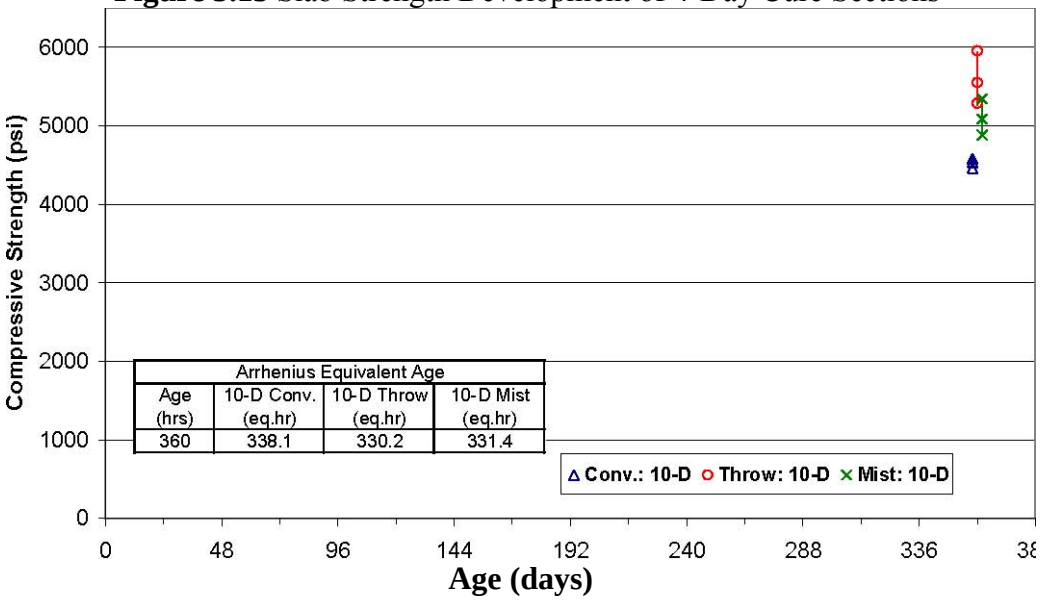

Figure 5.16 Slab Strength Development of 10-Day Cure Sections

Again, the conventional treated section has the highest equivalent age (338.8 hours) at 360 hours, but has a slightly lower average compressive strength compared to the other sections. The lower strength associated with the conventional treatment can be due to the moisture state of the specimen at time of testing and the rate of drying experienced during maturation. Although slightly lower in compressive strength, the 10day conventionally cured section is still within 500 psi of the other two treated sections.

Compressive strength data for 10-day cure section is only available at 360 hours of age and therefore equivalent ages are only provided for this age (Figure 5.16). Regarding compressive strength for this set, the conventional treated cores had the lowest average strength (4527 psi)

compared to the other two treatments. However, it is noticed that more scatter exists among the strength data associated with "throw-on" and "mist" treatments. This variability is examined in more detail in the next section.

5.3.3 Slab Compressive Strength Coefficient of Variability

Referring to Figure 5.16, compressive data for the 10-day conventional cured section varied less than for the other two treatments. This generally was true of the 0-and 4-day conventional cured section (i.e. less variability among compressive strength data for conventional sections). Table 5.5 lists the coefficient of variability for each set of core specimens. The values in the table reveal lower variability among strength data for most of the conventional treated specimens at a given test age and cure duration.

This is more distinguishable if an average of the coefficient of variability is taken for each cure treatment and duration, (i.e. averaging the values of each column). These average values are tabulated in Table 5.6 and have been further averaged in the last row to depict the variability in strength for each cure treatment.

Table 5.5 Compressive Strength Coefficient of Variability for Slab Sections

Test Age		0-Day			4-Day			10-Day		
(day)	(hrs)	Conv.	"Throw"	"Mist"	Conv.	"Throw"	"Mist"	Conv.	"Throw"	"Mist"
5	120	1.7	13.0	17.7	3.6	21.1	9.0	-	-	-
8	192	5.3	5.3	9.6	2.7	3.8	4.3	-	-	-
15	360	8.3	13.9	4.8	6.0	11.1	10.5	1.3	6.0	4.6

-*Values are in percent*

Table 5.6 Strength Coefficient of Variability – Averaged

Cure	Cure Treatment		
Duration	Conv.	"Throw"	"Mist"
0-D	5.1	10.7	10.7
4-D	4.1	12.0	7.9
10-D	1.3	6.0	4.6
Average	3.5	9.6	7.7

-*Values are in percent*

Referring to the average values in Table 5.6, the conventional treatment has the lowest coefficient of variability among strength data when considering the different cure durations. Assuming all test specimens were handled and tested in the same manner, concrete cured in a conventional manner would produce a more consistent composition. Coefficients of variability of 9.6% and 7.7% for the "throw-on" and "mist" treatments, respectively, are substantially

higher when compared to 3.5% for the conventional treatment.

The lower variability of the conventional treatment could be due to the curing compound. When applied to slab surfaces, curing compound forms a membrane that retards mix water evaporation and, quite possibly to some degree, the ingress of moisture for moist cure treatments. As a result, the pore humidity of the conventionally treated concrete is more constant throughout its age and experiences less internal moisture fluctuations. This is fairly noticeable when examining pore humidity profiles for the 0- and 4-day cure durations (Figures 5.7a and 5.8a). "Throw-on" and "mist" treatments typically absorbed the most moisture during water coring and dried out quicker compared to sections treated with a curing compound.

5.4 Cylinder Strength Comparison

The six-inch diameter cylinders were not subjected to the different cure treatments of the slabs. Rather, they were exposed to the more traditional treatments of test cylinders with some modifications. Handling and curing of test cylinders are described in Chapter 4. Since cure treatments were not compared for test cylinders, strength data is used as a representative of the strength behavior development of the AMA concrete mixture to cure duration effects. Figure 5.17 displays the strength data for each of the three durations at each test age. Cylinders were tested at Days 1, 3, 7, 14, and 28. Similar to previous strength graphs, a horizontal line is provided to distinguish the standard deviation from each side of the mean value. Trend lines have also been provided with the solid, dotted, and broken lines corresponding to the 0-, 4-, and 10-day cured cylinders, respectively.

It is apparent the 0-day cured cylinders have lower strength values compared to cylinders receiving some duration of curing in the lime bath. Non-moist-cured cylinders reach an approximate compressive strength of 3000 psi and level off. The 4- and 10-day cure cylinders continuously gain strength and are similar in strength at 336 hours and somewhat at 672 hours.

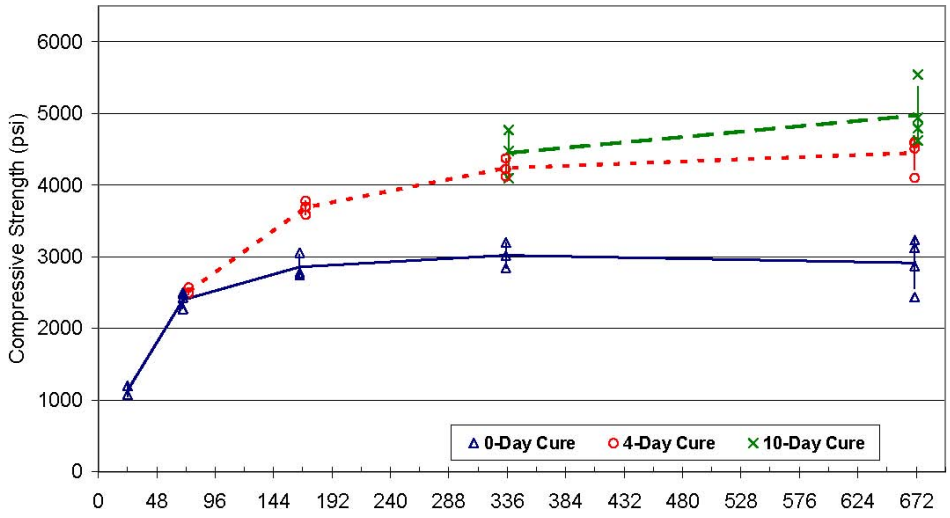

Figure 5.17 AMA Cylinder Strength Development.

Compressive strengths from the 6-inch cylinders are more representative of strengths for the conventional treated sections. Cylinder strengths on Days 7 and 14 were usually slightly lower than corresponding core strengths from the conventional cured sections. Differences between cylinder strengths and conventional cured cores were typically less than 500 psi. The lower strengths from cylinders are due to the larger size of the specimen, (i.e. size effects). Although correction factors were applied to core strengths, it is believed that this will not always be a true 1 to 1 correlation between specimens of different height and diameter. Ultimately, the test cylinder (6-inch diameter by 12-inch height) serves as an acceptable means to correlate strength with drilled cores.

5.5 AMA Permeability

Permeability results for the AMA mixture are somewhat limited. RCPT data for 10 days of curing was not available for "throw-on" and "mist" treatments. Instead RCPT data for the 14-day cure duration is presented when comparing the three different cure treatments (Table 5.2 and Figure 5.18). RCPT data was available for all cure durations of the conventional treated slab and thus included in some of the comparisons made in upcoming sections. Water soluble integral chloride results for the prismatic ponding blocks are presented in Figure 5.20. These blocks were not exposed to the three different cure treatments, but rather submerged in a lime bath as describe in Chapter 4. Water soluble integral chloride results from ponding blocks depict the resistance to chloride permeability with increasing cure duration.

5.5.1 AMA RCPT

Since 10-day cure RCPT results for the "throw-on" and "mist" sections are not available, it is assumed the 14-day cure duration results (which were available) would be fairly representative of a 10-day cure period. RCPT values for the different cure treatments and durations are presented and are the average of three tested specimens (Table 5.7 and Figure 5.18). All treatments for the 0-day cure sections had approximate

RCPT values from 4200 to 4800 coulombs. These RCPT values correspond to concretes having a high permeability based on ASTM C1202 classification criteria (Table 2.5). RCPT values for the three treatments were generally lower with 4 and 14 days of curing when compared to no curing. Conventional cured concrete had a high reduction in electrical conductance with 4- and 14-days of moist-curing. RCPT values were 1858 and 2342 for the 4- and 14-day cures, respectively. Both these values are on the borderline of a "low" and "moderate" permeable classification based on ASTM C1202.

"Throw-on" treated sections had a lower reduction in RCPT values when compared to the conventional cured concrete. The RCPT values between the 4- and 14day "throw-on" cure are 2783 and 3096 respectively. These values indicate that the "throw-on" treatment for this concrete mixture would produce a "moderate" permeable concrete.

Table 5.7 AMA RCPT Core Data

Cure Duration	Cure Treatment		
	Conv.	"Throw"	"Mist"
0-D	4427	4796	4198
4-D	1858	2783	4269
14-D	2342	3096	3352

- Values are in coulombs

"Mist" treated sections did not show an improvement in electrical resistivity with a 4-day cure duration. A lower RCPT value is noticed with 14 days of curing. A drop of about 850 coulombs is noticed between the 0- and 14-day cure for the "mist" treated sections. From the results, it appears the "mist" cure would produce a moderately high permeable concrete for the AMA concrete mixture.

The only noticeable trends for electrical resistivity are for both the conventional and "throw-on" treatments. Since RCPT is highly variable, it is difficult to determine any clear trends. This is obvious when comparing the 0-day cure data for both the "throw-on" and "mist" treatments. The six specimens used for RCPT for the 0-day "throw-on" and "mist" sections are practically the same. The same concrete mixture was used for both and no cure protection was provided. Nevertheless, RCPT data between them differs by an average of 600 coulombs. It is also noticed that RCPT values slightly increased when the curing duration went from 4 days to 14 days. This was not expected since, intuitively, increased curing duration should promote hydration and lessen permeability potential.

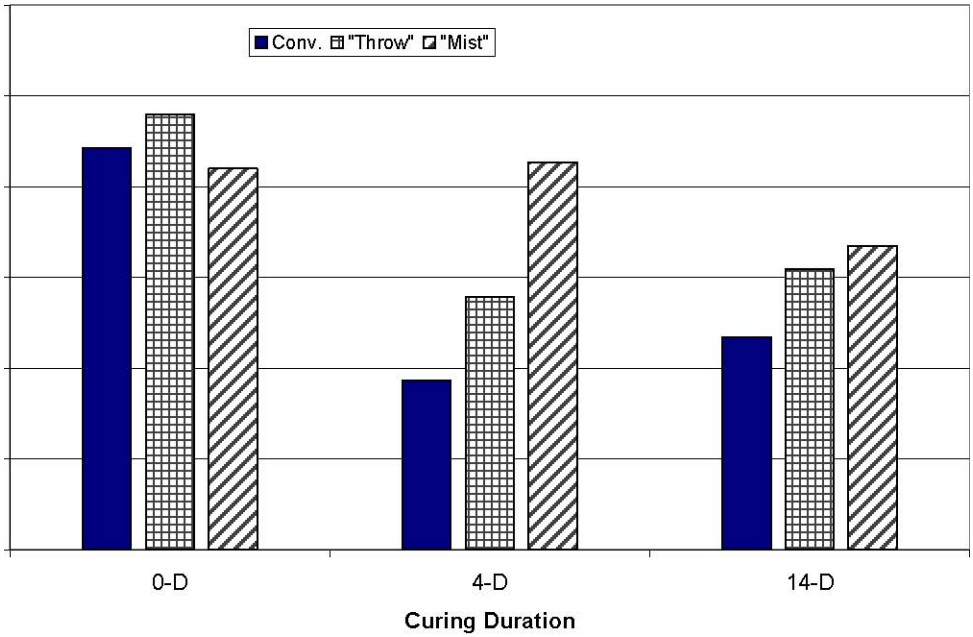

Figure 5.18 AMA Core RCPT Comparison

5.5.2 AMA In Situ Strength and RCPT Relationship

A relationship between in situ strength and RCPT for the three cure treatments are shown in Figure 5.19. Strength and RCPT for all cure durations of the conventional treated slab are included in Figure 5.19. Additional RCPT data was not available for the other two cure treatments due to limited sampling time.

Since RCPT data is limited, an accurate correlation between compressive strength and permeability via RCPT cannot be established. The data available indicates that RCPT readings appear to decrease with increasing strength, but this trend is broad. If RCPT data for the conventional treatment is isolated from the other cure treatments, a more distinct linear RCPT decline is noticed with increasing strength. The RCPT trend for the conventional treatment is shown with a solid line, while those for the "throw-on" and "mist" treatments are shown with a broken and dotted line, respectively.

A correlation between strength and RCPT is not as distinct as the previous correlation made from the field site study for several reasons. First, AMA RCPT core samples were anywhere from 100 to 109 days old when tested compared to 56 days of age for the previous concrete mixtures. Also, in situ strengths for the established comparison were for 15 days of age compared to 28 days of age.

An important factor to consider is the composition of the AMA mixture. This mixture contains siliceous gravel and such aggregate type usually yields higher and erratic RCPT results. This was observed for the PHR and ATL mixtures. Another difference of this mixture is the amount of binder, (i.e. cement and fly ash). This mixture is a 6 sack mixture whereas all mixtures from the field study had a 6.5 sack quantity. Additionally curing temperature can influence permeability as well. Owens (1985) found that concrete containing fly ash had lower permeability when cured at higher temperatures. Curing temperatures for the AMA slabs were generally below 70 °F for the entirety of their age whereas field decks presented in Chapter 3 were well above this temperature.

5.5.3 AMA Ponding Permeability

Water soluble integral chloride was determined from 12-inch by 12-inch block specimens. These specimens were not subjected to the three different cure treatments as the slabs in the structures laboratory. Results shown in Figure 5.20 only display the effect cure durations have on permeability. Permeability plots for both the 10- and 14day cures are included. Both of these are presented since previous RCPT and compressive strength discussions have been primarily with the 10-day cure duration and recent RCPT data results were only available for the 14-day cure sections. Water soluble integral chloride is determined by procedures detailed in Appendix A.

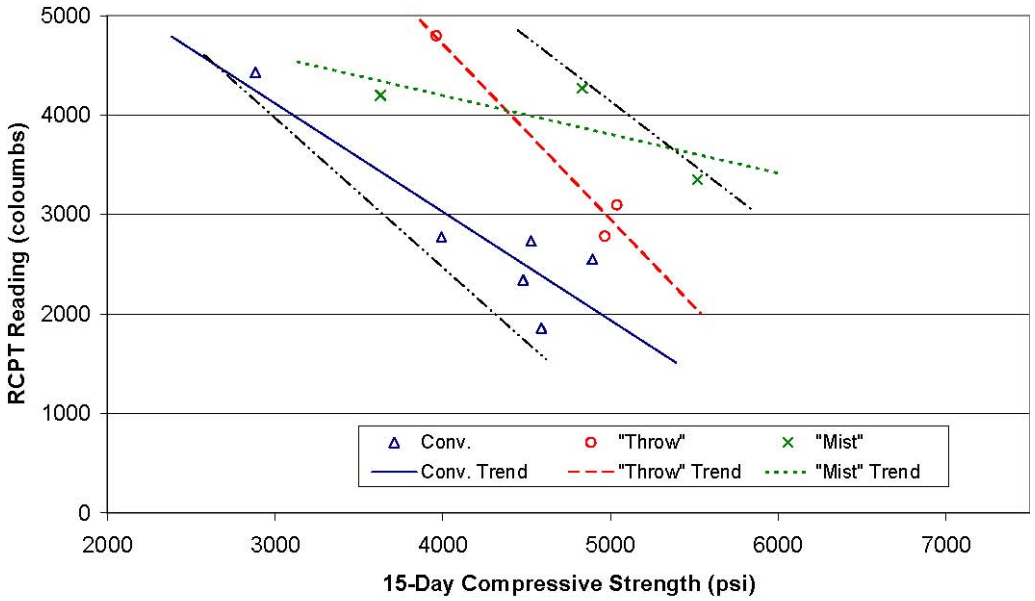

Figure 5.19 AMA Core Strength & RCPT Relationship.

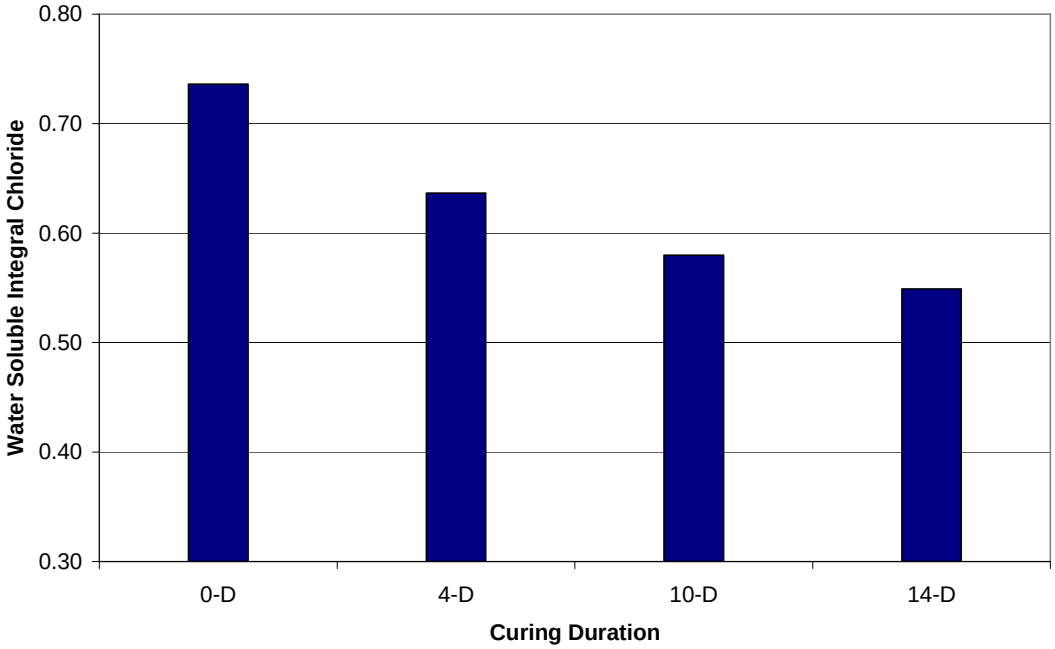

Figure 5.20 AMA Permeability for Varying Cure Durations

The content of water soluble integral chloride decreases with increasing cure periods. Decrease in chloride content is initially relatively large with the introduction of a moist curing period. Thereafter, chloride permeability is gradually lowered, with increasing cure periods.

The AMA ponding test presents much clearer results than the RCPT. The ponding test minimizes the influence siliceous gravel may have on the results. Ponding specimens are in a more controlled environment since they are completely submerged in a lime water bath during

curing. This eliminates the constant attention required of the three cure treatments such as periodic saturation of cotton mats. In addition, RCPT samples may experience some damage during drilling or sawing. This activity may introduce micro-cracks into the concrete matrix thus allowing a higher permeability reading. Ponding samples do not have to undergo the same degree of potential damage.

5.5.4 AMA Cylinder Strength and Integral Chloride Relationship

Cylinder compressive strengths and integral chloride contents from block specimens are displayed in Figure 5.21 to distinguish the relationship between these two parameters. Data points reveal increasing compressive strength results in lower chloride permeability. The trend for this relationship is more evident in this plot than in Figure 5.19. Chloride content data is not as variable compared to RCPT results and is not extremely affected by the type of aggregate used. Also, cylinder compressive strengths give more consistent results compared to 4-inch diameter drilled cores of varying heights. Therefore, the type of specimens and test results used for this comparison give a better relationship.

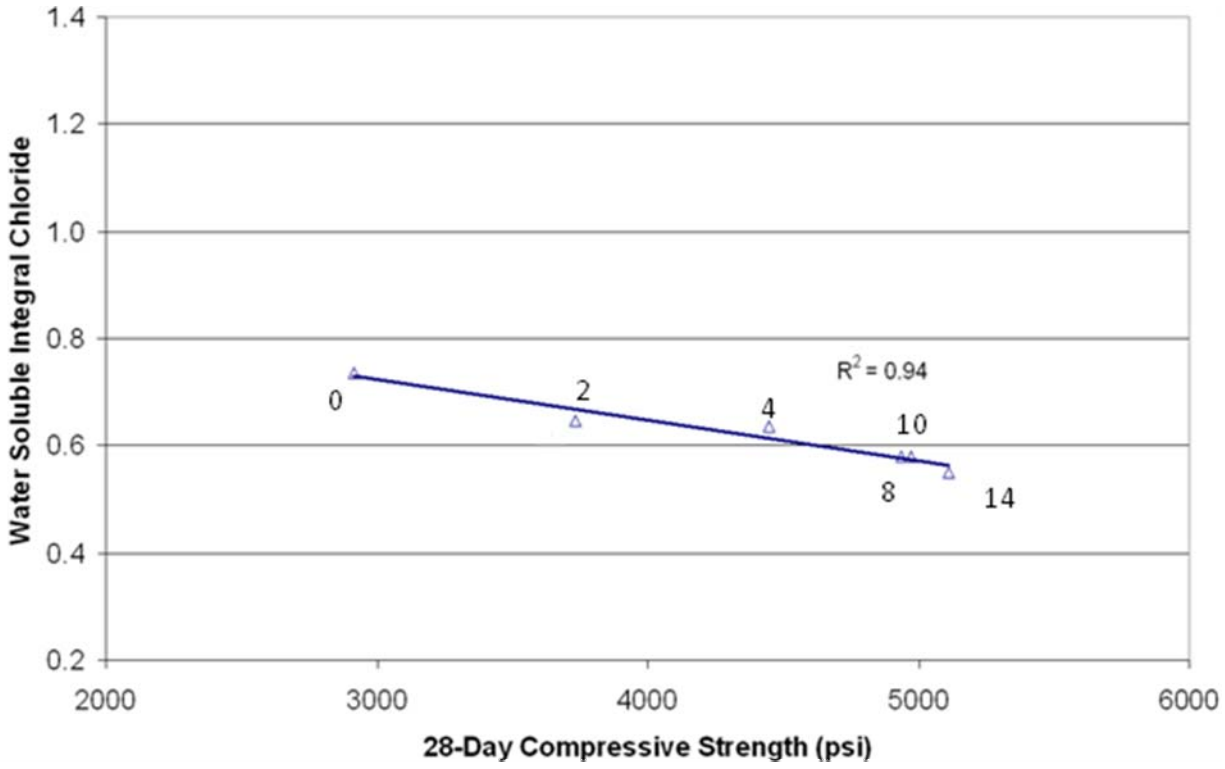

Figure 5.21 AMA Cylinder Strength and Integral Chloride Relationship

5.5.5 AMA RCPT and Integral Chloride Relationship

Figure 5.22 correlates RCPT and chloride content for the AMA mixture. Each data point is accompanied by a number indicating the duration of moist curing. Intuitively, one would expect permeability resistance to increase with prolonged curing. This is not the case when an

assessment is based on RCPT. It would be expected that the 0-day data would be the farthest to the right in Figure 5.22 (which is true for this set of data) followed by data points with ascending cure durations to the left. Instead, the 4-day cure data point is farthest to the left with a cluster of remaining data points in no particular order between the two extreme points. Based on established criteria for RCPT readings the data classify the AMA mixture as having "high" to "low" permeability depending on cure duration.

On the other hand, ponding test data do follow an anticipated pattern. The 0-day data point is expected to be the highest point in Figure 5.22 followed by data points with ascending cure durations downward. With regard to this pattern, there is more confidence in chloride content results from ponding tests.

Paired RCPT and integral chloride do not lie within the boundaries established. These points lie at the lower boundary and may be due to the siliceous gravel within the mixture. Substituting the coarse aggregate in the mixture with a less conductive aggregate, such as limestone, may theoretically result in lower RCPT readings and thus would potentially shift data points to the left. In this case, paired data points may then lie within the boundaries. Ponding data classify all cure durations for the AMA mixture as a "low" permeable concrete from findings of Whiting's work.

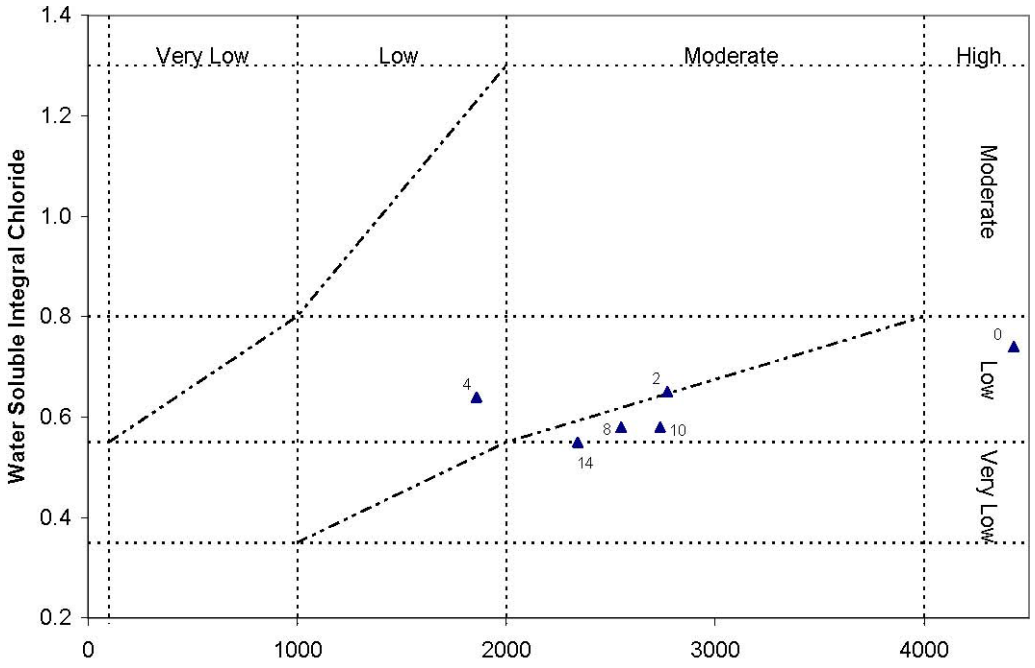

Figure 5.22 AMA RCPT and Integral Chloride Correlation

5.6 Summary of Results for Different Cure Treatments

Temperature history plots demonstrate higher and more consistent concrete temperatures are maintained with longer cure durations. It is also observed that the curing compound does affect the initial peak temperature of concrete slabs. This is demonstrated by the 0-day sections. The

0-day conventional section, which had a curing compound application, had a slightly higher peak temperature when compared to the other two 0-day treatments.

Moisture monitoring revealed less moisture fluctuation associated with the sections receiving a curing compound application. Conventionally cured sections underwent lower adsorption during water coring and usually had lower drying rates.

There is some improvement in moisture retention with the "mist" treatment is kept in place for 10 days. However, a 4-day "mist" treatment does not yield the satisfactory properties associated with the 10-day duration. Sections exposed to "throw-on" treatments had unusual drying trends. Drying trends did not suggest a lowering or increasing drying rate with an extended curing duration.

In situ compressive strengths were somewhat lower for conventional treated sections compared to the two other treatments. Most often, pore humidity was highest in the conventional sections. The higher pore humidity content suggested a more saturated sample and may be responsible for lower compressive strength values. In addition, less variability was noticed among compressive data for the conventional cured sections. The "throw-on" and "mist" sections both had overall standard deviations that were more than two times higher than the conventional treated sections. The lower strength variability associated with the conventional treated section may indicate a more consistent concrete matrix.

Equivalent ages were not affected by the type of curing treatment. For example, the 10-day equivalent ages at 360 hours of age (Figure 5.16) were similar for all three treatments. Equivalent ages are affected to some degree by the length of treatment. In the extreme case between the 0- and 10-day conventional cure sections at Day 15, average compressive strengths differ by 1500 psi but only differ by 4 equivalent hours. Equivalent age therefore should consider concrete moisture during curing to determine a better degree of hydration and progression of concrete maturity.

All concrete sections which received no moist curing exhibited high RCPT values. Slab sections undergoing conventional treatment for 4 and 10 days showed the most improvement in RCPT readings. "Mist" treated section had the highest RCPT values when a cure treatment was in place. Intermediate RCPT values resulted from the "throw-on" treatment. Since the AMA mixture contained siliceous gravel, RCPT values may be higher than expected. But with the acquired results, it can be assumed that the conventional treatment offers the best protection against permeability relative to the "throw-on" and "mist" treatments.

Chloride penetration via ponding was not conducted for the three different cure treatments. It was however tested for varying cure durations in a lime bath. Results from the ponding test reveal that permeability resistance increases with prolonged curing duration. The correlation between RCPT coulomb readings and water soluble integral chloride demonstrate the ponding test is the better choice to determine permeability if time is not an issue.

Findings from the AMA study will be used in the next chapter to establish improvements to current maturity functions. With an improved method, strength and durability can be better assessed. The scope of this modification encompasses moisture as a parameter to calculate equivalent ages.

CHAPTER 6

DEVELOPMENT OF A CONCRETE STRENGTH DURABILITY INDEX (SDI)

The maturity method when implemented under ideal conditions, (i.e. near 100% pore humidity and minimal concrete temperature fluctuations) can be a very effective strength prediction tool. However, field-cast conditions are rarely ever ideal and one cannot say with certainty how much moisture is available within a hydrating concrete to determine an appropriate equivalent age. Results from field cast deck slabs (i.e. ELP, FTW, SAT and HOU) under varying curing durations have demonstrated that compressive strength cannot be properly assessed with current maturity models. This was also true of the AMA deck slabs which were in a much more controlled environment when compared to field cast specimens. The following chapter re-emphasizes the results from the tested mixtures and sets the framework and ideology for a proposed strength durability index (SDI).

6.1 Arrhenius Equivalent Age and Compressive Strength for Field Deck Slabs

Figure 6.1 shows normalized equivalent ages and compressive strength for each concrete mixture tested in the field with respect to its 10-day cured section at a test age of 29 days. Arrhenius equivalent ages for 10-day cured sections for ELP, FTW, SAT, and HOU at this age are 1193, 764, 1306, and 1141 equivalent hours, respectively. Accompanying compressive strengths for the 10-day cured sections for ELP, FTW, SAT, and HOU at this age are 5086, 4262, and 6464, and 6937 psi. By normalizing Arrhenius equivalent age and strength data for each concrete mixture with respect to its 10-day section, a comparison of calculated Arrhenius equivalent ages and compressive strength among the three cure durations can be made.

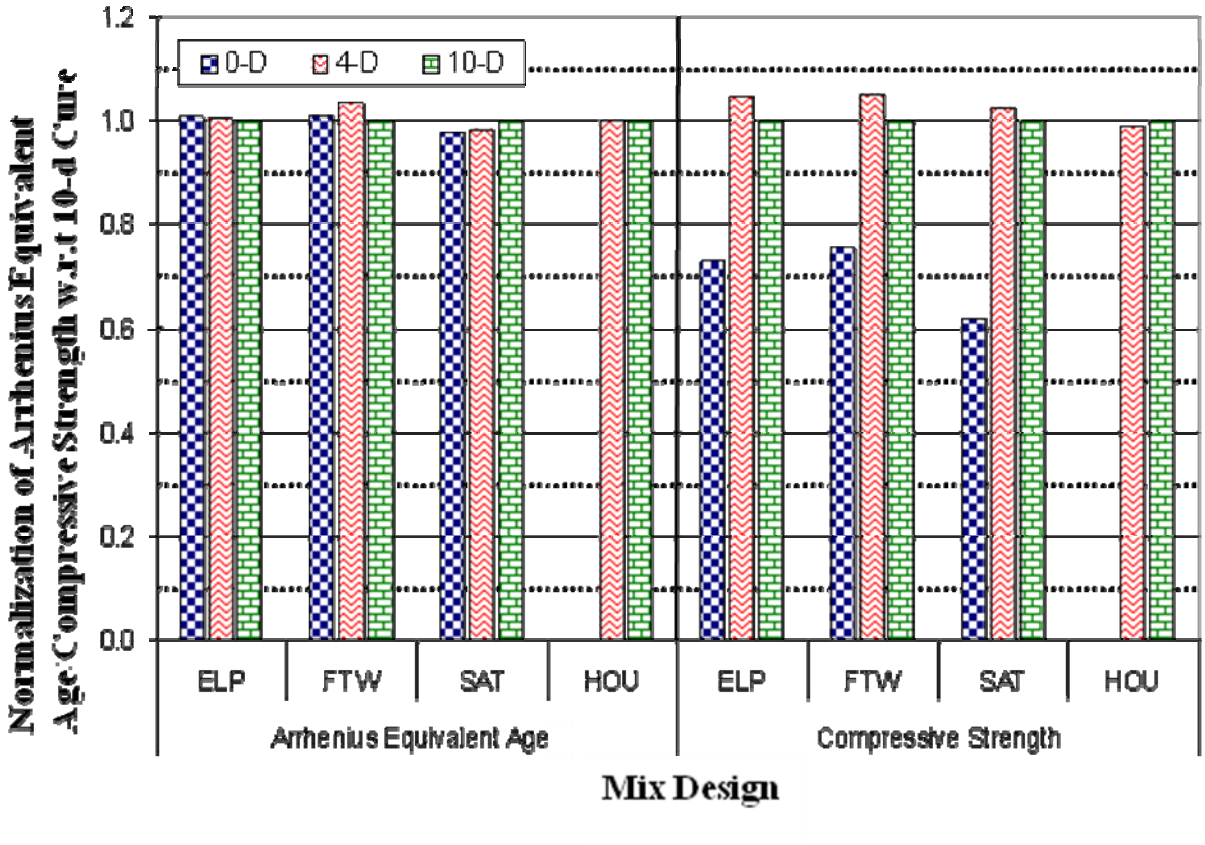

Figure 6.1 Normalized Calculated Arrhenius Equivalent Age and Observed Compressive Strength at 29-Day Age

The maturity method implies that two maturing concretes with similar equivalent ages should have similar strengths. Observing the left-side of Figure 6.1, the three different cure durations for a given concrete mixture yield very similar equivalent ages. For example, the 10-day equivalent age for ELP at 29 days of age is 1193 equivalent hours, and the corresponding 0- and 4-day bar graphs for ELP (Figure 6.1), show similar equivalent ages. This in turn would suggest that the 0-, 4-, and 10-day cure durations all would produce concretes with similar strength. This is not the case when observing the right-side of Figure 6.1. The 0-day cured sections yielded compressive strengths relatively lower when compared to their 4- and 10-day cured counterparts. Compressive strengths from 0-day cured HOU cores were not available but it is concluded that these strengths would be lower than the 4- and 10-day cured sections. On the other hand, 4- and 10-day cured sections for each respective concrete mixture in Figure 6.1 had reasonably similar compressive strengths to each other. With respect to the ELP, FTW, SAT, and HOU compressive strengths shown in Figure 6.1, one can infer that the 4- and 10-day wet-mat cure durations would result in similar concretes.

6.2 Arrhenius Equivalent Age and RCPT for Field Deck Slabs

Figure 6.1 demonstrated that the 4- and 10-day cure durations for a given concrete mixture produced similar compressive strengths at a test age of 29 days. Figure 6.2 examines the 56-day permeability of each concrete mixture and its respective equivalent age at 29 days of age. The left-hand side bars are the same in Figure 6.1 while the right-hand side bars represent RCPT for each concrete mixture with respect to its respective 10-day cure section.

Figure 6.2 reveals that the 0-day cure sections had much higher RCPT values when compared to the 4- and 10-day wet-mat cured sections. The 0-day section of each concrete mixture varied differently when compared to the two other cure durations. The mixture constituents and proportions affected the degree of permeability for the 0-day cured concrete. The 4- and 10-day cured wet-mat sections had very similar RCPT values. For the given concrete mixtures tested, it appears that a 4- and 10-day wet-mat cure would produce concretes with similar strengths and permeability.

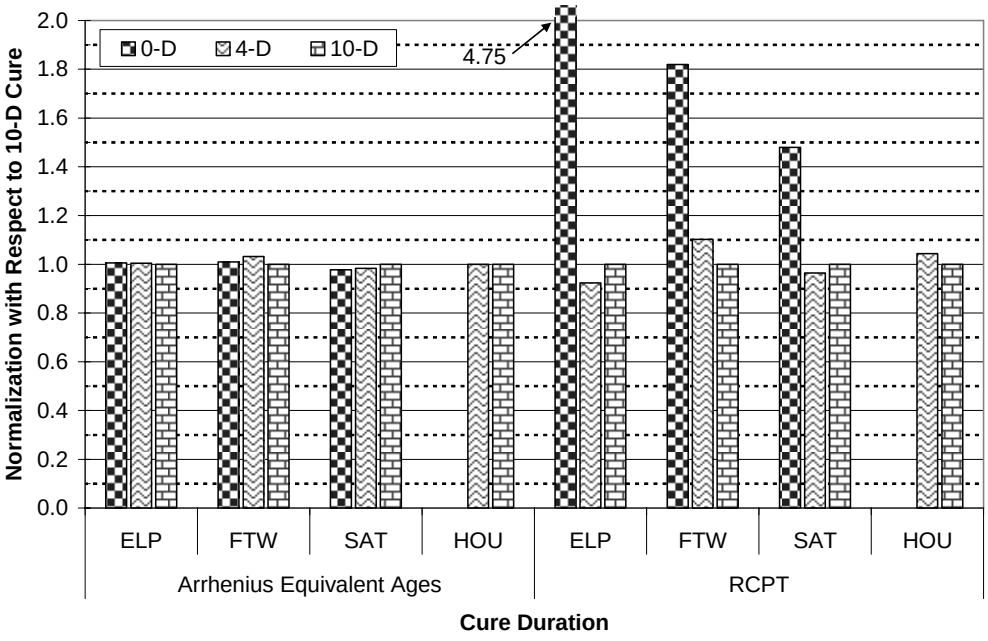

Figure 6.2 Normalized Calculated Arrhenius Equivalent Age and Observed RCPT at 29-Day Age.

6.3 Arrhenius Equivalent Age and Compressive Strength for AMA Slabs

Figure 6.3 displays the Arrhenius equivalent age at a concrete age of 15 days for each cure duration and treatment with respect to the 10-day conventionally cured section. The Arrhenius

equivalent age of the 10-day conventional cure section at test age of 15 days is 338 hours. Compressive strengths at 15 days of age are shown on the right-hand side of Figure 6.3. These strengths are relative to the 10-day conventionally cured strength of 4527 psi.

The bars on the left-hand side, representing equivalent age, are all relatively close to a value of one. This means that the three different cure durations and treatments used for the AMA mixture would produce concretes with similar equivalent ages under similar ambient conditions. Therefore in theory, all the concrete sections shown in Figure 6.3 would have similar compressive strength characteristics. The bars on the right-hand side dispute this claim. If the concrete strengths were similar, then the bars on the right-hand side would all be relatively close to a value of one. The 0-day cured sections for the three different treatments were fairly lower when compared to the 10-day conventionally cured section. Since the 0-day cured sections received no additional moisture, proper hydration could not continue to increase compressive strength.

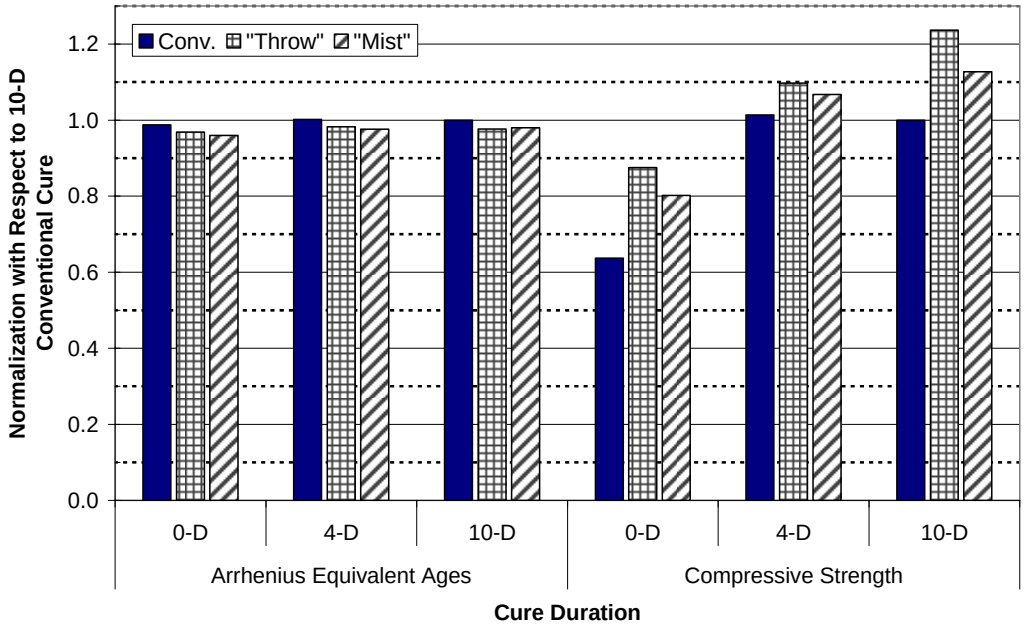

Figure 6.3 Normalized Calculated AMA Arrhenius Equivalent Age and Observed Compressive Strength at 15-Day Age.

The 4- and 10-day conventional cured sections show a similar trend as with the wet-mat cured sections in Figure 6.1. Both Arrhenius equivalent ages and compressive strengths for the 4- and 10-day conventionally cured sections were similar at 15 days of age. Therefore the amount of moisture available for hydration is critical for strength development for the period prior to 4 days.

The 4- and 10-day "throw-on" and "mist" sections developed slightly higher compressive strengths when compared to the 10-day conventional section at 15 days of age. This suggests that not only does the duration of cure affect strength gain, but that the curing treatment employed will also affect it.

6.4 Arrhenius Equivalent Age and RCPT for AMA Slabs

The right-hand side of Figure 6.4 displays the RCPT values with respect to the 14-day conventional section at an age of approximately 105 days. The RCPT value for the 14-day conventional section is used as opposed to the 10-day conventional section since no RCPT cores were available for any of the 10-day cure treatments. The 14-day conventional section has a RCPT value of 2342 coulombs.

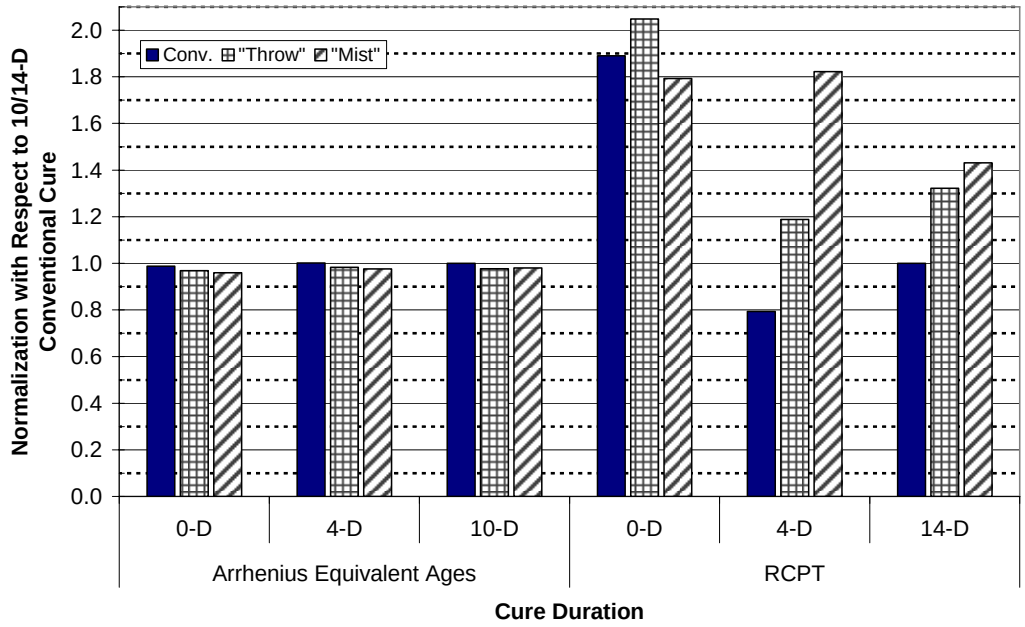

Figure 6.4 Normalized Calculated AMA Arrhenius Equivalent Age at 15-Day Age and Observed RCPT at Approximately 105-Day Age.

When comparing the relative RCPT values to the relative Arrhenius equivalent ages on the left-hand side of Figure 6.4, it is obvious that similar equivalent ages do not result in similar RCPT readings. The 0-day cured sections for the three cure treatments and the 4-day "mist" cure section yielded substantially higher RCPT values. Sections cured with the 4- and 10-day "throw" treatment and the 14-day "mist" treatment had fairly high RCPT values compared to the 14-day conventional section.

The 4-day conventional section had a lower RCPT value compared to the 14-day conventional section. This is unexpected since a prolonged curing period would typically hydrate more cement particles and produce a denser concrete matrix and thus reduce permeability. This inconsistency could have been caused by the siliceous gravel of the concrete mixture. Although all concrete was batched from the same concrete truck, the handling and placement of the concrete could have been slightly different for each section. One section may have had more segregation than the other causing a significant portion of the larger aggregate particles to settle to the bottom. Another explanation could be the handling and preparation of cores prior to testing.

6.5 Arrhenius Equivalent Age – Misrepresenting Concrete Properties

Figures 6.1 to 6.4 have shown that the Arrhenius equivalent age cannot depict compressive strength and permeability accurately when considering only concrete age and curing temperature. If these two parameters were the only ones needed, then the data in the right-hand side of Figures 6.1 to 6.4 would support this with values close to one. However, this is not the case. Therefore, considering the amount of moisture during hydration will help determine a more accurate equivalent age for any given concrete. This ideology is explored in more detail in the following sections.

6.5.1 Equivalent Hydration Period

Bažant and Najjar (1972) introduced the equivalent hydration period, t_e, to determine water diffusion of concrete. The equivalent hydration period can be expressed as follows:

$$t_e = \int_0^t \alpha_a \cdot \beta_h dt \,. \qquad \text{(Eq. 6.1)}$$

In Equation 6.1, β_h is considered to be the relative hydration rate expressed as a function of pore humidity. The α_a term in Equation 6.1 is the same parameter as the age conversion factor used in the Arrhenius equivalent age function and is defined in Equation 3.1 The equivalent hydration equation is similar to the Arrhenius equation with the exception of the addition of the relative hydration rate.

It has been reported that hydration of concrete slows down considerably or stops completely when concrete pore humidity is equal to or less than 80% (Powers 1947, Mindess et al. 2002). Bažant and Najjar (1972) have approximated the dependence of the relative hydration rate to pore humidity, h, with the following equation:

$$\beta_h = \frac{1}{1 + (7.5 - 7.5 \cdot h)^4} \,. \qquad \text{(Eq. 6.2)}$$

Equation 6.2 takes the s-curve shape shown in Figure 6.5. This curve, however, does not consider hydration to stop altogether when pore humidity is less than 80%. The relative hydration rate is low, approximately 0.15 at 80% pore humidity.

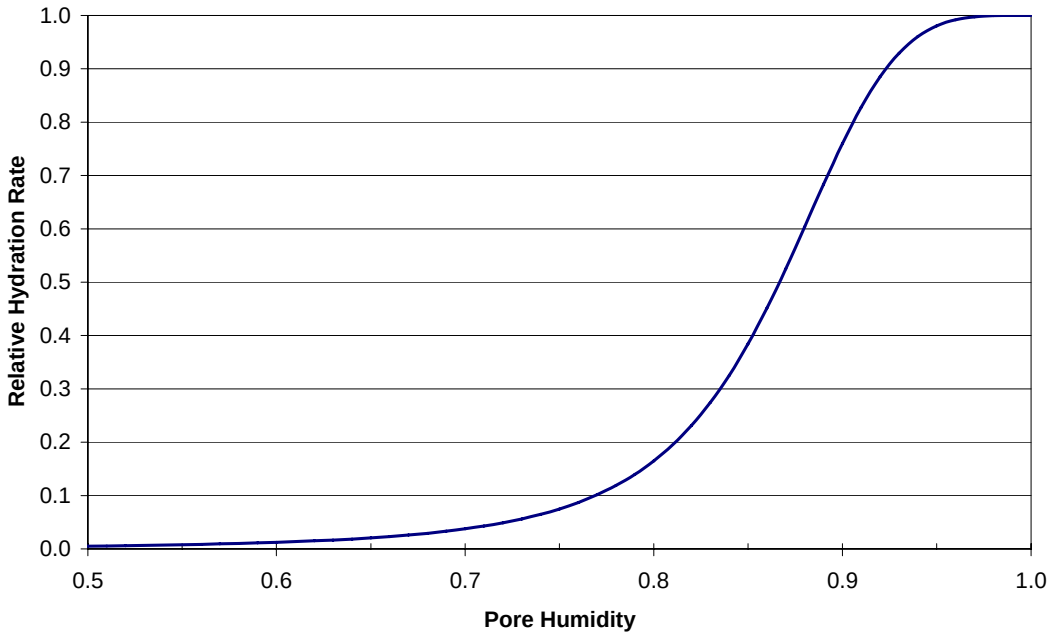

Figure 6.5 Relationship between Pore Humidity and Relative Hydration Rate.

6.5.2 Relative Hydration Age Factor

Equation 6.2 can be expressed in a more generic form as shown in Equation 6.3.

$$\beta_{af} = \frac{1}{1 + (\phi - \phi \cdot h)^n} \qquad \text{(Eq. 6.3)}$$

The shift factor, ϕ, moves the s-curve either to the left or the right while the power, n, alters the slope of the s-curve. Equation 6.3 can be expressed in terms of an inflection pore humidity

tolerance, h_c. For the value of $\phi = 7.5$ as suggested by Bažant and Najjar (1972), it is determined that the corresponding h_c would be 86.67%. From this known relationship, ϕ can be expressed as shown in Equation 6.4.

$$\phi = \frac{1}{1 - h_c} \qquad \text{(Eq. 6.4)}$$

Substituting Equation 6.4 into 6.3 expresses the relative hydration factor with respect to concrete pore humidity and an inflection pore humidity tolerance. The resulting equation is shown in Equation 6.5.

$$\beta_{af} = \frac{1}{1 + \left(\frac{1 - h}{1 - h_c} \right)^n} \qquad \text{(Eq. 6.5)}$$

The h_c parameter is similar to ϕ, in that different values shift the s-curve either to the left or right. Figure 6.6 demonstrates the various positions of the s-curve when h_c = 80, 85, 90, and 95% with n = 4. The curve proposed by Bažant and Najjar (1972) would correspond to a curve that is approximately between the curves with h_c equal to 0.85 and 0.90 in Figure 6.6.

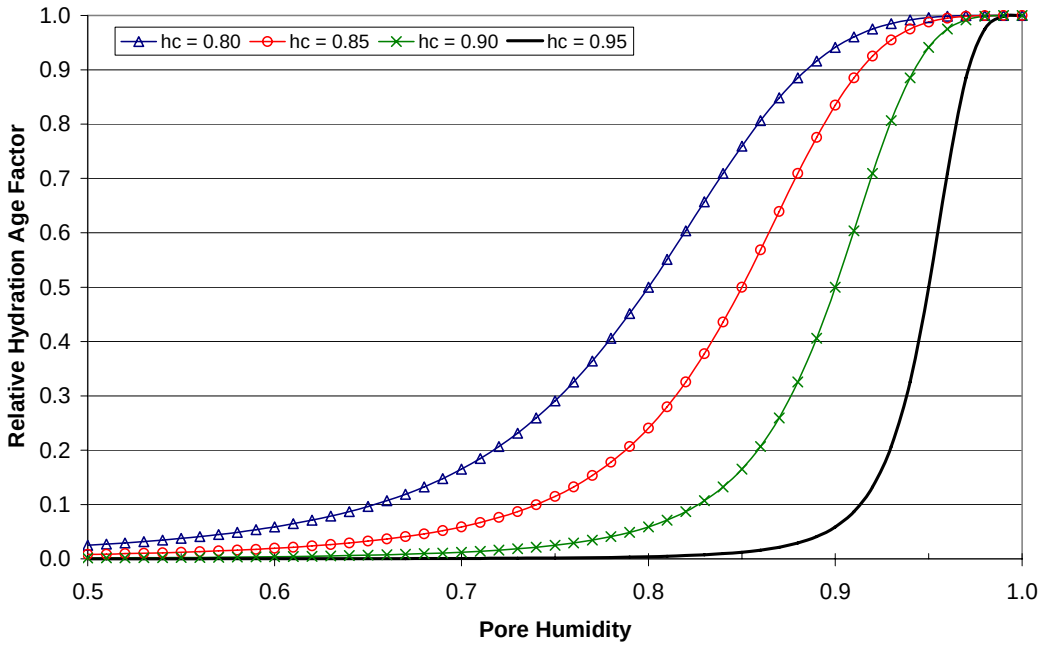

Figure 6.6 Relative Hydration Rate with Different h_c Values and $n = 4$.

The position of a curve that most closely represents hydration slowing down or stopping completely when pore humidity is equal to or less than 80% in Figure 6.6 would lie to the right of $h_c = 0.90$, (i.e. any curve with $h_c \geq 0.90$). Therefore, the relative hydration age factor with $h_c = 0.95$, an arbitrary value greater than 0.90, is plotted with various values of n in Figure 6.7 to demonstrate the effect this parameter has on the relative hydration age factor. All curves in Figure 6.7 have the same inflection humidity point of 0.95 and have half the relative hydration age factor at this point. Whether the relative hydration rate is actually one-half can only be revealed with additional research on this subject.

The Bažant and Najjar (1972) proposed curve indicates the relative hydration rate to be one-half when $h_c = 86.67\%$ (Figure 6.5), but no scientific explanation is given for the use of this value other than experimental data fits this curve well. It is the belief of the author that each concrete mixture behaves differently and the constituents and proportions of the mixture and the cure method used will dictate the values of h_c and n. These values however cannot be determined with the insufficient amount of data available from this research.

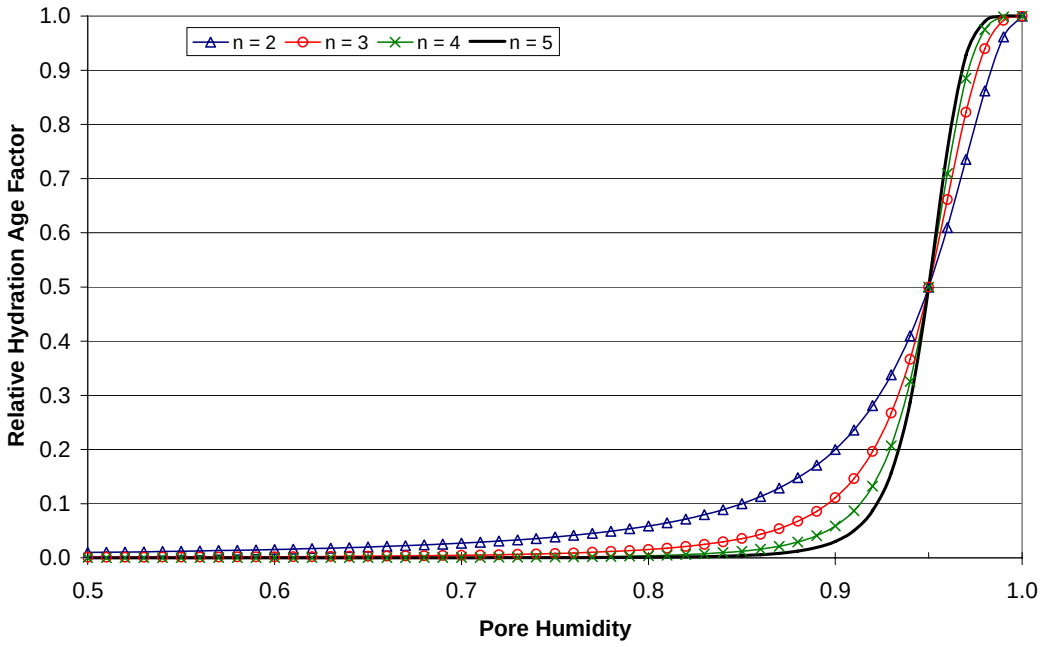

Figure 6.7 Relative Hydration Rate with Different n Values and $h_c = 0.95$.

6.6 Strength Development with Arrhenius Equivalent Age

Strength prediction based on compressive strength and Arrhenius equivalent ages can typically be quite accurate if adequate moisture is provided during curing. In this study, curing was intentionally altered to simulate poor curing conditions, (i.e. 0-day) and several treatment schemes were also studied. To understand the differences curing conditions could have on strength development or prediction, Arrhenius equivalent ages, as determined by Equation 2.5, were determined for the different cure treatments and durations. These equivalent ages are plotted with its corresponding average compressive strength in Figure 6.8. The plotted data is accompanied with the best-fit Freiesleben Hansen (FH) strength gain model (Equation 3.1). The parameters of best fit for the data in Figure 6.8 are as follows: $S_{inf} = 4636.75$ psi, $\tau = 72.04$ hrs, $\alpha = 2.08$.

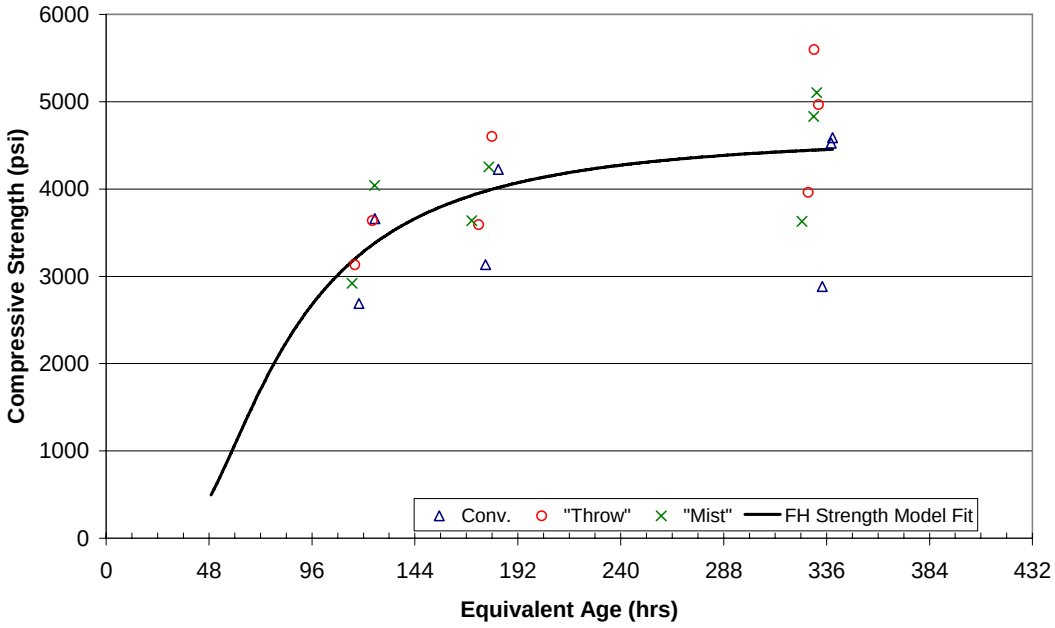

Figure 6.8 Arrhenius Equivalent Age and Strength Data for AMA Slabs.

From Figure 6.8, it is observed that data is highly scattered vertically along three different areas. These areas coincide with the test ages of 5, 8, and 15 days. As test age increases, so does the range of compressive strength. If the plotted FH Strength Model in Figure 6.8 was used as a reference strength-maturity curve, compressive strengths could not be accurately predicted given the variation in curing methods and current equivalent age determination.

6.7 Strength Development with an Equivalent Hydration Period

The equivalent hydration period as proposed by Bažant and Najjar (1972) is investigated to see how well strength data correlates with their proposed age. The equivalent hydration period in Equation 6.1 is modified for ease of calculation and Equation 6.2 is used for β_h. The resulting equation is shown in Equation 6.6 where all its parameters have been defined previously. The equivalent hydration ages and corresponding compressive strengths are plotted in Figure 6.9 with the parameters of best-fit for the FH strength gain model as the following: $S_{inf} = 5352.43$ psi, $\tau = 59.05$ hrs, $\alpha = 1.06$.

$$t_e = \sum_0^t e^{\left[\frac{E}{R}\left(\frac{1}{T_r}-\frac{1}{T}\right)\right]} \cdot \frac{1}{1+(7.5-7.5\cdot h)^4} \cdot \Delta t \qquad (6.6)$$

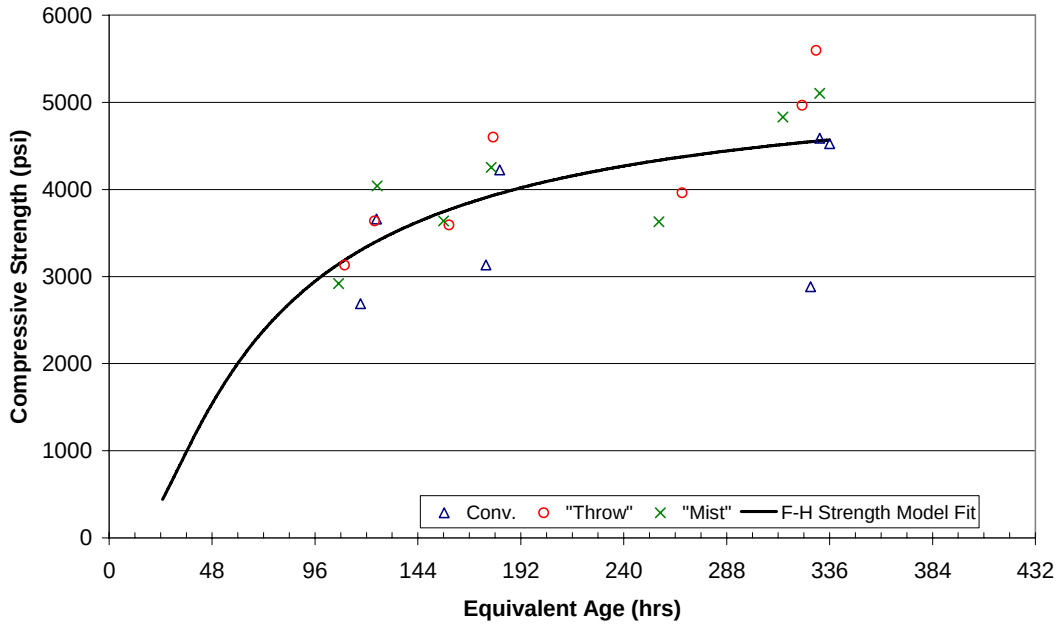

Figure 6.9 Equivalent Hydration Age and Strength Data for AMA Slabs.

The data in Figure 6.9 no longer lines up vertically along test dates, but appears to shift with the adjustment made from the relative hydration rate, β_h. This, however, does not give very satisfactory results when attempting to predict compressive strength with the provided FH strength gain model. The range of compressive strength at an equivalent age of about 336 hours is between 3000 and 5500 psi. The adjustment made with the relative hydration rate demonstrates that equivalent ages can possibly be altered to account for the availability of moisture during curing. An initial proposition to the correction of Arrhenius equivalent ages by applying the relative hydration age factor (Equation 6.5) is discussed in the following section and referred to as the Strength Durability Index (SDI).

6.8 Modeling of Strength Development with Strength Durability Index (SDI)

The compressive strength of concrete can be accurately modeled provided correct parameters are being used. In the previous sections, the Arrhenius equivalent age and the equivalent hydration period were used to characterize the strength development of the AMA mixture under three different cure durations and treatments. Both performed poorly when assigning an equivalent age to its corresponding compressive strength. The introduction of the strength durability index (SDI), t_{sdi}, attempts to improve the determination of a concrete equivalent age. The SDI is an altered form of the equivalent hydration period, t_e. It is believed that each concrete mixture and cure method will have a unique relative hydration age factor as opposed to the values suggested

by Bažant and Najjar (1972). The SDI is expressed as shown in Equation 6.7 and all its parameters have been defined in previous sections.

$$t_{sdi} = \sum_{0}^{t} e^{\left[\frac{E}{R}\left(\frac{1}{T_r}-\frac{1}{T}\right)\right]} \cdot \frac{1}{1+\left(1-h/1-h_c\right)^{n}} \cdot \Delta t \qquad (6.7)$$

Initially when determining values for h_c and n, all AMA compressive strengths for the various cure durations and treatments were treated as a single set. This, however, did not yield equivalent ages resulting in strengths in the proximity of the best-fit FH strength model. Therefore, the cure durations for each specific cure treatment were treated as one set of data to determine the parameters of the relative hydration age factor. For example, the 0-, 4-, and 10-day conventionally cured sections were grouped in a single data set while the 0-, 4-, and 10-day "throw-on" cured sections were grouped in another data set and the same was performed for the "mist" cured sections.

First, SDI values for a particular set of h_c and n parameters were plotted against their corresponding compressive strengths. These data points were fitted with a best-fit natural log curve. The natural log curve was used since compressive strength has been shown to follow this trend at an early age (Plowman 1956). The corresponding R^2 value for the best-fit natural log curve was used as a measure of how well the data was corrected. This process was iterated until a set of h_c and n values generated a R^2 closest to 1. The resulting relative hydration age factor parameters along with the R^2 values for each cure treatment are listed in Table 6.1. It is interesting to see that the h_c values are relatively close to 0.95 since Parrott (1991) has stated that "the rate of cement hydration is halved when the relative humidity drops to ~ 95%." The determined h_c values in Table 6.1 would coincide with such a statement.

Table 6.1 Parameters for Relative Hydration Age Factor.

Parameter	Cure Treatment		
	Conv.	"Throw"	"Mist"
h_c	0.97	0.93	0.93
n	6	4	4
R^2	0.87	0.97	0.96

Table 6.1 shows that both the "throw-on" and "mist" treatments had the same parameters with very similar R^2 values. These treatments did not receive a curing compound application but the conventional sections did. The conventional treatment had values different from the other two treatments and had a lower R^2 value. The parameters in Table 6.1 suggest that the "throw-on" and "mist" treatments would produce concretes with similar strengths, since these parameters were primarily determined from strength data.

Using the parameters listed in Table 6.1, the SDI for the AMA mixture can be determined at any age and treatment by considering the pore humidity history during curing. The SDI at any given test age are given for each of the cure treatments and durations in Table 6.2 along with the Arrhenius equivalent age and the equivalent hydration period.

Table 6.2 Equivalent Age Values for Three Different Functions.

Cure Duration	Conc. Age (hrs)	Conventional			"Throw"			"Mist"		
		Arr. [a] (eq. hr)	t_e [b] (eq. hr)	SDI (eq. hr)	Arr. [a] (eq. hr)	t_e [b] (eq. hr)	SDI (eq. hr)	Arr. [a] (eq. hr)	t_e [b] (eq. hr)	SDI (eq. hr)
0-D	120	117.9	117.3	52.0	116.0	109.8	73.1	114.7	107.0	67.8
	192	177.0	175.7	63.4	173.7	158.5	90.7	170.5	156.0	88.0
	360	334.0	327.1	77.2	327.5	267.2	118.7	324.5	256.4	111.0
4-D	120	125.3	124.7	92.7	124.2	123.8	119.6	125.2	125.0	124.6
	192	182.9	182.2	115.5	179.9	179.1	171.1	178.5	178.2	176.1
	360	338.8	331.4	128.8	332.2	323.2	265.3	330.0	314.2	248.8
10-D	360	338.1	336.0	185.0	330.2	329.7	324.5	331.4	331.4	331.1

[a] Arrhenius Equivalent Age

[b] Equivalent Hydration Period

The SDI values in Table 6.2 are plotted in Figure 6.10 with its corresponding compressive strength at age of testing. The data is fit with a FH strength gain curve with the following parameters: $S_{inf} = 7335.88$ psi, $\tau = 54.36$ hrs, $\alpha = 0.62$.

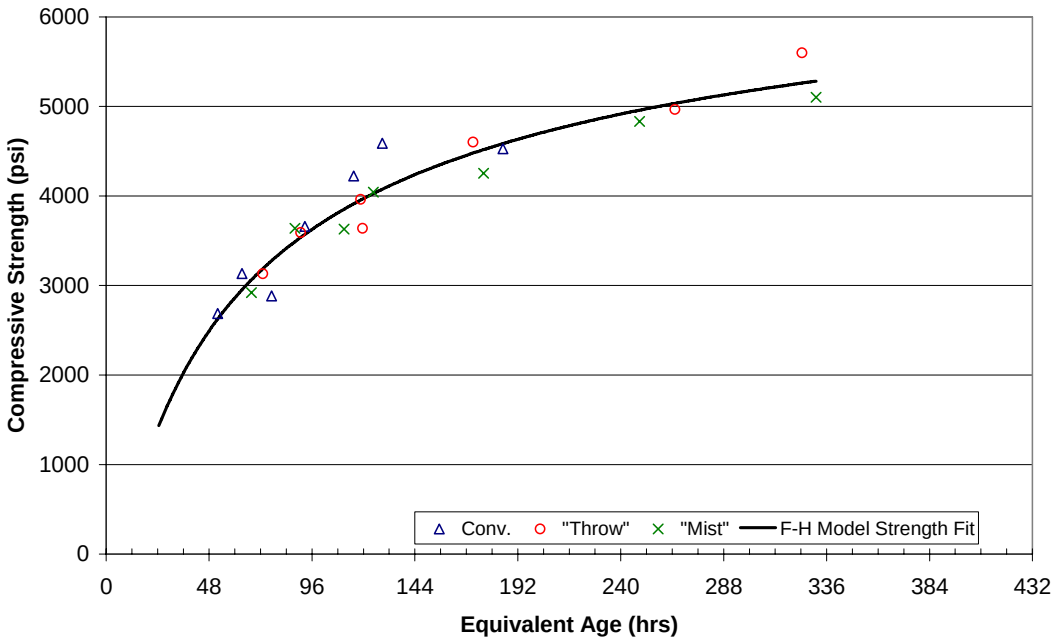

Figure 6.10 SDI Age and Strength Data for AMA Slabs.

The data in Figure 6.10 correlates relatively well with the F-H strength gain curve. The erratic scatter of the Arrhenius equivalent ages has been minimized by adjusting the equivalent ages to consider the dependency of moisture for proper concrete hydration. The FH strength gain curve depicted in Figure 6.10 could potentially be used for any cure treatment or duration for an AMA mixture. Therefore it could be thought of as the reference SDI-strength curve.

6.8.1 Using the SDI to Determine In Situ Strength

The key factor to using this curve as a strength assessment tool is the proper determination of an appropriate relative hydration age factor which in turn allows a more accurate portrayal of the concrete age. The parameters for the relative hydration age factor can be determined for a particular concrete mixture by subjecting it to various cure treatments which explore poor and good curing prior to casting in the field. In this study, poor curing consisted of the 0-day cure sections with and without curing compound. Good curing was represented with the 10-day cure sections with the various cure treatments. The 4-day cure sections are thought to have intermediate curing. The determination of the relative hydration age factor can be further refined if additionally intermediate curing treatments are used.

Once proper parameters of the relative hydration age factor are determined, a reference SDI-strength curve can be established with the FH strength gain model similar to Figure 6.10. Field concrete can then be monitored for temperature and moisture to determine a SDI.

This SDI can be used with the reference curve to determine the approximate in situ strength. Keeping in mind that the cure treatment used in the field can dictate which relative hydration age curve should be used. If the AMA mixture is placed in the field and a curing compound is applied to the surface, then the parameters used to determine the SDI would coincide with the values for the conventional cure treatment in Table 6.1. However, if curing is performed without a curing compound, similar to the "throw-on" and "mist" treatments, then the SDI can be determined using the "throw-on" and "mist" parameters in Table 6.1.

6.8.2 RCPT and Arrhenius Equivalent Age

Compressive strength is usually the primary property used to determine the quality of concrete and usually dictates when it can be loaded. Although this measure of concrete quality is convenient and has been widely accepted, other durability related parameters such as concrete chloride permeability must be considered to determine the potential ingress of deleterious substances which may cause concrete or reinforcing steel deterioration.

RCPT values for the three cure durations and treatments are plotted with the 15-day Arrhenius equivalent ages in Figure 6.11. RCPT values are for ages between 100 to 109 days. Arrhenius equivalent ages are not available for concrete age at time of RCP testing. It is assumed that the differences between the 15-day Arrhenius equivalent ages of the different cure durations and treatments would be fairly constant as the concrete ages.

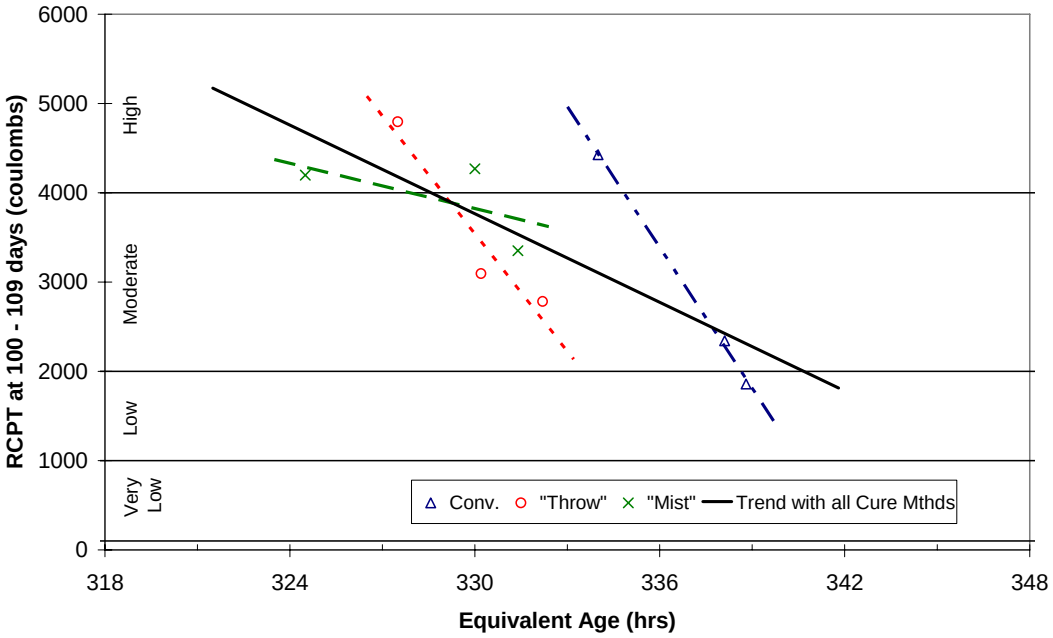

Figure 6.11 Arrhenius Equivalent Age and RCPT for AMA Slabs.

The RCPT and Arrhenius equivalent age trends suggest that increasing equivalent age results in lower permeability. Figure 6.11, however, also suggests that the AMA concrete can have a high variability of coulomb readings within a period of 15 Arrhenius equivalent hours. RCPT values range between 4800 and 1900 coulombs within this period and encompass the "low", "moderate", and "high" permeability classifications. Intuitively, a broader range in equivalent age would be expected to see such changes in the degree of permeability resistance. It would therefore be more appropriate to adjust the Arrhenius equivalent age to reflect a longer equivalent age period to realize these changes in permeability.

6.8.3 RCPT and SDI

A comparison between RCPT and equivalent hydration period is not given since the equivalent hydration period values are similar to Arrhenius equivalent ages as observed in Table 6.2. This data comparison would have been similar to Figure 6.11. Therefore only the relationship between RCPT and SDI are examined. Again, similar to the Arrhenius equivalent age scenario, SDI values were not available at 100 – 109 days during the time of RCP testing. The RCPT data is plotted against the 15-day SDI values, (i.e. calculated values at 360 hours as shown in Table 6.2), in Figure 6.12.

The data in Figure 6.12 does not produce a clear trend among the three cure treatments. "Throw-on" and "mist" treatments have similar permeability trends with increasing SDI. The increase in permeability resistance for these treatments is slow when compared to the conventional cured sections. "Throw-on" and "mist" treatments had a range of approximately 216 equivalent hours

(11 equivalent days) where permeability went from a “high” to a mid “moderate” classification based on ASTM C1202 guidelines.

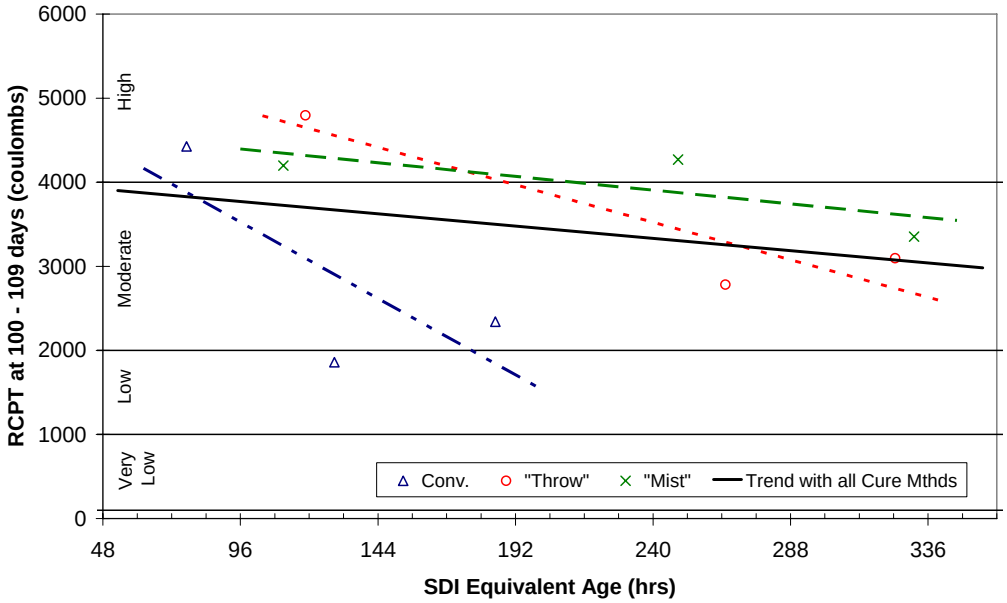

Figure 6.12 SDI Age and RCPT for AMA Slabs.

The conventional cure reacts differently and permeability is reduced in a shorter range of equivalent hours when compared to other two cure treatments. The approximate SDI range is 120 equivalent hours (5 equivalent days) for a change of permeability from “high” to “low”.

It is quite interesting that the conventional cured sections develop permeability resistance differently from the “throw-on” and “mist” sections. This is also apparent in the parameters used for the relative hydration age factor in Table 6.1, which the conventional cure did not have the same values as the two other cure treatments. The application of a curing compound on the conventionally cured sections has clearly affected the manner in which concrete properties develop. It appears as if the application of a curing compound acts as the equivalent of having an extra layer of concrete above the concrete layer that is being tested. This could be the reason the conventional cure sections are less sensitive to the lack or prolonged curing since moisture appears to vary less over the age of the concrete. This however has to be studied in more detail to determine if this is the case.

6.8.4 SDI as a Durability Tool

SDI can be used both as a strength and durability assessment tool for a particular concrete mixture if sufficient data has been gained on a number of tests. First the concrete mixture should be subjected to a number of cure treatment scenarios to cover poor and good curing conditions. Concrete properties for each cure scheme should be determined. With these data and some best fit curve optimization, a reference SDI-strength curve and quite possibly a SDI-permeability

curve can be determined. These curves can serve as a tool to determine the progress of concrete durability. Between these two curves an optimal SDI value can be suggested to attain a durable concrete.

For the AMA mixture in this study, if a compressive strength of 4000 psi is desirable to allow construction equipment on a concrete pavement, then a SDI value of approximately 130 hours (based on Figure 6.10) must be attained to reach this strength. This SDI value can be attained by several ways. One method would be to conventionally cure a section for 4 days and wait until day 15 to reach this approximate SDI values as suggested by Table 6.2. Alternatively, the "throw-on" and "mist" treatments can be used for 4-days and wait approximately 2 more days later to attain a SDI of 130 equivalent hours. Of course, it would probably be more assuring to continuously cure concrete until this equivalent age is reached.

Little can be stated at this stage about an acceptable SDI value for permeability since data was limited. If RCPT data was available at different stages of the concrete age, a more well defined SDI-permeability curve could be produced such as the SDI-strength curve in Figure 6.10. Such curve could indicate the SDI when an appropriate permeability resistance is reached. This can then lead to the termination of curing and help contractors complete construction sooner.

The SDI can be used effectively if the technique is enhanced with future research which is devoted to monitoring temperature, internal relative humidity and other important variables during curing. Discussion and recommendations on the SDI are provided in the following chapter.

CHAPTER 7
CONCLUSIONS AND RECOMMENDATIONS

7.1 Conclusions

7.1.1 Strength and Maturity

The objective of this research is to compare the compressive strengths of in-situ 4-inch diameter cores to predicted strengths based on strength-maturity curves developed from field-cured maturity (FMAT) cylinders and lab-cured maturity (LMAT) cylinders. Also, a comparison was made between in-situ strength and the conventional (CONVT) cylinder strength method. These tasks were performed through field and lab testing. Field testing involved full-scale bridge decks along with numerous field cast specimens and lab testing consisted of lab cast specimens in a more controlled environment. The curing durations discussed in this thesis is for 0, 4, and 10 days of curing with the addition of the 7-day cure for the lab testing portion of this project.

The findings from this research confirm what was previously known about the maturity method. The maturity method can be successfully implemented to determine in-situ strength of concrete. Though, these results match better than might be expected, the prediction could be further improved if moisture levels were also considered. Although, some discrepancies did exist during the analysis of the data, most of these are explained by differences in testing procedures and construction practices, including at times, a lack of quality control. These issues are discussed in the thesis. The following is a quick list of what was found:

- Maturity method is successful in assessing in-situ strength provided strict quality control is in place.
- Maturity equivalent age calculation can be misleading at times due to the lack of moisture or humidity variable in the Arrhenius and Nurse-Saul functions.
- Conventional cylinders are satisfactory when assessing in-situ strength in this manner, but involve much guesswork to determine when desired strengths have been achieved.
- Quality Control at field sites do not seem to be strongly enforced (i.e., addition of excessive water to concrete, thus altering final strength gain of concrete).

7.1.2 Strength Determination Based on the Maturity Method

The use of the maturity method, whether using the Arrhenius or Nurse-Saul Equivalent Age function, presented satisfactory results when using strength-maturity curves developed from concrete mix designs that are nearly identical. Developed strength-maturity curves from FMAT cylinders usually predicted compressive strength values within 10% of the in-situ concrete strength.

The exception to these findings was from the 0-day cure section of the bridge deck and the FMAT cylinders. As mentioned previously, the surface of the 0-day cure section of the bridge deck did not receive moist curing but was treated only with a curing compound. Therefore, in-situ strengths for the 0-day cure section were considerably lower compared to other sections of the bridge deck.

Also, strength gain models did not predict in-situ strengths well for the 0-day cure section based on developed strength-maturity curves from the 0-day cure FMAT cylinders. Again, this difference was attributed to differences in the curing environment between the 0-day FMAT cylinder and the 0-day field slab. Although, the 0-day cure FMAT cylinders did not receive any applied moist curing, they were completely sealed for the first 24 hours, which proved to be critical in strength development. Since evaporation of mix water was essentially prevented, the 0-day cure FMAT cylinders were more capable of gaining sufficient strength in the first 24 hours, as opposed to the 0-day, essentially unprotected, cure section of the bridge deck. As a result, strength correlations between the in-situ concrete and strength-maturity curves are not reliable for the 0-day cure. In contrast, for the other wet mat curing times, as shown in Tables 3.6, 3.7, and 3.8, the correlation between the strength-maturity curves and the in-situ concrete strength development is strong provided constituent proportions are nearly identical.

As discussed, the use of the maturity method appears to be a good indicator of in-situ strengths as long as curing durations, curing method, and mix design proportions are nearly identical for both the maturity cylinders and for the in-situ concrete. From LMAT generated strength-maturity curves, it became apparent that the typical field concrete was not similar enough to lab mixed concrete for strength prediction purposes. The difference from field and lab concrete appeared to be primarily due to the addition of water to the truck-delivered field concrete mix by the contractor prior to concrete placement. In general, water was added at the jobsite for the deck pour. Other possible reasons for the differences include control of mix proportions and differences in ingredients (actual water content). As a result, overall strength gain for the field concrete was decreased with the increase of the water-cement ratio. However, the final 28-day deck compressive strength (f_c') was greater than the 4 ksi design strength in all cases with the exception of the 0-day cure slabs.

When differences in mix proportions occur, a comparison between the in-situ concrete strength and the predicted lab strength (from strength-maturity curves) is not valid as indicated by Saul's maturity rule. This rule states that concrete of the *same mix* will have approximately the same strength when based on maturity. Strengths from lab-generated strength-maturity curves are compared to in-situ strengths, but are not indicative of a true "maturity-based" comparison due to differences in mix proportions, (i.e., amount of water).

When comparing strength gain trends from developed strength-maturity relationships, whether from FMAT or LMAT cylinders, it is observed that 4 days of moist curing provided similar strength gain as for the 10-day cure specimens. This was further verified with the addition of the 7-day cure to the laboratory portion of this research project. The strength gain trends for the 4-, 7-, and 10-day cure LMAT cylinder were almost identical with the exception of the San Antonio mix. The deviation of the 4-day cure trend for San Antonio was probably due to an inconsistency in mix design during batching in the lab. Overall, it can be suggested that 4 days of moist curing can provide similar strength gain when compared to longer curing durations, but

currently it is not known what effects, if any, 4 days of curing, as opposed to longer curing durations, will have on the durability of concrete.

7.1.3 CONVT Strength Determination Findings

In-situ strength determination based on CONVT cylinder breaks was found to be less accurate than the maturity method in general. Also, CONVT cylinders typically yielded strengths anywhere from 3 to 24% higher or 2 to 25% lower than in-situ concrete strengths. Although, when the use of maturity method is not an option, strength determination based on CONVT cylinders has been shown to be reasonable when compared to in-situ strength.

The use of CONVT cylinders for strength determination also increases the amount of labor the contractor must perform. Since it is unknown when in-situ concrete will gain a desirable strength, contractors must cast numerous field specimens. Cylinders are then tested on days when in-situ concrete is believed to have gained sufficient strength. These testing days are either based on experience, written specifications, or educated guesses. Even then, based on these testing criteria, the CONVT cylinder may not confirm the desired compressive strength. With this in mind, more CONVT cylinders will have to be tested at a later time to verify if the desired strength has been achieved. This process may take several trials; thus, many cylinders have to be cast to anticipate the possibility of numerous cylinder tests. With the use of the maturity method, less CONVT cylinders have to be cast to verify if a desired strength has been achieved.

In conclusion, utilizing the maturity method to determine the strength of in-situ concrete appears to be more accurate than conventional cylinders, provided that mix proportions used to develop strength-maturity curves are the same for the bridge deck. It should be noted that this reliability is high only if (a) the same nearly identical mix is used for both the cast-in-place slab and maturity cylinders used to develop a strength-maturity relationship, and (b) proper curing is applied to the bridge deck.

Also, a 4-day curing duration seems to provide sufficient strength gain. In other words, the difference in the 28 day compressive strength (f_c') for a 4-and 10-day cure cylinder is negligible. It is not known yet what effect the 4-day curing duration has on the durability aspects of the concrete.

7.1.4 Comparative Assessment of Three Curing Methods

The objective of this research was to establish the developing framework for a strength durability index (SDI) parameter. This parameter has been developed with the aim to determine concrete quality, both in terms of compressive strength and durability. First, the current Arrhenius equivalent age function was used to determine maturity and to examine corresponding in situ strengths for field-cast deck slabs under various cure durations, (i.e. curing ranging from none to 14 days). The pairings of these two parameters at times did not accurately predict in situ strengths for a particular equivalent age. A more accurate assessment can be made if it is assured that sufficient moisture is available throughout the curing process. This, however, may not be realized out in the field. Therefore if pore humidity is monitored during curing, a more accurate

equivalent age can be assigned to a maturing concrete as opposed to just considering concrete age and curing temperature.

Thus, pore humidity as well as temperature in the concrete during curing became the major focus in the experimental laboratory setup for the AMA mixture. Slabs with this concrete mixture were cast and cured using three different methods while also varying the duration of the cure treatments. The three cure treatments are the conventional, "throw-on" and "mist" treatments as defined in Chapter 4. The cure durations investigated for this research ranged from 0 to 14 days. However, only cure durations of 0, 4, and 10 days are discussed since these are the only sections which were monitored for moisture during curing. Findings from the AMA tests are discussed and recommendations are given in the following sections.

7.1.4.1 Influence of Cure Treatment & Duration on Concrete Temperature

From the AMA test setup in the structures lab, it was found that concrete temperature over the curing period on the concrete was not affected by the cure treatment used. All the 0-day sections had similar temperature profiles throughout their age with a slight exception for the 0-day conventional section. This section had a slightly higher peak temperature (approximately 2 °F higher) at 24 hours. The 4-day cure sections all experienced the same concrete temperature history irrespective of the cure treatment used. This was also true of the 10-day cure group.

Cure duration did affect the concrete temperature for the AMA laboratory setup. Prolonged moist-cure durations usually helped maintain higher and consistent temperatures during this period. This was noticeable between the 0-day sections and the other sections receiving some duration of moist-curing. During the first 24 hours, the concrete temperature for the 0-day sections peaked at approximately 65 to 67 °F and then followed the laboratory temperature. The concrete temperature for the 4- and 10-day sections both peaked at approximately 77 °F during this same period. Sections from both of these cure durations gradually decreased in temperature. Curing media used for these cure durations helped maintain temperature by providing insulation. Once cure treatment media were removed from the 4-day section, this section experienced a quick drop in temperature and then followed laboratory temperatures. The 10-day cure sections did not experience this quick drop in temperature once coverings were removed since the majority of the heat of hydration had dissipated by this time.

Comparing temperature profiles between the AMA setup and the field setup for the ELP, FTW, SAT, and HOU sites yielded different results regarding effect of cure duration on concrete temperature. In the field, differences in concrete temperature between cure durations were not detected. Additionally, nothing can be stated regarding concrete temperature affected by cure treatments since only one type of treatment (i.e. conventional) was used for all field sites. The reason temperature differences are noticed in the laboratory setup between cure durations is that these slabs were housed in a laboratory with an average temperature of 65 °F. This low constant laboratory temperature allowed variations in concrete temperature to be more detectable. Field-cast concrete, on the other hand, experienced significant variation in temperatures which ultimately dictated concrete temperature. Since concrete slabs had a large surface area to volume ratio, heat could be easily transmitted into and out of the concrete.

7.1.4.2. Influence of Cure Treatment & Duration on Concrete Moisture

Pore humidity for the AMA slabs was affected by both the cure treatment and duration. Of the three treatments, all cured durations of the conventional cure treatment appeared to provide more stable pore humidity throughout the concrete age when compared to the fluctuations observed from the other two treatments. At an age of 14 days, "throw-on" and "mist" treatments with 0 days of curing went from producing a concrete with lower pore humidity to higher pore humidity with 10 days of curing when compared to the conventional treatment.

Among the three 0-day sections, the conventional section had a higher pore humidity profile. This, however, changed when the cure duration increased to 4 days. At this cure duration, all treatments had similar pore humidity profiles throughout the age of the concrete. With 10 days or curing, both the "throw-on" and "mist" treatments had higher pore humidity profiles when compared to the conventional section with this same cure duration.

7.1.4.3 Influence of Cure Treatment & Duration on Compressive Strength

Under the laboratory conditions for the AMA mixture, all sections with 0 days of curing had lower compressive strengths when compare to section with 4 and 10 days of curing. Compressive strengths from the conventional, "throw-on" and "mist" treatments with no days of moist-curing were relatively close to each other except at a test age of 15 days. At this age, the 0-day conventional section produced lower strengths compared to the 0-day "throw-on" and "mist" treatment. This was not expected since the 0-day conventional section received a curing compound which helped maintain higher pore humidity throughout its age. The higher pore humidity in this case caused a negative effect on compressive strength results but does not mean it is a weaker concrete.

The higher pore humidity for the 0-day conventional specimens suggests the possibility of a higher degree of hydration which could have led to a more brittle concrete. This in turn may have caused more micro-cracking in the 0-day conventional specimens during coring. Additionally, these specimens were in a more moist state when observing the pore humidity prior to testing. This moisture condition may have also been a factor in lowering the compressive strength.

At test age of 15 days, "throw-on" and "mist" treatments with cure durations of 4 and 10 days had higher compressive strengths when compared to the 4- and 10-day conventionally cured sections. Typically the 4- and 10-day sections for a given cure treatment yielded similar compressive strengths at 15 days. This was also evident of the 4- and 10- day cure sections of the field-cast deck slabs at test ages of 14 and 29 days. This suggests that a prolonged cure period beyond 4 days for a slab will not significantly increase compressive strength.

7.1.4.4 Influence of Cure Treatment & Duration on Concrete Permeability

From the limited AMA RCPT data available, results show that 0-day cure sections had a "high" permeability for all three treatments. The most improvement in permeability resistance was within the conventionally cured sections. Increasing the cure duration to 4 and 14 days for this treatment resulted in concrete with a permeability bordering between "low" and "moderate". There was some improvement with an increase in cure duration for the "throw-on" treatment. Both the 4- and 10-day cure durations for this treatment produced a "moderate" permeable concrete. However, there was hardly any improvement for the 4-day "mist" cured section. This section remained at a "high" classification for 4 days of curing. Permeability was reduced to "moderate" with 14 days of "mist" curing. These results imply that permeability can be reduced by utilizing a curing compound in conjunction with a period of moist-curing. Moist-curing with the absence of a curing compound will limit the improvement in resistance to permeability for this mixture.

RCPT results for the 0-day field-cast decks slabs revealed higher electrical conductivity when compared to the 4- and 10-day sections. Cure durations of 4 and 10 days had similar permeability values. This implies little improvement in permeability resistance will be achieved between 4 and 10 days of curing. This is the same pattern noticed with compressive strength development.

Ponding results from the ELP, FTW, SAT, and HOU concrete mixtures revealed that 0 days of curing produce the highest chloride concentrations when compared to counterpart specimens with some duration of cure. The 4-day cure for these mixtures generally identified the curing threshold for an improved resistance against chloride permeability. Curing past 4 days typically resulted in little to no improvement in permeability resistance. Similarly, the AMA mixture demonstrated an increasing resistance to chloride ion ingress with prolonged curing durations.

7.1.5 Arrhenius Equivalent Age, Equivalent Hydration Period, and SDI

Results of the Arrhenius equivalent age – compressive strength relationship show a wide scatter from the best-fit Freiesleben Hansen (FH) strength gain curve. The reason of the wide scatter is because Arrhenius equivalent ages are computed using age and concrete temperature history. Although this method has been shown to work when adequate moisture is provided during concrete, it is not certain that these conditions may exist in the field. It was the intention of this study to subject concrete to a variety of curing conditions. Therefore to improve the determination of the equivalent ages, pore humidity was monitored throughout the age of the concrete.

With a pore humidity profile for each cure treatment and duration, an equivalent hydration period was determined for each section. The equivalent hydration period was first suggested by Bažant and Najjar (1972) to determine water diffusion in concrete. Using their suggested relative hydration curve parameters, these equivalent hydration ages were plotted with their corresponding compressive strengths. The data points were slightly altered but still scattered from the best-fit FH strength gain curve.

Therefore in finding ways to improve on the calculation of equivalent hydration period, the author was not restricted to the relative hydration rate proposed by Bažant and Najjar (1972). It is believed that each concrete mixture and cure treatment poses its own characteristics and thus will dictate the relative hydration rate. These revised hydration curves are referred to as relative hydration age factor curves to distinguish them.

The combination of the Arrhenius equivalent age function and the relative hydration age factor resulted in the strength durability index (SDI). With this improvement, SDI values were plotted with corresponding compressive strengths. The result was a better agreement between observed data points and the predicted best-fit FH strength gain curve. This shows some evidence that Arrhenius equivalent ages can be adjusted to account for the moisture history of the concrete by incorporating a relative hydration age factor.

The limited amount of RCPT data suggests that an increasing SDI will result in a lower permeable concrete. This however must be investigated further to determine its validity to many concrete mixtures.

Intuitively, it is considered that each concrete mixture has a given SDI value it must reach for it to attain adequate strength and permeability resistance. With the development of SDI-strength and SDI-permeability curves, an optimal SDI value can be determined and used as a guideline to terminate curing or load concrete pavement.

7.2 Recommendations

Though the maturity method has shown to be a good indicator of strength development, more research is needed to further improve the method and gain more confidence. Since there was a considerable difference in strength determination between field and lab conditions, it would be of good use if these setups could be duplicated under strict quality control guidelines. Such a setup would again have the same three portions: bridge deck, field and lab cylinders. Concrete for the deck and cylinders would be batched and delivered from the same mixing plant. The pour would be performed in a similar fashion with the exception of allowing extra water to be added to the concrete mix. All of these steps would be under strict constant supervision.

The bridge deck, field and lab cylinders would all be cured in the same manner with the exception of the 0-day cure. All testing procedures and data gathering would be performed in the same manner to develop strength-maturity relationships. These developed maturity curves would be further compared to in-situ strengths to verify the reliability of the maturity method. Also, strength gain trends from the strength-maturity curves could be further studied to support if a 4-day curing duration is sufficient to gain strength and provide durability.

For the 0-day cure cylinders, it would be more appropriate to deviate from ASTM C31 and C192 and not cap the cylinders, but rather apply a curing compound as such is the case for the 0-day cure slab of the bridge deck. By preparing 0-day cure cylinders in this manner, a strength correlation from developed strength-maturity curves could possibly be made with the 0-day cure in-situ strength of the bridge deck.

Another area of future research includes the monitoring of heat development in concrete with the development of adiabatic heat signature (AHS) curves. The use of AHS curves could be used to determine the effects of strength gain due to varying the proportions of a mix design (i.e., cement, mineral admixture, w/c ratio, etc.). With the use of AHS curves, the amount of total heat generation can be determined and used to label certain concrete mixes as either having high, low, and/or delayed heat generation. This could be helpful when specifying a concrete mix for a construction project.

Also, atmospheric factors on the field site could affect strength gain during and after the pour considerably. Some of these factors include, ambient temperature, wind velocity, humidity, and weather conditions (i.e., cloud cover, fog, direct sunlight, etc.). The development of a curing matrix in future research could help determine an appropriate wet mat curing time. If all the variables are known (i.e., atmospheric conditions, concrete type, size of section, maturity, etc.) curing durations based on a curing matrix could be specified to ensure proper strength gain and help ensure durable concrete.

The SDI has shown promise that it can better assess a true concrete age from the gathered temperature, pore humidity, and compressive strength data for the AMA mixture. The idea of improving Arrhenius equivalent ages with a relative hydration age factor, resulting in a SDI, must be examined with other concrete mixtures and conditions to gain confidence in this method.

It is still unknown how concrete mixture composition and cure treatment directly affect the relative hydration age curve. This relationship could be defined by conducting sensitivity studies on various concretes. For example, a concrete mixture with a certain amount of cement and no pozzolanic material may first be tested to determine values of h_c and n for the relative hydration age curve. Ensuing studies may test the same concrete mixture with variations of pozzolanic material replacement to determine the change in the relative hydration age curve. An extensive database of such tests for different concrete mixtures will help reveal general values and guidelines for h_c and n for an array of concrete mixtures.

This study was conducted in a laboratory environment with an average temperature of 65 °F and absence of direct sunlight, wind, and natural precipitation. This is unrealistic of a field-cast environment and thus the SDI method should be tested and validated under field conditions. With further research, both in the laboratory and in the field, the SDI method can be further refined and become a useful tool when assessing quality and durability of concrete in the field.

REFERENCES

AASHTO. (1998). "Standard Method of Test for Resistance of Concrete to Chloride Ion Penetration." *T259-80*. American Association of State Highway and Transportation Officials. Washington, D.C.

AASHTO. (1998). "Standard Method for Sampling and Testing for Chloride Ion in Concrete and Concrete Raw Materials." *T260-94*. American Association of State Highway and Transportation Officials. Washington, D.C

ACI. (2001). "Guide to Curing Concrete." ACI 308R-01. *Manual of Concrete Practice*. American Concrete Institute, Farmington Hills, MI.

Afroze, M. (2002). *Effect of Curing on Permeability and Freeze-thaw Durability of Bridge Deck Concrete*. Master's thesis. Texas Tech University.

Aïtcin, P. Miao, B., Cook, W.D., and Mitchell, D. (1994). "Effect of Size and Curing on Cylinder Compressive Strength of Normal and High-Strength Concretes." *ACI Materials Journal.* Volume 91. No. 4. 349.

Alexander, K. M., and Taplin, J. H. (1962). "Concrete Strength, Paste Strength, Cement Hydration and the Maturity Rule." *Australian Journal of Applied Science*. Volume 13. No. 4 277.

Alsayed, S.H. and Amjad, M.A. (1994). "Effect of Curing Conditions on Strength, Porosity, Absorptivity, and Shrinkage of Concrete in Hot and Dry Climate." *Cement and Concrete Research.* Volume 24. No. 7. 1390.

ASTM. (2002). "Standard Practice for Estimating Concrete Strength by the Maturity Method." *C 1074-98*. American Society for Testing Materials. Philadelphia, PA.

ASTM. (2002). "Standard Practice for Making and Curing Concrete Test Specimens in the Field." *C 31-98*. American Society for Testing Materials. Philadelphia, PA.

ASTM. (2002). "Standard Practice for Making and Curing Concrete Test Specimens in the Laboratory." *C 192-98*. American Society for Testing Materials. Philadelphia, PA.

ASTM. (2002). "Standard Specification for Portland Cement." *C 150-99*. American Society for Testing Materials. Philadelphia, PA.

ASTM. (2002). "Standard Test Method for Compressive Strength of Cylindrical Concrete Specimens." *C 39-99*. American Society for Testing Materials. Philadelphia, PA.

ASTM. (2002). "Standard Test Method for Electrical Indication of Concrete's Ability to Resist Chloride Ion Penetration." *C 1202-97*. American Society for Testing Materials. Philadelphia, PA.

ASTM. (2002). "Standard Test Method for Obtaining and Testing Drilled Cores and Sawed Beams of Concrete." *C 42-99*. American Society for Testing Materials. Philadelphia, PA.

Ballim, Y., and Graham, P.C. (2003). "A Maturity Approach to the Rate of Heat Evolution in Concrete." *Magazine of Concrete Research*. Volume 55. Number 3. 249-256.

Bartlett, F.M., and MacGregor. J.G. (1994). "Effect of Moisture Condition on Concrete Core Strength." *ACI Materials Journal*. Volume 91. No. 3. 227.

Bazant, Z.P., and Najjar, L.J. (1972). "Nonlinear Water Diffusion in Nonsaturated Concrete." *Materials and Structures*. RILEM, Paris. No. 5. 3-20.

Bergstrom, S.G. (1953). "Curing Temperature, Age and Strength of Concrete." *Magazine of Concrete Research*. Volume 5. Number 14. 61.

Bickley, J.A. (1975). "Practical Application of the Maturity Concept to Determine In-situ Strength of Concrete." *Transportation Research Record.* No. 558. 45.

Bloem, D.L. (1965). "*Concrete Strength Measurement – Cores versus Cylinders*." Proceedings of the American Society for Testing and Materials. Volume 65. 668.

Bloem, D.L. (1968). "*Concrete Strength in Structures*." Proceedings of the ACI Journal. Volume 65. Number 3. 176.

Cable, J.K., Wang, K., and Ge, Z. (2003). "Investigation into Improved Curing Materials and Techniques: Part 2 (Phase III)." *Research Report Number TR-479*. Center for Portland Cement Concrete Pavement Technology, Iowa State University. Ames, IA.

Carino, N.J. (1984). "The Maturity Method: Theory and Application." *Cement, Concrete, and Aggregates*. Volume 6. Number 2. Gaithersburg, MD.

Carino, N.J., Lew, H.S., and Volz, C.K. (1982). "Early Age Temperature Effects on Concrete Strength Prediction by the Maturity Method." *Journal of American Concrete Institute*. Volume 80. Number 2. 93.

Chanvillard, G., and D'Aloia, L. (1997). "Concrete Strength Estimation at Early Ages: Modification of the Method of Equivalent Age." *ACI Materials Journal*. Volume 94. Number 6. 520.

Chengju, G. (1989). "Maturity of Concrete: Method for Protecting Early-Stage Strength." *ACI Materials Journal*. Volume 86. Number 4. 341.

Conroy-Jones, A.G. (2004). "Effect of Curing on the Tensile Strength of Medium to High Strength Concrete." *Magazine of Concrete Research.* Volume 56. Number 3. 151-158.

Constantino, C.A., and Carrasquillo, R.L. (1998). "Investigation of the Maturity Concept as a New Quality Control/Quality Assurance Measure of Concrete." *Research Report Number 1714-3*. Center for Transportation Research, The University of Texas. Austin, TX.

Dong, Y., et al. (2002). "Use of the Maturity Method during Highway Bridge Construction." *Concrete International*. Volume 24. Number 2. 61-66.

Freiesleben, H.P., and Pedersen, E.J. (1985). "Curing of Concrete Structures." *CEB Information Bulletin*. 166.

Freiesleben, H.P., and Pedersen, E.J. (1977). "Maturity Computer for Controlled Curing and Hardening of Concrete." *Nord. Betong.* Vol. 1. No. 19.

Ghanem, H.A. (2004). *Chloride Ion Transport in Bridge Deck Concrete under Different Curing Conditions.* Master's thesis. Texas Tech University.

Hulshizer, A.J. (2001). "Benefits of the Maturity Method for Cold-Weather Concreting." *Concrete International*. Volume 23. Number 3. 68-72.

Kehl, R.J., and Carrasquillo, R.L. (1998). "Investigation of the Use of Match Cure Technology in the Precast Concrete Industry." *Research Report Number 1714-2*. Center for Transportation Research, The University of Texas. Austin, TX.

Kehl, R.J, Constantino, C.A and Carrasquillo, R.L. (1998). "Match-Cure and Maturity: Taking Concrete Strength Testing to a Higher Level." *Project Summary Report 1714-S.* Center for Transportation Research, The University of Texas. Austin, TX.

Khan, A.A., Cook, W.D., and Mitchell, D. (1998). "Thermal Properties and Transient Thermal Analysis of Structural Members during Hydration." *ACI Materials Journal*. Volume 95. Number 3.

Klieger, P. (1958). "Effects of Mixing and Curing Temperature on Concrete Strength." *Journal of Amercian Concrete Institute*. Volume 54. Number 12. 1063.

Lew, H.S., and Reichard, T.W. (1978). "Mechanical Properties of Concrete at Early Ages." *Journal of Amercian Concrete Institute*. Volume 75. Number 10. 533.

Malhotra, V.M. (1977). "*Contract Strength Requirements – Cores Versus In Situ Evaluation*." Proceedings of the ACI Journal. Volume 74. Number 4. 163.

Malhotra, V.M., and Carino, N.J. (2004). "The Maturity Method." *Handbook on*

Nondestructive Testing of Concrete. CRC Press. Ann Arbor, MI.

McIntosh, J.D., (1956). "The Effects of Low-Temperature Curing on the Compressive Strength of Concrete." *Proceedings of the RILEM Symposim: Winter Concreting, Theory and Practice*. Session BII. Danish Institute for Building Research, Copenhagen.

McIntosh, J.D. (1949). "Electric Curing of Concrete." *Magazine of Concrete Research*. Volume 1. Number 1.

Mindess, S., Young , J.F., and Darwin, D. (2002). *Concrete*. Second Edition. Prentice-Hall. Englewood Cliffs, NJ.

Myers, J.J.. (2001). "Permeability Performance of High Performance Concrete Subjected to Various Curing Regimes." *Transportation Research Record.* No. *1775*.

Nassif, H., and Suksawang, N. (2002). "Effect of Curing Methods on Durability of High-Performance Concrete." *Transportation Research Record.* No. *1798*.

Nurse, R.W., (1949). "Steam Curing of Concrete." *Magazine of Concrete Research*. Volume 1. Number 2.

Owens, P.L. (1985). "Effect of Temperature Rise and Fall on the Strength and Permeability of Concrete Made With and Without Fly Ash." *Temperature Effects on Concrete, ASTM STP 858*. T.R. Naik, Ed. American Society for Testing and Materials, Philadelphia. 134-149.

Parrott, L.J.. (1991). "Factors Influencing Relative Humidity in Concrete." *Magazine of Concrete Research*. Volume 43. Number 154.

PCA. (1988). *Design and Control of Concrete Mixtures.* 13th Edition. Skokie, IL.

PCA. (1992). *Materials for Concrete: Portland Cements*. VC118. (video). Skokie, IL.

PCA. (1995). "Portland Cements." *Design and Control of Concrete Mixtures*. 13th Edition. Skokie, IL.

PCA. (1997). "Portland Cement, Concrete, and the Heat of Hydration." *Concrete Technology Today.* Volume 18. Number 2. Skokie, IL.

Phelan, S., and Senadheera, S. (2001). "Effects of Wet Mat Curing and Earlier Loading on Long-Term Durability of Bridge Decks: Survey Results." *Research Report 2116-1*. Center for Multidisciplinary Research in Transportation, Texas Tech University. Lubbock, TX.

Plowman, J.M. (1956). "Maturity and the Strength of Concrete." *Magazine of Concrete Research*. Volume 8. Number 22.

Popovics, S. (1998). *Strength and Related Properties of Concrete: A Quantitative Approach*. John Wiley & Sons, Inc. New York, NY.

Powers, T.C. (1947). "A Discussion of Cement Hydration in Relation to the Curing of Concrete." *Proceedings of the Highway Research Board*. Washington, D.C.

Phelan, S., and Senadheera, S. (2001). "Effects of Wet Mat Curing and Earlier Loading on Long-Term Durability of Bridge Decks: Survey Results." *Research Report 2116-1*. Center for Multidisciplinary Research in Transportation, Texas Tech University. Lubbock, TX.

Quadrel. (2000). "Heat Signature, Maturity, and Simulation." Digital Site Systems, Inc. Pittsburgh, PA.

Rastrup, E., (1956). "The Temperature Function for Heat of Hydration in Concrete." *Proceedings of the RILEM Symposim: Winter Concreting, Theory and Practice*. Session BII. Danish Institute for Building Research, Copenhagen.

Saul, A.G.A. (1951). "Principles Underlying the Steam Curing of Concrete at Atmospheric Pressure." *Magazine Concrete Research*. Volume 2. Number 6.

Soroka, I., and Baum, H. (1994). "Influence of Specimen Size on Effect of Curing Regime on Concrete Compressive Strength." *Journal of Materials in Civil Engineering*. Vol. 6. No. 1. 15.

Stanish, K.D., Hooton, R.D., and Thomas, M.D.A. (1997). "Testing the Chloride Penetration Resistance of Concrete: A Literature Review." *Prediction of Chloride Penetration in Concrete.* FHWA Contract DTFH61-97-R-00022.

Tepke, D., and Tikalsky, P.J. (2001). "Concrete Maturity Progress: Survey of Departments of Transportation." *Transportation Research Record.* No. *1775*.

Texas Quality Initiative. (1999). *Reconstruction of the Dallas North Central Expressway – Dallas, Texas*. NQI Achievement Award.

TxDOT (1993). *Standard Specification for Construction of Highways, Streets and Bridges*. Texas Department of Transportation, Austin, TX.

TxDOT (1998). *Special Provision to Item 420 Concrete Structures*. Texas Department of Transportation, Austin, TX.

TxDOT. (1999). "Obtaining and Testing Drilled Cores of Concrete." Tex – 424 – A. *Manual of Testing Procedures*. Texas Department of Transportation, Austin, TX.

TxDOT. (2000). "Obtaining and Testing Drilled Cores of Concrete." Tex – 424 – A. *Manual of Testing Procedures*. Texas Department of Transportation, Austin, TX.

TxDOT (2004). *Standard Specification for Construction of Highways, Streets and Bridges*. Texas Department of Transportation, Austin, TX.

Topcu, I.B., and Toprak, M.U. (2005). "Fine Aggregate and Curing Temperature Effect on Concrete Maturity." *Cement and Concrete Research*. Volume 35. Number 4. 311.

Whiting, D. (1981). Rapid Determination of the Chloride Permeability of Concrete. Final Report No. FHWA/RD-81/119. Federal Highway Administration.

Wojcik, G.S. (2004). "Effect of Atmospheric and Construction Conditions on Concrete Equivalent Ages." *ACI Materials Journal*. Volume 101. Number 5. 376.

Wojcik, G.S., and Fitzjarrald, D.R. (2001). "Energy Balances of Curing Concrete Bridge Decks." *Journal of Applied Meteorology*. Volume 40. Number 11. 2003.